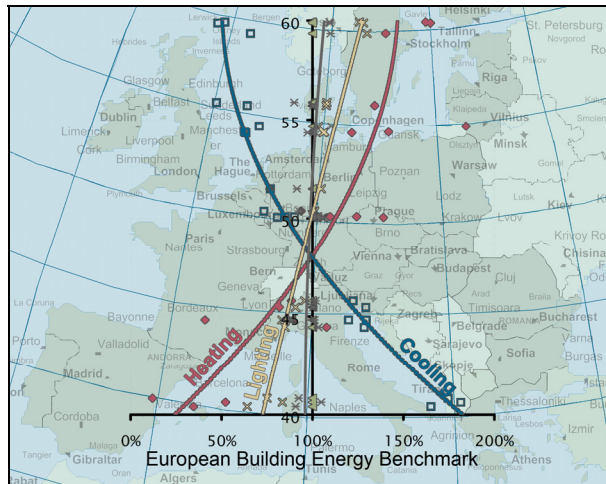


Climatic Influences on the Energy Demand of European Office Buildings



Dissertation

Approved by the

Faculty of Building

(Architecture and Civil Engineering)

Dortmund University of Technology

for the Degree of

Doctor of Science in Engineering (Dr.-Ing.)

by

Dipl.-Ing. Jörg Schlenger

Dortmund, Germany, 2009

Date of submission: 27.02.2009

Date of oral examination: 02.10.2009

Examination committee:

Chairman: Prof. Dr.-Ing. Mike Gralla

1st Examiner: Prof. Dr.-Ing Helmut F.O. Müller

2nd Examiner: Prof. Dr.-Ing. habil. Wolfgang M. Willems

Abstract

This dissertation analyses the total primary energy demand of office buildings in 25 European locations and the impact of the respective climatic conditions by the means of building simulation. An overview of existing climate classification systems and methodologies for comparison of buildings in different locations is followed by the definition of a representative office building model. Besides buildings with typical insulation levels per country, buildings with optimised façades in terms of insulation level and window proportion have also been analysed. Correlations between the location's degree of latitude, the climatic conditions and the energy demand for heating, cooling, ventilation and lighting have been evaluated. Furthermore, the impact of latent cooling loads has been analysed and the impacts of climate change on the building energy demand have been exemplified for two locations. From the findings in this work, a European Building Performance Climate Index (EBPCI) and a subsequent Classification (EBPCC) could be deducted.

Acknowledgements

This dissertation has been built during my activity as an assistant researcher and lecturer at the Chair of Environmental Architecture, Dortmund University of Technology, Germany. It would not be what it is without the help of many people, to which I owe thanks. Not all can be mentioned here, but some shall be pointed out:

My doctoral advisor Prof. Dr.-Ing. Helmut F.O. Müller (Dortmund University of Technology, Germany) supported this work with a strong personal interest and with lots of confidence in my work. The research activities at his chair were the basis for this dissertation, whereas the ultimate topic and scope has been developed in numerous fruitful discussions over time, which I enjoyed a lot.

Andreas Preißler (Dortmund University of Technology, Germany) is a great colleague and even was, when he was still a student. He has been involved substantially in developing the methodology of energetic parameterisation of façades and the subsequent building optimisation by parameter studies, which has been used in this work as well.

Lisa M. Meyer (Dortmund University of Technology, Germany) can be held responsible for the layout of the better looking images and diagrams in this work, especially the maps. Her help probably saved me several weeks of work.

Martin Goer (RWTH Aachen University, Germany) was a very capable partner for the discussions on impacts of climate change on the energy performance of buildings. I wish him all the best for the completion of his dissertation in this field.

Mark F. Jentsch (University of Southampton, United Kingdom) provided excellent support on his tool for the morphing of climatic data taking into account climate change in the UK.

Duanne Render (University of the Witwatersrand, Johannesburg, South Africa) spent a lot of his precious time on proof reading this work, despite the fact that he was writing his own thesis at the same time. I hope his help had the positive effect on his work that he expected to gain from doing this.

Dr.-Ing. Hans-Jürgen Schmitz and Lars Knabben (both: e²-Energieberatung GmbH, Germany) as well as Marcus Oetzel (bau+ GmbH, Germany) consistently provided their help and knowledge for handling special challenges of building simulation.

Prof. Olli Seppänen (Helsinki University of Technology, Finland), Prof. Francis Allard (University of La Rochelle, France) and Prof. Cristian Ghiaus (INSA Lyon, France) gave a lot of important input on the matter in discussions during and after our joint research project EULEB.

Andrea Griesinger (last, not least) supported me and backed me up during the whole process, but especially during the last year after our son was born. This was an invaluable contribution to this dissertation, which I highly appreciate.

Table of Contents

1. Introduction.....	1
2. Motivation and Objectives	3
3. Methodology.....	4
4. Existing Climate Classifications.....	6
4.1. General	6
4.2. Traditional Climate Classifications.....	7
4.3. Building-related Climate Classifications	8
5. Existing Methodologies for Building Comparison	10
5.1. General	10
5.2. Climate Surfaces (B. Keller).....	10
5.3. Energy Estimation by Robust Regression (C. Ghiaus).....	11
6. Selection of Locations and Analysis of Climatic Data.....	12
6.1. General	12
6.2. Selection of Locations	13
6.3. Original Data Sets	15
6.4. Building-relevant Climate Elements.....	15
6.5. Deducted Climatic Terms.....	15
6.6. Climate Comparison of Selected Locations.....	19
7. Methodology for Calculation of Resulting Energy Demand	24
7.1. General	24
7.2. Standard Building Model	24
7.3. Findings from Previous Studies.....	26
7.4. Energetic Parameterisation	27
7.5. Definition of “Typical” Buildings	34
7.6. Definition of “Optimised” Buildings	37
8. Energy Demand of Typical Buildings.....	43
8.1. Detailed Example: Praha.....	43
8.2. Comparison of 25 Locations (per Latitude)	44
8.3. Comparison of 25 Locations (per Climatic Term)	45
8.4. Comparison relative to European Average.....	45
9. Energy Demand of Optimised Buildings	47
9.1. Detailed Example: Praha.....	47
9.2. Comparison of 25 Locations (per Latitude)	48
9.3. Comparison of 25 Locations (per Climatic Term)	48

9.4.	Comparison relative to European Average.....	49
10.	Comparison of Typical and Optimised Buildings	51
10.1.	Comparison of Results among Each Other	51
10.2.	Exemplary Benchmarking of Results with Target Values from VDI 3807	53
11.	Influences of Supply Air Dehumidification	57
11.1.	General	57
11.2.	Typical Buildings.....	58
11.3.	Optimised Buildings	59
11.4.	Impact of the Humidity Ratio Setpoint.....	60
12.	EBPCC - European Building Performance Climate Classification	62
13.	Impacts of Climate Change	65
13.1.	General	65
13.2.	Scenarios and Predictions	65
13.3.	Exemplary Impacts of Climate Change on the Building Energy Demand	74
14.	Conclusions.....	82
15.	Summary	84
16.	German Summary (Deutsche Zusammenfassung)	91
17.	References	99
18.	List of Diagrams	103
19.	List of Tables	113
20.	Appendix	114
20.1.	Boundary Conditions of Building Simulation	114
20.2.	Characteristics of Selected Locations.....	125
20.3.	Climatic Data and Results of Selected Locations	126

1. Introduction

The reduction of the world wide energy demand and the associated emissions of greenhouse gases (GHG) is one of the biggest challenges of our time. Since the “Intergovernmental Panel for Climate Change (IPCC)” published its reports on the ongoing climate change and its effects on vegetation, animals and human beings, these challenges are no longer doubted, neither are the anthropogenic influences on the greenhouse effect worldwide. Fig. 1 shows the significant rise of air temperatures during the industrial area in the 20th century, Fig. 2 shows the correlating concentrations of carbon dioxide (CO₂) in the atmosphere during the same period.

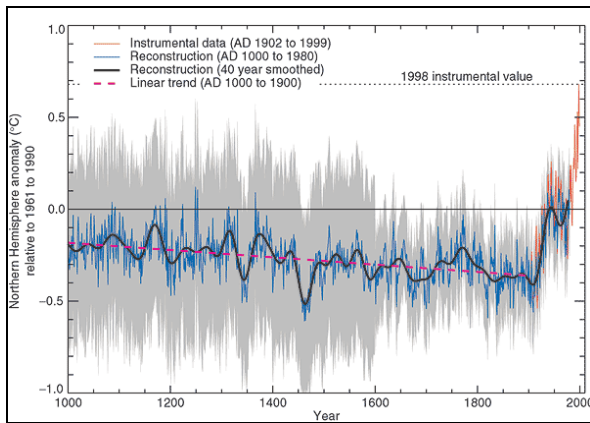


Fig. 1: Variations of the Earth's Surface Temperature on the Northern Hemisphere for the Past 1000 Years [IPCC-3 WG I].

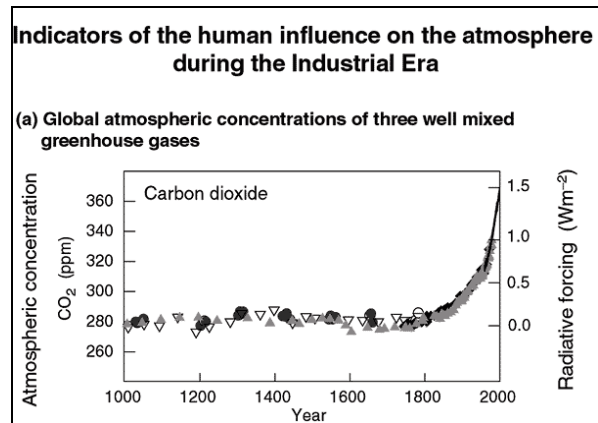


Fig. 2: Concentration of Carbon Dioxide (CO₂) in the Atmosphere for the Past 1000 Years [IPCC-3 WG I].

The energy consumption of buildings plays a significant role in these effects and therefore offers a huge potential for influencing the use of limited fossil energy resources and its negative effects on the climate. The buildings' share in the GHG-emissions amounts in the global average of countries to 15,3% (see Fig. 3). In industrialised countries such as the USA this share increases up to 27,3% (see Fig. 4). As a result, the need for energy efficient buildings has become obvious and fortunately an increasing number of buildings with low primary energy demand is being realised.

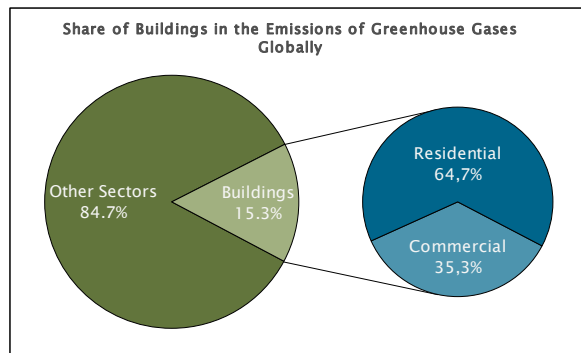


Fig. 3: Share of Buildings in the Global GHG-Emissions [WRI].

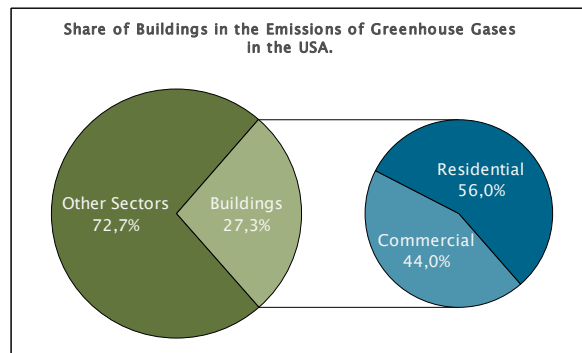


Fig. 4: Exemplary Share of Buildings in the GHG-Emissions of the USA [WRI].

One important part of the building sector are commercial buildings, which globally amount for 35,3% of the GHG-emissions of buildings (44,0% in the USA) [WRI]. Due

to their often intense use and high requirements on indoor comfort, office buildings offer huge potential for improvement.

The total energy demand of office buildings consists of several subdivisions such as heating, cooling, ventilation and lighting. With the “Energy Performance of Buildings Directive” [EPBD] the European Commission has provided a guideline for the European member states to evaluate buildings in these subdivisions. This guideline shall be implemented by the member states in their national requirements and standards for construction and refurbishment of buildings. The implementation of this directive in the EU-member states partly has taken place already, in others it is still in progress.

Generally the energy performance of buildings is influenced by many factors, such as

- climatic conditions of the building’s location
- design and quality of the building envelope
- technical systems
- internal conditions and loads
- user behaviour

As a result, the comparison and benchmarking of buildings is a complex issue which has to take these factors into account as much as possible. As one of these aspects the challenges resulting from the different climatic conditions will be analysed in detail in this work.

2. Motivation and Objectives

In the European research project “EULEB – EUropean high quality Low Energy Buildings” 25 energy efficient buildings from all over Europe were analysed and presented on a CD and website [EULEB]. Fig. 5 shows the locations of the buildings analysed in EULEB and their allocation to the building types “education”, “office” and “leisure facilities”.



Fig. 5: Locations and Types of Buildings analysed in [EULEB] (© www.ReginaMueller.de).

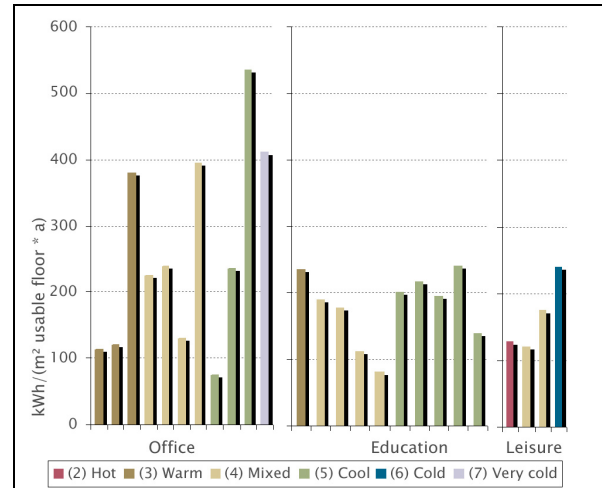


Fig. 6: Total Primary Energy Demand of EULEB-Buildings, grouped by Building Type and Climatic Zone according to [ASHRAE].

At the time of the data collection for EULEB all buildings have been in use for at least two years, so their energy performance, user acceptance etc. could be evaluated from measured data, user surveys etc. Fig. 6 exemplifies the resulting total primary energy demand of the 25 buildings, grouped by building type and climatic zone according to ASHRAE 4610/4611 [ASHRAE] (see chapter 4.3.1).

The strong variance of the results in Fig. 6 shows the difficulty of comparing the energy performance of buildings in a European scale. On the one hand, the results vary between the climatic zones within one building type, but also within one climatic zone the differences between building types are significant.

Therefore the motivation of this work was to analyse the climatic influence on the energy performance of office buildings in a European context. The bandwidth of the specific primary energy demand for heating, cooling, ventilation and lighting should be investigated and correlations to the location and the respective climatic conditions should be determined. From the analyses, suggestions for a classification of European climates with regard to the Energy Demand of Buildings should be deduced, allowing the estimation of relative energy demand based on a location’s climate.

3. Methodology

As a first step existing climate classifications and their applicability for buildings will be compared. A special classification system, which has been developed for the use with buildings, will be reviewed in terms of evaluation of the total primary energy demand of buildings. Furthermore, two methodologies for the estimation of building energy demands from climatic data will be discussed, as they offer the possibility of comparing climatic influences as well.

As a second step a number of locations from all over Europe will be selected for further analysis in this work. Statistical climatic data for these locations will be generated from a data base. Representative characteristics will be deduced from the original sets of climatic data. Additionally, climatic terms with significance for the building energy demand will be deduced and analysed in detail. Both the characteristics and the climatic terms will be analysed and brought into context with each other and their geographic location. This will give a first overview on the climatic variety of the European continent and the climatic boundary conditions for buildings respectively.

Afterwards, a representative standard office building model will be defined in a third step. Using dynamic simulation tools, this model will be used for the calculation of the energy demand for heating, cooling, ventilation and lighting. Here, two types of buildings will be analysed in parallel: One with typical and one with optimised thermal façade qualities. This split way of analysis was chosen in order to tackle the challenge of different insulation levels in European countries. The results achieved from the building simulation with both building types will be analysed and compared with each other.

From the comparison of the calculated energy demand with the climatic analyses correlations between the two will be deduced. The variation of primary energy demand for heating, cooling, ventilation and lighting will be analysed in detail with regard to the location and its climatic conditions.

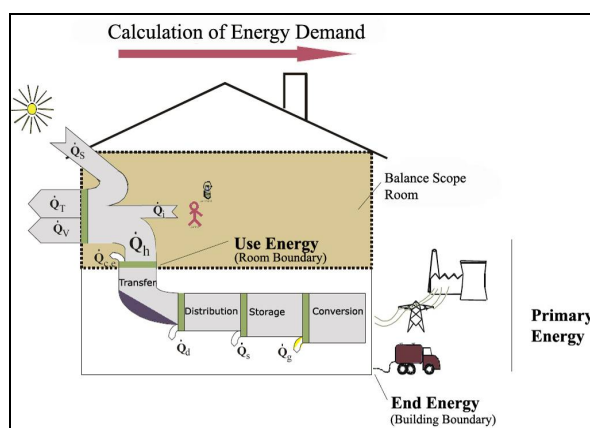


Fig. 7: Calculation of Primary Energy Demand [DIN V 4701-10].

All calculations of energy demand will be done on a "primary energy" level, i.e. including the losses resulting from conversion, storage, distribution and transfer of energy within the building as well as losses from extraction and transportation of energy to the building. Fig. 7 visualises the principle of primary energy calculation.

Summing up energy demands covered by different resources has low significance on a level of use or end energy. As primary energy represents the actual energy demand, taking into account advantages and disadvantages of different energy resources, it is the only energy level with significant results from the addition of energy demands from different resources.

Finally, from the correlations between climate and energy demand an evaluation system will be developed, allowing for the classification of climates with regard to the energy demand of buildings.

4. Existing Climate Classifications

4.1. General

“Weather” is defined as the atmospheric conditions at a certain location and a certain point of time. Contrary to this, “climate” is defined as the average weather conditions occurring at a certain location over a longer period of time. Usually a climate consists of more or less constant annual recurrences of certain weather conditions.

A climate can be described with the help of different climate elements influencing the climatic conditions. These climate elements can be air temperature, air pressure, solar radiation, cloud cover, direction and intensity of winds etc. Very often average, minimum and maximum values of a selection of these elements are used to describe a climate.

By the definition of thresholds for the selected climate elements different climates can be grouped together and a classification system can be defined. The selection of climate elements appropriate for the scope has a strong influence on the informative value of a classification system.

As solar radiation is the main driver of all weather and climate effects in the world and as precipitation is the second most important factor for the life of creatures and vegetation, a rough definition of “solar zones” in the world has become common. Fig. 8 shows the global distribution of this rough climatic classification. Apart from some regions dominated by local influences a certain correlation to the degree of latitude can be noticed, allowing a rough horizontal separation of cool, temperate, arid and tropical zones. With this low grade of detail, most of the European continent belongs to the “temperate” zone, only the very northern parts is marked as “cool”.

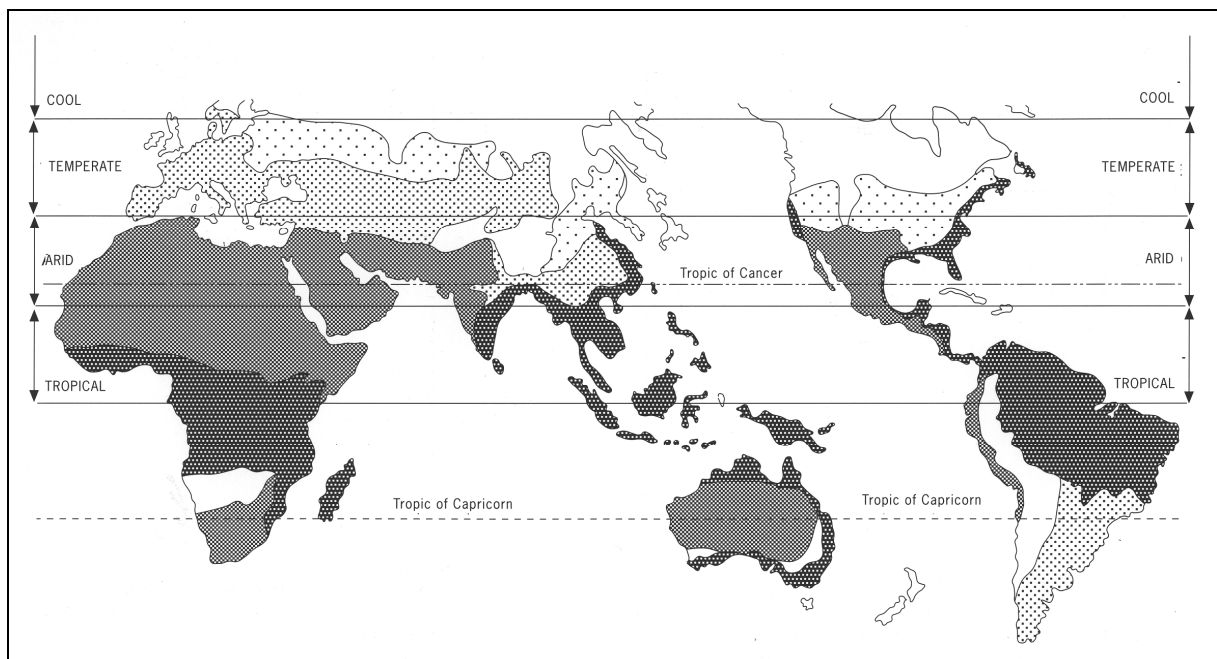


Fig. 8: Global Distribution of Climatic Zones [Yeang].

Most of the traditional classification systems have been created to describe the climatic conditions for creatures and vegetation and therefore have been based on the rough classification described above. Despite this fact these traditional systems are very common and often used in relation with buildings and other technical issues.

Other systems have been developed focussing on different correlations of climate and the energy demand of buildings. Examples of both types of classifications will be presented in this chapter.

4.2. Traditional Climate Classifications

4.2.1. Classification of KOEPPEN

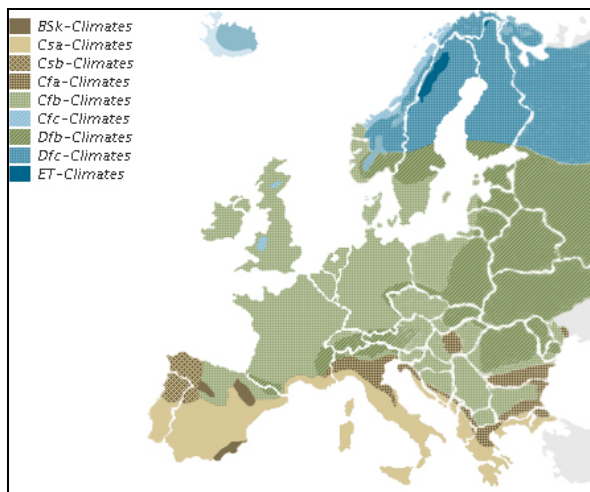


Fig. 9: Climate Classification of Europe according to KOEPPEN, based on [Straesser], (© www.ReginaMueller.de).

The classification system of Wladimir Köppen (1846–1940) is the most known and common climate classification. Furthermore it has been the basis for many other classifications and regulations. By analysis of the climate elements “air temperature” and “precipitation” in the KOEPPEN system five major climatic zones have been defined and named with capital letters: “A” (tropical), “B” (dry), “C” (temperate), “D” (continental) and “E” (polar) [Straesser].

Each of these zones has eight subdivisions (“types”) according to the type of winter and summer, described by lower case letters. In some climatic zones “subtypes” allow for a more detailed

subdivision. The combination of the letters for climatic zone, type and subtype (if applicable) leads to a climate code describing a certain climate.

Fig. 9 shows the KOEPPEN classification of Europe, where the climate codes can be translated as followed:

- BSk: Mid-latitude steppe. Semiarid, cool or cold.
- Csa: Interior Mediterranean. Mild winter and dry hot summer.
- Csb: Coastal Mediterranean. Mild winter and dry, short, warm summer.
- Cfa: Humid subtropical. Mild winter and moist in all seasons.
- Cfb: Marine. Mild winter and moist all seasons. Warm summer.
- Cfc: Marine. Mild winter and moist all seasons. Short cool summer.
- Dfb: Humid continental. Severe winter, moist all seasons with a short warm summer.
- Dfc: Subarctic. Severe winter, moist all seasons with a short, cool summer.
- ET: Tundra. Very short summer.

The classification of KOEPPEN is quite detailed and covers the whole world with 23 climate types. Based on air temperature and precipitation it was made to be used in

context with creatures and vegetation so that for the use with buildings it lacks a relation to the resulting energy demand of buildings.

4.2.2. Classification of TROLL

The classification of Carl Troll (1899–1975) is even more detailed than the KOEPPEN system and focuses on the annual change of seasons. Compared to KOEPPEN it includes the solar radiation as a third parameter and distinguishes the climates of locations according to their height above sea level as well. This leads to five major categories: I (polar and sub polar), II (cold temperate), III (cool temperate), IV (warm temperate) and V (tropical). Together with up to twelve subdivisions a total of 29 climatic zones describe the climate around the world.

Similar to the KOEPPEN system the classification of TROLL was made to be used in context with creatures and vegetation and lacks a relation to the resulting energy demand for the use with buildings.

4.3. Building-related Climate Classifications

4.3.1. ASHRAE 4610/4611 (R.S. Briggs / R.G. Lucas / Z.T. Taylor)

The American Society of Heating, Refrigerating and Air-Conditioning Engineers (ASHRAE) developed a building related climate classification. By cluster analysis of climate data of about 5000 locations in the United States of America (USA), a detailed map of the USA has been created, dividing the country into three major climates (marine, dry and humid), subdivided with up to eight thermal zones: 1 (very hot), 2 (hot), 3 (warm), 4 (mixed), 5 (cool), 6 (cold), 7 (very cold) and 8 (sub arctic) [ASHRAE].

Contrary to the general classifications of KOEPPEN and TROLL, the ASHRAE classification uses heating and cooling degree days (HDD / CDD, see chapter 6.5) instead of air temperatures to evaluate the influence of climate on the heating and cooling energy demand of a building.

According to [ASHRAE], the methodology developed for the USA generally can be applied outside the USA. However with respect to application of the classification itself (i.e. the thresholds and their resulting categorisation) some caveats have to be considered. The appropriateness of the classification for other continents should be investigated further and new cluster analyses should be performed in order to achieve respective maps with the local distribution of the climatic zones on other continents.

Regardless of these caveats, Fig. 10 exemplifies the climate classification of European capitals according to the ASHRAE system.

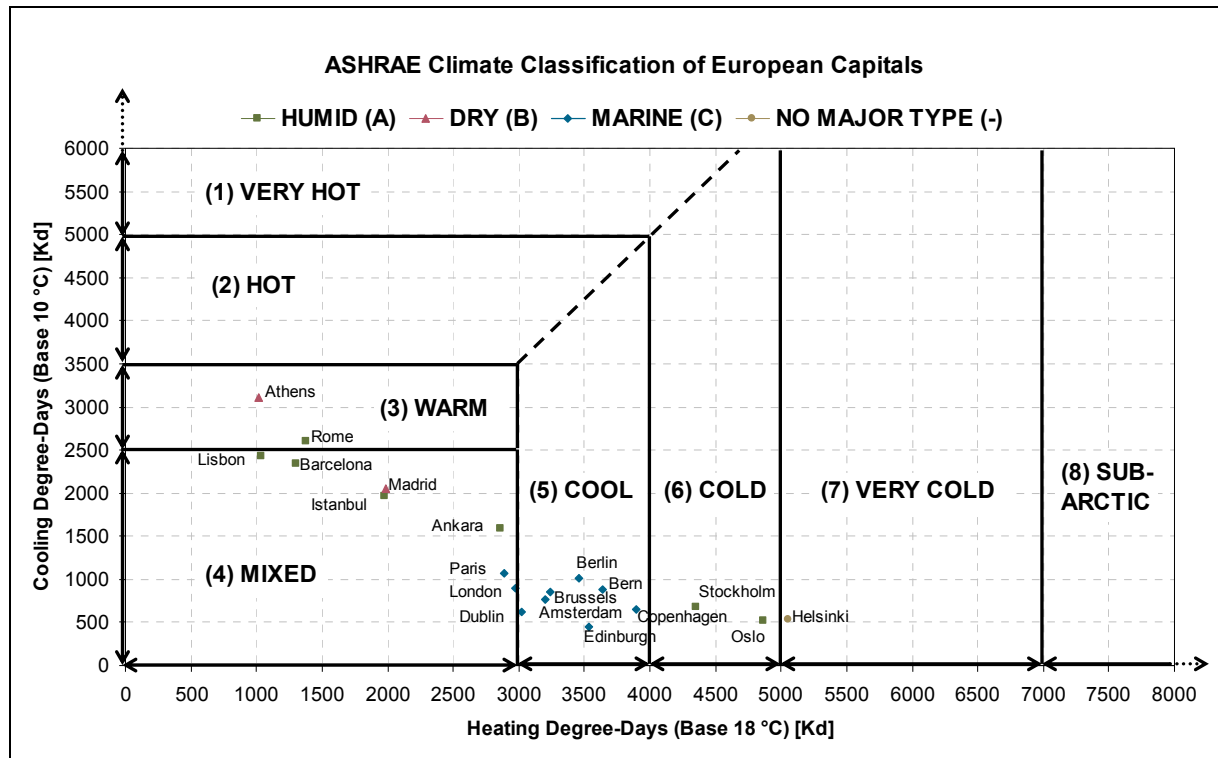


Fig. 10: Climate Classification of European Capitals according to ASHRAE 4610/4611.

The ASHRAE methodology offers a good possibility to evaluate and compare the heating and cooling energy demand of a building based on the climatic data of its location. However without further analysis the classification of climatic zones can not just be applied to European locations.

Treating only thermal aspects, the methodology is not sufficient looking at the total energy demand of buildings, i.e. the energy demand for heating, cooling, ventilation and lighting.

5. Existing Methodologies for Building Comparison

5.1. General

The prediction of the building energy demand is very important during the design process. Therefore several methodologies have been developed for the simple estimation of the energy demand of a building in advance. The idea is to analyse and optimise a design in order to maximise the indoor comfort and to minimise the energy demand at the same time without performing detailed calculations (for example dynamic simulations).

Some of these methodologies offer the opportunity to analyse the climatic influence and therefore to compare buildings in different locations. Therefore two of these will be described briefly in the following.

5.2. Climate Surfaces (B. Keller)

The methodology of “Climate Surfaces” described in [Keller] and [Pinpoint] has been developed in 1996 and allows the analysis of a single room with given parameters. These parameters have been reduced to only three most important parameters:

- A generalised loss factor K (related to the external surface of the room)
- The time-constant τ (depending on the thermal mass / inertia of the room)
- The solar gain-to-loss-ratio $\gamma = \Psi / K$ (where Ψ represents the solar gains through the apertures, related to the external surface of the room)

By calculation of generalised heating and cooling degree days $\Omega_{\text{heat/cool}}$ (or Ω_{tot} as the sum of both) depending on τ_{eff} and γ (i.e. taking into account thermal mass and solar gains of the room), a so-called climate surface can be created for the room based on a considered control strategy and a certain climate. Fig. 11 shows an example for the sum of heating and cooling energy demand of a room South facing room in Zürich (Switzerland) as described by a climate surface. The thick line indicates the limit between cooling loads equal and above zero.

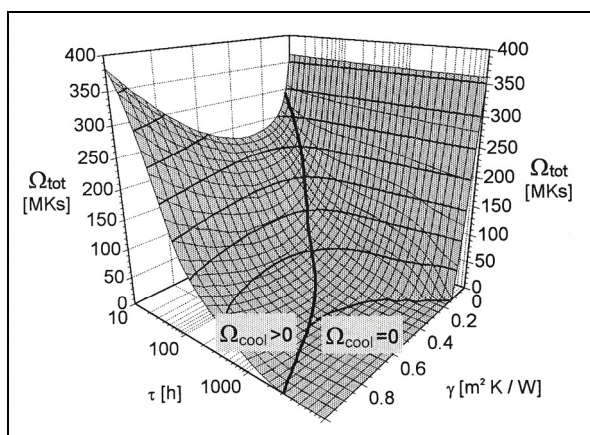


Fig. 11: Example of a Climate Surface (Sum of Heating and Cooling for Zürich, CH) [Keller].

With the help of these climate surfaces the energetic position of a room can be determined and the influence of modifications of room parameters such as insulation level, size of apertures, thermal mass etc. can be evaluated and visualised. It can be seen easily which modifications would have a strong effect on the energy demand under the given climate and which would not. Therefore strategies of best improvement can be found at a very early planning stage.

Furthermore by calculation of climate surfaces different climates can be com-

pared quantitatively. In this so called “climate surface algebra” the energetic effects of climate can be deduced from the differences between two climate surfaces.

A classification of climates based on climate surfaces could be created, but so far this has not been done. As the methodology focuses on thermal aspects only, other energetic aspects of a building such as lighting energy demand could not be considered therein.

5.3. Energy Estimation by Robust Regression (C. Ghiaus)

A rather new way of estimating energy performance indices like the heating curve of a building using robust regression of the heating and cooling losses on the outdoor temperature has been described in [Ghiaus].

By using the frequency distribution of the outdoor temperature to describe the climate and the free-running temperature to characterize the building behaviour, the thermal behaviour of the building, the thermal comfort range and the climate data could be uncoupled from each other. Therefore equivalence between the load curve and the free-running temperature of a building could be proved.

Fig. 12 in principle shows the resulting operating zones of the technical systems (HVAC – heating, ventilation and air-conditioning) depending on the outdoor temperature, the free running temperature and the limits for thermal indoor comfort of a building.

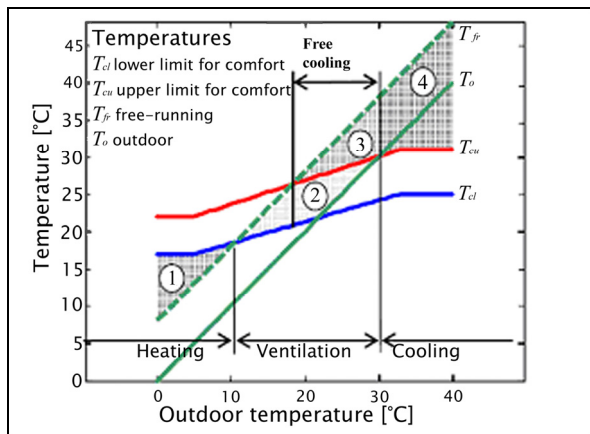


Fig. 12: HVAC Operating Zones according to [Ghiaus]: (1) Heating, (2) Ventilation, (3) Free-Cooling, (4) Mechanical Cooling.

This methodology gives the possibility to analyse and compare the energy consumption and comfort of one building in different climates, based on measured or statistical climatic data.

A respective climate classification system based on this methodology has not been deduced so far. Like the other building-related classification systems mentioned before, this classification system would deal with thermal aspects only.

6. Selection of Locations and Analysis of Climatic Data

6.1. General

The analyses in this work will be done at a certain number of locations all over Europe. The criteria for the selection of these locations will be described below.

For each of the selected locations a set of climatic data is required for the analysis of the locations' climate and as input for the dynamic calculations performed. As a result of the level of detail of the simulation (annual, at a time step of one hour) climate information for each hour of one year (i.e. 8.760 values per climate element) is required.

The source of the data sets used for this work was the software *Meteonorm* (version 5.0) [Meteonorm]. It consists of a data base with measured data from more than 7.000 weather stations all over the world and a number of algorithms allowing for calculation of climatic data for any location in the world. Therefore it can provide statistical sets of climatic data comprising both average weather conditions as well as extreme weather events that occur with a certain probability.

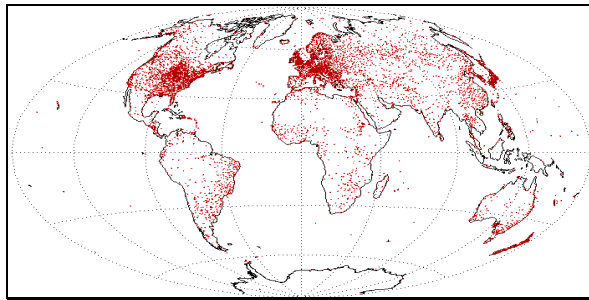


Fig. 13 shows the distribution of the weather stations included in *Meteonorm* 5.0. As a result of the very dense net of weather stations in Europe all locations selected in this work (see chapter 6.2.4) were represented with statistical interpretations of measured data from the actual location.

Fig. 13: Position of the 7.400 Weather Stations in the Software *Meteonorm* 5.0 [Meteonorm].

6.2. Selection of Locations

6.2.1. General

The locations analysed in this work have been selected according to two main criteria:

- Degree of latitude (and position within the particular east-west-dimension of Europe)
- Relevance for office buildings (city size)

6.2.2. Selection Criterion: Degree of Latitude

All climatic conditions in the world are significantly influenced by the solar radiation, which is also the main driver for all life in the world. Other climate elements such as air temperature, precipitation, wind etc. eventually are results of the solar radiation (and other factors).

Looking at the local distribution of annual solar radiation (see Fig. 14) a rough correlation with the degree of latitude can be determined. Therefore, a rough correlation between the general climatic conditions (and the resulting energy demands of buildings) and the latitude can be expected as well.

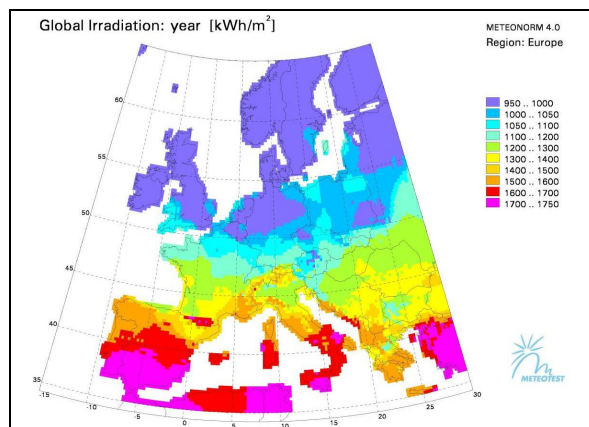


Fig. 14: Annual Global Irradiation in Europe [Meteonorm].

Therefore as a first step the locations have been selected in groups with similar geographical latitude. To cover most of the European continent, locations have been selected between latitudes of 60 °N and 40 °N in steps of 5°. As a result five groups of locations have been defined: 60 °N, 55 °N, 50 °N, 45 °N and 40 °N.

Secondly five locations have been selected within each group of latitude covering the particular east-west dimensions of the European continent as much as possible. Therefore a total of 25 locations have been selected.

6.2.3. Selection Criterion: Relevance for Office Buildings (City Size)

The second criterion for the selection of locations was the size of cities. It was assumed that starting from a population of more than 100.000 in the urban area the location has a significant relevance for office buildings. Although this is not mandatory for the analysis of the climate, it was considered as an additional benefit to choose such locations for further analysis.

The locations have been selected according to the population in their urban areas listed in [Butler].

6.2.4. Selected Locations

According to the above mentioned criteria the locations shown in Fig. 15 have been selected for the analyses in this work. Detailed information about the selected locations can be found in the appendix of this work.



Fig. 15: Map of Europe with Selected Locations.

6.3. Original Data Sets

For the selected locations climatic data have been obtained from [Meteonorm] on an hourly basis (see 6.1) comprising the following climate elements:

- Cloudiness factor [-]
- Wind direction [°]
- Wind speed [m/s]
- Precipitation [mm]
- Air pressure [hPa]
- Air temperature [°C]
- Relative humidity [-]
- Direct solar radiation on horizontal surface [W/m²]
- Diffuse radiation on horizontal surface [W/m²]
- Illuminance on horizontal surface [lux]
- Longwave radiation on horizontal surface [W/m²]
- Atmospheric counter radiation on horizontal surface [W/m²]

The data has been analysed according to [EN 15927-1] in order to achieve a statistical data sheet with climate characteristics for each of the 25 locations. These detailed climate data sheets give a first impression of the local climates and can be found in the appendix of this work.

6.4. Building-relevant Climate Elements

From the data contained in the Meteonorm data sets, the following climate elements were considered to have the main influence on the building energy demand and therefore have been selected for further analysis:

- Air temperature [°C]
- Direct solar radiation on horizontal surface [W/m²]
- Diffuse radiation on horizontal surface [W/m²]
- Illuminance on horizontal surface [lux]

The minor influences of other elements have been neglected in order to keep the complexity of the further analyses within feasible limits. In this context the influence of relative humidity on the cooling energy demand was considered minor for the comparison of European locations. As it highly depends on the technical systems applied, which should not be part of this study, its impact has been evaluated separately (see chapter 11).

6.5. Deducted Climatic Terms

6.5.1. General

From the analysis of existing climate classifications (see chapter 4) and methodologies for building comparison (see chapter 5) it was considered useful to translate the original climate elements to other climatic terms which have a stronger significance for the energy consumption of buildings.

For heating and cooling energy demand this could be done by degree days, for the energy demand resulting from artificial lighting the illuminance on horizontal surface proved to be a suitable term.

6.5.2. Heating Degree Days (HDD)

In international literature different definitions for the calculation of heating degree days (HDD) exist. All methods include the definition of a so called “base temperature” to which temperature differences are calculated. Some methods additionally include a “temperature threshold”, which has to be exceeded before the temperature differences are taken into account.

For this work, the calculation of HDD is done according to the definition in the European standard [EN 15927-6] which does not include a temperature threshold but only a base temperature.

In this standard the base temperature is defined as a “conventional temperature, for example the indoor design temperature minus the decrements resulting from internal and / or solar gains”. This makes it obvious that the base temperature actually is depending on many building parameters such as size and orientations of apertures, insulation level, shading facilities and their control, internal loads etc. Despite this fact it is common to use standard base temperatures which do not reflect the properties of a certain building, in order to make HDD comparable between climates.

[EN 15927-6] recommends a standard base temperature of 12 °C, but “other integer base temperatures are possible at which multiples of 2 °C are preferred (for example 10 °C, 12 °C, 14 °C, 16 °C, 18 °C and 20 °C)”.

Because of dependence on [ASHRAE] (see chapter 4.3.1) a base temperature of 18 °C has been used in this work for the calculation of HDD.

The hourly temperature differences $\Delta\Theta_h$ are calculated for each hour of the summation period using the equations

$$\Delta\Theta_h(\Theta_b) = (\Theta_b - \Theta_{hm}) \quad \text{if } \Theta_{hm} < \Theta_b \quad [\text{K}]$$

and

$$\Delta\Theta_h(\Theta_b) = 0 \quad \text{if } \Theta_{hm} \geq \Theta_b \quad [\text{K}]$$

where

$\Delta\Theta_h(\Theta_b)$: Hourly temperature differences [K]

Θ_b : Base temperature [°C]

Θ_{hm} : Hourly mean values of outside air temperature [°C]

Fig. 16 shows the principle of calculation of heating degree hours (HDH).

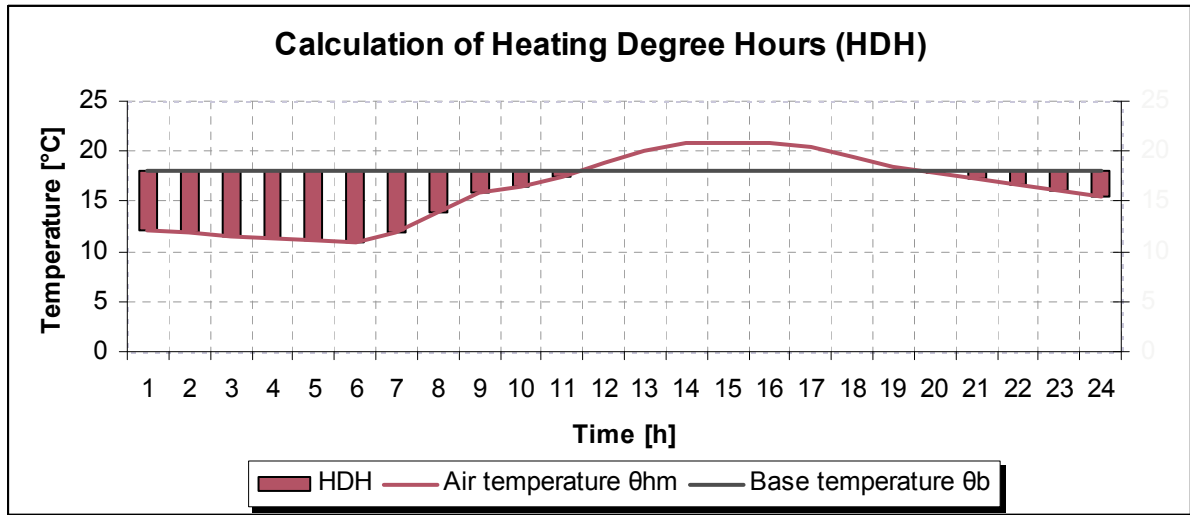


Fig. 16: Principle of Calculation of Heating Degree Hours (HDH).

For the period of n hours the accumulated hourly temperature differences are calculated as the sum of the $\Delta\theta_h$ – values using the equation

$$\theta_{\sum_h}(\theta_b) = \sum_{h=1}^n \Delta\theta_h(\theta_b) \quad [\text{Kh}]$$

The accumulated hourly temperature difference $\theta_{\sum_h}(\theta_b)$ can be expressed in degree days using in the equation

$$\theta_{\sum_{h(d)}}(\theta_b) = \theta_{\sum_h}(\theta_b) / 24 \quad [\text{Kd}]$$

6.5.3. Cooling Degree Days (CDD)

According to [EN 15927-6] the equations for the calculation of HDD “in principle can be reversed in order to calculate cooling degree days (CDD)”. Because of the influences of solar radiation and humidity not taken into account the significance of a CDD-term is put into question in this standard.

As described before (see 6.4), the impacts of dehumidification have been examined separately. From the results of this analysis (see chapter 11), it was decided not to take humidity into account in this work. The solar radiation will be considered very precisely within the dynamic simulations. Since first tests showed a good correlation between CDD and the calculated cooling energy demand, it was decided to use the CDD-term in dependence on ASHRAE 4610/4611 [ASHRAE].

Therefore the hourly temperature differences $\Delta\Theta_h$ were calculated for each hour of the summation period in dependence on [EN 15927-6] using the equations

$$\Delta\Theta_h(\Theta_b) = 0 \quad \text{if } \Theta_{hm} \leq \Theta_b \quad [\text{K}]$$

and

$$\Delta\Theta_h(\Theta_b) = (\Theta_b - \Theta_{hm}) \quad \text{if } \Theta_{hm} > \Theta_b \quad [\text{K}]$$

where

$\Delta\Theta_h(\Theta_b)$: Hourly temperature differences [K]

Θ_b : Base temperature [°C]

Θ_{hm} : Hourly mean values of outside air temperature [°C]

The base temperature for CDD is subject to the same restrictions described in chapter 6.5.2. Because of dependence on ASHRAE 4610/4611 [ASHRAE] (see chapter 4.3.1) it has been defined at 10 °C for this work. Fig. 17 shows the principle of calculation of cooling degree hours (CDH).

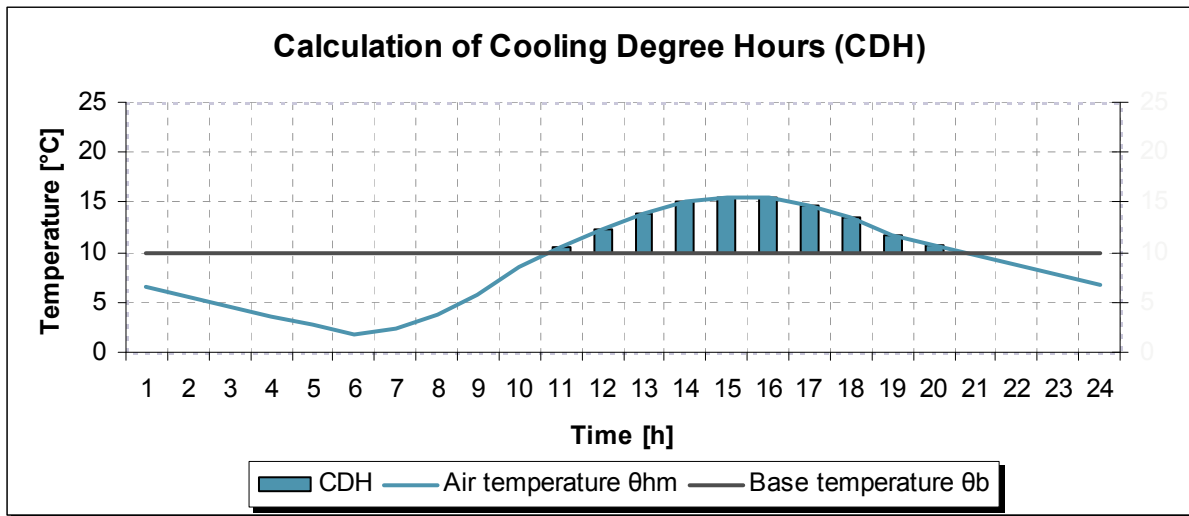


Fig. 17: Principle of Calculation of Cooling Degree Hours (CDH).

For the period of n hours the accumulated hourly temperature differences are calculated as the sum of the $\Delta\Theta_h$ – values using the equation

$$\Theta_{\sum h}(\Theta_b) = \sum_{h=1}^n \Delta\Theta_h(\Theta_b) \quad [\text{Kh}]$$

The accumulated hourly temperature difference $\theta_{\sum h}(\theta_b)$ can be expressed in degree days using in the equation

$$\theta_{\sum h(d)}(\theta_b) = \theta_{\sum h}(\theta_b) / 24 \text{ [Kd]}$$

6.5.4. Total Annual Illumination

The energy demand for artificial lighting is influenced (amongst building and user specific parameters) by the availability of daylight outside and therefore depending on the solar radiation. Therefore the total annual illumination has been used as a third climatic term for the comparison of climates. It can be obtained easily from the original data set by summing up the hourly values.

If the illumination is not part of a set of climatic data, it can be estimated from the global radiation on a horizontal surface using the equation

$$\text{Illumination [lux]} = \text{Global Radiation [W/m}^2\text{]} * 110 \text{ [lm / (W/m}^2\text{)]}$$

Due to the joint dependency on the solar radiation of both cooling degree days and annual illumination, a correlation between the two could be expected and has been analysed in chapter 6.6.3.

6.6. Climate Comparison of Selected Locations

6.6.1. Temperatures and Degree Days

The comparison of annual mean temperatures as well as maximum and minimum monthly temperatures of the 25 selected locations in relation to the latitude of the locations is shown in Fig. 18.

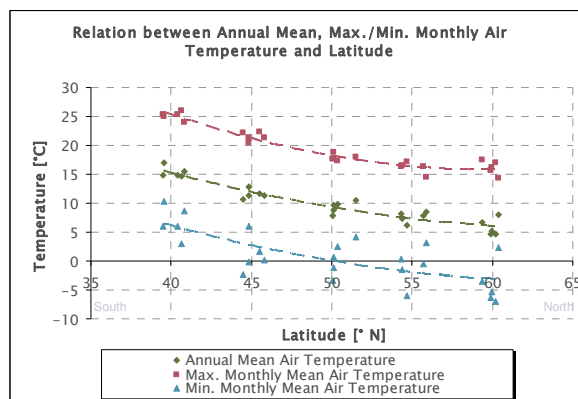


Fig. 18: Mean, Max. and Min. Air Temperatures as Functions of the Locations' Latitudes.

It can be stated that the maximum monthly air temperatures show a good correlation to the latitude. This can be traced back to the strong influence of solar radiation on the daily temperatures and the correlation of solar radiation and latitude (see chapter 6.2.2).

Contrary the minimum monthly air temperatures vary much more independently from the latitude as a result of local influences on the climate in winter (for example the distance to the sea or the ocean). Nevertheless the annual mean air temperatures correlate well with the latitude.

The heating and cooling degree days of the 25 selected locations are shown in Fig. 19 as functions of the latitude.

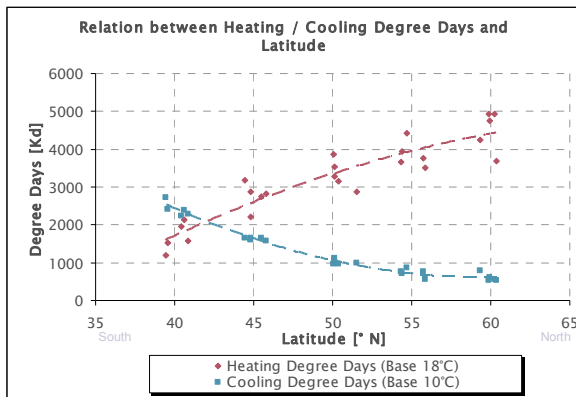


Fig. 19: Heating and Cooling Degree Days as Functions of the Latitude.

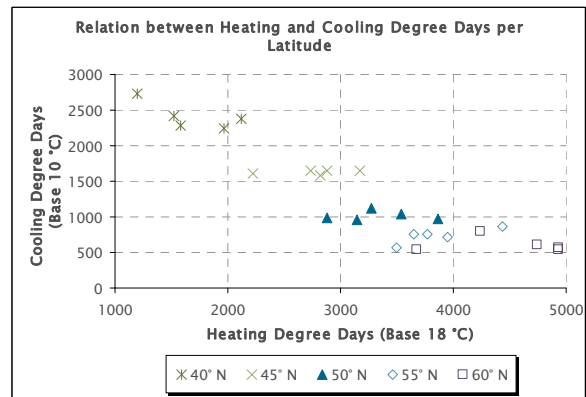


Fig. 20: Heating and Cooling Degree Days of Selected Locations grouped by Latitude.

The good correlation of cooling degree days with the latitude can be traced to the strong influence of solar radiation, just as the maximum monthly air temperatures. Similarly to the minimum monthly air temperatures, the heating degree days show a stronger variation independent of the latitude.

It can be observed that from North to South the dominant climatic term changes from heating to cooling degree days. Furthermore within each group of latitude the cooling degree days are much more consistent than the heating degree days, which again is a result of the observed minimum monthly air temperatures (see Fig. 18).

Fig. 20 shows the heating and cooling degree days of the 25 selected locations grouped by latitude. The trend of this correlation, shown in Fig. 21, can be described by the ratio between heating and cooling degree days. The higher this ratio, the more the climate is dominated by heating loads, i.e. the colder is the climate. This HDD/CDD-Ratio shows a clear trend as function of the latitude (see Fig. 22), whereas the southern latitudes are the warmer climates (low HDD/CDD-ratio), the northern locations are colder (high HDD/CDD-ratio).

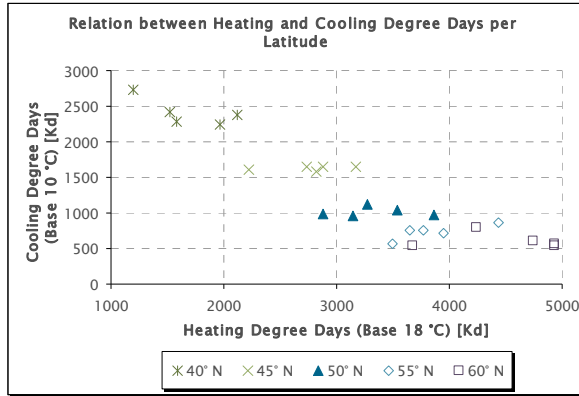


Fig. 21: Correlation between Heating and Cooling Degree Days.

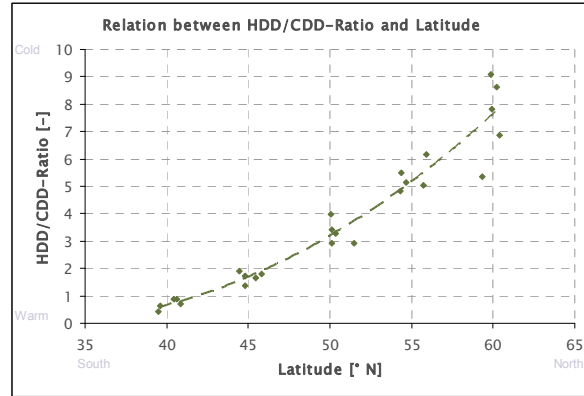


Fig. 22: Ratio between Heating and Cooling Degree Days as Function of Latitude.

6.6.2. Global Radiation and Illumination

As described in chapter 6.5.4, the annual total illumination is strongly dependant on global radiation. Therefore both terms are mainly dependant on the sun path (angle of incidence and length of days) and the weather conditions (especially cloudiness).

The sun path and correspondingly the daylight hours vary depending on the latitude of a location, with seasonal differences increasing from South to North (at the equator the daylight hours are constant all over the year). Fig. 23 shows these correlations for the annual mean daylight hours as well as for the daylight hours in June and December, comprising the longest and shortest days of the year. It can be seen, that northern locations generally have more daylight hours in summer, but less daylight hours in winter, compared to southern locations. Despite these seasonal differences, the annual mean number of daylight hours is almost the same in all locations.

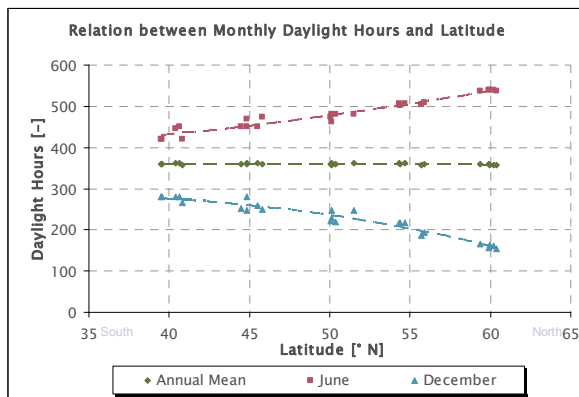


Fig. 23: Relation between Daylight Hours and Latitude.

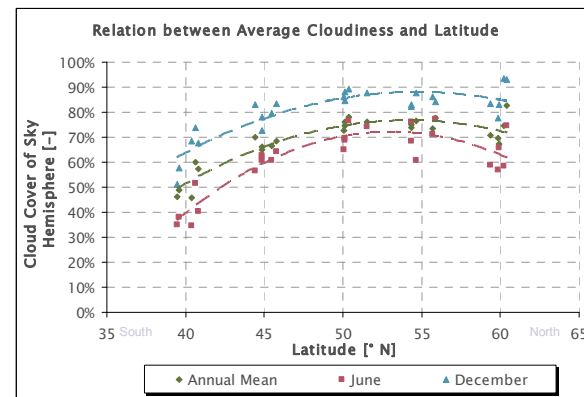


Fig. 24: Relation between Average Cloudiness and Latitude.

The correlation of the average cloudiness (described by the fraction of the sky hemisphere covered with clouds) with the latitude is shown in Fig. 24. Despite a significant variance of the results due to local influences, an increasing trend from South to North can be observed. The slight decrease north of 55 °N might be an accidental result of the selected locations. Further investigations using a larger number of locations could clarify this issue, but have not been carried out in this work.

The impacts of daylight hours and cloudiness on the resulting illumination has been exemplified in Fig. 25: Despite the fewer daylight hours in winter, Madrid (40 °N) has much higher illumination than Bergen (60 °N) during all months of the year. This is a result of lower cloudiness in Madrid (annual average: 45%) than in Bergen (82,5%). The resulting annual average illumination, calculated per daylight hours, in Madrid is more than twice as high as in Bergen. This shows that regardless the different length of days, the daylight hours in the South are much brighter than in the North.

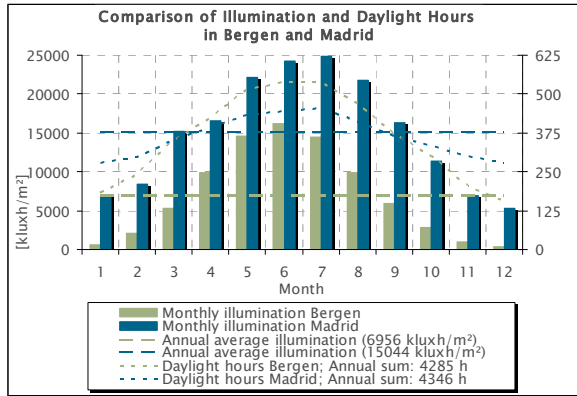


Fig. 25: Monthly and Annual Average Illumination in Bergen and Madrid.

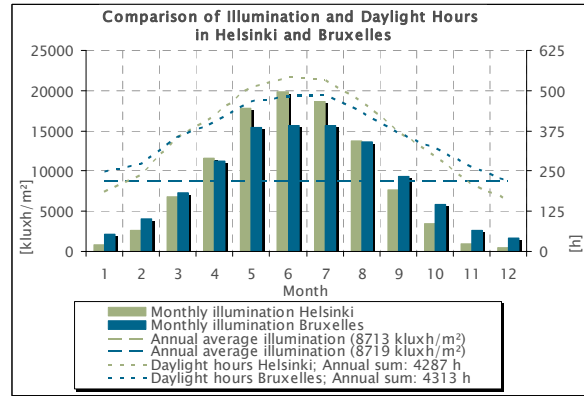


Fig. 26: Monthly and Annual Average Illumination in Helsinki and Bruxelles.

In some cases, this general coherence can be dominated by local influences like cloudiness. Fig. 26 exemplifies the monthly illumination in Helsinki (60 °N) and Bruxelles (50 °N), where again the more northern location (Helsinki) has fewer daylight hours in winter and more in summer. But contrary to the general tendency, here the more southern location (Bruxelles) has a higher average cloudiness than Helsinki (Helsinki: 74,5%; Bruxelles: 77,9%). Therefore, the illumination in Helsinki is lower in winter and higher in summer, compared to Bruxelles, resulting in almost the same annual average illumination per daylight hours.

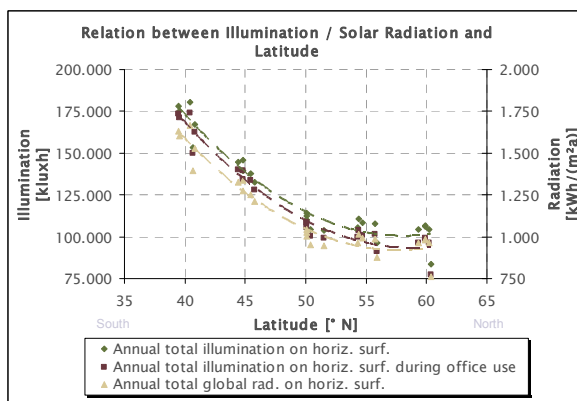


Fig. 27: Global Radiation and Total Illumination on Horizontal Surface as Functions of Latitude.

Despite these local influences both the global radiation and the total illumination on horizontal surface show a good correlation to the latitude, decreasing from South to North (see Fig. 27).

Calculating the annual total illumination for an assumed office use from 8 to 18 hours, a slight difference compared to the overall illumination can be observed in Fig. 27. But as this difference was only minor and the correlation almost proportional it was decided to use the overall annual illumination as more general climatic term for the illumination.

6.6.3. Degree Days and Illumination

Since the outside illumination and the outside air temperature both significantly depend on the solar radiation, an almost linear correlation between the total annual illumination and the cooling degree days of a location can be observed (Fig. 28). Therefore, a correlation between the HDD/CDD-ratio and the annual illumination can be found as well (Fig. 29). A rough distinction between “warm and bright” locations on the one hand and “cold and dark” locations on the other hand can be made.

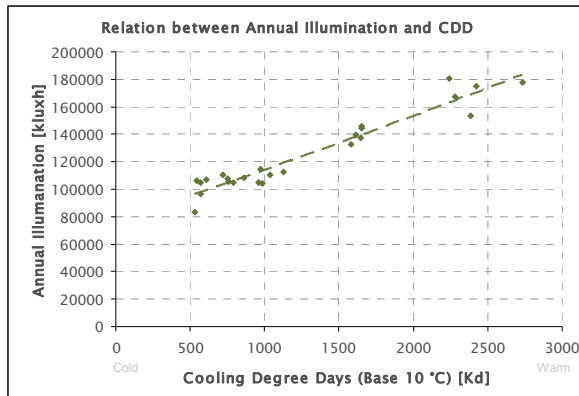


Fig. 28: Total Annual Illumination as Function of Cooling Degree Days.

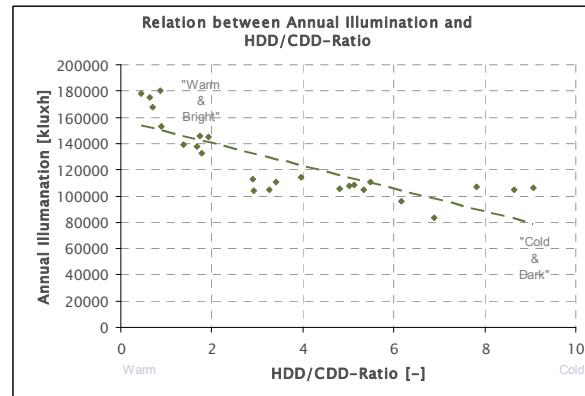


Fig. 29: Correlation between Heating/Cooling Degree Days Ratio and the Annual Illumination.

7. Methodology for Calculation of Resulting Energy Demand

7.1. General

The calculations of energy demand in this work have been carried out using the transient system simulation program TRNSYS (version 16.01.0003), developed by the Solar Energy Laboratory at the University of Wisconsin-Madison, USA. This program allows the dynamic simulation of multi-zone-buildings and their technical systems taking into account all physical phenomena (heat transfer, heat storage etc.) and internal or external influences (weather conditions, thermal loads from solar radiation, technical equipment, user behaviour, artificial lights, control strategies etc.).

All calculations comprised the period of one year in time steps of one hour (i.e. 8.760 hours per simulation run). Statistical weather data on an hourly basis have been obtained from the software Meteonorm (see chapter 6.1).

Inputs for the calculation of the energy demand for artificial lighting have been obtained from Relux-Vision, a software program using the “Radiance” kernel for the precise calculation of daylight and artificial light in buildings.

The post-processing of the obtained results has been done using Microsoft Excel.

As a matter of principle, the precise energetic simulation of buildings requires a lot of inputs, many of which have to be defined or assumed in case of notional buildings. This usually leads to the definition of one specific situation, whose results can not necessarily be transferred to other situations. At the same time, the influences on energy performance of buildings are too complex to consider all possible combinations of parameters, so parameters have to be chosen representing combinations as common as possible.

Therefore it had to be decided which parameters of the simulation will be varied and which will have to be fixed with values representing a building as typical as possible. In doing so the question “what is typical in different parts of Europe” was an important challenge. This challenge could be met on the one hand by using findings from previous studies and references, on the other hand by performing separate parameter studies which led to substantiated assumptions.

7.2. Standard Building Model

The calculations in this work have been carried out using a standard single office room based on previous studies (such as [Müller], [Preißler] and [BBR]). The room has a floor area of 2,50 m x 4,45 m (i.e. 11,125 m²). Between the raised floor and the concrete ceiling a clear height of 3,00 m leads to a volume of 33,375 m³. The side walls and the rear wall are made from plasterboard; the façade is made of transparent and opaque elements with different thermal qualities. Fig. 30 shows a visualisation of the room with exemplary furniture.



Fig. 30: Relux-Visualisation of Standard Office Room (here: with a Band Façade).

The room is occupied by one person with a computer and a printer. The occupancy period has been assumed from 8 to 18 h.

The outside air infiltration due to leakages has been assumed with an air change rate of $0,2 \text{ h}^{-1}$. During the occupancy an additional ventilation air change rate of $1,395 \text{ h}^{-1}$ has been assumed in dependence on [EN 15251]. A heat recovery from exhaust air has been considered with an average efficiency of 50%.

Heating and cooling devices have been assumed to have unlimited power, in order to achieve the net energy demand of the room as a simulation result. The indoor air temperatures have been kept between 22 °C and $24,5 \text{ °C}$ according to the recommendations for energy calculations given in [EN 15251].

The room is artificially lit by fluorescent lights (13 W/m^2) providing a total of 500 lux on the desk level. To avoid unnecessary energy demand, the lights are self-dimming depending on the daylight availability in the room.

The windows are equipped with both an internal blind screen to prevent glare and an external venetian blind to prevent overheating from solar radiation. Both systems have been controlled according to the radiation on the façade and to the outside air temperatures. The venetian blind has been operated in two levels: A cut-off position of the lamella (45° , preventing transmission of direct radiation but still allowing for diffuse light to enter the room) and a fully closed position (10° , with maximum sun protection).

The control strategies of internal and external blinds represent a combination of an automatically controlled (or ideal user controlled) external sun shading system and a user-controlled internal blind screen, preventing direct radiation to enter the room at any time. Therefore, the daylight availability inside the room could be estimated using the outside illumination and the daylight factor (defined for overcast sky conditions). Therefore the effects of the internal and external blinds on the availability of daylight and the resulting requirement of artificial light with its thermal effects could be taken into account in each hourly time step of the simulation.

All net energy demands obtained from the building simulation have been calculated to primary energy demand, i.e. including losses resulting from extraction, conversion and transport of energy to the building as well as losses from provision and distribution of energy in the building (see chapter 3). Therefore, standard values for the efficiency of technical systems (gas heater, compression chiller etc.) and primary energy factors from [DIN V 18599-1] have been used.

The calculations of energy demand have been carried out using this standard room in the four main orientations North, East, South and West. In this work mainly com-

bined results from an arithmetic mean of the four orientations are presented (if not stated otherwise).

Further details can be obtained from the appendix of this work.

7.3. Findings from Previous Studies

Some of the building parameters in this work have been defined based on the findings from the detailed parameter analysis of [Preißler]: There, the following parameters have been varied in five equidistant steps of a given bandwidth (according to products usual in the market or according to standard requirements):

- Effective ventilation rate (i.e. including impacts of heat recovery)
- Heat transmission (U-value) of the façade
- Window proportion
- Shading factor (efficiency of variable shading systems)
- Solar heat gain coefficient (SHGC) of the glazing
- Light transmission factor of the glazing (τ -value)

Together with an analysis in the four main orientations (North, East, South, West), this led to the simulation of more than 15.000 possible façade configurations for a single office room. For each of these simulations the total primary energy demand has been calculated and the influence of the individual parameters as well as their combined influences have been analysed. Therefore, the total primary energy demand has been analysed as a function of two parameters. From the level, slope and shape of the resulting surface a standardised gradient could be calculated, representing the relative degree of influence of the two parameters from its direction and length (Fig. 31).

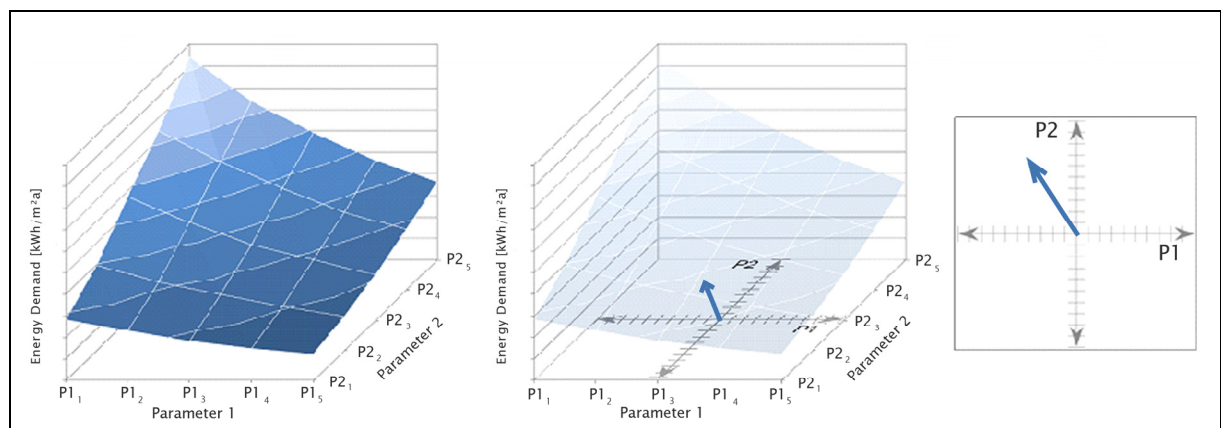


Fig. 31: Principle of Analysing the Combined Influences of Parameters by Deduction of Standardised Gradients in [Preißler].

The generally large bandwidth of the results showed the strong influence of the building envelope on the total energy performance of a building. Comparing the parameters' degree of influence, a ranking of relevance could be established which is represented by the above-given order of parameters (i.e. highest relevance: Ventilation rate; lowest relevance: τ -value), whereas window proportion and shading factor were on the same level.

Furthermore it was discovered that almost equally good results can be obtained from different parameter combinations. Nevertheless, looking at the best results (“Top10”) some increased frequencies could be detected:

- The window proportion of the Top10-results has been most often 65% (band façade) with a maximum deviation of one parameter step below (47,5%) or above (82,5%).
- The shading factor of the Top10-results was always the one with the highest efficiency (reduction of solar transmission by 75%, i.e. to 25%).
- Low SHGC values among the Top10-results always correlated with high τ -values, so sun protection glazing should have a high selectivity.

From these findings the following decisions have been deduced for this work:

- The effective ventilation rate has a strong influence on the primary energy demand, but is mainly depending on the type of building use, the occupancy and the technical systems. Therefore it will be considered fixed in this work (see chapter 7.2).
- The U-value and the window proportion of the façade have strong influence as well. Therefore they will be considered in detail in this work.
- Shading systems with high efficiency have shown to be crucial for optimised results. Therefore, an external shading system (venetian blinds) will be considered in all simulations in this work (see chapter 7.2).
- The SHGC and the τ -value have less influence. Therefore they will be considered as combinations of U-value, SHGC and τ -value, which are usual in the market (taking into account high selectivity for sun protection glazing).

The resulting parameters “U-Value”, “window proportion” and “sun protection characteristic” were considered to differ within the European scale. Therefore two different analyses have been performed, in order to obtain a bandwidth of results:

- Definition of “typical” buildings with statistically relevant parameter values for each location
- Definition of “optimised” buildings using the methodology described in [Preißler], representing a solution for minimised primary energy demand for each location.

For the definition of optimised buildings an energetic parameterisation was crucial to perform a respective variation of parameters.

7.4. Energetic Parameterisation

7.4.1. Methodology

Based on the findings in [Preißler] and the deduced decisions described in chapter 7.3, the parameters “window proportion”, “U-value” and “sun protection characteristic” have been considered in detail in this work.

By performing a study on these three parameters, the resulting primary energy demand could be analysed for each possible combination and the best solution (i.e. with the lowest primary energy demand) could be found.

The window proportion and the U-value have been varied in five equidistant steps within a bandwidth usual in the market.

The insulation level has been varied in five steps. U-Values of glazing, window frames and opaque façade elements have been adjusted proportionally.

The window proportion has been varied between 30% and 100%. The frame proportion has been adjusted proportionally. Following technical limitations, U-Value, SHGC and light transmission factor (τ) of glazing are interdependent. Therefore, each glazing per insulation level will be analysed as a normal and as a sun protection glazing usual in the market (i.e. 10 glazing types). Light transmission will be considered depending on glazing type whereas high selectivity of sun protection glazing will be assumed as far as usual and available in the market.

This led to a number of 250 annual simulation runs per each of the 25 location, each with results for the four main orientations. To reduce the amount of data, the parameter variations have been performed for only five locations considered representative (see chapter 7.5) for each group of latitude. The results of each of these five locations then have been applied to the other locations in the same group.

7.4.2. Definition of Parameter Values

7.4.2.1. Window Proportion „w“

In this work the window proportion “w” has been defined as

w = Proportion of window area (including frame) of the wall area.

The minimum for w has been defined to 30%. This meets the requirements of window sizes according to [DIN 5034-1] in order to ensure a minimum of daylight in the room, to guarantee a view to the outside etc. The maximum for w was 100%, representing a fully glazed façade. The equidistant partition of this bandwidth in five steps leads to values of 30,0 / 47,5 / 65,0 / 82,5 / 100 %

Based on the wall area of 2,5 m x 3,0 m = 7,5m² and a maximum parapet height of 0,80 m the window dimensions for w = 30% have been defined as

- One window, horizontally centred, reaching from 80cm above floor level to the ceiling (i.e. height of 2,20 m, resulting width for w=30% is 1,02 m)






The following window proportions have been developed according to the following order of criteria:

- From w=47,5%: Two windows of same dimensions, equally distributed in horizontal direction
- Window width increasing up to 2,50 m
- After a width of 2,50 m is reached, the window height increases up to 3,00 m.

This led to the window dimensions shown in Tab. 1. For information the aperture proportions (Def.: Relation between window area and floor area of the room) of the five window proportions have been listed as well.

For the precise analysis the fraction of glazing and frame had to be known as well. Therefore the frame proportion “f” (Def.: Proportion of Frame area of the window area) had to be calculated. As the width of the frames is considered to always be 10 cm, the frame proportion of the window area can be calculated from the window dimensions and can also be found in Tab. 1.

Tab. 1: Visualisations and Dimensions of different Window Proportions.

	w1	w2	w3	w4	w5
Visualisation					
Window proportion [%]	30,0	47,5	65,0	82,5	100,0
Aperture proportion [%]	20,2	32,0	43,8	55,6	67,4
Window area [m²]	2,250	3,563	4,875	6,188	7,500
Wall area [m²]	5,250	3,938	2,625	1,313	0,000
Window height [m]	2,200	2,200	2,200	2,475	3,000
Window width [m]	1,023	1,619	2,216	2,500	2,500
Frame area [m²]	0,605	0,724	0,843	0,955	1,060
Frame proportion [%]	26,9	20,3	17,3	15,4	14,1

7.4.2.2. Insulation Levels “U”

7.4.2.2.1. *General*

Five levels of insulation (U1 to U5) have been defined. Therefore, within a range of products usual in the market, five glazing types with different levels of insulation have been defined first.

Based on the U-values of these glazings, the U-values of the window frames and the opaque wall partitions then have been selected accordingly within a range of appropriate maximum and minimum values.

The mean façade-U-values could then be calculated according to the area ratios listed in Tab. 1.

7.4.2.2.2. *U-Value of Glazing „U_g“*

Within the five insulation levels, glazing has been defined, covering the range from a single glazing over double glazing with heat protection sheets and Argon gas filling up to a 3-layer glazing with krypton gas filling. Each of these glazing types were considered with and without a sun protection sheet (low-emission layer), resulting in ten different glazing types overall.

For identification purposes each glazing type has been given a unique WinID which will be used further on in this work. Here, the last figure represents the SHGC level (1: without sun protection layer, 2: with sun protection layer), the last but one figure represents the insulation level. The characteristics of the ten different glazing types are shown in Tab. 2.

Tab. 2: Characteristics of Selected Glazing Types.

Insulation level	WinID	Description	Design	U _g	SHGC	τ	Mean U-value	
							U _g	Distr.
				[W/(m ² K)]	[-]	[-]	[W/(m ² K)]	[%]
U1	1011	Single glass	6	5,73	0,85	0,896	5,735	100%
	1012	Single glass sun protection	6	5,74	0,453	0,752		
U2	1021	Double glass heat protection, Air	4/16/4	2,92	0,77	0,820	2,910	45%
	1022	Double glass sun protection, Air	6/16/4	2,90	0,391	0,681		
U3	1031	Double glass heat protection, Ar	4/16/4	1,40	0,60	0,799	1,375	14%
	1032	Double glass sun protection, Ar	6/16/4	1,35	0,373	0,677		
U4	1041	Triple glass heat protection, Ar	4/8/4/8/4	1,03	0,47	0,710	1,020	7%
	1042	Triple glass sun protection, Ar	4/8/4/8/4	1,01	0,34	0,601		
U5	1051	Triple glass heat protection, Kr	4/8/4/8/4	0,65	0,47	0,709	0,640	0%
	1052	Triple glass sun protection, Kr	4/8/4/8/4	0,63	0,335	0,600		

Due to slight differences between the glazing types within one insulation level, a mean U-value of the glazing types had to be calculated per insulation level. These mean values have been expressed as percentages within their range between min (0%) and max (100%).

7.4.2.2.3. *U-Value of Frame „U_f“*

Based on the distribution of the mean U_g-values (100 / 45 / 14 / 7 / 0 %) within their given bandwidth, the frame U-values U_f have been distributed accordingly. The upper and lower limit of frames usual in the market have been represented by maximum (metal frame without thermal separation) and minimum (wood/aluminium/foam composite frame) U_f-values. The resulting U_f-values are shown in Tab. 3 and Fig. 32.

Tab. 3: U_f-Values of Frames

Insulation level	Glazing (Mean value)	Distribution	Frame
	[W/(m ² K)]	[%]	[W/(m ² K)]
U1	5,735	100%	7,000
U2	2,91	45%	3,562
U3	1,375	14%	1,694
U4	1,02	7%	1,262
U5	0,64	0%	0,800

7.4.2.2.4. U-Value of Opaque Parts „U_{Wall}“

The U_{Wall}-values of the opaque parts of the façade (i.e. of parapets and the wall elements on both sides of the windows, if applicable) have been defined in the same way, i.e. based on the distribution of the mean U_g-values.

The range extends from a wall with almost no insulation (equal to a non-insulated concrete wall of 25 cm thickness) to a highly insulated wall (for example a sandwich panel with 40 cm of insulation (thermal conductivity of 0,040 W/(mK) or a respective multilayer wall).

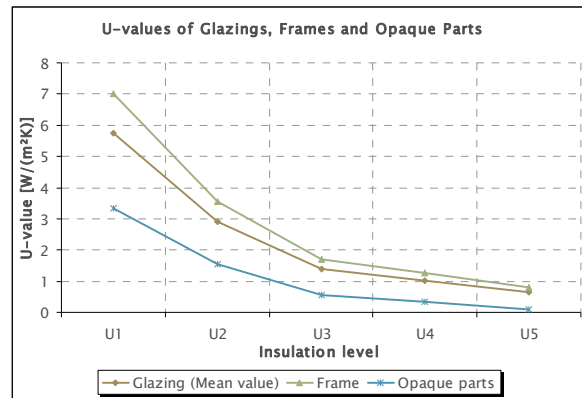


Fig. 32: U-Values of Glazing Types, Frames and Opaque Parts Depending on Insulation Level.

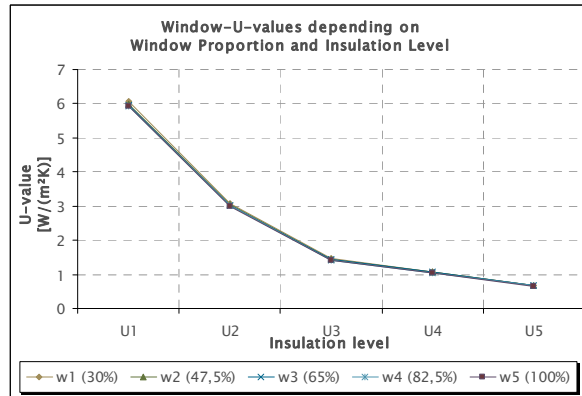
Fig. 32 shows the U-values of glazing types, frames and opaque parts of the façade

Tab. 4: U_{Wall}-Values of Opaque Parts of the Façade.

Insulation level	Glazing (Mean value)	Distribution	Opaque parts
	[W/(m ² K)]	[%]	[W/(m ² K)]
U1	5,735	100%	3,349
U2	2,91	45%	1,545
U3	1,375	14%	0,565
U4	1,02	7%	0,339
U5	0,64	0%	0,096

7.4.2.2.5. Resulting U-Values of Windows „ U_W “

As the frame proportions of the windows vary slightly with the window proportions of the façade, the U-values of the windows have to be calculated separately for each window proportion by assessing the U-values of the glazing types and the frames. Here, this has been done in a simplified way for information only, not taking into account the thermal edge bond of the glazing. In the simulation this is taken into account in detail.



The resulting U-values of the windows are shown in Tab. 5 and Fig. 33.

Fig. 33: Window U-Values depending on Window Proportion and Insulation Level.

Tab. 5: Window U-Values depending on Window Proportion and Insulation Level.

Window U-values		U1	U2	U3	U4	U5
		[W/(m²K)]	[W/(m²K)]	[W/(m²K)]	[W/(m²K)]	[W/(m²K)]
Glazing U-Value		5,735	2,91	1,375	1,02	0,64
Frame U-Value		7,000	3,562	1,694	1,262	0,800
Window prop.	Frame prop					
w1 (30,0%)	26,9%	6,075	3,085	1,461	1,085	0,683
w2 (47,5%)	20,3%	5,992	3,043	1,440	1,069	0,673
w3 (65,0%)	17,3%	5,954	3,023	1,430	1,062	0,668
w4 (82,5%)	15,4%	5,930	3,011	1,424	1,057	0,665
w5 (100%)	14,1%	5,914	3,002	1,420	1,054	0,663

7.4.2.2.6. Resulting U-Values of Façades „ $U_{Façade}$ “

As the U-values of the windows vary with the window proportions of the façade, the U-values of the façade have to be calculated separately for each window proportion by assessing the U-values of the windows and the opaque parts.

The resulting façade U-values are shown in Tab. 6 and Fig. 34

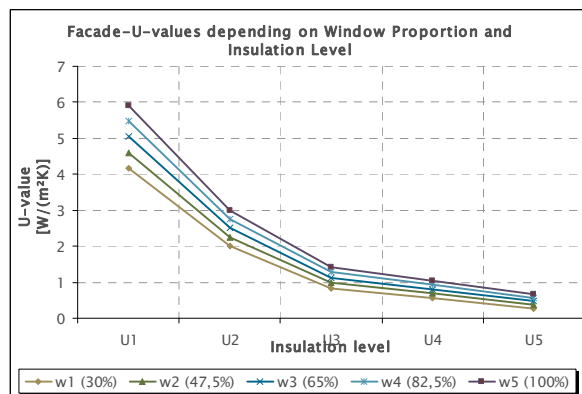


Fig. 34: Façade U-Values depending on Window Proportion and Insulation Level.

Tab. 6: Façade U-Values depending on Window Proportion and Insulation Level.

Façade U-Values	U1	U2	U3	U4	U5
	[W/(m ² K)]	[W/(m ² K)]	[W/(m ² K)]	[W/(m ² K)]	[W/(m ² K)]
w1 (30,0%)	4,121	1,937	0,922	0,465	0,226
w2 (47,5%)	4,525	2,155	1,048	0,551	0,290
w3 (65,0%)	4,929	2,373	1,174	0,637	0,355
w4 (82,5%)	5,332	2,590	1,300	0,722	0,419
w5 (100,0%)	5,733	2,806	1,425	0,807	0,482

7.4.2.3. Solar Heat Gain Coefficient (SHGC) and Light Transmission (τ)

To take into account the influence of the SHGC, each of the glazing selected per insulation level has been analysed as a solar protection glazing as well.

The effects of the sun protection function on the light transmission have been factored with high selectivity of the glazing types, i.e. providing as much light transmission as possible despite low solar transmission (see Tab. 2).

7.4.3. Resulting Daylight Factors

For each window proportion and each glazing type a distribution of the daylight factor (Def.: ratio between outside illuminance on horizontal surface and inside illuminance on desk level at diffuse sky conditions) in the room had to be calculated. From the distribution of the daylight factor in the room (without furniture, see Fig. 35) an average value has been calculated.

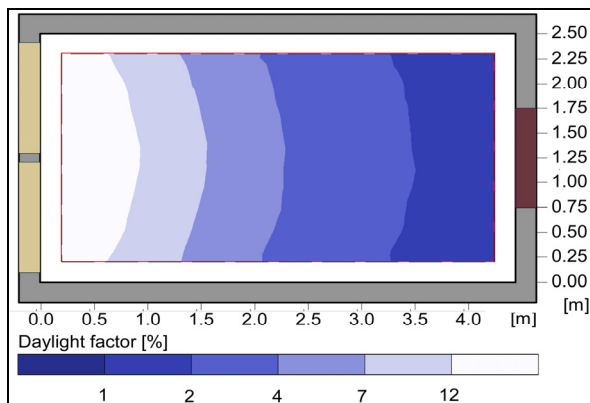


Fig. 35: Exemplary Distribution of Daylight Factor (w3=65%, WinID=1031).

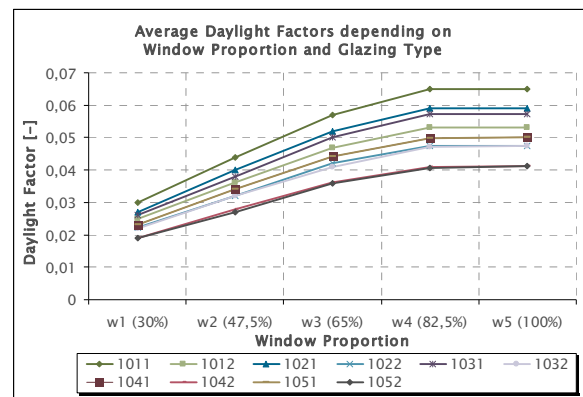


Fig. 36: Average Daylight Factors depending on Window Proportion and Glazing Type.

Depending on the window geometries (see Tab. 1) of the five window proportions and the light transmission (τ) of the 10 glazing types (see Tab. 2) the average daylight factors shown in Fig. 36 have been calculated.

An almost linear relation between window proportion and daylight factor can be observed from window proportions of 30% to 65%. Higher window proportions result in a smaller increase of the daylight factor (especially between w4 and w5, where the increasing window proportion results from additional glazing below the desk level).

Fig. 37 shows exemplary visualisations of the daylight situation inside the office at diffuse sky conditions with the five different window proportions (here: heat protection glazing WinID1031).

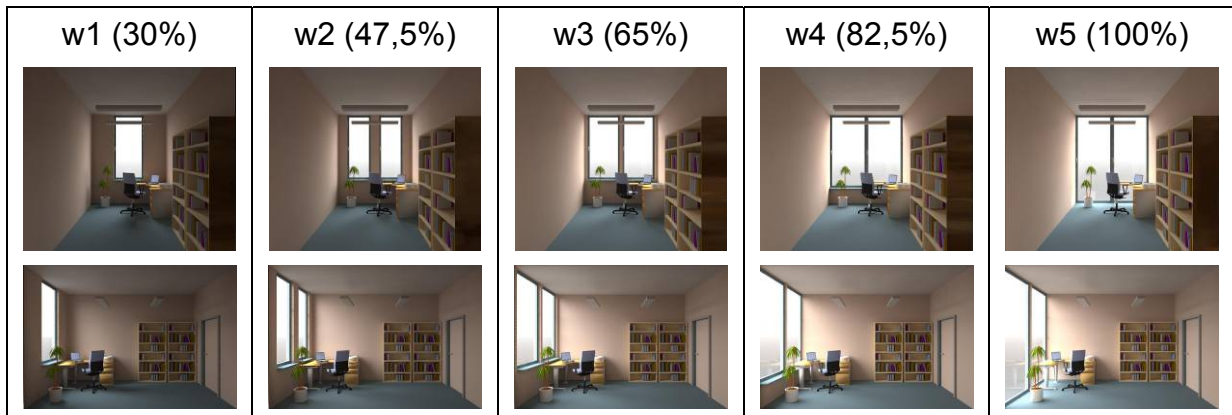


Fig. 37: Exemplary Visualisation of Daylight Situation inside the Office at Diffuse Sky Conditions.

7.5. Definition of “Typical” Buildings

The level of insulation of a building in reality depends on several factors such as cost efficiency, insulation requirements from national standards or building traditions. Therefore, typical U-values of the façade have been obtained from [EnPer-TEBuC]. In this study the U-values for the building envelope have been analysed for different European countries. The U-values gathered therein are not required by the respective national regulations, but normally applied to meet the energy performance requirements. Fig. 38 shows the results of this analysis for the European countries considered therein. It was determined, that as a result of climatic conditions and much stricter requirements affecting applied components, the insulation level tends to be higher (i.e. lower U-values) in northern countries than in southern countries of Europe.

Typical U-Values [W/(m²K)]	Roofs						Outer Walls						Ground Floor						Windows				
	0.15	0.25	0.35	0.45	0.55	0.65	0.15	0.25	0.35	0.45	0.55	0.65	0.15	0.25	0.35	0.45	0.55	0.65	1.25	1.75	2.25	2.75	3.25
Sweden	█						█						█						█				
Norway								█															
Finland								█															
Denmark								█															
Lithuania									█														
Ireland										█													
Russian Federation											█												
United Kingdom												█											
Netherlands													█										
Austria																							
Germany																							
Switzerland																							
France																							
Belgium																							
Italy																							
Portugal																							
Spain																							

Fig. 38: Typical U-values in European Countries [EnPer-TEBuC].

Based on these U-values for the outer walls and windows, typical façade U-values could be calculated. This has been done uniformly for a window proportion of 65% (w3) representing an average value and a very common façade type for office buildings at the same time.

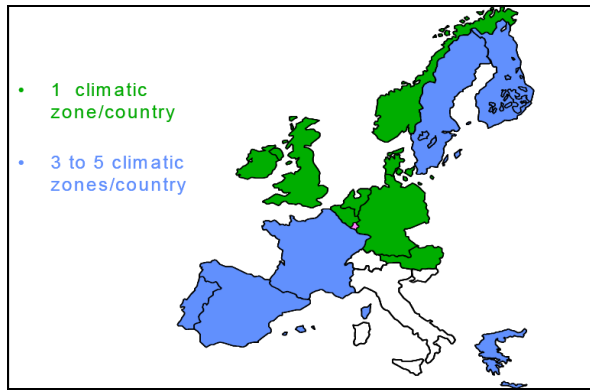
To homogenise the boundary conditions and to improve the comparability of the results of typical and optimised buildings, the resulting façade U-values have been allocated to the five insulation levels defined in chapter 7.4.2.2. As a result of the bandwidths given for some countries in Fig. 38, the façade U-values sometimes had to be assigned to a bandwidth of insulation levels as well (see Tab. 7).

Tab. 7: Assignment of Typical U-Values in EU-Countries to Insulation Levels.

Country	Outer walls		Windows		Façade (w=65%)		Insulation level	
	from	to	from	to	from	to	from	to
Sweden	0,15		1,25		0,865		U4	
Norway	0,25		1,25		0,9		U4	
Finland	0,25		1,75		1,225		U3	
Denmark	0,25		1,25	1,75	0,9	1,225	U4	U3
Lithuania	0,25		1,75	2,25	1,225	1,55	U3	
Ireland	0,25		1,75	2,25	1,225	1,55	U3	
Russian Federation	0,15		1,75	3,25	1,19	2,165	U3	U2
United Kingdom	0,35		1,75	2,25	1,26	1,585	U3	
Netherlands	0,25	0,35	1,75	2,25	1,225	1,585	U3	
Austria	0,35		1,25		0,935		U4	
Germany	0,55		1,25		1,005		U3	
Switzerland	0,35		1,25		0,935		U4	
France	0,45		1,75	2,25	1,295	1,62	U3	
Belgium	0,55		1,75	2,25	1,33	1,655	U3	
Italy	0,45		2,75	3,25	1,945	2,27	U2	
Portugal	0,65		2,25	2,75	1,69	2,015	U3	U2
Spain	0,65		2,75	3,25	2,015	2,34	U2	

The countries considered in [EnPer-TEBuC] have been grouped according to their climatic variety into two groups (one or multiple climatic zones per country) as shown in Fig. 39.

From the assignments shown in Tab. 7 insulation levels for typical buildings could be defined for the 25 selected locations in this work. Where bandwidths of insulation levels resulted from the data obtained from [EnPer-TEBuC] and the respective country had been classified in Fig. 39 to have multiple climatic zones per country, the upper or lower insulation level has been selected according to the position of the location within the respective country (higher insulation level for northern locations and vice versa).



For countries where no insulation levels could be deducted from [EnPer-TEBuC], assumptions have been made correlating with the insulation levels resulting for other locations in the same group of latitude.

All typical buildings have been assumed to have heat protection glazing. The resulting parameter definitions are listed in Tab. 8.

Fig. 39: Number of Climatic Zones in European Countries according to [EnPer-TEBuC].

Tab. 8: Definition of Window Proportions, Insulation Levels and Glazing Types for Typical Buildings.

Group of Latitude	Location Number	Location Name	Window Proportion	Insulation Level	WinID / Glazing Type
60 ° N	01	Bergen (N)	w3 (65,0%)	U4	1041 (Heat protection)
	02	Oslo (N)	w3 (65,0%)	U4	1041 (Heat protection)
	03	Uppsala (S)	w3 (65,0%)	U4	1041 (Heat protection)
	04	Stockholm (S)	w3 (65,0%)	U4	1041 (Heat protection)
	05	Helsinki (FIN)	w3 (65,0%)	U3	1031 (Heat protection)
55 ° N	06	Glasgow (GB)	w3 (65,0%)	U3	1031 (Heat protection)
	07	Kiel (D)	w3 (65,0%)	U3	1031 (Heat protection)
	08	Kobenhavn (DK)	w3 (65,0%)	U3	1031 (Heat protection)
	09	Gdansk (PL)	w3 (65,0%)	U3	1031 (Heat protection)
	10	Vilnius (LT)	w3 (65,0%)	U3	1031 (Heat protection)
50 ° N	11	London (GB)	w3 (65,0%)	U3	1031 (Heat protection)
	12	Bruxelles (B)	w3 (65,0%)	U3	1031 (Heat protection)
	13	Frankfurt/Main (D)	w3 (65,0%)	U3	1031 (Heat protection)
	14	Praha (CZ)	w3 (65,0%)	U3	1031 (Heat protection)
	15	Krakow (PL)	w3 (65,0%)	U3	1031 (Heat protection)
45 ° N	16	Bordeaux (F)	w3 (65,0%)	U3	1031 (Heat protection)
	17	Milano (I)	w3 (65,0%)	U2	1021 (Heat protection)
	18	Zagreb (HR)	w3 (65,0%)	U3	1031 (Heat protection)
	19	Beograd (SRB)	w3 (65,0%)	U3	1031 (Heat protection)
	20	Bucuresti (RO)	w3 (65,0%)	U3	1031 (Heat protection)
40 ° N	21	Madrid (E)	w3 (65,0%)	U2	1021 (Heat protection)
	22	Valencia (E)	w3 (65,0%)	U2	1021 (Heat protection)
	23	Palma de Mallorca (E)	w3 (65,0%)	U2	1021 (Heat protection)
	24	Napoli (I)	w3 (65,0%)	U2	1021 (Heat protection)
	25	Salonika (GR)	w3 (65,0%)	U2	1021 (Heat protection)

7.6. Definition of “Optimised” Buildings

7.6.1. General

From the inhomogeneous insulation levels in European countries, resulting from the differences in national regulations, building traditions etc. (see chapter 7.5), a poor correlation between climatic conditions and the building energy demand at different locations could be expected. Therefore, an optimised building has been defined using the methodology described in chapter 7.4.1.

This methodology by principle creates a remarkable quantity of data which would have to be post-processed and concentrated after the simulation. Based on the good correlations found in chapter 6.6 it was decided that the optimisation does not have to be done for each of the 25 selected locations separately. Instead, the optimisation has been carried out in one representative location per group of latitude, which then could be considered representative for the other four locations in the same group.

7.6.2. Definition of Representative Locations

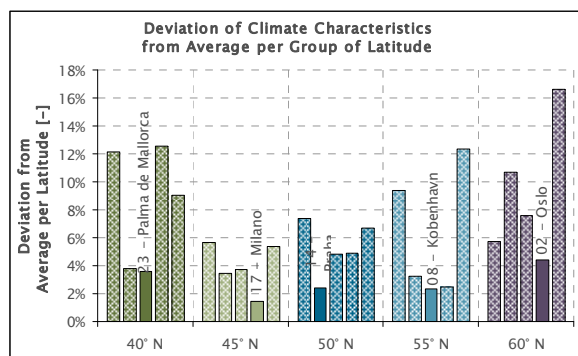


Fig. 40: Selection of Representative Locations per Group of Latitude.

For the selection of representative locations, the climate characteristics relevant for the building energy demand (see chapter 6.4) have been compared within one group of latitude and their deviation from the groups' average has been calculated. From these analyses the locations with the lowest overall deviation have been selected as representatives of their group.

The results of this selection can be found in Fig. 40.

7.6.3. Results of Building Optimisation

The simulation of all possible combinations of the parameters produced a series of results for the primary energy demand for heating, cooling and lighting (ventilation considered constant, see chapter 7.3) for each location. The following diagrams demonstrate the primary energy demand for heating (Fig. 41), cooling (Fig. 42) and lighting (Fig. 43) as well as the total primary energy demand (Fig. 44, including ventilation) for Praha using heat protection glazing. The lowest values per diagram have been marked with a red circle. Reading these diagrams in the different directions of their base axes, the interdependent influences of insulation level and window proportion can be analysed.

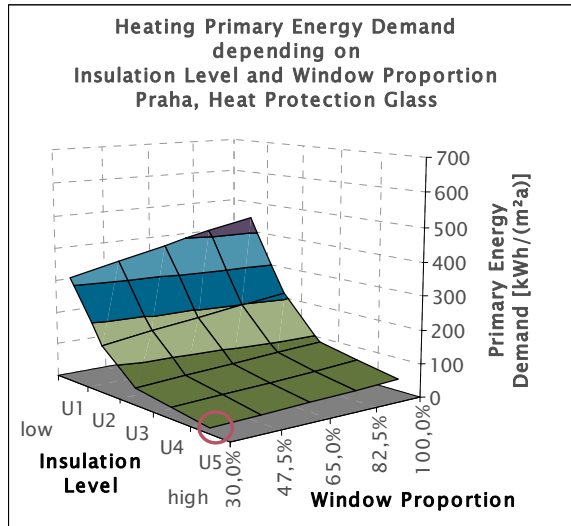


Fig. 41: Heating Primary Energy Demand, Praha, Heat Protection Glass.

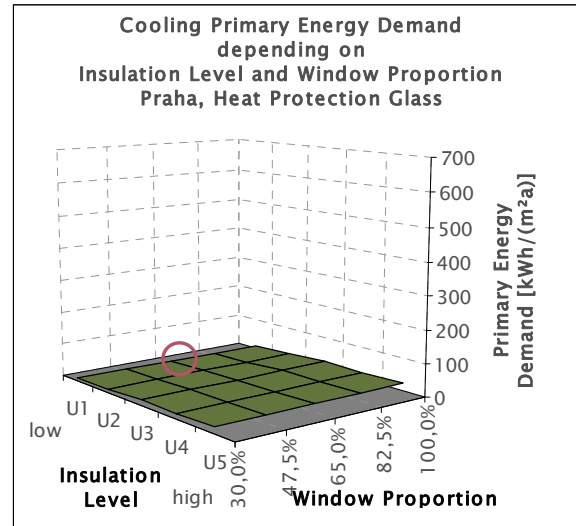


Fig. 42: Cooling Primary Energy Demand, Praha, Heat Protection Glass.

Fig. 41 shows a significant increase of the heating primary energy demand with the reduction of insulation level. Secondly, the heating primary energy demand increases with increasing window proportion, which can be traced to the different U-values of windows and opaque parts. This effect decreases with an increasing insulation level as the particular U-values become similar (see Fig. 34). The lowest heating primary energy demand therefore can be obtained with the lowest window proportion and the highest insulation level.

The cooling primary energy demand shown in Fig. 42 generally is on a much lower level than the heating energy demand. This mainly results from lower CDD than HDD of the location (see Fig. 19 and Fig. 20). As a result of lower solar heat gains, the cooling primary energy demand decreases with decreasing window proportions and generally increases with an increasing insulation level (so-called “heat trap”). This second effect is overcompensated at very low insulation levels by the high SHGC of single glazing. Therefore a slight minimum of cooling primary energy demand could be observed at the lowest insulation level and a window proportion of 65%.

The influence of insulation level and window proportion on the primary energy demand for lighting can be seen in Fig. 43. The increase of light transmission of the glazing types with decreasing insulation levels and the increasing daylight availability from higher window proportions result in a minimum lighting primary energy demand at the highest window proportion and the lowest insulation level.

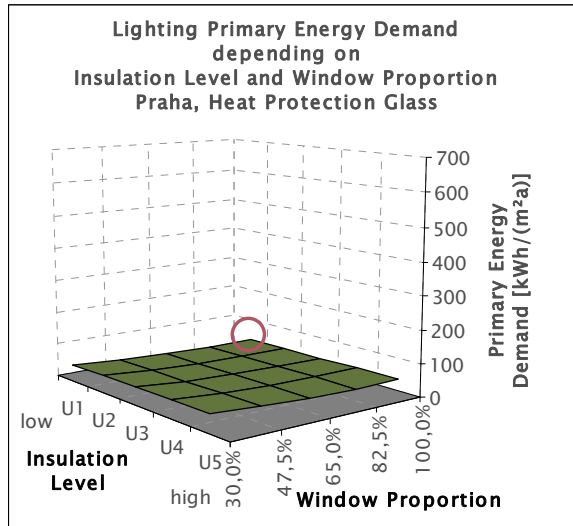


Fig. 43: Lighting Primary Energy Demand, Praha, Heat Protection Glass.

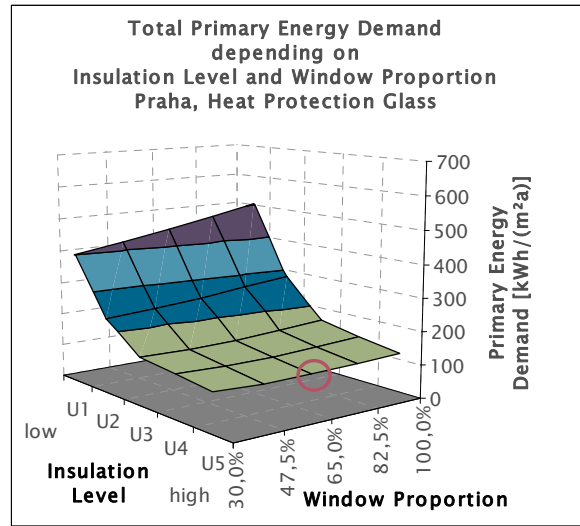


Fig. 44: Total Primary Energy Demand, Praha, Heat Protection Glass.

Summarising these results (also taking into account the constant primary energy demand for ventilation) a domination of the heating energy demand can be observed (Fig. 44). The total primary energy demand increases with decreasing insulation level. At low insulation levels, the total primary energy demand increases with increasing window proportions, at high insulation levels the effect of the cooling energy demand becomes more dominant and leads to slightly lower values at medium window proportions. Therefore the minimum total primary energy demand could be observed at the highest insulation level and a window proportion of 65%.

The same parameter variation with sun protection glazing qualitatively brought the same results. As the direct comparison of Fig. 45 and Fig. 46 shows, both heat and sun protection glazing led to the lowest total primary energy demand at the highest insulation level and a window proportion of 65%.

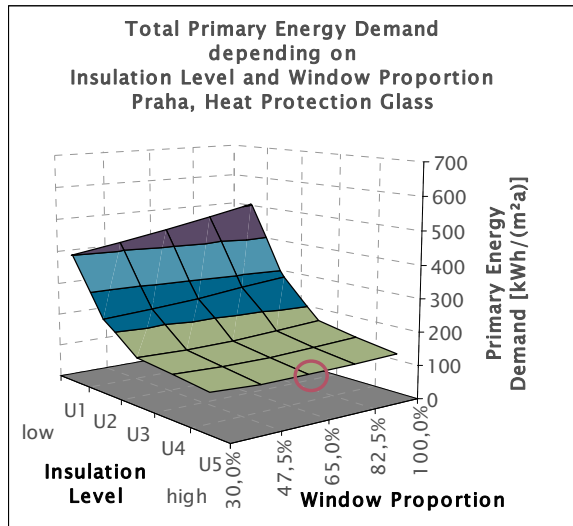


Fig. 45: Total Primary Energy Demand, Praha, Heat Protection Glass.

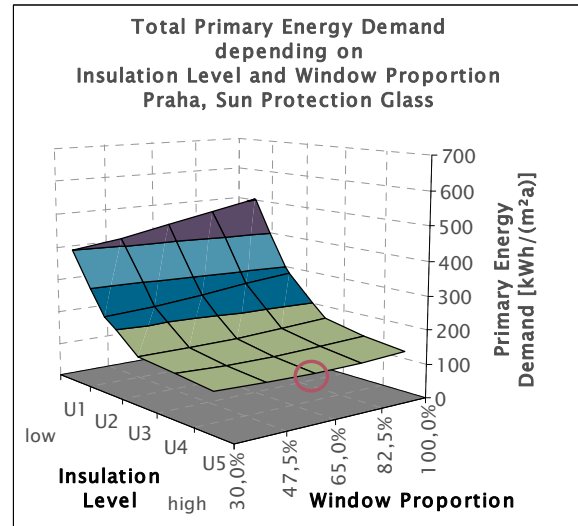


Fig. 46: Total Primary Energy Demand, Praha, Sun Protection Glass.

Furthermore, both results are on comparable levels, at which the minimum of the heat protection glass is slightly lower than the minimum of the sun protection glass. Therefore, in terms of minimum total primary energy demand a high insulated building with 65% window proportion (band façade) and heat protection glazing can be considered optimum for Praha and the other locations in the group of 50 °N latitude.

Repeating this optimisation process for the other four representative locations led to respective results in terms of heating, cooling and lighting. The best parameter combinations for each simulation can be found in Tab. 9.

The detailed analysis of the optimisation results per orientation and the comparison with the average of orientations per location (see Tab. 9) showed only minor differences. In all cases, the lowest total primary energy demand has been achieved with the highest insulation level (U5). Due to the high insulation level, the deviations from the average of orientations are predominantly very low and therefore have low significance in terms of absolute results.

As a result of the slightly lower U-values at low window proportions (see chapter 7.4.2.2.6), there is a slight trend to smaller windows in very cold climates (especially 60 °N) and low solar gains (North offices). By contrast, as a result of lower energy demand for artificial light some South offices (Oslo and Palma de Mallorca) seem to be better with slightly larger windows, whereas the deviation from average is not significant (-0,2% and +0,1%). The advantage of a sun shading glazing in the North office in Palma de Mallorca results from a total primary energy demand 0,12 kWh/(m²a) lower than the heat protection glazing – therefore both solutions can be seen as equivalent.

Tab. 9: Results of Optimisation with lowest Total Primary Energy Demand per Orientation and for Average of Orientations.

Group of Latitude	Location	Orientation	Window-Proportion (w)					Insulation-Level (U)					Glazing Type		Total Primary Energy Demand	
			30%	47,5%	65%	82,5%	100%	U1 (low)	U2	U3	U4	U5 (high)	Heat Protection	Sun Protection	[kWh/(m ² a)]	Deviation from Average
60°N	Oslo	North	x								x	x		112.50	-5.0%	
		East		x							x	x		119.00	0.5%	
		South			x						x	x		118.20	-0.2%	
		West		x							x	x		119.90	1.3%	
		Average		x							x	x		118.40	0.0%	
55°N	London	North		x							x	x		106.30	-2.4%	
		East			x						x	x		108.90	0.0%	
		South			x						x	x		108.10	-0.7%	
		West			x						x	x		110.40	1.4%	
		Average			x						x	x		108.90	0.0%	
50°N	Praha	North		x							x	x		108.85	-1.6%	
		East			x						x	x		109.90	-0.6%	
		South			x						x	x		111.81	1.1%	
		West			x						x	x		110.80	0.2%	
		Average			x						x	x		110.57	0.0%	
45°N	Milano	North			x						x	x		109.20	0.5%	
		East			x						x	x		108.30	-0.4%	
		South			x						x	x		109.10	0.4%	
		West			x						x	x		108.30	-0.4%	
		Average			x						x	x		108.70	0.0%	
40°N	Palma de Mallorca	North			x						x		x	101.70	1.5%	
		East			x						x	x		100.60	0.4%	
		South				x						x	x	100.30	0.1%	
		West			x							x	x	97.81	-2.4%	
		Average			x							x	x	100.20	0.0%	

Accepting the few minimal deviations of some results per orientations from the average of orientations, the building parameters for the further analyses with optimised buildings have been defined according to the average values marked bold in Tab. 9.

Besides the qualitatively similar results for all representative locations, the graphs in Fig. 47 show the quantitative aspect in the European scale. For more detailed consideration, the maximum and minimum total primary energy demands per representative location have been extracted and compared in Fig. 48.

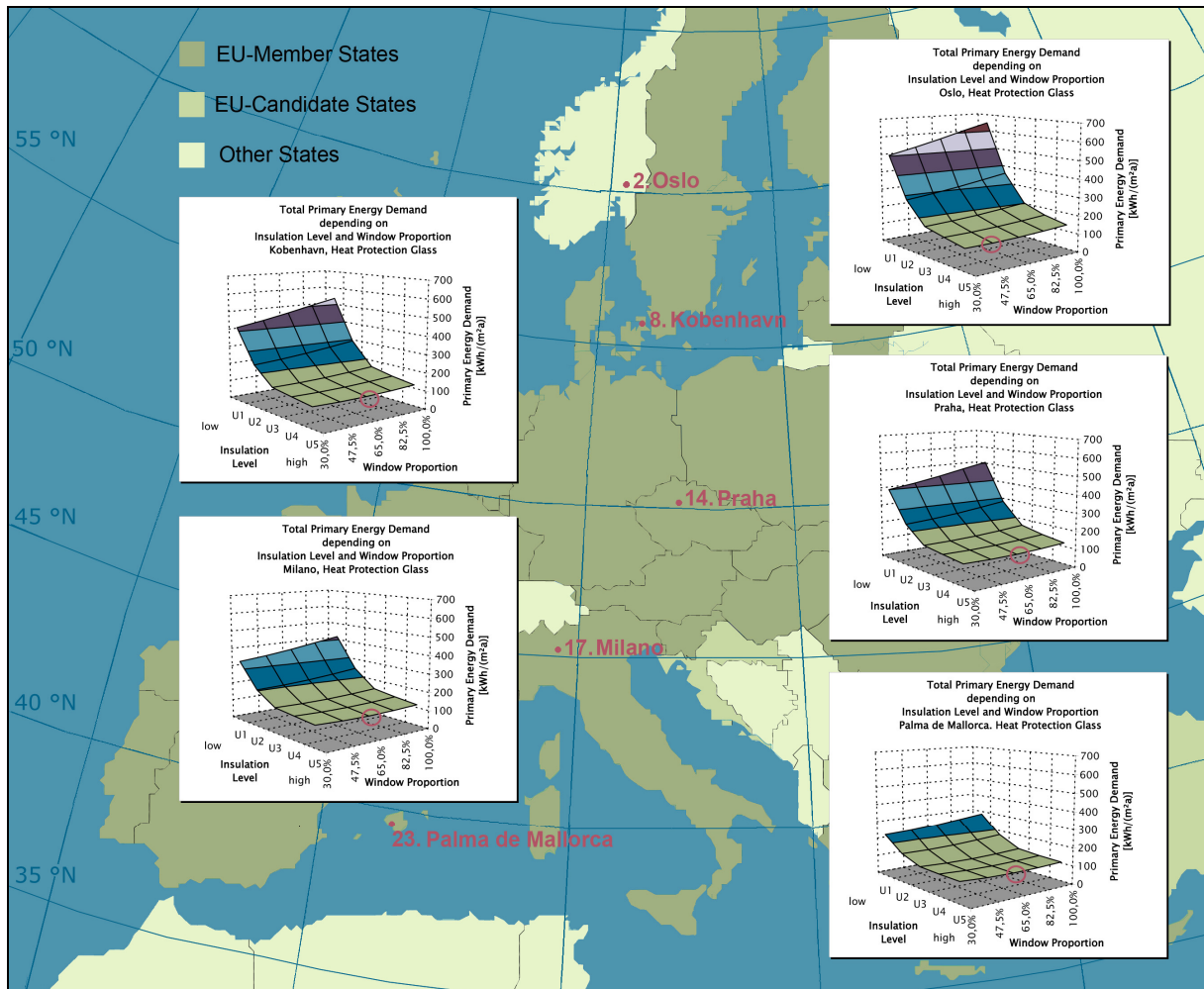


Fig. 47: Results of Building Optimisation in Representative Location.

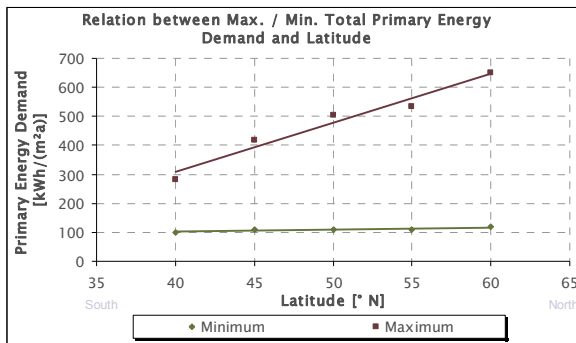


Fig. 48: Maximum and Minimum Total Primary Energy Demand of Representative Locations.

It can be stated that with optimised buildings (especially with high insulation levels) almost the same minimised total primary energy demand can be achieved independent from the location. By the use of high insulation levels, the buildings are uncoupled from climatic effects of the location.

In all locations, the highest total primary energy demand was determined with fully glazed façades and the lowest insulation level.

Furthermore it can be stated that the negative effects of sub-optimal buildings on the total primary energy demand increases from South to north. This can mainly be traced to the generally higher level of HDD compared to CDD. Therefore, the heating energy demand in the North is influenced stronger by a low insulation level than the cooling energy demand in the South.

8. Energy Demand of Typical Buildings

8.1. Detailed Example: Praha

Using the given building parameters described in chapters 7.2 and 7.5, the primary energy demand for heating, cooling, ventilation and lighting has been calculated for a typical building in each of the 25 selected locations. The hourly results from the simulation of a period of one year have been obtained separately for each main orientation and have been summarised to monthly values. These monthly results have been exemplified in Fig. 49 as specific values (i.e. relative to the floor area of the room) for a south-orientated room in Praha. Detailed results for other orientations and locations can be found in the appendix of this work.

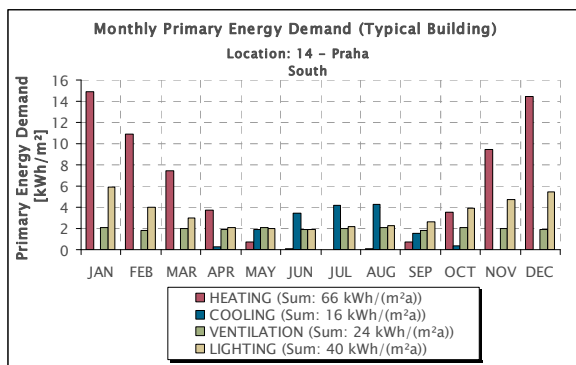


Fig. 49: Monthly Primary Energy Demand of a South-Office in a Typical Building in Praha.

The results for Praha show an overlapping of the heating and cooling period in April/May and September/October. Due to the way of calculation, the ventilation energy demand varies only slightly as a result of different lengths of months. The lighting energy demand is much higher in winter than in summer due to differences in daytime length and reduced radiation intensity.

for the different fractions of the energy demand. The heating energy demand is highest in the North as a result of lower solar gains.

In Fig. 50 the annual sums per orientation are exemplified for the same location. Slight variations can be determined

As a result of the control strategy (depending on the direct and total radiation) of the internal blind and the external shading system, the cooling energy demand is also highest in the North and lowest in the South: On the northern façade, the use of the internal blind and the partly closed (45° cut-off-position) external lamella system suffices more often than on the southern façade. This results in slightly higher cooling loads but also in lower lighting energy demand in the North compared to the South, where the external lamella have to be used and be fully closed more often. This effect could be reduced by the use of a sun shading system with daylight redirection in the South, which has not been taken into account in this work.

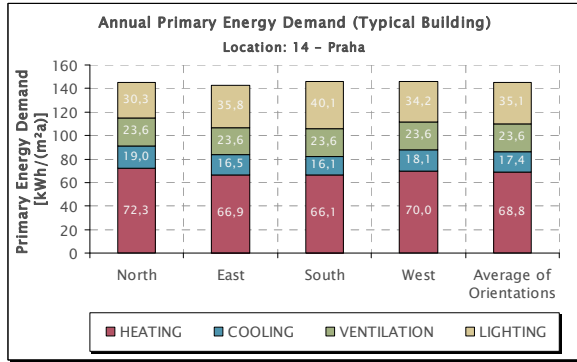


Fig. 50: Annual Primary Energy Demand of a Typical Building in Praha.

Due to these contrary effects, the differences of the sums per orientation are small and average values have been calculated for the location. Here, it can be seen that the primary energy demand for heating already amounts for about 50% of the total primary energy demand, which could be improved by a better insulation level. The primary energy demand for lighting amounts to about 25%.

8.2. Comparison of 25 Locations (per Latitude)

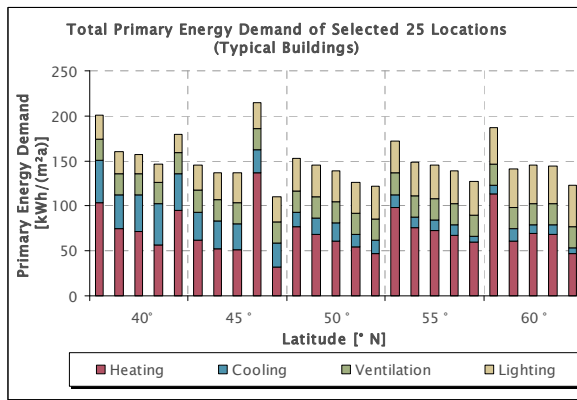


Fig. 51: Total Primary Energy Demand of Typical Buildings in Selected 25 Locations.

Fig. 51 shows the total primary energy demand of the typical buildings in the 25 selected locations. The results vary a lot both within as well as between the groups of latitude. This variation mainly results from the heating energy demand.

The subdivisions of the primary energy demand as functions of the latitude can be found in Fig. 52. The heating energy demand shows a strong variation, whereas the energy demands for cooling and lighting correlate much better with the latitude. The strong variation of heating energy demand can be traced to a

combination of the variation of heating degree days (see Fig. 19) and the variation of insulation levels defined for typical buildings per country (see chapter 7.5).

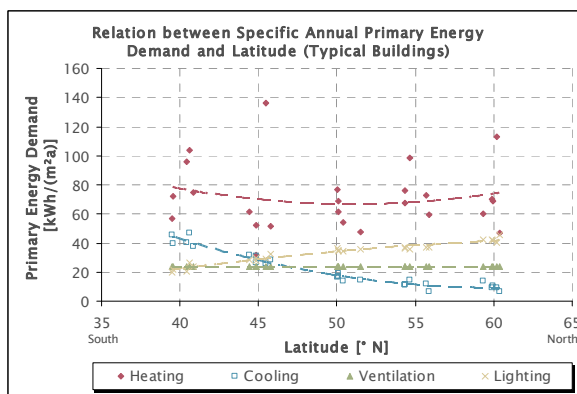


Fig. 52: Annual Primary Energy Demand for Heating, Cooling, Lighting and Ventilation in Typical Buildings as Function of Latitude.

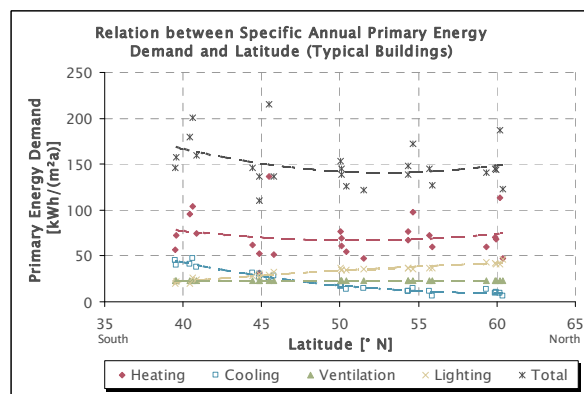


Fig. 53: Total Annual Primary Energy Demand of Typical Buildings as Function of Latitude.

As a result, the total primary energy demand shown in Fig. 53 varies as well. With the constraints of the variation of results, the buildings between 50° and 55° northern latitude generally seem to be designed most appropriate to the location, as the minimum of the trend line indicates.

8.3. Comparison of 25 Locations (per Climatic Term)

From the findings of different correlations described in chapter 6.6.1, a better correlation could be expected between the energy demand and the climatic terms deducted in chapter 6.5.

The correlation of the primary energy demand with degree days and annual illumination shows a strong variation of the heating energy demand as well. The energy demands for cooling and lighting correlate much better, as expected (see Fig. 54).

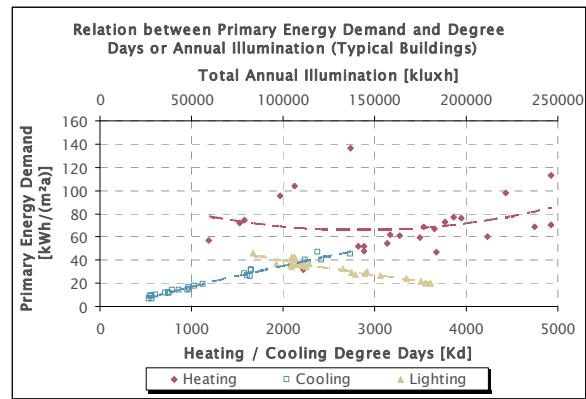


Fig. 54: Primary Energy Demand of Typical Buildings as Function of Degree Days and Annual Illumination.

Therefore, as a result of the different insulation levels in European countries, no significant correlation between the Heating Degree Days and the heating energy demand of typical buildings can be observed.

8.4. Comparison relative to European Average

As the absolute energy demand depends on many influences resulting from the building use (e.g. occupancy, internal loads etc.) which had to be fixed assumptions in this analysis, the estimations of absolute values from the climatic conditions would have low significance. Therefore, the absolute results have been qualified with respect to the European bandwidth of results. An average value of the subdivisions of primary energy demand calculated from all 25 locations can be defined as 100% and can be used as European benchmark for the influence of climate on the energy demand at any given location.

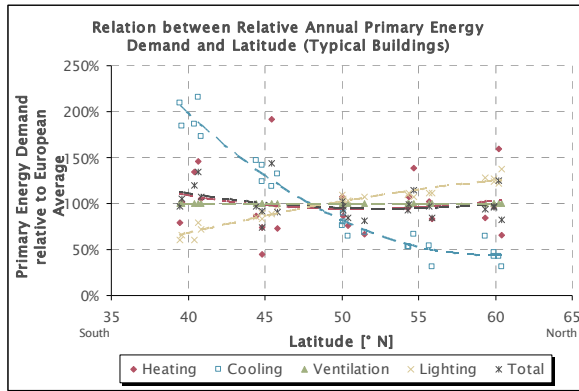


Fig. 55: Relative Primary Energy Demand of Typical Buildings as Function of Latitude.

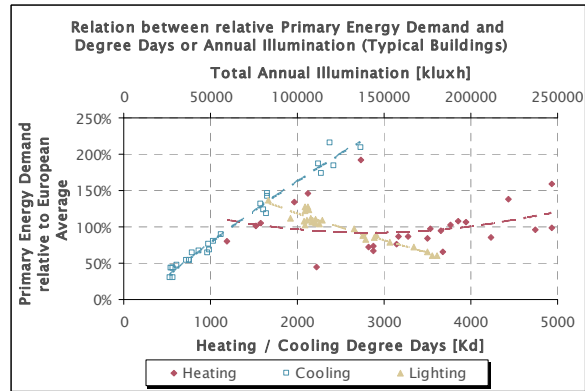


Fig. 56: Relative Primary Energy Demand of Typical Buildings as Function of Degree Days and Annual Illumination.

The calculation of the primary energy demand relative to the European average shows the same poor correlation of the heating energy demand. Referred to the latitude, from South to North the relative primary energy demands are decreasing for cooling and increasing for lighting (Fig. 55). For heating and in consequence also for the total primary energy demand no trend can be determined as a result of poor correlation.

In reference to heating degree days (Fig. 56), the relative primary energy demand for heating shows a minimum at about 2750 HDD. Due to the bad correlation the significance of this result has to be doubted. The relative primary energy demands for cooling and lighting show a good correlation with the cooling degree days and the annual illumination respectively.

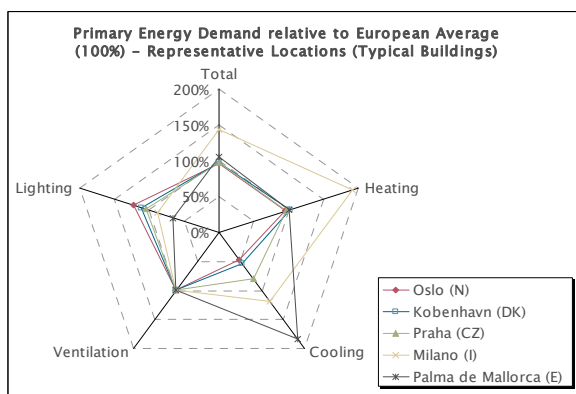


Fig. 57: Primary Energy Demand of a Typical Building in Selected Locations relative to European Average (100%).

Fig. 57 shows the relative primary energy demand of typical buildings in the five representative locations. The very high heating demand in Milano shows that this is one of the locations where the insulation level is not very suitable for the climatic conditions of the location. This also has an effect on the total primary energy demand of Milano.

The other locations have similar heating and total primary energy demands, whereas decreasing cooling and increasing lighting energy demand can be observed from South to North.

9. Energy Demand of Optimised Buildings

9.1. Detailed Example: Praha

The calculations described before have been performed again using the parameters defined for optimised buildings in chapter 7.6.3. Again, the monthly results have been exemplified in Fig. 58 as specific values (i.e. relative to the floor area of the room) for a south-orientated room in Praha. Detailed results for other orientations and locations can be found in the appendix of this work.

The results for Praha show a more distinct separation between the heating and cooling period in April and October, than the typical building. Again, the ventilation energy demand varies only slightly and the lighting energy demand is much higher in winter than in summer.

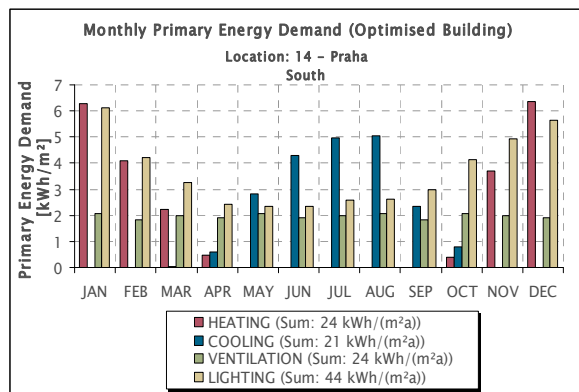


Fig. 58: Monthly Primary Energy Demand of a South-Office in an Optimised Building in Praha.

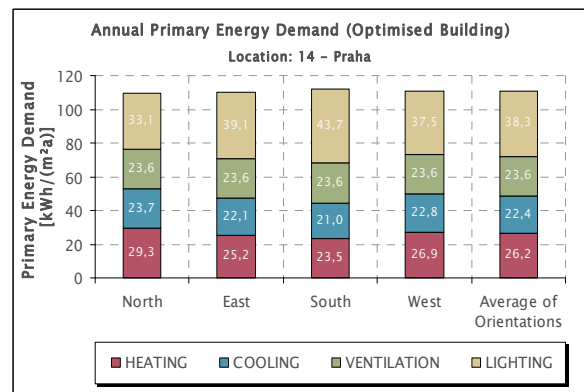


Fig. 59: Annual Primary Energy Demand of an Optimised Building in Praha.

In Fig. 59 the annual sums per orientation are exemplified for the same location. Qualitatively the same differences between the orientations can be observed as in the typical building.

The differences of the sums per orientation are predominantly small again. As a result of the good thermal insulation level, the primary energy demand for heating and cooling together amounts to less than 50% of the total primary energy demand. In contrast, the energy demand for lighting amounts to almost 40% of the total as a result of the generally lower level of total primary energy demand compared to the typical building.

9.2. Comparison of 25 Locations (per Latitude)

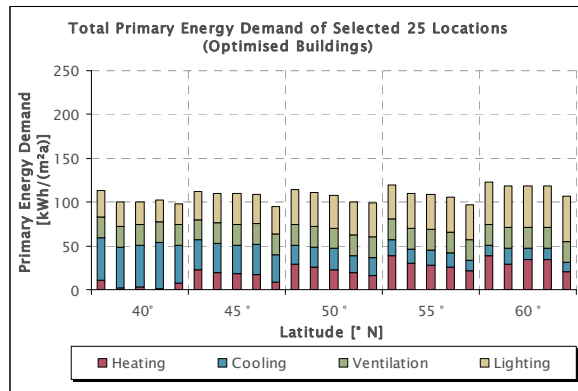


Fig. 60: Total Primary Energy Demand of Optimised Buildings in Selected 25 Locations.

The results of the optimised buildings in all 25 locations (average values of orientations) have been contrasted with each other in Fig. 60, grouped by latitude. It can be seen that despite the differences in the subdivisions the variation of the total primary energy demand is quite low. A more detailed view on the subdivisions of primary energy demand is given in Fig. 61 as functions of latitude. From South to North the heating and lighting energy demands are increasing, the cooling energy demand is decreasing. The ventilation energy demand again is constant due to the ventilation strategy defined in this work. The heating energy demand shows a comparatively large spread as a result of the spreading winter temperatures observed in chapter 6.6.1. The results of cooling and lighting energy demand show a good correlation with the latitude of the location.

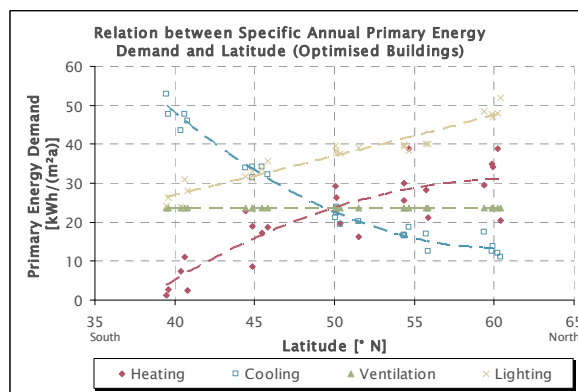


Fig. 61: Annual Primary Energy Demand for Heating, Cooling, Lighting and Ventilation in Optimised Buildings as Functions of Latitude.

The results of the optimised buildings in all 25 locations (average values of orientations) have been contrasted with each other in Fig. 60, grouped by latitude. It can be seen that despite the differences in the subdivisions the variation of the total primary energy demand is quite low.

A more detailed view on the subdivisions of primary energy demand is given in Fig. 61 as functions of latitude. From South to North the heating and lighting energy demands are increasing, the cooling energy demand is decreasing. The ventilation energy demand again is constant due to the ventilation strategy defined in this work. The heating energy demand shows a comparatively large spread as a result of the spreading winter temperatures observed in chapter 6.6.1. The results of cooling and lighting energy demand show a good correlation with the latitude of the location.

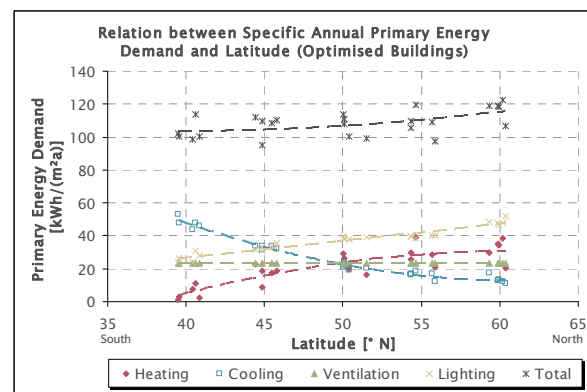


Fig. 62: Total Annual Primary Energy Demand of Optimised Buildings as Function of Latitude.

Summing up the subdivisions, the total primary energy demand as function of the latitude can be added to the diagram (Fig. 62). Despite a certain spread of results mainly caused by the heating energy demand, the results for the optimised buildings are within a close range independent from the latitude.

9.3. Comparison of 25 Locations (per Climatic Term)

In Fig. 63 the primary energy demands for heating and cooling have been correlated to the heating and cooling degree days and the primary energy demand for lighting has been correlated to the total annual illumination on a horizontal surface. As a result of the high insulation level, even the heating energy demand correlates well with the HDD.

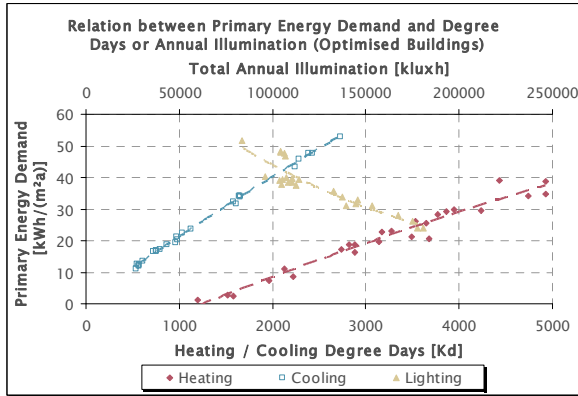


Fig. 63: Primary Energy Demand of Optimised Buildings as Function of Degree Days and Annual Illumination.

The correlations shown in Fig. 63 in principle could be used to estimate the respective primary energy demands of a building from the deducted climatic terms of the building's location.

But as described before, the absolute energy demand depends on many influences resulting from the building use so that these estimations of absolute values from climatic conditions would have low significance.

9.4. Comparison relative to European Average

Like in chapter 8.4 for the typical buildings, the absolute results have been qualified with respect to the European bandwidth of results.

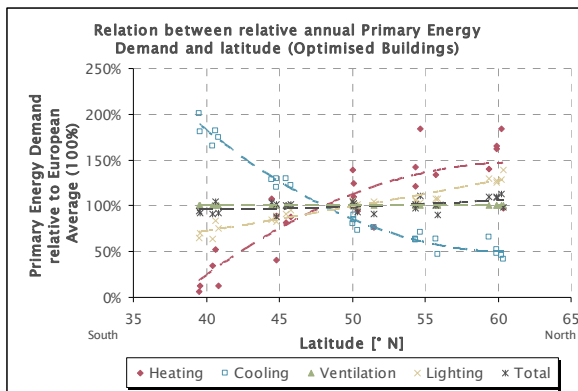


Fig. 64: Relative Primary Energy Demand of Optimised Buildings as Function of Latitude.

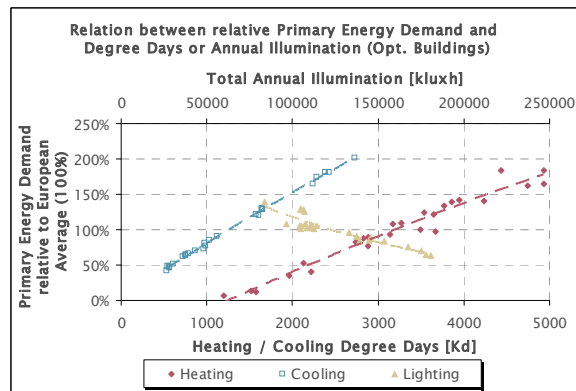


Fig. 65: Relative Primary Energy Demand of Optimised Buildings as Functions of Degree Days and Annual Illumination.

The relative primary energy demand of optimised buildings is shown in Fig. 64 as function of the latitude and in Fig. 65 as function of degree days and annual illumination. Again, from South towards North an increasing heating and lighting energy demand and a decreasing cooling energy demand can be observed. The total primary energy demand of optimised buildings is almost constant regardless the location.

Fig. 66 demonstrates the relative primary energy demands for heating, cooling, ventilation and lighting plus the total of each of the five representative locations from each group of latitude relative to the respective European average value (100%). More detailed results for the other locations analysed in this work can be found in the appendix.

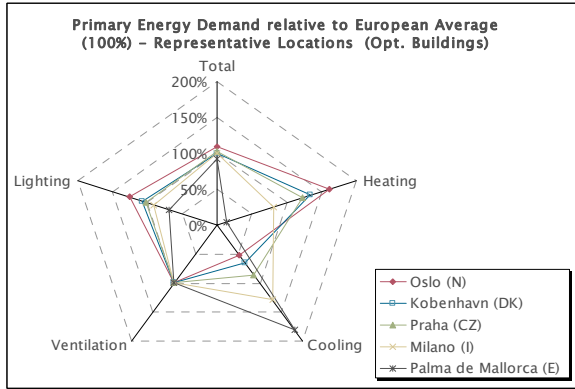


Fig. 66: Primary Energy Demand of Optimised Buildings in Selected Locations relative to European Average (100%).

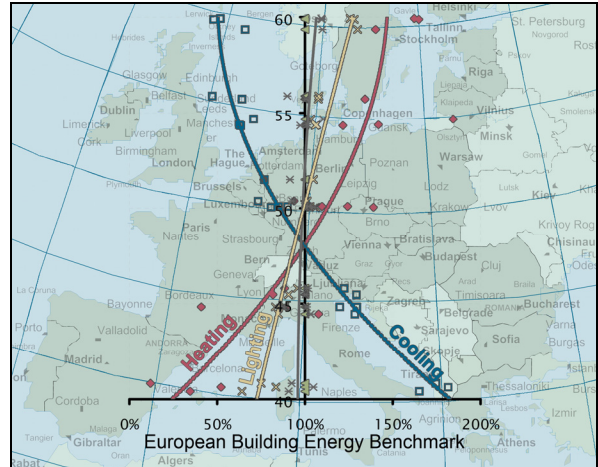


Fig. 67: European Building Energy Benchmark (EBEB) for Heating, Cooling and Lighting depending on the Latitude.

From these results a rough estimation of the climatic influences on the energy demand can be deduced from the latitude of a location, leading to a rough “European Building Energy Benchmark” (EBEB). Fig. 67 visualises the primary energy demand for heating, cooling and lighting in optimised buildings relative to the European average (100%) and depending on the latitude.

10. Comparison of Typical and Optimised Buildings

10.1. Comparison of Results among Each Other

10.1.1. Comparison of Primary Energy Demand for Heating

The graphs in Fig. 68 show generally lower heating energy demand for the optimised buildings compared to the typical buildings for all locations. The optimised buildings have higher heating energy demands from South to North with a distinctly variance of results. The heating energy demand of the typical buildings varies even more as a result of different insulation levels usual per country. About 50 °N the trend-line shows an optimum for the typical buildings, but given the strong variation of results, this cannot be seen significant.

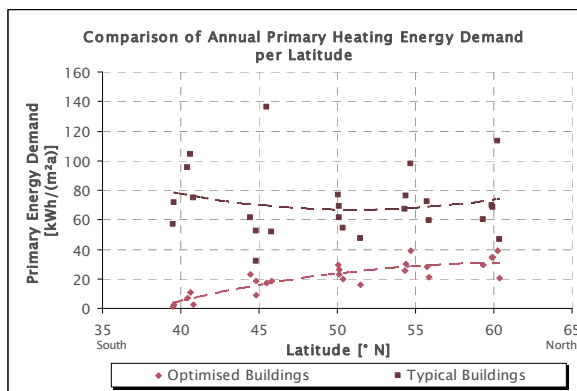


Fig. 68: Comparison of Primary Energy Demand for Heating of Typical and Optimised Buildings per Latitude.

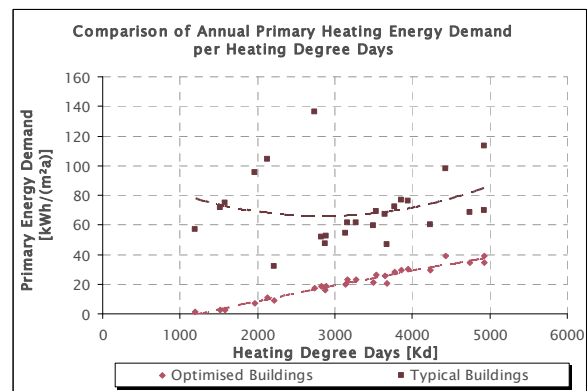


Fig. 69: Comparison of Primary Energy Demand for Heating of Typical and Optimised Buildings per Heating Degree Days.

The heating energy demands as functions of the heating degree days again show a strong variation of the results of typical buildings (Fig. 69). Contrary, the heating primary energy demand for optimised buildings correlates very well with the heating degree days.

Overall the increased level of insulation of the optimised buildings leads to significant lower heating energy demands, independent from the location. Accepting a certain inaccuracy even the latitude can be used for the estimation of heating energy demand, although an estimation based on the heating degree days would be more accurate. For typical buildings both estimations seem to have low significance.

10.1.2. Comparison of Primary Energy Demand for Cooling

The cooling primary energy demand of both optimised and typical buildings correlate well with the latitude (Fig. 70) and the cooling degree days (Fig. 71), while the latter correlation is more accurate. From South to North the cooling energy demands for both types of buildings decrease.

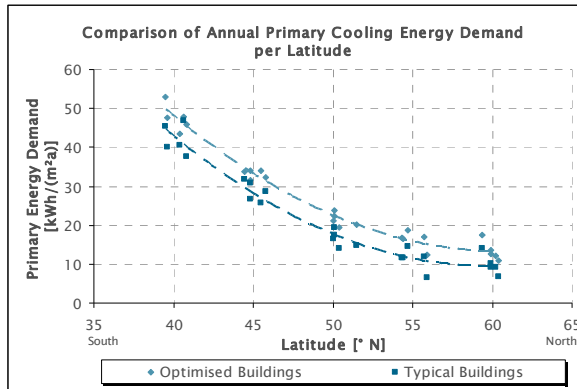


Fig. 70: Comparison of Primary Energy Demand for Cooling of Typical and Optimised Buildings per Latitude.

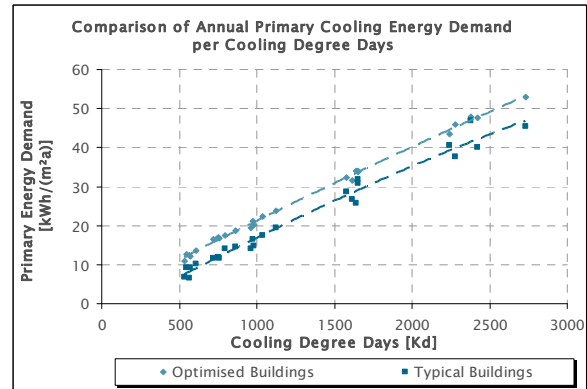


Fig. 71: Comparison of Primary Energy Demand for Cooling of Typical and Optimised Buildings per Cooling Degree Days.

Overall, the higher insulation level of the optimised buildings leads to higher energy demands for cooling compared to typical buildings.

10.1.3. Comparison of Primary Energy Demand for Lighting

The primary energy demand for lighting correlates with the latitude (Fig. 72) as well as with the annual illumination (Fig. 73). For typical as well as for optimised buildings the lighting energy demand increases from South to north.

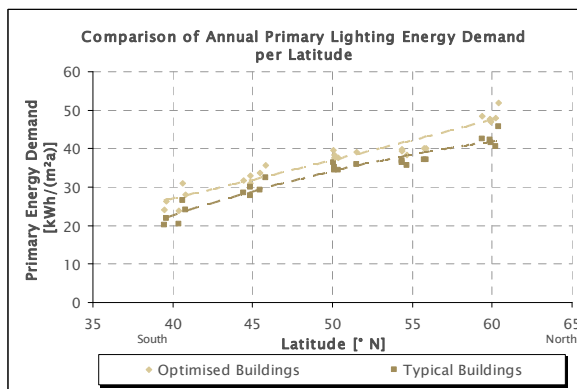


Fig. 72: Comparison of Primary Energy Demand for Lighting of Typical and Optimised Buildings per Latitude.

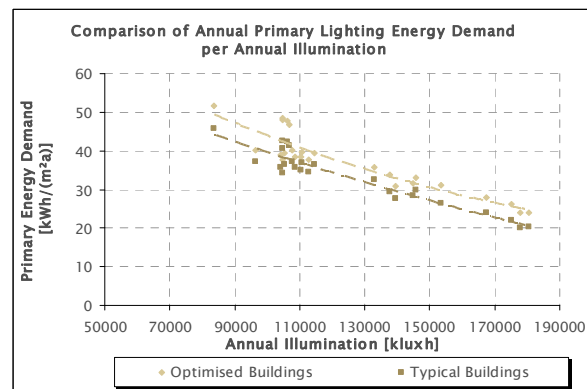


Fig. 73: Comparison of Primary Energy Demand for Lighting of Typical and Optimised Buildings per Annual Illumination.

Overall the reduced light transmittance of the glazing of the optimised buildings with high insulation levels lead to higher lighting energy demand compared to typical buildings.

10.1.4. Comparison of Total Primary Energy Demand

The total primary energy demand for typical and optimised buildings as functions of the latitude is shown in Fig. 74. As a result of the strong variation of heating energy demands of typical buildings, the same effect can be observed for the total primary

energy demand. Again, there seems to be an optimum around the latitude 50 °N, but this cannot be trusted given the strong variation of results.

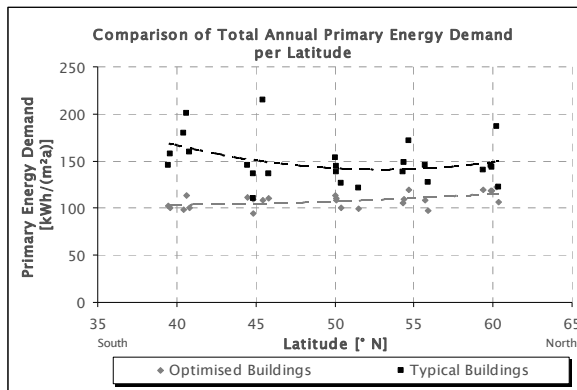


Fig. 74: Comparison of Total Primary Energy Demand of Typical and Optimised Buildings per Latitude.

cooling energy demand is stronger than the reductions of heating and lighting energy demand. The optimised buildings are almost unaffected by from influences outdoor temperature.

Therefore, regardless the location, almost the same low level of total primary energy demand can be achieved. As local influences are minimised by the high level of insulation even the latitude could be used for a rough energetic comparison of optimised buildings.

10.2. Exemplary Benchmarking of Results with Target Values from VDI 3807

The German VDI-Guideline 3807 provides characteristic values of energy and water consumption of buildings. These values can be used to countercheck the results and therefore to proof the methodology used for calculation of energy demand in this work.

As the guideline provides statistical consumptions of German buildings (offices and other building types) it can be used best to countercheck the results of a location in Germany. Therefore, the results of Frankfurt/Main will be used for this comparison.

Reference values for the heating energy demand will be taken from [VDI 3807-2]. This guideline provides mean values (see Fig. 75) and guide values (see Fig. 76), whereas the latter is a lower quartile mean value and shall be used as a target value for new and refurbished buildings.

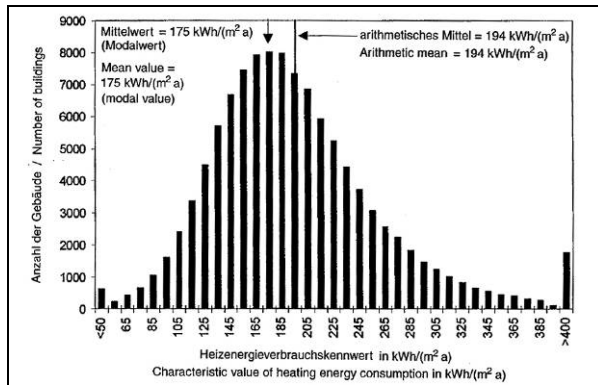


Fig. 75: Exemplary Determination of Mean Values in [VDI 3807-2].

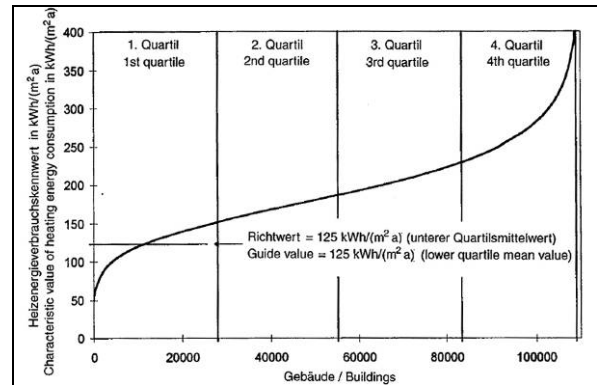


Fig. 76: Exemplary Determination of Guide Values in [VDI 3807-2].

The benchmark values for counterchecking cooling, ventilation and lighting energy demand can be taken from [VDI 3807-4]. Here a more detailed subdivision of area-related electrical energy demands is given for five demand classes:

- Very high
- High
- Average
- Low
- Very low

As the limit which has to be achieved by new or refurbished buildings, this guideline specifies the demand class “low”. The demand class “very low” is specified as the target value. For each of these demand classes, typical boundary conditions are given. For the comparison of the results calculated for typical and optimised buildings with the values in VDI 3807, some assumptions have to be made:

- The mean values for heating in [VDI 3807-2] have been measured in the early 1990s. The guide values should be taken as target values to be achieved when carrying out energy saving measures at the time of 1998. Therefore the guide values seem to be more appropriate for comparison of the typical buildings defined in this work.
- Besides the insulation level, the “typical” building already represents a quite a good design in terms of size and position of windows, type and control of luminaires etc., so the comparison with the demand level “low” (single office) seems to be appropriate.
- For the definition of a (here called) best-practice-building (demand class “very low”) according to VDI 3807, lower heating energy demand has to be assumed. It can be expected that the reduction of heating energy demand is comparable to the reduction of cooling energy demand between demand classes “low” and “very low”. Therefore a reduction of cooling energy demand by 60% (from 5 to 2 kWh/(m²a)) has been assumed.
- The ventilation type is the same for both typical and optimised buildings, therefore it will be kept at “low” level (which best meets the definition of the ventilation strategy, see appendix) for the best-practice-building according to VDI 3807.

- The values of end energy demand given in VDI 3807 have to be calculated to primary energy demand using the primary energy factors described in the appendix.

Tab. 10 shows the calculation of the values used for the comparison.

Tab. 10: Comparison of Results for Typical and Optimised Buildings in Frankfurt/Main with VDI 3807.

Comparison of Energy Demands [kWh/(m ² a)]		HEATING	COOLING	VENTILATION	LIGHTING
Results Typical Building (Frankfurt/Main)		61,34	19,35	23,62	34,46
VDI 3807 ("Low" Values)	Data Source	[VDI3807-2] Guide Value	[VDI 3807-4] "low"	[VDI 3807-4] "low"	[VDI 3807-4] "low"
	End energy demand (VDI 3807)	65	5	8	19
	PE-Factor [-]	1,1	2,7	2,7	2,7
	Resulting primary energy demand (VDI 3807)	71,5	13,5	21,6	51,3
Results Optimised Building (Frankfurt/Main)		23,16	23,74	23,62	37,68
VDI 3807 ("Best Practice")	Data Source	[VDI3807-2] 2/5 of Guide Value	[VDI 3807-4] "very low"	[VDI 3807-4] "low"	[VDI 3807-4] "very low"
	End energy demand (VDI 3807)	26	2	8	6
	PE-Factor [-]	1,1	2,7	2,7	2,7
	Resulting primary energy demand (VDI 3807)	28,6	5,4	21,6	16,2

The total primary energy demand of the typical building shown in Fig. 77 is a bit lower than the "Low"-Value-Building in VDI 3807. This results from the heating and lighting energy demands.

In 1995 a new building regulation with higher insulation requirements came into force in Germany. Therefore, the lower heating energy demand can be traced to better insulation levels resulting from the time between the construction of the buildings (before 1995), measured for [VDI 3807-2], and the typical values used according to [En-Per-TEBuC] to fulfil the standard requirements of that time (after 1995).

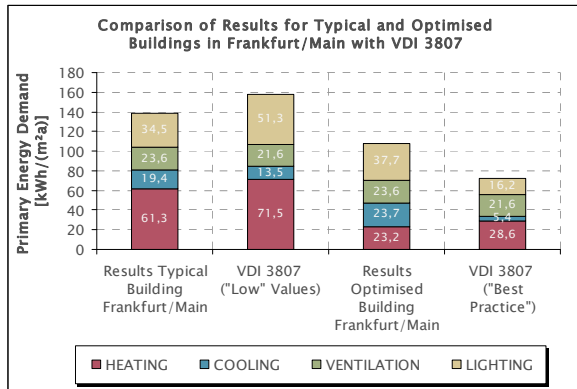


Fig. 77: Comparison of Results for Typical and Optimised Buildings in Frankfurt/Main with VDI 3807.

The lower lighting energy demand results from the classification in [VDI 3807-4], which does not exactly meet the configuration of the typical building. With some factors (e.g. room reflectance) of the "low" demand class and some of the "very low" demand class (e.g. luminaires and control strategy), the lighting of the typical building is ranked between these demand classes.

Overall, the results for the typical building seem to be realistic for a typical up-to-date building design, although many new buildings perform much worse, some do better.

The total primary energy demand of the building with optimised insulation level and window proportion is another 20% lower than the demand of the typical building. With a total primary energy demand of about 110 kWh/(m²a) it is very close to the target of the German research project "SolarBau", where office buildings not exceeding 100 kWh/(m²a) have been planned, realised and monitored [Voss].

The best-practice building is another 30% lower as a result of the "very low" lighting energy demand and the reduced cooling and heating energy demand, whereas the latter was based on assumptions (see above). It is very close to a total primary energy demand of 75 kWh/(m²a), which is the limit for buildings attending the new German research project "EnBau" [EnOB-EnBau].

Overall the optimised building performs on a high level, although there is even more potential to be tapped, as the comparison with the best-practice-building shows. This potential results from optimisation of the numerous parameters which have been unchanged in this work (efficiency of technical systems, primary energy factors of energy sources used etc.).

11. Influences of Supply Air Dehumidification

11.1. General

In terms of cooling energy, the analyses in this work have been focussed on the sensible (i.e. dry) cooling loads in the room and the resulting primary energy demand for cooling. Depending on type and operation mode of cooling facilities, additional cooling energy demand can result from the dehumidification of the supply air.

These so-called latent cooling loads occur inevitably as soon as the air is cooled below the saturation temperature corresponding to the absolute air humidity (i.e. humidity ratio). In many buildings there is no humidity control as such, but in some cooling systems and especially in hot and humid climates such additional loads may occur. For these eventualities, a lateral analysis has been done and will be described in this chapter.

The analyses of various locations with significant cooling loads in Europe and the USA by [Colliver] showed that on average latent cooling loads account for about 80% of the total loads for supply air cooling (see Fig. 78). It is obvious, that the European locations analysed by [Colliver] have only low cooling loads compared to the locations in the USA. Looking at the European locations in detail (see Fig. 79) it can be found that only the more southern locations (here: in France) have significant cooling loads and a significant fraction of latent cooling loads at the same time.

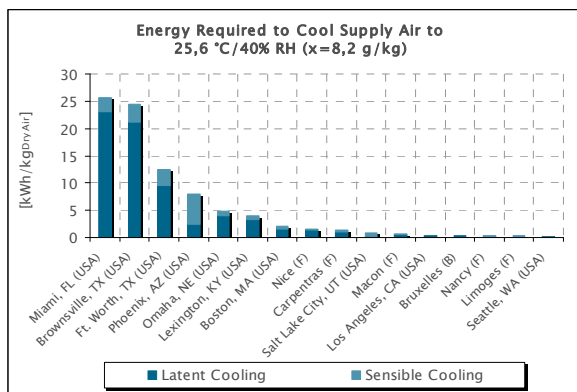


Fig. 78: Latent and Sensible Loads for Cooling of Supply Air in Selected Locations according to [Colliver].

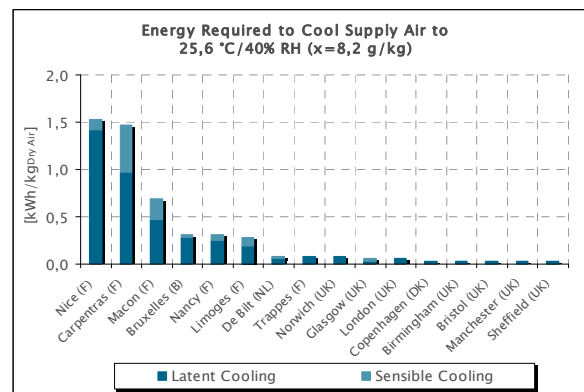


Fig. 79: Latent and Sensible Loads for Cooling of Supply Air in Selected European Locations according to [Colliver].

Contrary to [Colliver], in this work the impacts of latent cooling have been analysed compared to the total primary energy demand of the building, i.e. including cooling energy demand resulting from internal and external thermal loads.

As mentioned before, the dehumidification of air and the respective latent cooling loads are highly depending on the technical systems used in a building and their operation mode (i.e. surface temperature of cooling devices, etc.). In order not to take into account the wide variety and efficiencies of possible equipment, in this work only those latent cooling loads have been considered, which are required to cool and dehumidify the ventilated air to a certain setpoint of room condition. It was also assumed that the air enters the room at the same conditions as the indoor air setpoint.

It should be recognized that the energy demand resulting from this procedure is for the minimum required enthalpy changes of the air only. This procedure for example represents a ventilation system delivering the minimum (hygienically) required air change rate at setpoint temperatures and humidity of the room. Cooling loads are mainly covered by other systems (e.g. cooling ceilings, recirculating air chillers etc.). Effects of indoor sources and sinks of moisture (persons, equipment, moisture storage in materials etc.) are not taken into account.

Therefore, due to the design and efficiency of the cooling system, the actual latent cooling energy demand may be larger than calculated in chapters 11.2 and 11.2. The impact of other degrees of dehumidification will be analysed in chapter 11.4.

With the above assumptions, the latent cooling load can be calculated from the differences of humidity ratios of outdoor conditions and indoor setpoint conditions, i.e. from the amount of moisture which must be removed from the supply air. With reference to the air temperature for cooling (see appendix) the setpoint has been assumed as the following:

- Air temperature: 24,5 °C
- Relative humidity: 60% (acc. to class II in [EN 15251])
- Corresponding humidity ratio at setpoint: 0,0115 kg_{Water} / kg_{Dry Air}
- Corresponding dewpoint temperature: 16,2 °C.

11.2. Typical Buildings

The typical buildings have been simulated in all 25 locations, taking into account latent cooling loads. The resulting primary energy demand can be found in Fig. 80 and Fig. 81. For the dehumidification of supply air to the given setpoint, latent cooling loads only occur in the locations South of the latitude of 50 °N.

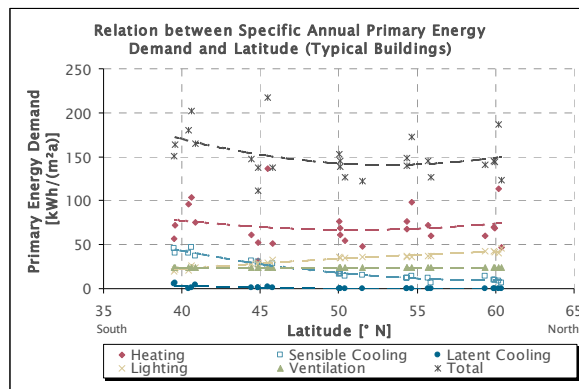


Fig. 80: Annual Primary Energy Demand of 25 Typical Buildings including Latent Cooling (Humidity Ratio Setpoint: 0,0115 kg_{wa-ter}/kg_{Dry Air}) as Function of the Latitude.

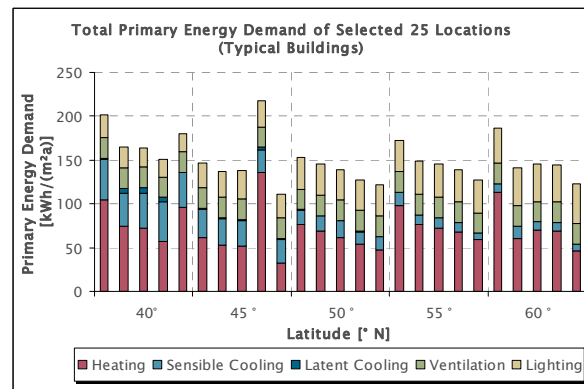


Fig. 81: Annual Primary Energy Demand of 25 Typical Buildings including Latent Cooling (Humidity Ratio Setpoint: 0,0115 kg_{wa-ter}/kg_{Dry Air}) grouped by Latitude.

An increasing trend southwards can be observed. The maximum share of latent cooling in the total primary energy demand is only 4% (Palma de Mallorca). Therefore, no significant change in the correlation to the latitude can be stated.

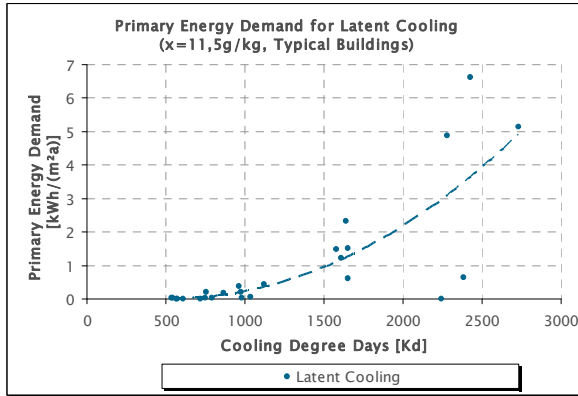


Fig. 82: Annual Primary Energy Demand of 25 Buildings for Latent Cooling (Humidity Ratio Setpoint: 0,0115 kg_{Water}/kg_{Dry Air}) as Function of the Cooling Degree Days.

The correlation of the annual primary energy demand for latent cooling with the cooling degree days (CDD) of the location in Fig. 82 shows an increasing trend for warmer (i.e. cooling dominated) climates. As a result of local influences (mainly humid climates at locations close to the sea) the variance of the results increases southwards as well. Given the overall low values compared to the total primary energy demand, the correlation still seems to be acceptable.

11.3. Optimised Buildings

Since all relevant parameters remained unchanged, the primary energy demand for latent cooling in the optimised buildings is the same as in the typical buildings in terms of absolute values (see Fig. 83 and Fig. 84). Again, no significant influence on the total primary energy demand can be observed. As a result of the generally lower energy demand compared to the typical buildings, the share of latent cooling in the total primary energy demand is slightly higher in the optimised buildings: Still, the maximum share in all 25 locations is only 6,2% (Palma de Mallorca).

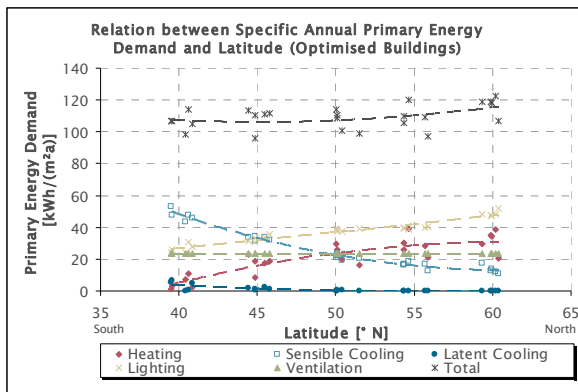


Fig. 83: Annual Primary Energy Demand of 25 Optimised Buildings including Latent Cooling (Humidity Ratio Setpoint: 0,0115 kg_{Water}/kg_{Dry Air}) as Function of the Latitude.

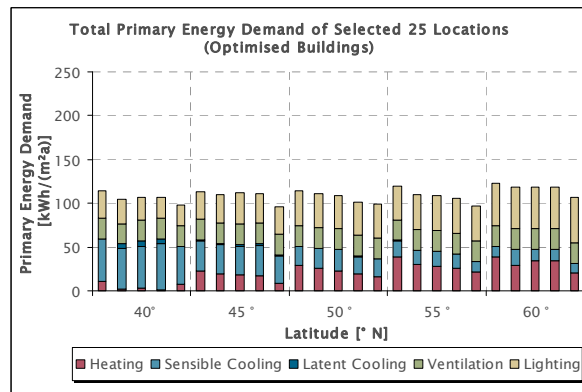


Fig. 84: Annual Primary Energy Demand of 25 Optimised Buildings including Latent Cooling (Humidity Ratio Setpoint: 0,0115 kg_{Water}/kg_{Dry Air}) grouped by Latitude.

The correlation of the annual primary energy demand for cooling with the cooling degree days (CDD) of the location in is the same as shown in Fig. 82.

11.4. Impact of the Humidity Ratio Setpoint

To evaluate the influence of different technical systems and ways of operation described in chapter 11.1, a variation of the setpoint conditions has been performed in the optimised buildings. Therefore the relative humidity of the setpoint has been reduced from 60% to 30% in four steps, resulting in reduced humidity ratios to which the supply air had to be dehumidified (see Tab. 11). Looking at the corresponding dewpoint temperatures, the range covers most of the technical systems up to chilling coils with a surface temperature of about 6°C and intensive cooling and dehumidification of the air.

Tab. 11: Variation of Setpoint Conditions in Terms of Humidity.

	Temperature	Relative Humidity	Humidity Ratio	Dewpoint Temperature
	[°C]	[%]	[g _{Water} /kg _{Dry Air}]	[°C]
x1	24,5	60	11,5	16,2
x2	24,5	50	9,6	13,4
x3	24,5	40	7,6	10,0
x4	24,5	30	5,7	5,8

Fig. 85 shows, that with decreasing setpoint humidity ratios latent cooling loads occur even in northern locations. With a setpoint humidity ratio of 5,7 g/kg the mean cooling energy demand at 60 °N roughly meets the maximum values at 40 °N and 11,5 g/kg.

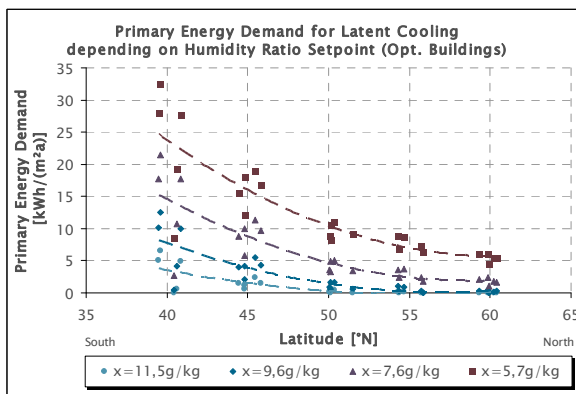


Fig. 85: Annual Primary Energy Demand for Latent Cooling with different Humidity Ratio Setpoints as Functions of the Latitude.

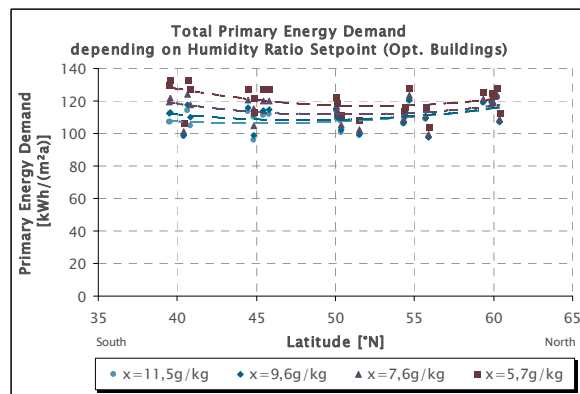


Fig. 86: Annual Total Primary Energy Demand including Latent Cooling with different Humidity Ratio Setpoints as Functions of Latitude.

The variances (i.e. the local influences) in the northern locations are low compared to southern locations. The influence of reduced humidity setpoints increases exponentially towards south. Therefore, in Fig. 86 the influence on the total primary energy demand is more obvious in southern than in northern locations. Depending on the humidity setpoint, the slight increase of total primary energy demand from South towards North changes to roughly the same levels as at 40 and 60 °N and a slight minimum around 50 °N.

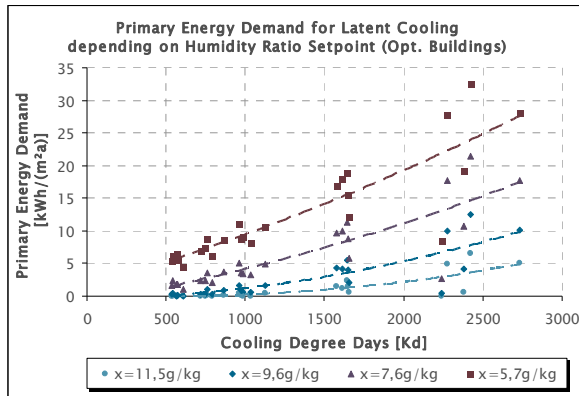


Fig. 87 shows a proportional increase of the latent cooling loads as functions of the cooling degree days under decreasing setpoint humidity ratios. Also, the variance of the results in warmer climates (i.e. with high cooling degree days) increases with the decrease of the setpoint humidity ratio.

Fig. 87: Influence of the Humidity Ratio Setpoint on the Annual Total Primary Energy Demand as Function of the Cooling Degree Days.

12. EBPCC - European Building Performance Climate Classification

From the results of the analyses with optimised buildings in chapter 11.3, a “European Building Performance Climate Classification” (EBPCC) with reference to the building energy demand in European locations could be deduced. Therefore, the European bandwidths of the results obtained in this work (absolute values) have been transformed to relative values, called “European Building Performance Climate Index” (EBPCI), whereas 0% represented the respective minimum, 100% represented the maximum (see Fig. 88) of the bandwidths.

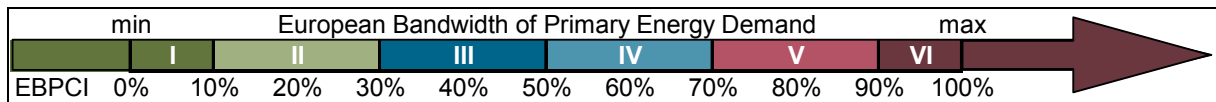


Fig. 88: Definition of Indices and Classes of Primary Energy Demand within the Bandwidth of Results.

These bandwidths have been divided into six classes, describing the due primary energy demand relative to the European bandwidth identified in this work. The highest and lowest classes I and VI should be seen open beyond their extremes, i.e. a classification of a location in one of these classes would mean a climatic influence resulting in an energy demand “below 10%” or “above 90%” of the bandwidth.

From the locations of the 25 buildings analysed in this work, a correlation to the climatic data could be deduced, decoupling the climatic conditions from the actual energy demand of a specific building. With the good correlation between the annual illumination and the cooling degree days (see Fig. 28), HDD and CDD seem to be appropriate terms for the integral classification of climates.

Fig. 89 to Fig. 93 show the resulting diagrams for the total primary energy demand and its subdivisions for heating, cooling (sensible and latent), ventilation and lighting. Depending on its respective primary energy demand, each of the 25 buildings has been allocated to an EBPCC-Class and has been plotted in the diagrams according to its heating and cooling degree days. The resulting EBPCC-Arrays represent the range of heating and cooling degree days resulting in a certain energy demand relative to the European bandwidth.

The overlapping of the EBPCC-Arrays on the one hand shows the transition regions between two classes. On the other hand, together with the gaps between the arrays they are a sign for limited accuracy of the system, resulting from the limited number of locations. With a larger basis of results, the arrays could be stated more precisely. But the trends and correlations are still well-defined. In each diagram the classification of a new location is exemplified for Dortmund, Germany (HDD₁₈=3021, CDD₁₀=1165).

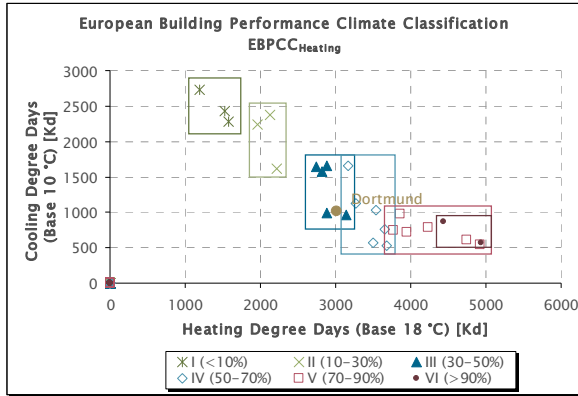


Fig. 89: Arrays for EBPCC_{Heating}-Classes I–VI depending on HDD and CDD with exemplary Classification of Dortmund, Germany.

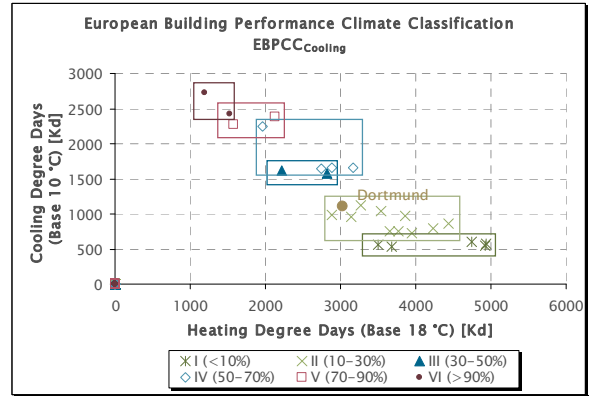


Fig. 90: Arrays for EBPCC_{Cooling}-Classes I–VI depending on HDD and CDD with exemplary Classification of Dortmund, Germany.

The EBPCC_{Heating}-Arrays in Fig. 89 show a clear trend from the top left to the bottom right corner of the diagram. The example of Dortmund is classified in classes III and IV. This is a sign for climatic conditions resulting in a heating energy demand of about 30-50% or 50-70% of the European Bandwidth. As the HDD/CDD values of Dortmund are close to the limits of the two classes, a heating energy demand of about 50% (EBPCI_{Heating}) of the European Bandwidth can be expected with regard to the climate.

The trend of the EBPCC_{Cooling}-Arrays in Fig. 90 is inverse compared to the diagram before. Dortmund is classified in class II, therefore an EBPCI_{Cooling} of about 30% can be expected.

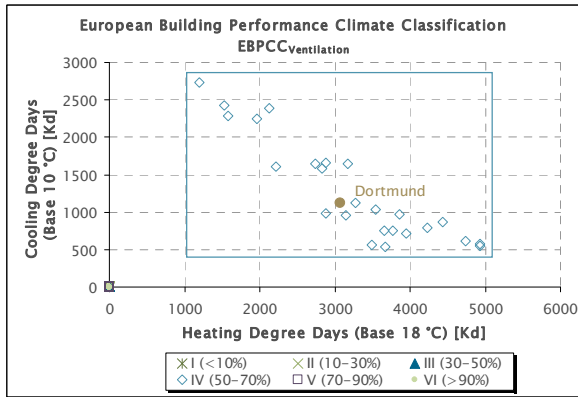


Fig. 91: Arrays for EBPCC_{Ventilation}-Classes I–VI depending on HDD and CDD with exemplary Classification of Dortmund, Germany.

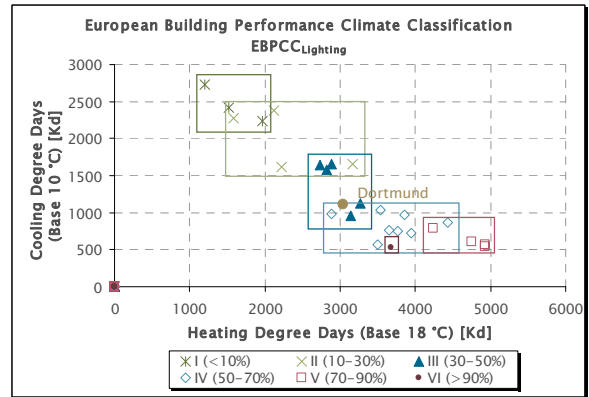


Fig. 92: Arrays for EBPCC_{Lighting}-Classes I–VI depending on HDD and CDD with exemplary Classification of Dortmund, Germany.

Since the analysis in this work did not comprise any changes affecting the ventilation energy demand, Fig. 91 consists only of average EBPCI-values of 50% (class IV).

Except class VI, which consists of only one data point, the EBPCC_{Lighting}-Arrays in Fig. 92 show a clear trend as well. This is a result of unusual local conditions (comparatively low annual illumination due to cloudiness) in Bergen. Dortmund is classified in classes III and IV resulting in an EBPCI_{Lighting} of about 50%.

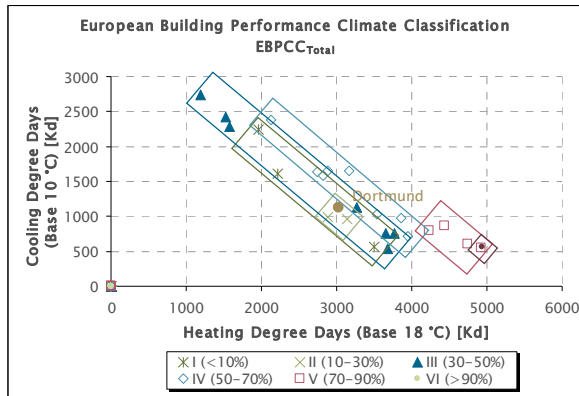


Fig. 93: Arrays for EBPCC_{Total}-Classes I–VI depending on HDD and CDD with exemplary Classification of Dortmund, Germany.

0% to 70%), so a classification in terms of the climatic influence on the total primary energy demand would have low significance.

As a result of the contrary trends of the EPCIs for heating and lighting on the one hand, and for cooling on the other hand, the arrays for the total primary energy demand in Fig. 93 are rotated within the diagram. Most of the arrays have a wide extent and multiple instances of overlapping occur.

This correlates with the almost horizontal array of results for the total primary energy demand of optimised buildings in Fig. 62. As a result, the example of Dortmund would meet EBPC-classes I to IV (corresponding EBPC-indices from

13. Impacts of Climate Change

13.1. General

The greenhouse effect described in chapter 1 will affect the climate world wide. As a result, the buildings of today will face different climatic conditions in the future, resulting probably in different energy demand for heating, cooling and lighting.

Several analyses of climate change have led to different scenarios and predictions of the respective impacts with regards to live on earth. In this chapter some of these predictions will be compared briefly and a qualified prediction of the effects on the energy demand of European office buildings will be given. Finally, an exemplary quantitative outlook on the change of building energy demand will be given.

13.2. Scenarios and Predictions

13.2.1. IPCC Assessment Reports

The most comprehensive and highly acknowledged scientific resources on climate change are the reports of the Intergovernmental Panel on Climate Change (IPCC), a scientific body set up by the World Meteorological Organization (WMO) and the United Nations Environment Programme (UNEP). It was established in 1998 to provide decision-makers and others interested in climate change with an objective source of information on the subject.

The IPCC does not conduct any research nor does it monitor climate related data or parameters. Its role is to assess on a comprehensive, objective, open and transparent basis the latest scientific, technical and socio-economic literature produced worldwide relevant to the understanding of the risk of human-induced climate change, its observed and projected impacts and options for adaptation and mitigation.

The main activity of the IPCC is to provide, in regular intervals, Assessment Reports of the state of knowledge on climate change. Four assessment reports have been completed in 1990, 1995, 2001 and 2007. The fourth (and last) volume is subdivided in a synthesis report and three reports of special working groups (WG):

- WG I: "The Physical Science Basis"
- WG II: "Impacts, Adaptation and Vulnerability"
- WG III: "Mitigation of Climate Change"

Since this fourth assessment report, more regional projections are available. Fig. 94 shows the observed and modelled temperature anomalies during the 20th century for Europe and the global average of land regions (sea regions have lower anomalies). The anomalies in Europe more or less meet the global average of land regions.

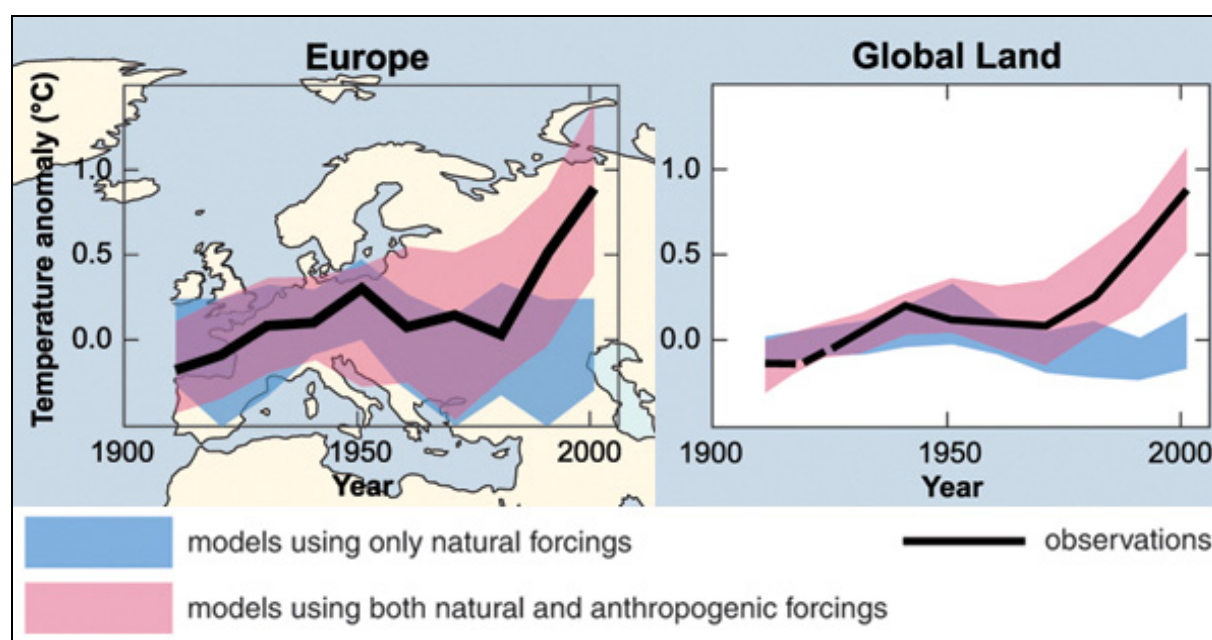


Fig. 94: Comparison of observed European and Global Changes in Surface Temperature with Results simulated by Climate Models using Natural and Anthropogenic Forcings [IPCC-4 WG I].

For the prediction of greenhouse gas (GHG) emissions and their effects on the climate, different scenarios have been developed. These scenarios explore alternative development pathways in terms of demographic, economic and technological driving forces and resulting GHG emissions for the 21st century. The scenarios are divided into four scenario families with different storylines, some with subdivisions describing alternative directions of technology change (see Tab. 12). Referring to the “Special Report on Emission Scenarios” where the scenario definitions have been published for the first time, they are usually called “SRES-scenarios”.

Tab. 12: SRES-scenarios on Emissions of Greenhouse Gases according to [IPCC-4 WG I].

Scenario family	Storyline	Scenario	Development pathways
A1	A world of very rapid economic growth, a global population that peaks in mid-century and rapid introduction of new and more efficient technologies.	A1FI	Technological change towards intensive fossil energy resources.
		A1T	Technological change towards non-fossil energy resources.
		A1B	Technological change towards a balance across all sources.
A2	A very heterogeneous world with high population growth, slow economic development and slow technological change.		
B1	A convergent world, with the same global population as A1, but with more rapid changes in economic structures toward a service and information economy.		
B2	A world with intermediate population and economic growth, emphasising local solutions to economic, social, and environmental sustainability.		

For these scenarios, the averages and assessed ranges for global emissions of greenhouse gases and the global surface warming obtained from different calculation models can be seen in Fig. 95.

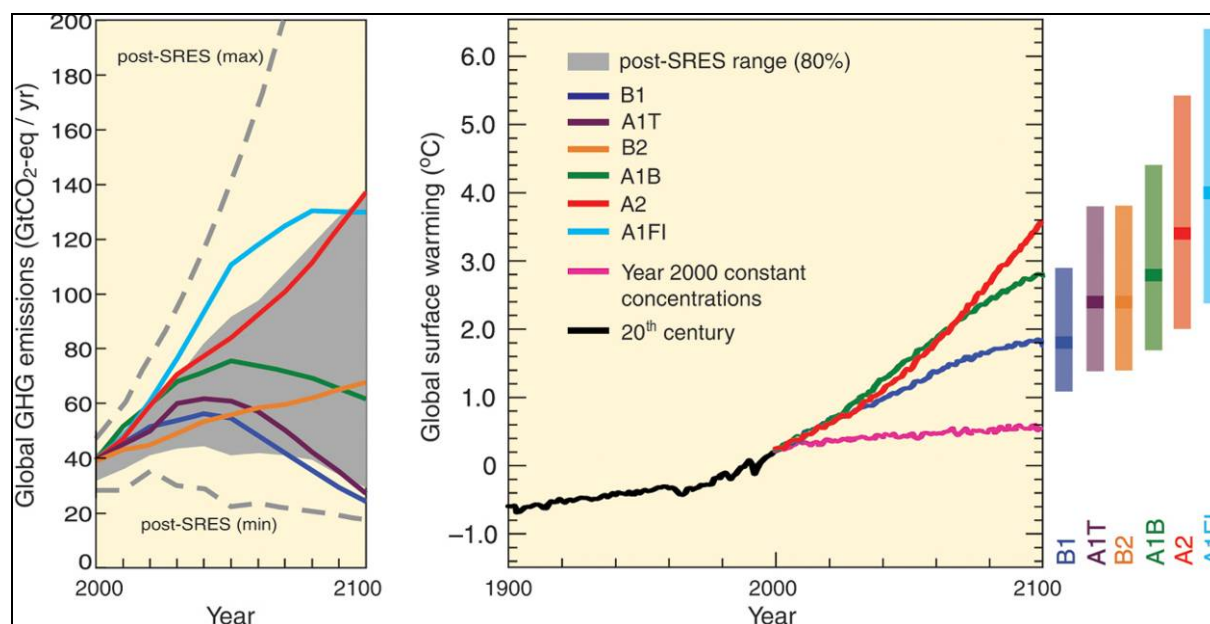


Fig. 95: Multi-model Averages and Assessed Ranges for Global Emissions of Greenhouse Gases and Global Surface Warming during the 21st century [IPCC-4 WG I].

Among the above mentioned scenarios “A1B” has been used for most of the further analyses, as it represents an average development which will be most likely from today’s point of view in the absence of additional climate policies. For this scenario, generally the following tendencies are generally expected for the future development with different probabilities:

- “Virtually certain” (>99% probability):
 - Warmer and fewer cold days and nights over most land areas
 - Warmer and more frequent hot days and nights over most land areas
- “Very likely” (>90% probability):
 - Warm spells / heat waves: Frequency increases over most land areas
 - Heavy precipitation events. Frequency (or proportion of total rainfall from heavy falls) increases over most areas
- “Likely” (>66% probability):
 - Area affected by droughts increases
 - Intense tropical cyclone activity increases

In this work only effects on air temperatures will be summarised.

Generally, it is very likely that all land regions will warm in the 21st century. Looking in detail at the effects in Europe, the annual mean temperatures are likely to increase

more than the global mean. Heat waves, like the summer 2003 in Europe, will become usual. Fig. 96 shows the projected anomalies of average temperatures in Europe for the 21st century according to emission scenario A1B.

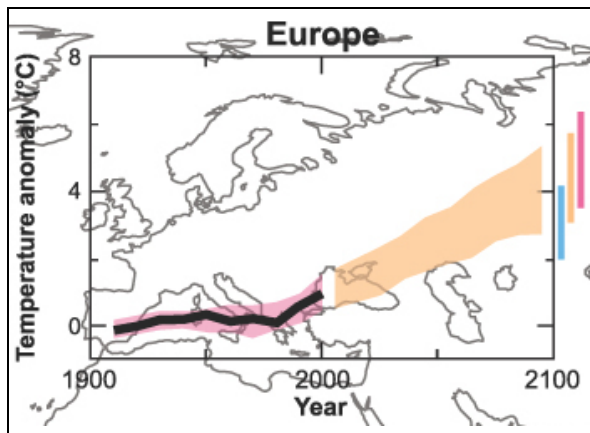


Fig. 96: Temperature Anomalies in Europe with Respect to 1901 to 1950. Observed (black line) and simulated (red envelope, 1906 to 2005) and Projected (orange envelope, 2001 to 2100, A1B scenario) [IPCC-4 WG I].

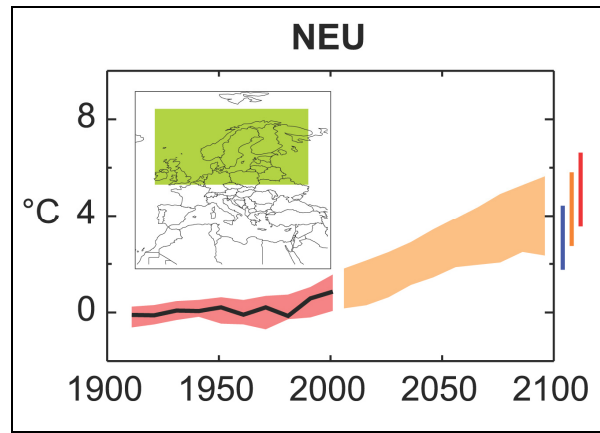


Fig. 97: Temperature Anomalies in Northern Europe with Respect to 1901 to 1950. Observed (black line) and simulated (red envelope, 1906 to 2005) and Projected (orange envelope, 2001 to 2100, A1B scenario) [IPCC-4 WG I].

The more detailed view on the European continent given in Fig. 97 and Fig. 98 shows stronger effects in Northern Europe (NEU) than in southern Europe including the Mediterranean coast (SEM). Also the effects over land are stronger than over sea, therefore a lower degree of effect can be expected on small islands in the Mediterranean Basin (MED, Fig. 99).

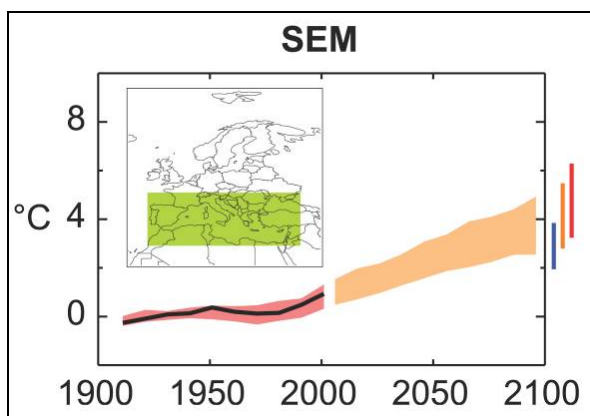


Fig. 98: Temperature Anomalies in Southern Europe including the Mediterranean Coast with Respect to 1901 to 1950. Observed (black line) and simulated (red envelope, 1906 to 2005) and Projected (orange envelope, 2001 to 2100, A1B scenario) [IPCC-4 WG I].

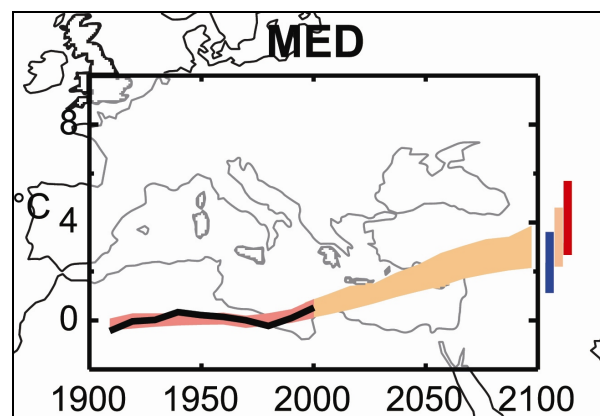


Fig. 99: Temperature Anomalies on Small Islands in the Mediterranean with Respect to 1901 to 1950. Observed (black line) and simulated (red envelope, 1906 to 2005) and Projected (orange envelope, 2001 to 2100, A1B scenario) [IPCC-4 WG I].

Seasonally, the largest warming is likely to be in northern Europe in winter (Dec./Jan./Feb. – DJF) and in the Mediterranean area in summer (Jun./Jul./Aug. – JJA) as shown in Fig. 100. In northern Europe, minimum winter temperatures are

likely to increase more than the European average. In southern and central Europe, maximum summer temperatures are likely to increase more than the average.

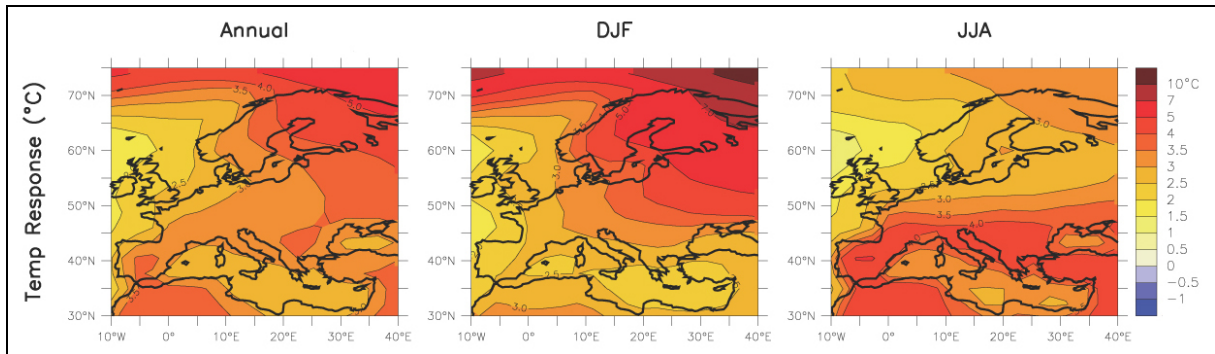


Fig. 100: Annual Mean, Winter (DJF) and Summer (JJA) Temperature Changes over Europe between 1980 to 1999 and 2080 to 2099, averaged over 21 Models (Scenario A1B) [IPCC-4 WG I].

The seasonal temperature change from the years 1980-1999 to 2080-2099 under the A1B scenario for northern (NEU) and southern Europe including the Mediterranean coast (SEM) as well as for the small islands in the Mediterranean (MED) are shown in Fig. 101.

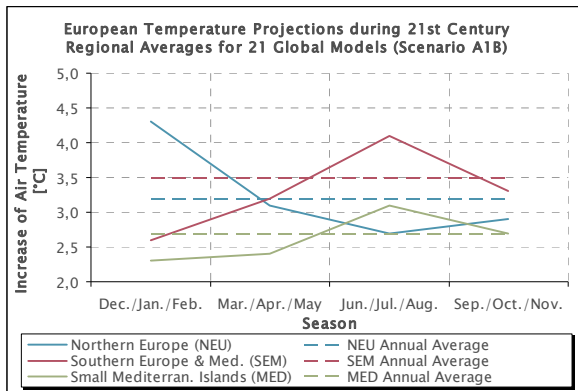


Fig. 101: Seasonal Averages for European Temperature Projections during the 21st Century (based on [IPCC-4 WG I]).

It is obvious that the annual average increasing of air temperatures is highest in northern, lower in southern Europe and lowest on the small islands in the Mediterranean. But whilst in northern Europe mainly the winters become milder, the rest of Europe above all will have significantly warmer summer periods.

Qualitatively these results are a sign for decreasing heating energy demand and less increasing cooling energy demand in northern Europe. In southern Europe slightly decreasing heating energy demand and stronger increasing cooling

energy demand can be expected. The small islands in the Mediterranean will face similar changes as in southern Europe but with reduced intensity.

13.2.2. Prediction of Climate Change in Germany

Based on the results of the IPCC described in chapter 13.2.1, more detailed scenarios per country are currently under development. For Germany, this has been done by a research project commissioned by the Federal Environmental Agency (“Umweltbundesamt”) [Spekat] [Jacob].

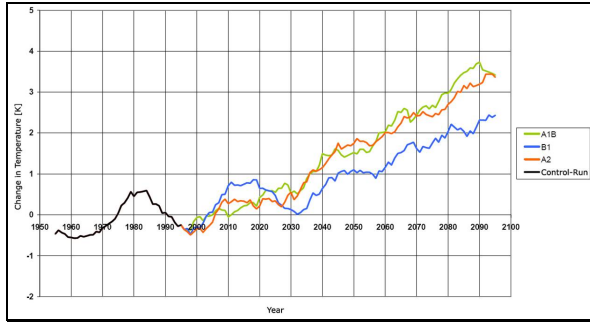


Fig. 102: Increase of Annual Mean Air Temperature (Mean Values of one Decade) in Germany during the 21st Century under the Scenarios A1B, A2 and B1 [Jacob] compared to 1951-1990.

The model used for the prediction of regional changes has been tested by comparison of the calculated and measured data for the period of 1961 to 1990. After this validation and control of the model it has been used for the prediction of regional impacts of climate change. The resulting temperature changes have been compared to the average temperatures from 1961 to 1990. Fig. 102 shows the increase of average air temperatures in Germany during the 21st century, given as mean values per three decades and compared to the period of 1961 to 1990.

For these three scenarios, local projections for Germany have been calculated using a 10km-grid and analysing the seasonal changes in detail. Fig. 103 shows the annual and seasonal increase of mean air temperatures for three emission scenarios. Generally, stronger effects can be observed in southern than in northern Germany. In Winter also the south-eastern parts are more affected than the North-West. In all scenarios the lowest temperature increases will be in spring, the highest in winter.

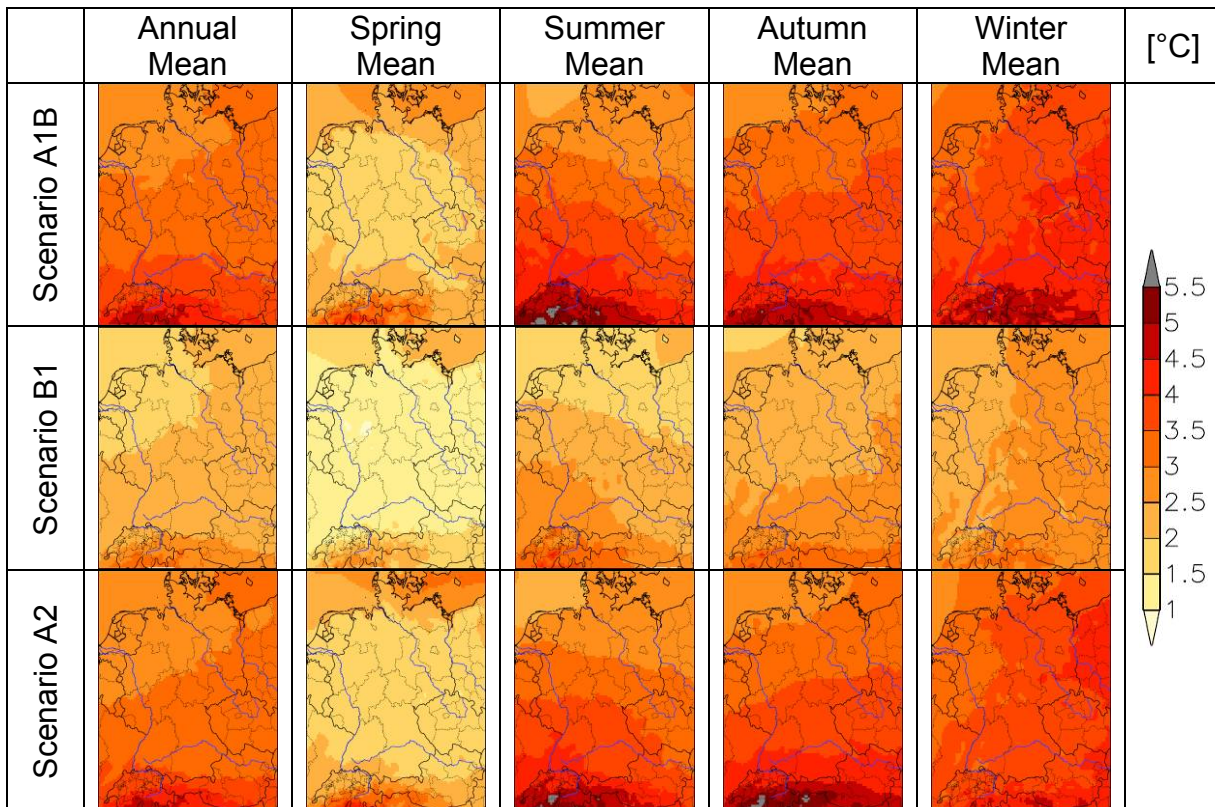


Fig. 103: Annual and Seasonal Temperature Changes in Germany by 2071-2100 compared to 1961-1990 under different SRES-Scenarios [Jacob].

From these projections, the resulting heating degree days have been calculated in [Jacob]. Contrary to the definition in this work (see chapter 6.5.2), a base tempera-

ture and a temperature threshold of 15°C has been used in [Jacob]. Fig. 104 shows the resulting local distribution of heating degree days in Germany during the reference period (1961-1990) and by the end of the 21st century under different emission scenarios. Depending on the emission scenario a reduction of heating degree days between roughly 18% (B2) and 30% (A1B) has been predicted.

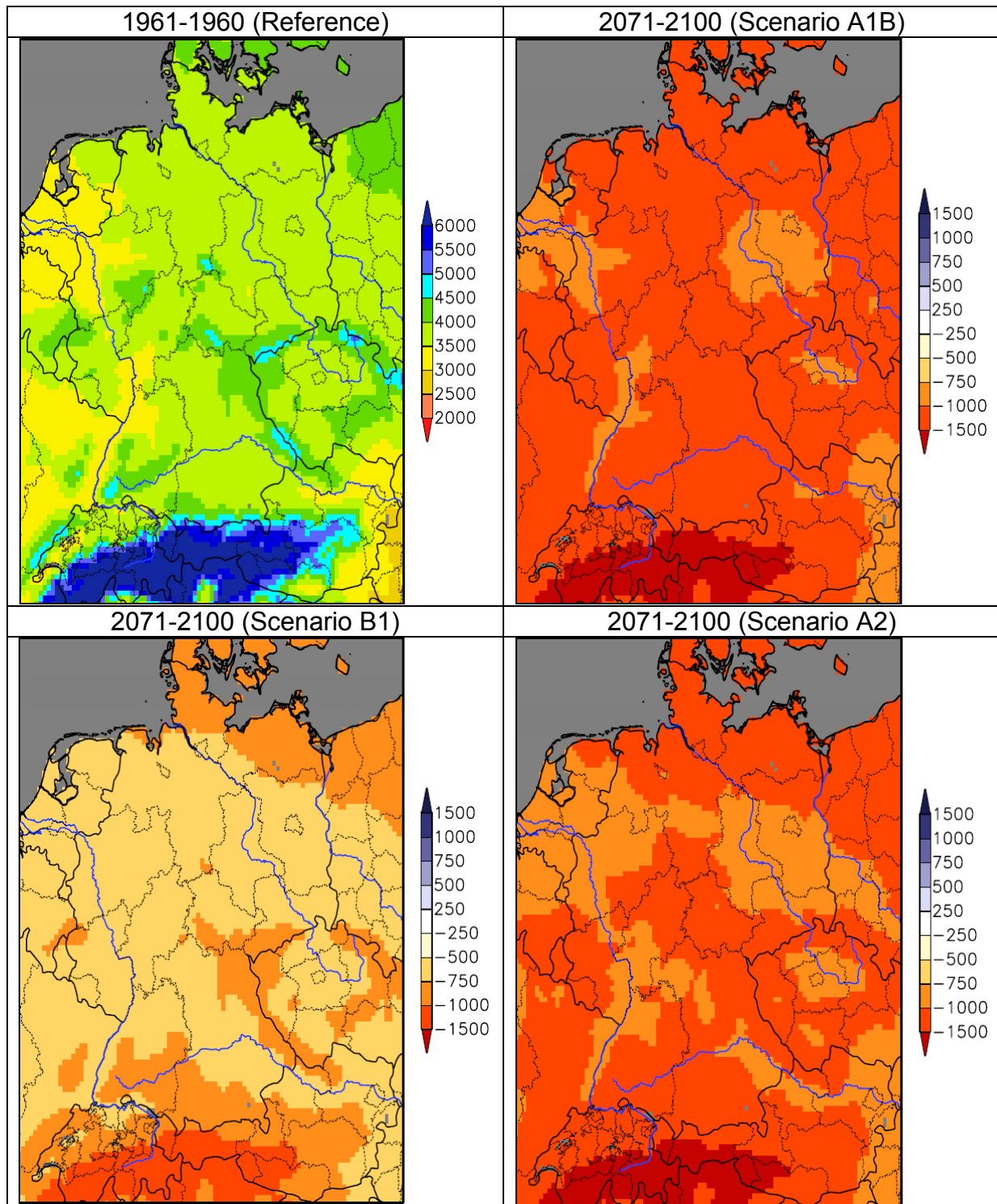


Fig. 104: Heating Degree Days in Germany during the Reference Period and during 2071-2100 under different SRES-Scenarios [Jacob].

The predicted reduction of heating degree days is a sign for significantly lower heating energy demands in Germany during the 21st century. From the predicted increase of air temperatures in summer and autumn (see Fig. 103) increasing cooling energy demand has to be expected.

13.2.3. Predictions of Climate Change in the United Kingdom

In the United Kingdom (UK) the national “Climate Impacts Programme” (UKCIP) commissioned a set of four scenarios of future climate change for the UK based on the current understanding of the science of climate change. In 2002, the resulting report “Climate Change Scenarios for the United Kingdom - The UKCIP02 Scientific Report” was published, summarising the changes already occurring in global and UK climate and presenting information about changes of average climate in the UK under four different scenarios [UKCIP02].

These scenarios have been based on global emission scenarios published in 2000 by the Intergovernmental Panel on Climate Change (IPCC, see chapter 13.2.1). Notwithstanding the SRES-scenarios of the IPCC, the emission scenarios in [UKCIP02] are:

- Low emission (based on B1-Scenario of IPCC)
- Medium-low emission (based on B2-Scenario of IPCC)
- Medium-high emission (based on A2-Scenario of IPCC)
- High emission (based on A1FI-Scenario of IPCC)

The worldwide emissions of carbon dioxide assumed for these scenarios are shown in Fig. 105.

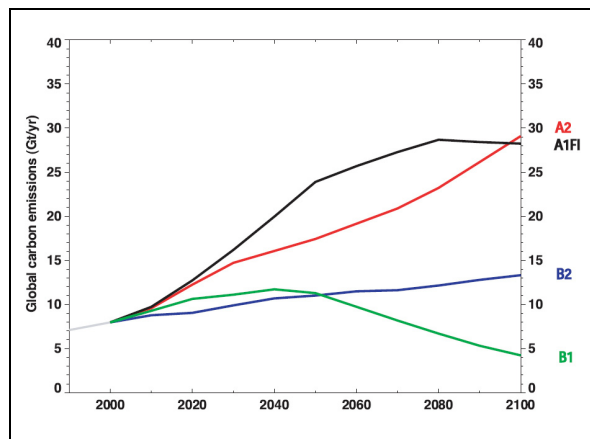


Fig. 105: Global Carbon Emissions from all Sources (Energy, Industry and Land-Use Changes) from 1990 to 2100 for the Four Scenarios used in [UKCIP02]. Observed Values to 2000 are grey.

For these four scenarios the annual and seasonal impacts on local climate in the UK have been calculated using a grid size of 50 km. The resulting projections of annual mean air temperatures are shown in Fig. 106.

For the high emission scenario, the seasonal projections can be obtained from Fig. 107. It can clearly be seen that the south-eastern part of the UK is affected most. From the seasonal projection a major effect during summer and autumn can be observed.

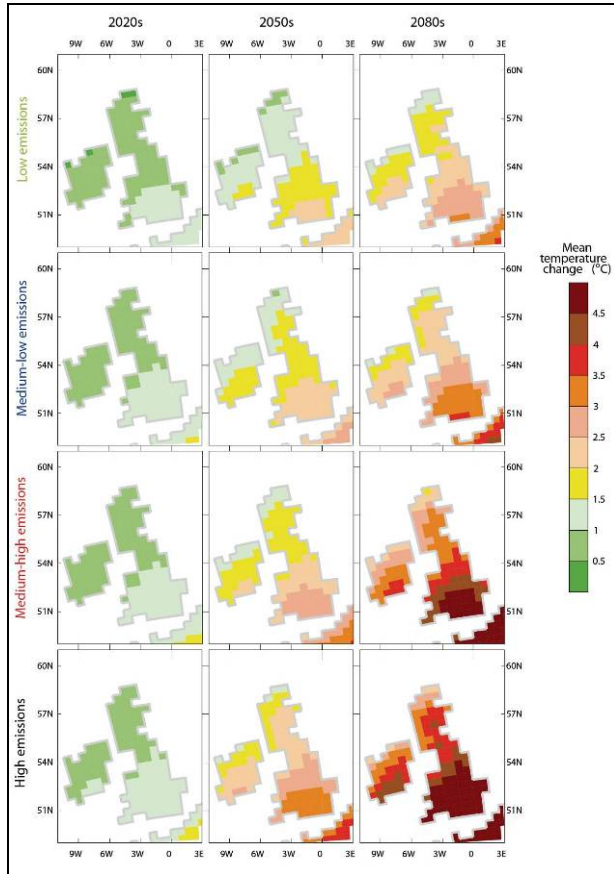


Fig. 106: Change in Average Annual Temperature in the UK (with Respect to the Model-Simulated 1961-1990 Climate) for Thirty-Year Periods centred on the 2020s, 2050s and 2080s under different Emission Scenarios [UKCIP02].

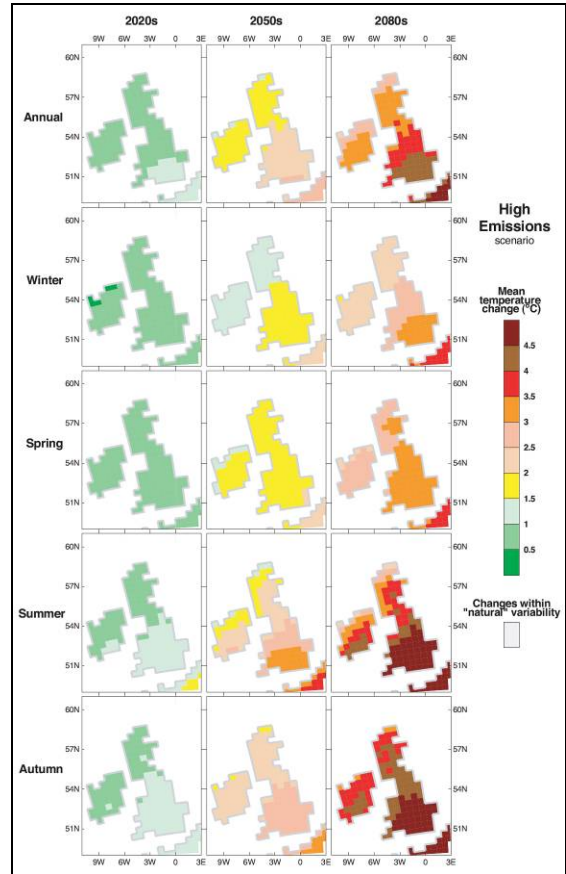


Fig. 107: Change in Average Annual and Seasonal Temperature in the UK (with Respect to the Model-Simulated 1961-1990 Climate) for Thirty-Year Periods centred on the 2020s, 2050s and 2080s under the High Emission Scenario [UKCIP02].

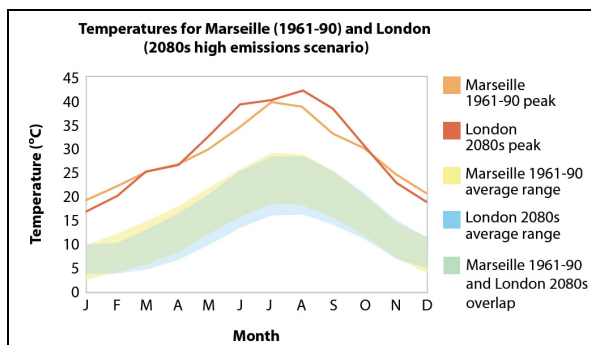


Fig. 108: Comparison of Predicted Average and Maximum Temperatures in London in the 2080s under the High Emissions Scenario with those in Marseille for 1961-90 [UKCIP].

Based on the high emissions scenario in [UKCIP02] a climatic situation in London in the 2080s comparable to Marseille between 1961 and 1990 has been predicted (see Fig. 108).

Overall, the predictions in [UKCIP02] and [UKCIP] are a sign for decreasing heating energy demand and (depending on the emission scenario) significantly increasing cooling energy demand, especially in the south-east of UK.

13.3. Exemplary Impacts of Climate Change on the Building Energy Demand

13.3.1. Switzerland (Th. Frank)

The impacts of climate change on the energy demand of buildings in Switzerland have been analysed in [Frank]. During the period from 1981 to 2003 hourly weather data has been recorded and analysed in a weather station in Zürich (Switzerland), which is considered representative for typical climatic conditions in the Swiss Central Plateau. An increase of mean annual air temperatures of $0,52\text{ }^{\circ}\text{C}$ per decade could be observed (see Fig. 109), whereas no significant increase of the annual mean solar radiation could be observed (see Fig. 110).

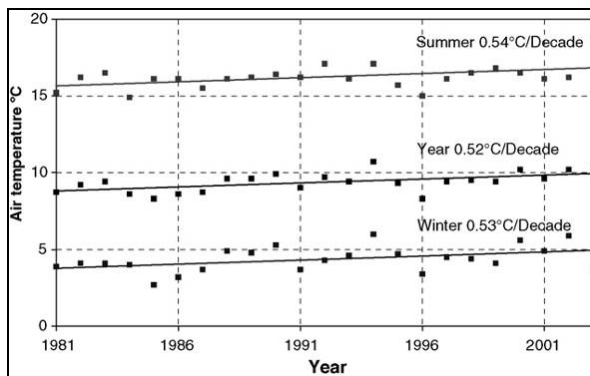


Fig. 109: Trends for mean annual and seasonal air temperature at Zürich-Kloten from 1981 to 2003 [Frank].

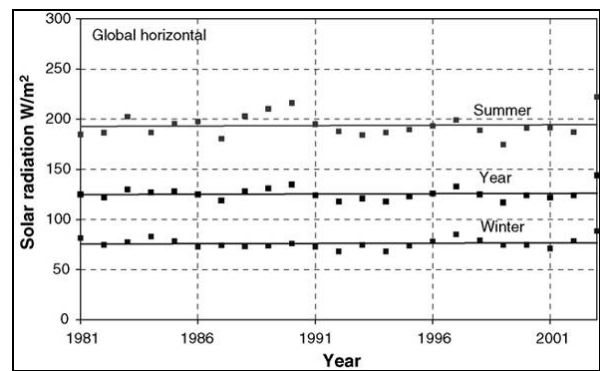


Fig. 110: Trends for mean annual and seasonal mean solar radiation at Zürich-Kloten from 1981 to 2003 [Frank].

For an office building, the energy demand for heating and cooling has been calculated taking into account three levels of insulation, representing the varying building code framework between 1970 and 2000, i.e. large parts of the Swiss building stock:

- Level 1: Representing Swiss building code 1970
($U_{\text{Wall/Roof}} = 0,8\text{ W}/(\text{m}^2\text{K})$, $U_{\text{Floor}} = 0,8\text{ W}/(\text{m}^2\text{K})$, $U_{\text{Window}} = 2,7\text{ W}/(\text{m}^2\text{K})$)
- Level 2: Representing Swiss building code 1980
($U_{\text{Wall/Roof}} = 0,4\text{ W}/(\text{m}^2\text{K})$, $U_{\text{Floor}} = 0,4\text{ W}/(\text{m}^2\text{K})$, $U_{\text{Window}} = 1,9\text{ W}/(\text{m}^2\text{K})$)
- Level 3: Representing Swiss building code 2000
($U_{\text{Wall/Roof}} = 0,2\text{ W}/(\text{m}^2\text{K})$, $U_{\text{Floor}} = 0,2\text{ W}/(\text{m}^2\text{K})$, $U_{\text{Window}} = 1,4\text{ W}/(\text{m}^2\text{K})$)

Furthermore, the level of internal sensible gains has been varied between standard (building 1) and high (building 2) values.

Four different scenarios with different climatic conditions have been calculated, referring to the climatological normals still used as boundary conditions for building design according to actual standards:

- Scenario A: Climatological normals
 (World Meteorological Organisation WMO reference period of 1961-1990)
- Scenario B: Temperature rise +0,7 °C
 (design reference year based on 1981-1990)
- Scenario C: Temperature rise +1,0 °C
 (reference year, based on the measured temperature increase 1984-2003)
- Scenario D: Temperature rise +4,4 °C
 (warm reference year, based on the measured temperature increase 1984-2003 and the projections for 2050-2100 in the third IPCC assessment report [IPCC-3 WG I])

The resulting heating and cooling energy demands of building 1 (Fig. 111) and building 2 (Fig. 112) both show decreasing heating and increasing cooling energy demand over time. Compared to the reference scenario “A”, in building 2 the heating energy demand decreases by up to 58% and the cooling energy demand increases by up to 1050% by the second half of the 21st century. Less strong effects can be observed with lower internal loads (building 1).

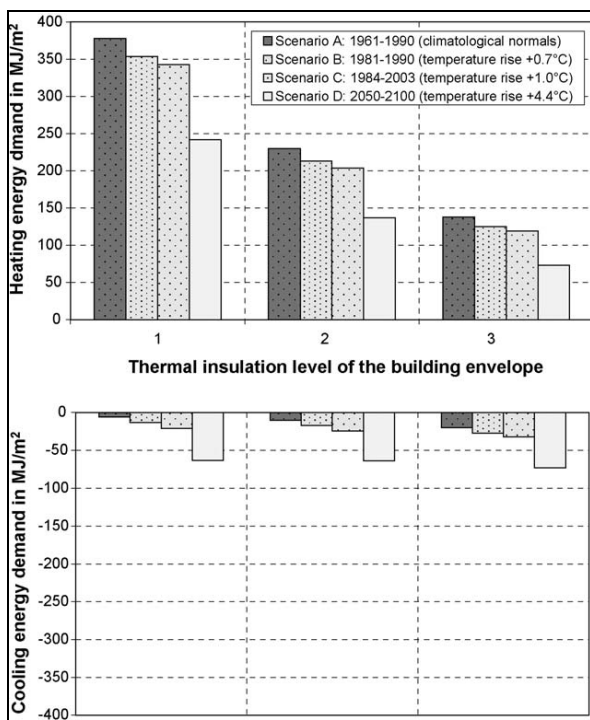


Fig. 111: Annual Heating and Cooling Energy Demand of Office Building 1 for Three Levels of Thermal Insulation [Frank].

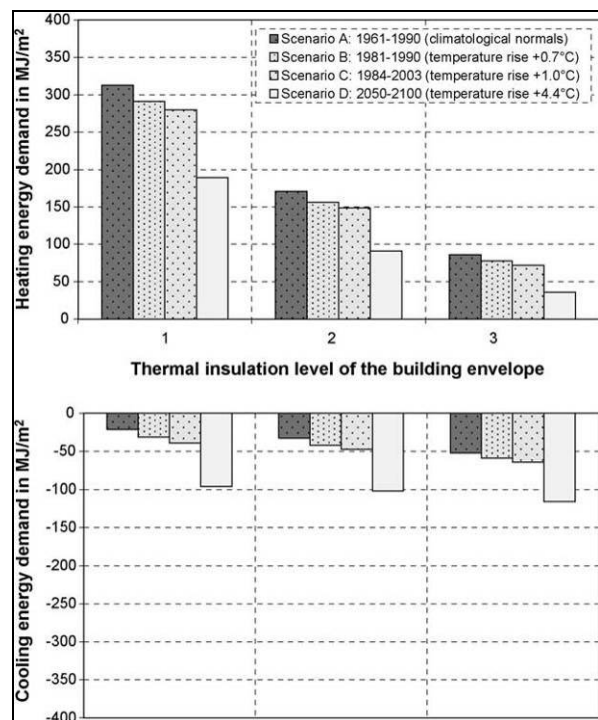


Fig. 112: Annual Heating and Cooling Energy Demand of Office Building 2 for Three Levels of Thermal Insulation [Frank].

A holistic evaluation of the contrary effects of climate change and insulation on heating and cooling energy demand have not been performed by [Frank], since primary energy demand has not been calculated.

13.3.2. United Kingdom (Hacker / Belcher / Connell)

Based on the local climate changes predicted in [UKCIP02] (see chapter 13.2.3), the impacts on different building types significant to the UK building stock have been analysed in [UKCIP]. The results have been calculated for buildings located in London under the medium-high emissions scenario, while the impacts have not been expressed in energy demand, but in resulting discomfort room temperatures and CO₂-emissions.

One of the case studies was a 1960's office building, which has been analysed in a state "as built" as well as in an "adapted" state. The adaptation of the building comprised the increase of the insulation level (windows, walls, roof etc.), the increase of the air tightness, the introduction of solar shading, a mechanical ventilation system with heat recovery, night ventilation in the summer, cooling beams etc.

Fig. 113 and Fig. 114 show the discomfort temperatures and CO₂-emissions in the "as built" situation. A significant increase of hours with discomfort temperatures could be observed as a result of climate change to the 2080s. The CO₂-emissions develop in opposite direction over the time, resulting from reduced heating loads (boiler) and the lack of a cooling facility.

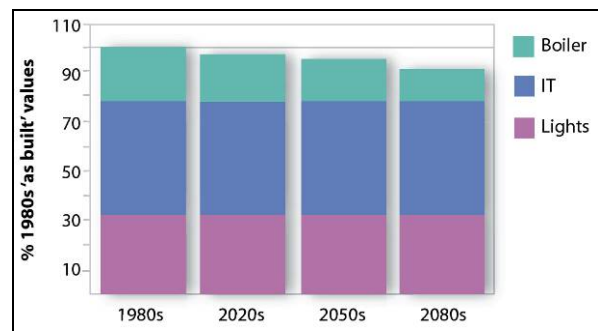
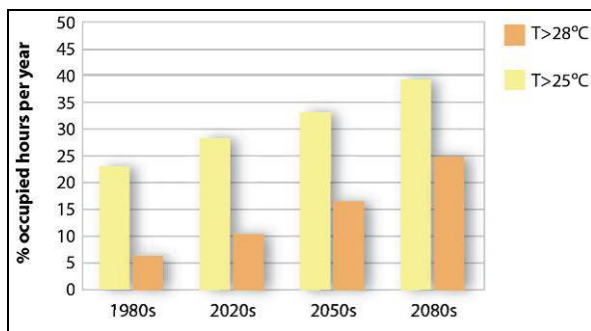


Fig. 113: Average Discomfort Temperatures, Office Building "as built" [UKCIP].

Fig. 114: CO₂-emissions, Office Building "as built" [UKCIP].

Fig. 115 and Fig. 116 show the same results in the "adapted" situation. The number of hours with discomfort temperatures still increases over time due to climate change, but they could be reduced to some incidences of hours between 25 and 28 °C resulting from the cooling and control strategy. The CO₂-emissions now comprise additional emissions from energy for mechanical ventilation (fan) and cooling (chiller).

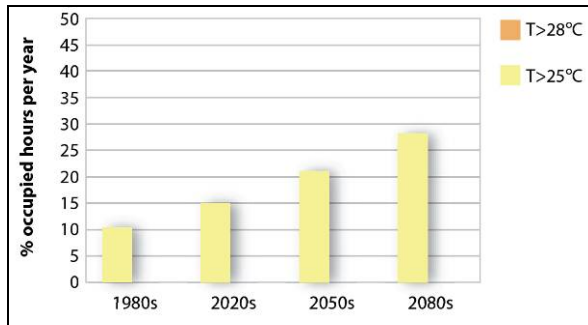


Fig. 115: Average Discomfort Temperatures, Office Building “adapted” [UKCIP].

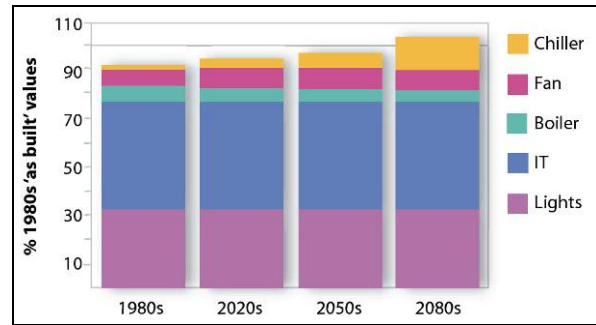


Fig. 116: CO₂-emissions, Office Building “adapted” [UKCIP].

Compared to the “as built” situation the total emissions in the 1980s are lower despite the additional emissions from air transport (Fan) and Cooling (Chiller). Over time, the emissions from heating (boiler) are still decreasing and the emissions from cooling increase significantly, both due to climate change. Only between the 2050s and 2080s the total 1980s “as built” total emission values will be exceeded.

The influence of solar shading on the energy demand for artificial lighting, which is responsible for more than 30% of the emission in 1980s “as built” situation has not been considered in this study.

13.3.3. Example: „Typical“ and „Optimised Buildings“ in London and Glasgow

Based on the results of [UKCIP02] a tool for the generation of new statistical weather files for the use in building simulation programs has been developed [Jentsch]. This allows the dynamic simulation of building models under climatic conditions in the United Kingdom (UK) while taking into account impacts of climate change.

Using this tool, weather data has been generated for the two locations in UK analysed in this work, London and Glasgow for the reference period (1961-1990) as well as for the 2020s, 2050s and 2080s and for each of the four emission scenarios described in 13.2.3. Fig. 117 and Fig. 118 show the annual mean air temperatures increasing in these weather data both with emissions and over time. Independent from climate change, the temperature level is generally higher in London than in Glasgow.

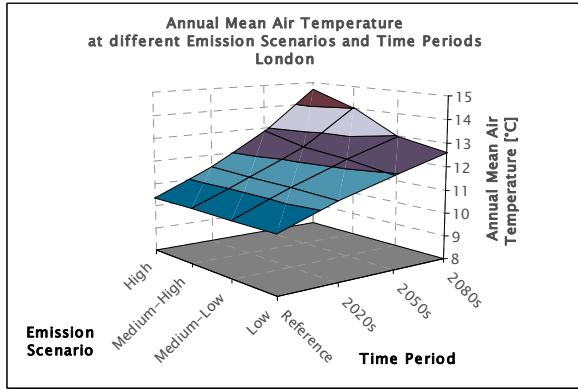


Fig. 117: Annual Mean Air Temperature in London during the 21st Century under different Emission Scenarios and Periods.

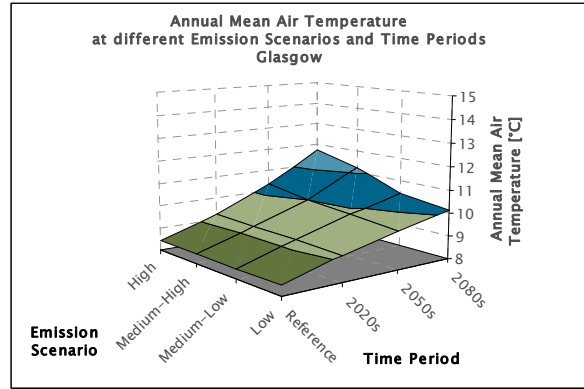


Fig. 118: Annual Mean Air Temperature in Glasgow during the 21st Century under different Emission Scenarios and Periods.

The annual solar radiation on a horizontal surface (Fig. 119 and Fig. 120) shows the same variations, whereas again the level is generally higher in London than in Glasgow. Therefore, independent from the emissions scenario and the time period, increasing solar radiation and annual mean air temperatures in both locations have to be expected in the future.

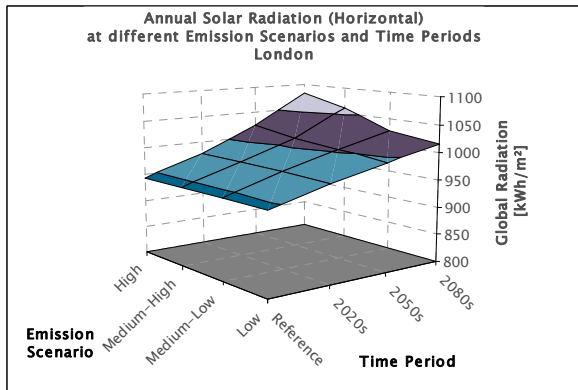


Fig. 119: Annual Solar Radiation in London during the 21st Century under different Emission Scenarios and Periods.

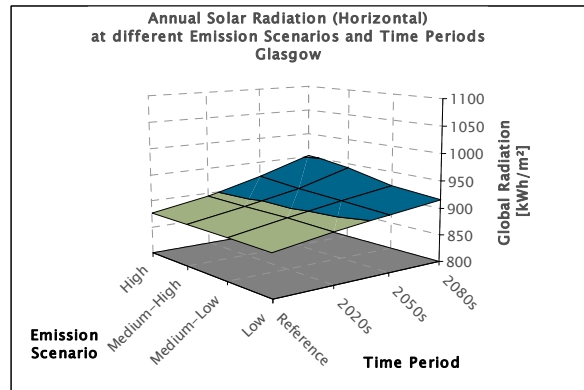


Fig. 120: Annual Solar Radiation in Glasgow during the 21st Century under different Emission Scenarios and Periods.

For further analysis the increase of air temperature over the year has been grouped to average values of three months, representing roughly the seasons winter (DJF), spring (MAM), summer (JJA) and autumn (SON). Fig. 121 and Fig. 122 exemplify the variation of mean air temperatures per season for both locations under the high emissions scenario.

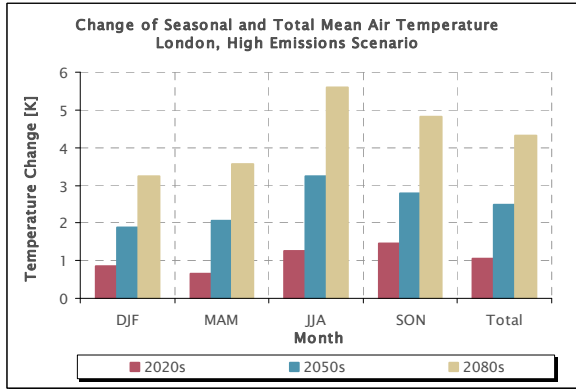


Fig. 121: Change of Seasonal Mean Air Temperatures during the 21st Century in London under High Emissions Scenario.

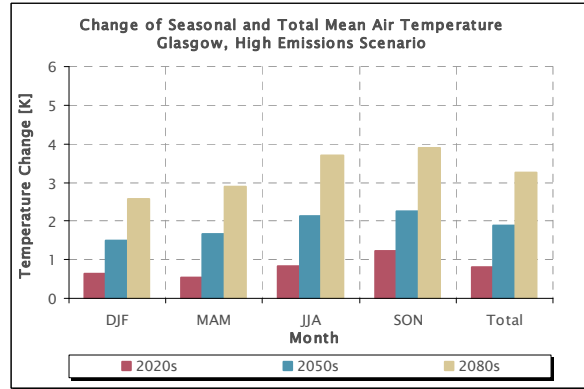


Fig. 122: Change of Seasonal Mean Air Temperatures during the 21st Century in Glasgow under High Emissions Scenario.

For all seasons and periods a significant temperature change can be observed, whereas the increase of temperatures in summer and autumn is higher than in winter and spring and the effects are stronger in London than in Glasgow. These findings correlate with the results described in chapter 13.2.3.

The simulation of the two building types specified in this work (optimised and typical buildings) with these new weather data gives a detailed view on the impact of climate change on the primary energy demand of these buildings.

Starting with the optimised building, Fig. 123 and Fig. 124 exemplify the total primary energy demand and its partial values for the reference period as well as for three future periods of the 21st century under the high emissions scenario. Both locations show a significant decrease of heating and increase of cooling energy demand over time. In London, where the cooling demand is slightly higher than the heating energy demand during the reference period, this difference increases over time. Glasgow, which is rather heating dominated during the reference period, will become cooling energy demand dominated during the middle of the 21st century under the high emissions scenario.

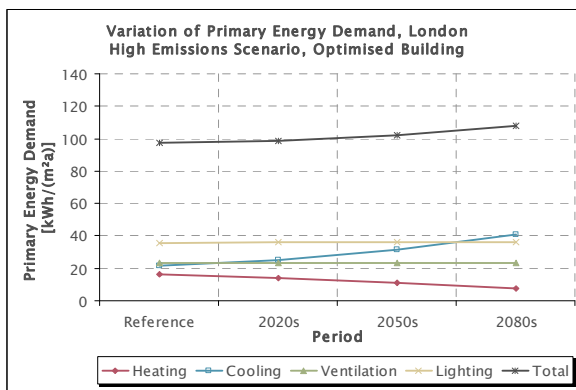


Fig. 123: Variation of Primary Energy Demand of an Optimised Building in London during the 21st Century under High Emissions Scenario.

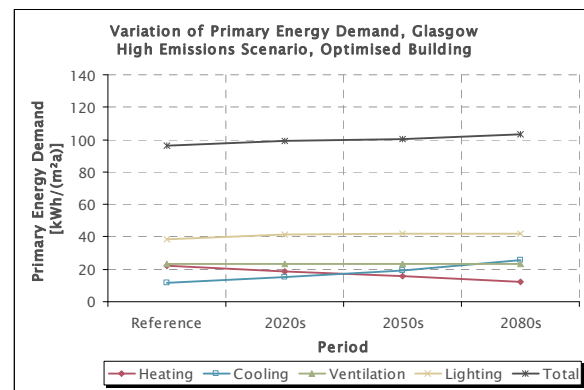


Fig. 124: Variation of Primary Energy Demand of an Optimised Building in Glasgow during the 21st Century under High Emissions Scenario.

The lighting energy demand slightly increases as a result of increasing solar radiation and therefore more frequent activation of the shading systems. Generally, a good correlation between the primary energy demand and the climatic conditions can be observed with the optimised buildings.

Overall, these contrary variations even out partially and only a slight increase of the total primary energy demand over the time can be observed in both locations. Like before (see chapter 9), the optimised buildings in both locations perform on a comparatively good (i.e. low) level, even taking into account the changing climate under the high emissions scenario. Under all scenarios, the total primary energy demand increases with both emissions and time, whereas the maximum increase compared to the reference period is about 10% for both locations (see Fig. 125 and Fig. 126).

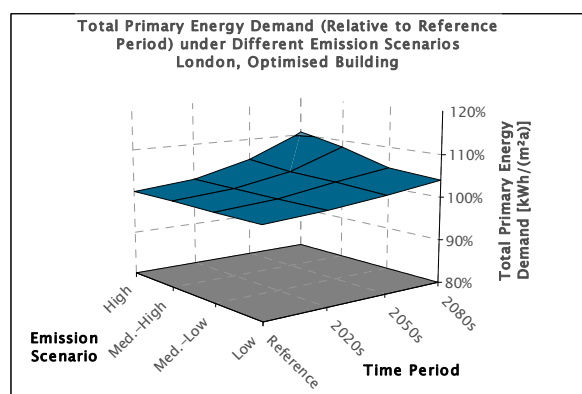


Fig. 125: Variation of Primary Energy Demand of an Optimised Building in London during the 21st Century under different Emissions Scenarios and Periods.

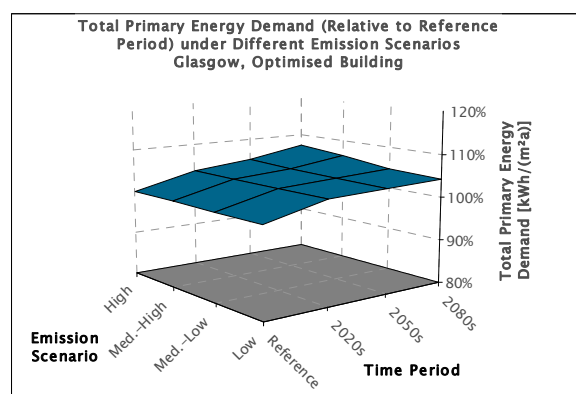


Fig. 126: Variation of Primary Energy Demand of an Optimised Building in Glasgow during the 21st Century under different Emissions Scenarios and Periods.

In the typical buildings under the high emissions scenario heating energy demand decreases and cooling energy demand increases over time as well. But as a result of the lower level of insulation the building responds much more on the climatic conditions. Both locations are heating dominated in the reference period, whereas the difference between heating and cooling energy demand is much higher in Glasgow than in London. Therefore, under the high emissions scenario the building in London becomes cooling dominated in the second half of the 21st century (see Fig. 127), whereas the building in Glasgow remains heating dominated with a decreasing difference between heating and cooling energy demand (see Fig. 128).

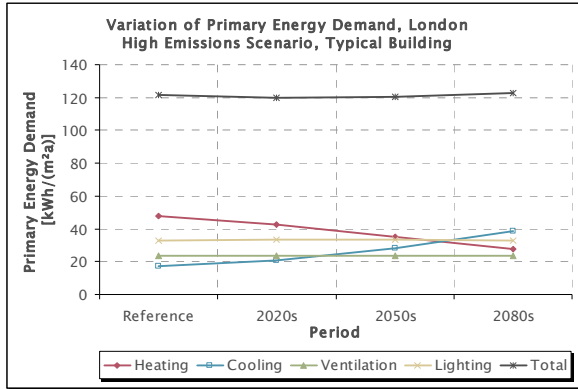


Fig. 127: Variation of Primary Energy Demand of a Typical Building in London during the 21st Century under High Emissions Scenario.

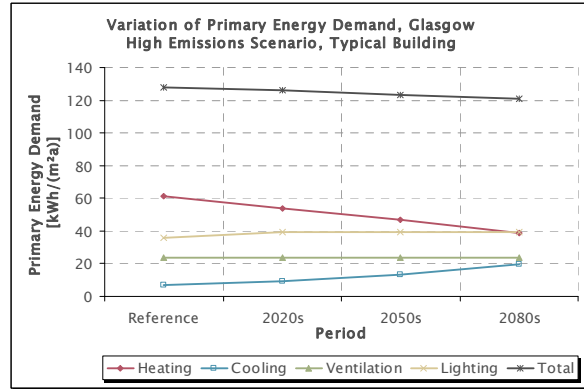


Fig. 128: Variation of Primary Energy Demand of a Typical Building in Glasgow during the 21st Century under High Emissions Scenario.

Due to these differences the total primary energy demand slightly decreases by the mid (London) or end (Glasgow) of the 21st century. Nevertheless, it is higher than in the optimised buildings at any time. The maximum relative variation of total primary energy demand under all emission scenarios during the 21st century is less than 2% (London, Fig. 129) and 5% (Glasgow, Fig. 130).

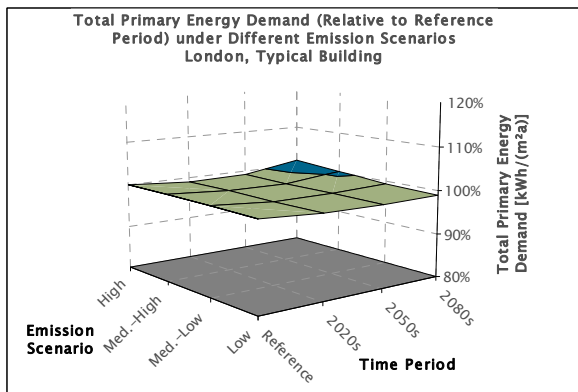


Fig. 129: Variation of Primary Energy Demand of a Typical Building in London during the 21st Century under different Emissions Scenarios and Periods.

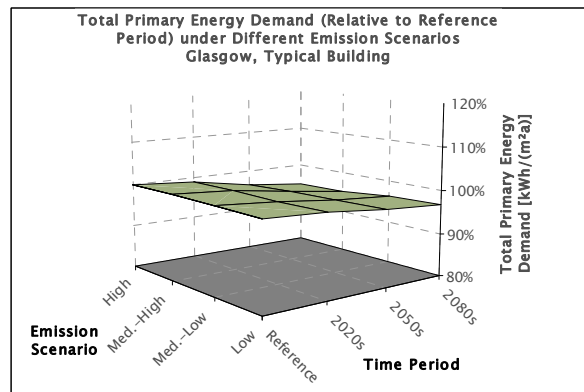


Fig. 130: Variation of Primary Energy Demand of a Typical Building in Glasgow during the 21st Century under different Emissions Scenarios and Periods.

Summarising the results of these analyses, only slight variations of the total primary energy demand could be observed even under the high emissions scenario. Although the decreasing heating and increasing cooling energy demand may even out more or less, the sometimes significant differences between both demonstrate that impacts of climate change should be taken into account in building design. By tapping the potentials resulting from these developments and designing buildings optimised for the conditions predicted for their period of life, the performance can be improved.

Despite increasing cooling loads in the future and decreasing energy loads in Glasgow over time, the “optimised” buildings with high insulation level in both locations generally perform better than the “typical” buildings.

14. Conclusions

A rough correlation of climatic conditions with the latitude can be observed. Variances mainly occur with winter temperatures, which are influenced for example by a locations' distance from the sea. Due to such local influences on the climate, deducted climatic terms represent the climate of a location more precisely and are more appropriate for the use with buildings.

Typical buildings in Europe have very different insulation levels, depending on national regulations, building traditions etc. Therefore, a strong variation of heating energy demand of typical buildings can be observed. This results in a poor correlation of heating and subsequently total primary energy demand with both the latitude and the heating degree days. Better correlation can be observed for cooling and lighting energy demands, which are more dominated by solar radiation.

Amongst energetic relevant parameters of the façade, the insulation level and the window proportion have the main influence on the total primary energy demand of a building. Despite the contrary influences on heating, cooling and lighting energy demand, the optimisation of buildings in terms of window proportion and insulation level results in very similar optimised buildings all over Europe. The lowest total primary energy demand can be achieved with medium window proportions and a very high insulation level. In all locations the highest demand results from fully glazed façades with low insulation level. The difference between the lowest and the highest total primary energy demand per location (i.e. the significance of building optimisation) increases from South to North, mainly due to the higher heating energy demand in colder climates. Only minor differences between different orientations of the façades could be observed.

With buildings optimised in this way, generally lower heating and higher cooling and lighting energy demand than in the typical buildings can be expected, while the total primary energy demand is significantly lower in the optimised buildings. Independent from the location in Europe, almost the same level of total primary energy demand can be achieved.

In optimised buildings, a good correlation of the primary energy demand with the latitude can be observed, especially in terms of cooling and lighting energy. Heating, cooling and lighting energy demand correlate even better with the deducted climatic terms of heating / cooling degree days and the total annual illumination of a location. Therefore, these correlations can be used to analyse the climatic influence on the energy demand of European office buildings.

As long as efficient ventilation and cooling systems with low dehumidification rates are used, the latent cooling loads resulting from the dehumidification of supply air even in southern Europe have low significance compared to the total primary energy demand. An exponential increase of latent cooling energy demand has to be expected even in middle or northern Europe for higher dehumidification rates, which should be avoided as much as possible.

Based on the good correlation of the energy demand in optimised buildings with deducted climatic terms, a classification of climates with respect to the building energy

demand can be deducted. As the absolute values of energy demand depend on many other factors specific to a certain building, this classification should correlate the energy demand relative to the European bandwidth with deducted climatic terms. Since the annual illumination correlates well with the solar radiation, lighting energy demand can be correlated to cooling degree days as well. Therefore, a “European Building Performance Climate Classification” (EBPCC) can be based on the heating and cooling degree days of a location’s climate. The classification has to focus separately on heating, cooling and lighting, since the very narrow bandwidth of total energy demand of optimised buildings in Europe is not suitable as a benchmark.

The change of climate resulting from the greenhouse effect will have an impact on the energy demand of European office buildings. Depending on different scenarios for the emission of greenhouse gases in the future, these impacts will be more or less significant. Local differences of the impacts of climate change have to be expected.

Generally, increasing cooling and decreasing heating loads have to be expected. These contrary impacts will partly even out, so that depending on the location, increasing, unchanged or even decreasing total primary energy demand has to be expected. Nevertheless, European office buildings in the future might face climatic conditions significantly different from the climate in the past, which is still today the basis for a buildings’ design.

The possible impacts of climate change on the energy demand of buildings should be taken into account in the planning process in order to avoid increasing energy demand and tap the full savings potential resulting from it. Therefore, there is a strong need for adapted sets of climatic data, taking into account the impacts of climate change on the local climates in Europe. Once this new data is available, planning tools like the EBPCC could be adapted, focussing on probable future situations instead of the past.

15. Summary

The change of climate as a result of greenhouse gas emissions leads to increasing efforts to reduce these emissions worldwide. The global share of buildings in the emissions of greenhouse gases is about 15%, of which about 35% can be traced to commercial buildings (see Fig. 131). Because of this and the increasing energy prices, the importance of the energy efficiency of office buildings has increased.

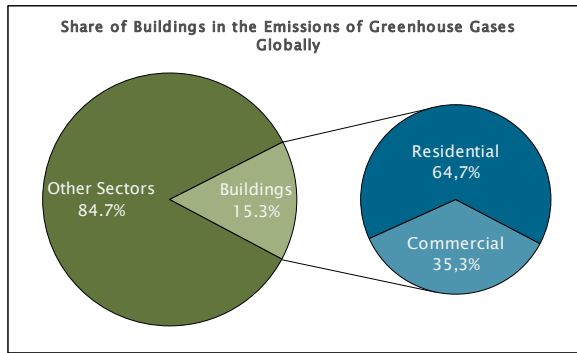


Fig. 131: Share of Buildings in the Global GHG-Emissions [WRI].

demand relevant for the total energy performance of office buildings, i.e. heating, cooling, ventilation and lighting.

In this work, the climatic influences on the total primary energy demand of European office buildings have been analysed by the use of dynamic building simulation tools. Therefore, 25 locations from all over Europe between 60 and 40 degree northern latitude have been selected, grouped in steps of 5° northern latitude (see Fig. 132).

The climate in these locations has been analysed by statistical evaluation of air temperatures, solar radiation, horizontal illumination and other climatic elements. Furthermore, building specific climatic terms such as heating and cooling degree days have been deducted.

Correlations between the latitude and the statistical and building specific climatic terms have been analysed and could be proved with different accuracy, whereas local particularities have been detected mainly from the lowest temperatures during the winter season. Fig. 133 exemplifies the correlation between heating and cooling degree days (HDD / CDD) and the latitude, of which the variance of the HDD has been stronger than of the variance of the CDD.

As the energy demand of buildings depends on many factors, a comparison between different buildings usually has low significance. The climatic conditions of a buildings' location are one of the aspects weakening the benchmark of buildings in a larger geographic scale, for example within Europe.

Existing systems for the classification of climates often are not related to the energy demand of buildings at all or at least do not consider all parts of the energy



Fig. 132: Map of Europe with Selected Locations.

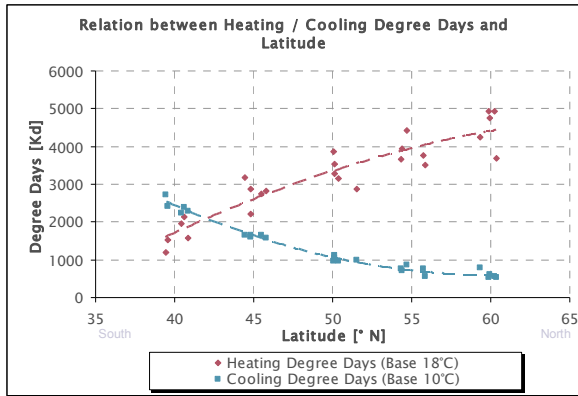


Fig. 133: Heating and Cooling Degree Days as Functions of the Latitude.

For each of the 25 locations the primary energy demand for heating, cooling, ventilation and lighting has been calculated by annual simulations in time steps of one hour. By definition of a uniform ventilation system, the ventilation energy demand did not vary, but has been taken into account for the calculation of the total primary energy demand.

The simulation model comprised a single office room of about 11 m², which has been analysed in four orientations (North, East, South, West).

For the simulation, many assumptions had to be made, representing a standard office building. In previous studies, the window proportion and the insulation level of the façade turned out to have major influence on the total energy performance of office buildings. Therefore, these characteristics have been parameterised in five equidistant steps within a typical bandwidth. Fig. 134 shows external and internal visualisations of the five façade types (window proportions w1 – w5) with the resulting daylight situations at diffuse sky conditions, which have been taken into account for the calculation of the lighting energy demand.

w1 (30%)	w2 (47,5%)	w3 (65%)	w4 (82,5%)	w5 (100%)
Aperture Proportion: 20,2%	Aperture Proportion: 32,0%	Aperture Proportion: 43,8%	Aperture Proportion: 55,6%	Aperture Proportion: 67,4%

Fig. 134: Exemplary Visualisation of five Façades with different Window Proportions and resulting Daylight Situations inside the Office at Diffuse Sky Conditions.

The window proportion in Fig. 134 describes the ratio between the window area and the area of the whole façade segment. The resulting aperture proportion describes the ratio between the window area and the floor area of the room.

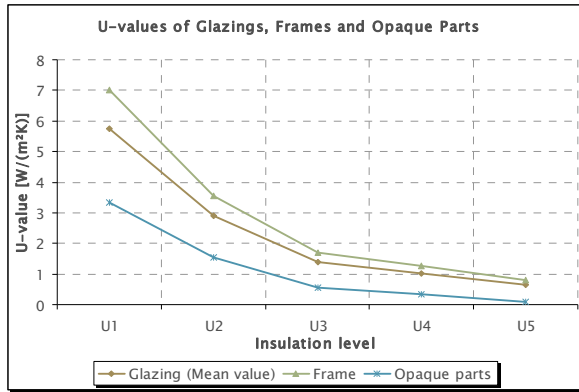


Fig. 135: U-values of Glazings, Frames and Opaque Parts Depending on Insulation Level.

The insulation level has been varied in five steps as well, while the upper and lower limits of the bandwidth have been defined by technical limitations. Fig. 135 shows the proportional variation of U-values for glazing types, frames and opaque parts of the façade within five insulation levels.

As the insulation level of a building often depends on local influences such as national building regulations, building traditions etc. two analyses have been carried out.

One analysis has been defined as “Typical Buildings”, comprising façade U-Values typical in the respective country of the location and assuming a window proportion of 65% (average value of the bandwidth).

Secondly, a parameter analysis has been performed, minimising the annual total primary energy demand by variation of the window proportion and the insulation level in five steps each. This analysis has been repeated for one representative location per group of latitude, also analysing the differences between heat and sun protection glazing.

Fig. 136 exemplifies the results of the parameter variation in Praha (50 °N) using a heat protection glazing. The lowest total primary energy demand has been achieved with a window proportion of 65% and the highest insulation level (red circle).

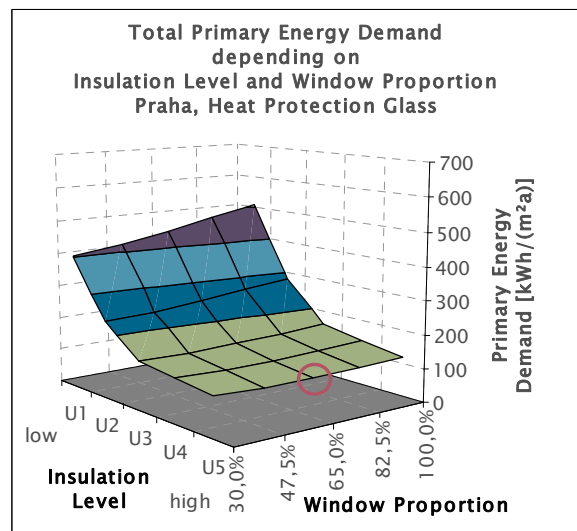


Fig. 136: Total Primary Energy Demand of an Optimised Building in Praha with Heat Protection Glass as Function of Insulation Level and Window Proportion.

By performing this analysis for the five representative locations, a set of “Optimised Buildings” could be defined for each location, wherein the results have been very similar. Despite significant, but partly contrary differences of the primary energy demands for heating, cooling and lighting, in almost all groups of latitude the lowest total primary energy demand was found with the highest insulation level, a window proportion of 65% (exception: 60 °N with a window proportion of 47,5%) and a heat protection glazing. The highest energy demand always occurred with fully glazed façades ($w_5=100\%$) and the lowest insulation level. The difference between the lowest and the highest total primary energy demand per location (i.e. the significance of building optimisation) increased from South to North, mainly due to the higher heating energy demand in colder climates.

The simulation of both the typical and optimised buildings in all 25 locations brought two series of results which have been compared to the latitude and the climatic conditions of the locations. As a result of the national differences of the insulation levels, the total primary energy demand of the typical buildings showed a poor correlation with the latitude as well as with the climatic conditions. Especially the variance of the heating energy demand was strong and affected the total primary energy demand accordingly.

Generally, the optimised buildings had lower total primary energy demand in all locations, so a high insulation level with moderate window proportions proved to be best in all locations over Europe.

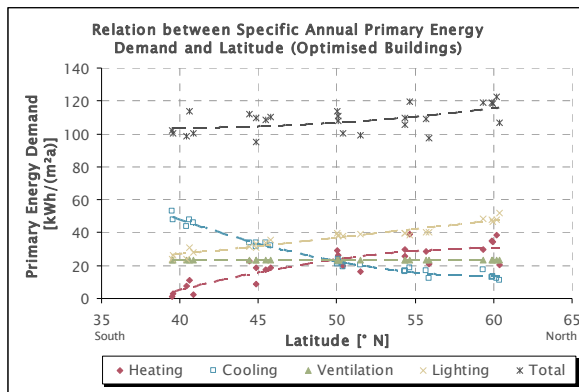


Fig. 137: Annual Primary Energy Demand of Optimised Buildings as Function of Latitude.

From these results a rough estimation of the climatic influences on the energy demand could be deduced from the latitude of a location. Due to the many other influences on the absolute energy demand, the results obtained from the optimised buildings have been referred to the average values of their respective bandwidths. This resulted in a rough “European Building Energy Benchmark” (EBEB).

Fig. 138 visualises the primary energy demand for heating, cooling and lighting in optimised buildings relative to the European Average (100%) and depending on the latitude.

Fig. 137 shows the results of the optimised buildings as functions of the latitude. The graphs predominantly correlate well with the latitude. Increasing trends for the heating and lighting, decreasing trends for the cooling energy demand from South to North can be observed, whereas only the heating energy demand shows a remarkable variance of the results. This also affects the variance of the total primary energy demand which only slightly increases from South to North, but overall in the European comparison varies about only 10%.

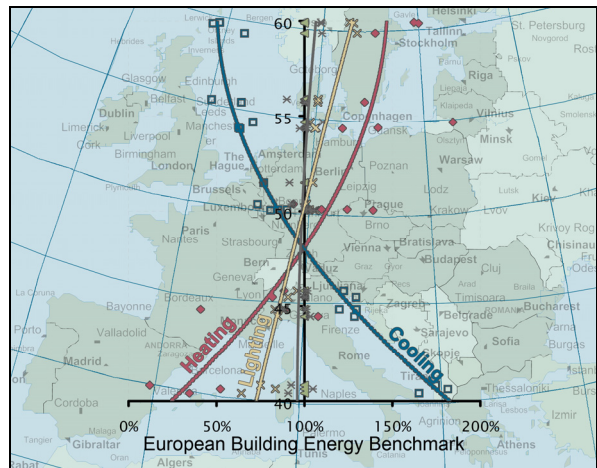


Fig. 138: European Building Energy Benchmark (EBEB) for Heating, Cooling and Lighting depending on the Latitude.

From the analyses of climates, an even better correlation of results with the deduced climatic terms has been expected and could be proved. Fig. 139 shows the correlation of heating and cooling energy demand with the respective degree days as well as the correlation of lighting energy demand with the total annual illumination on a horizontal surface. Since both cooling and lighting energy demand are strongly de-

pending on the solar radiation, a correlation between lighting energy demand and cooling degree days could be proved.

The correlations in Fig. 139 show the actual climatic influences of a location on the energy demand of a building.

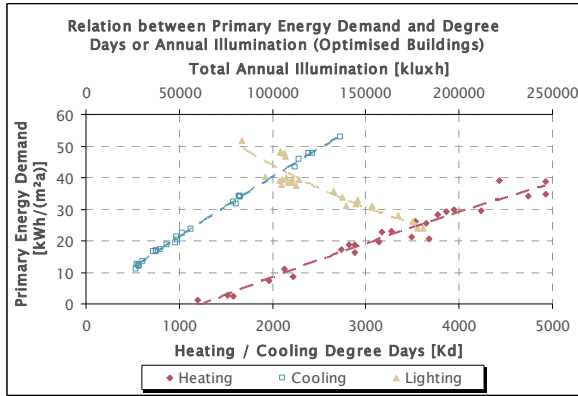


Fig. 139: Primary Energy Demand of Optimised Buildings as Function of Degree Days and Annual Illumination.

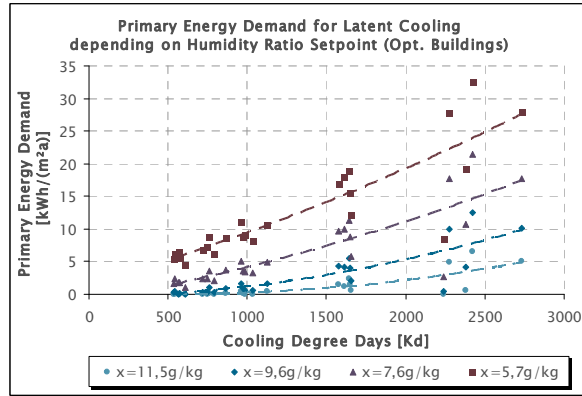


Fig. 140: Influence of the Humidity Ratio Setpoint on the Latent Cooling Energy Demand as Function of the Cooling Degree Days.

The influence of latent cooling loads, resulting from the dehumidification of supply air, has been evaluated in a separate parameter analysis, varying the setpoint to which the air is dehumidified. Fig. 140 shows the primary energy demand for latent cooling in the 25 locations with different setpoints (humidity ratio) of the supply air. A strong influence of the setpoint and an increasing influence with increasing cooling degree days (i.e. from North to South) could be detected.

However it could be proven, that as long as efficient ventilation and cooling systems with low ventilation and dehumidification rates are used, latent cooling even in southern Europe has low significance compared to the total primary energy demand (max. 6% in optimised buildings at $x=5,7\text{g/kg}$, 4% for typical buildings). Therefore, the minimisation of both ventilation rates and the dehumidification of air could be proven to be important for the minimisation of energy demand, especially in warm and humid climates.

Since the actual energy demand is influenced by many more factors than the climate, the estimation of absolute values would have low significance. Therefore, the results obtained from the analysis of the 25 optimised buildings have been qualified within their own bandwidth. Fig. 141 visualises the allocation of the resulting “European Building Performance Climate Index” (EBPCI) to six classes of the corresponding climate classification system (EBPCC).

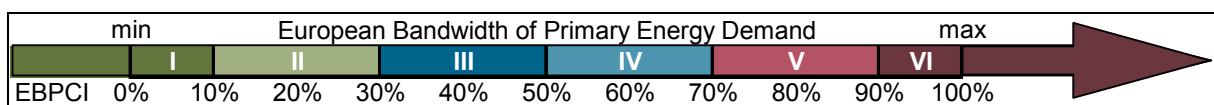


Fig. 141: Definition of Indices and Classes of Primary Energy Demand within the Bandwidth of Results.

From the good correlations proven between the heating energy demand and heating degree days on the one hand and between cooling and lighting energy demand and the cooling degree days on the other hand, the EBPC allows the estimation of the climatic influence on the relative energy demand of a building from the heating and cooling degree days of a location's climate.

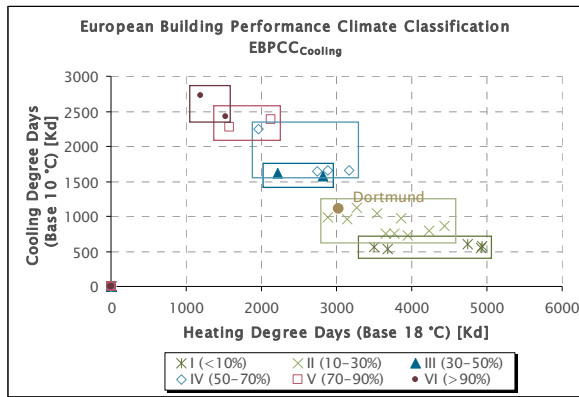


Fig. 142: Arrays for EBPCC_{Cooling}-Classes I–VI depending on HDD and CDD with exemplary Classification of Dortmund, Germany.

a result of the climatic conditions in Dortmund, a cooling energy demand between 10% and 30% of the European bandwidth can be expected. Respective diagrams have been developed for heating and lighting energy demand as well.

It has to focus on heating, cooling and lighting separately, since the very narrow bandwidth of total energy demand of optimised buildings in Europe is not suitable as a benchmark.

Fig. 142 exemplifies the resulting arrays for the relative cooling energy demand (including latent cooling energy demand) that can be expected depending on the heating and cooling degree days of the location. As an example, Dortmund (Germany, HDD₁₈=3021, CDD₁₀=1165) has been plotted into the diagram. The location meets the array of class II, so as

The impacts of climate change on the energy demand of European office buildings have been analysed in a lateral analysis of two locations in the United Kingdom (UK). Therefore a new weather file generator has been used providing weather files for the changing climate in the UK for the use in building simulations.

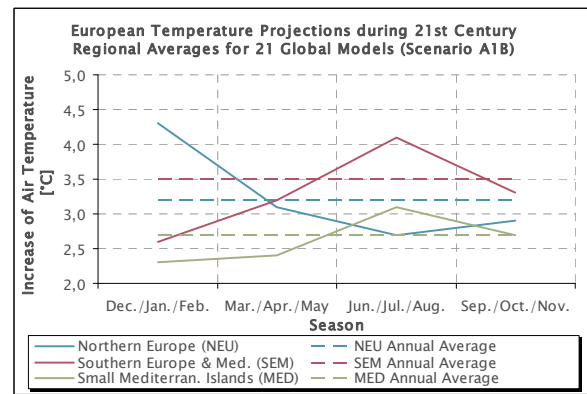


Fig. 143: Seasonal Averages for European Temperature Projections during the 21st Century (based on [IPCC-4 WG I]).

Fig. 143 shows the expected seasonal temperature changes in different parts of Europe according to the fourth IPCC-report. It is obvious that the impacts of climate change regionally and seasonally will be significantly different.

Based on local predictions, the impacts of climate change for typical and optimised buildings in London and Glasgow have been analysed under different scenarios of greenhouse gas emissions. Fig. 144 shows the variation of the total primary energy demand of an optimised building in London during the 21st century for different emission scenarios. Depending on the scenario, an increase of the total primary energy demand of more than 10% can be expected by the end of the 21st century, compared to the end of the 20th century.

The corresponding split of the total primary energy demand for the high emissions scenario can be found in Fig. 145. A significant increase of the cooling energy demand and decrease of the heating energy demand can be observed, resulting in an increase of the total primary energy demand.

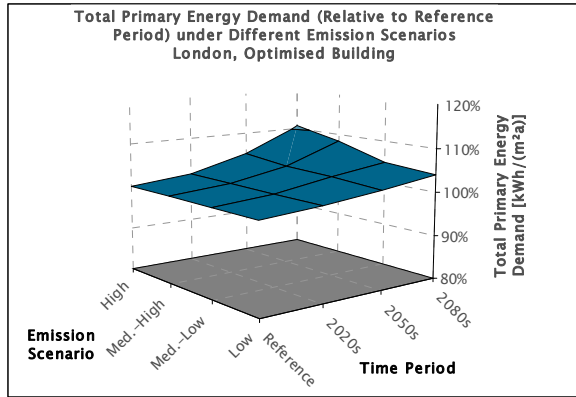


Fig. 144: Variation of Primary Energy Demand of an Optimised Building in London during the 21st Century under different Emission Scenarios and Periods.

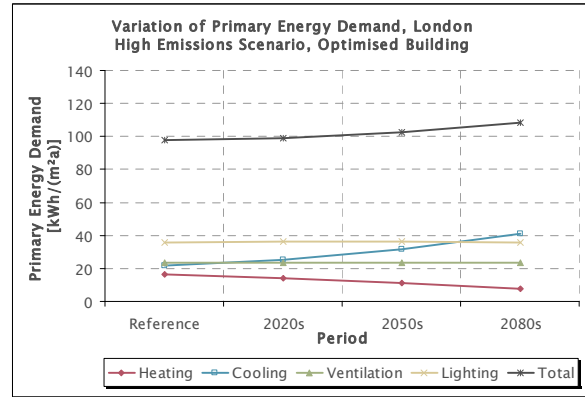


Fig. 145: Variation of Primary Energy Demand of an Optimised Building in London during the 21st Century under the High Emissions Scenario.

These results showed that the significantly different climatic conditions today's buildings will face during their lifetime might have strong impacts on their energy demand. Therefore, the design should be based on predictions of future boundary conditions of the climate instead of statistical weather data from the past, which is still the common approach. To avoid additional energy demand from the changing climate and rather tap the full saving potentials resulting out of it, there is a strong need for adapted sets of climatic data, taking into account the impacts of climate change on local climate in Europe and beyond.

16. German Summary (Deutsche Zusammenfassung)

Die Veränderungen des Klimas infolge der Emission von Treibhausgasen führen zu verstärkten Bemühungen, diese Emissionen weltweit zu vermeiden. Der globale Anteil von Gebäuden an der Emission von Treibhausgasen liegt bei etwa 15%, wovon etwa 35% auf gewerbliche Gebäude zurückgeführt werden (siehe Fig. 146). Aus diesem Grunde und infolge steigender Energiepreise hat die Bedeutung der Energieeffizienz von Bürogebäuden zugenommen.

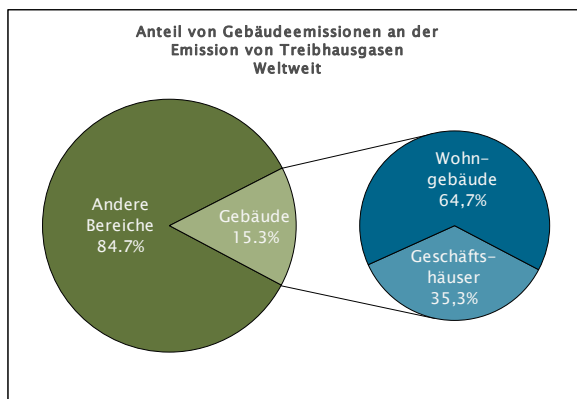


Fig. 146: Anteil von Gebäudeemissionen an den weltweiten Treibhausgasemissionen [WRI].

Bestehende Systeme zur Klimaklassifikation beziehen sich häufig gar nicht auf den Gebäudeenergiebedarf oder berücksichtigen nicht alle relevanten Bestandteile des Gesamtenergiebedarfes, d.h. Heizung, Kühlung, Lüftung und Beleuchtung.

In dieser Arbeit wurden mit Hilfe dynamischer Gebäudesimulationen die klimatischen Einflüsse auf den Gesamtenergiebedarf europäischer Bürogebäude untersucht. Dazu wurden 25 Standorte in Europa zwischen 60 und 40 Grad nördlicher Breite in Gruppen von 5° nördlicher Breite ausgewählt (siehe Fig. 147).

Das Klima an diesen Standorten wurde durch statistische Auswertung von Lufttemperatur, Solarstrahlung, Helligkeit auf horizontaler Fläche und anderen Klimaelementen untersucht. Weiterhin wurden gebäudespezifische Klimakennwerte wie Heiz- und Kühlgradtage abgeleitet.

Korrelationen zwischen der geographischen Breite und den gebäudespezifischen Klimakennwerten wurden untersucht und konnten mit unterschiedlicher Genauigkeit nachgewiesen werden, wobei lokale Besonderheiten im Wesentlichen bei den jeweils niedrigsten Temperaturen im Winter festgestellt wurden. Fig. 148 zeigt beispielhaft den Zusammenhang zwischen Heiz- bzw. Kühlgradtagen (HDD /

Da der Energieverbrauch von Gebäuden von einer Vielzahl von Faktoren abhängt, hat ein Vergleich verschiedener Gebäude üblicherweise eine geringe Aussagekraft. Die unterschiedlichen klimatischen Bedingungen der Gebäudestandorte sind einer der Aspekte, welche die Bewertung von Gebäuden in einem größeren Rahmen, z.B. innerhalb Europas, erschweren.

Bestehende Systeme zur Klimaklassifikation beziehen sich häufig gar nicht auf den Gebäudeenergiebedarf oder berücksichtigen nicht alle relevanten Bestandteile des Gesamtenergiebedarfes, d.h. Heizung, Kühlung, Lüftung und Beleuchtung.



Fig. 147: Landkarte Europas mit ausgewählten Standorten.

CDD) und der geographischen Breite, wobei die Streuung der Heizgradtage größer ist, als die der Kühlgradtage.

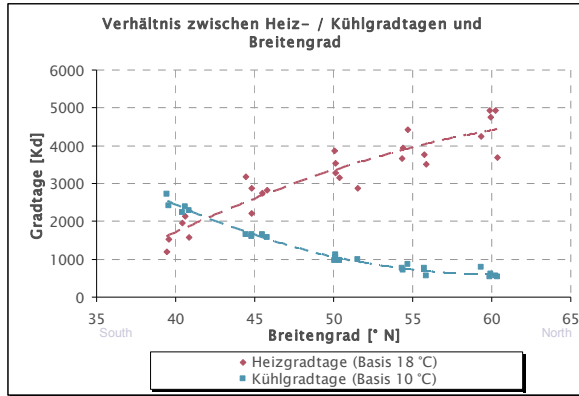


Fig. 148: Heiz- und Kühlgradtage der ausgewählten Standorte als Funktion der geographischen Breite.

Für jeden der 25 Standorte wurde mit Hilfe von Jahressimulationen mit einer Schrittweite von einer Stunde der Primärenergiebedarf für Heizung, Kühlung, Lüftung und Beleuchtung ermittelt. Durch die Festlegung eines einheitlichen Lüftungssystems hat sich der Lüftungsenergiebedarf nicht verändert, er wurde jedoch bei der Berechnung des Gesamtprimärenergiebedarfes miteinbezogen. Das Simulationsmodell bestand aus einem Einzelraum mit einer Größe von etwa 11 m², der in vier Himmelsrichtungen (Nord, Ost, Süd, West) untersucht wurde.

Für die Simulation mussten einige Annahmen getroffen werden, um ein Standardbürogebäude zu definieren. In früheren Studien haben sich der Fensterflächenanteil und der Wärmedämmstandard von Fassaden als wesentliche Einflussgrößen auf den Gesamtenergiebedarf von Bürogebäuden erwiesen. Daher wurden diese Kennwerte in fünf gleich großen Schritten innerhalb einer üblichen Bandbreite parametrisiert. Fig. 149 zeigt Außen- und Innensichtungen der fünf Fassadentypen (Fensterflächenanteile w1 – w5) mit der resultierenden Tageslichtsituation bei bedecktem Himmel, die für die Berechnung des Kunstlichtenergiebedarfes berücksichtigt wurde.

w1 (30%)	w2 (47,5%)	w3 (65%)	w4 (82,5%)	w5 (100%)
Öffnungsflächenanteil: 20,2%	Öffnungsflächenanteil: 32,0%	Öffnungsflächenanteil: 43,8%	Öffnungsflächenanteil: 55,6%	Öffnungsflächenanteil: 67,4%

Fig. 149: Beispielhafte Visualisierung von fünf Fassaden mit unterschiedlichen Fensterflächenanteilen und resultierender Tageslichtsituation im Büroraum bei bedecktem Himmel.

Der Fensterflächenanteil in Fig. 149 beschreibt das Verhältnis zwischen der Fensterfläche und der Fläche des gesamten Fassadenabschnittes. Der resultierende Öffnungsflächenanteil beschreibt das Verhältnis zwischen der Fensterfläche und der Grundfläche des Raumes.

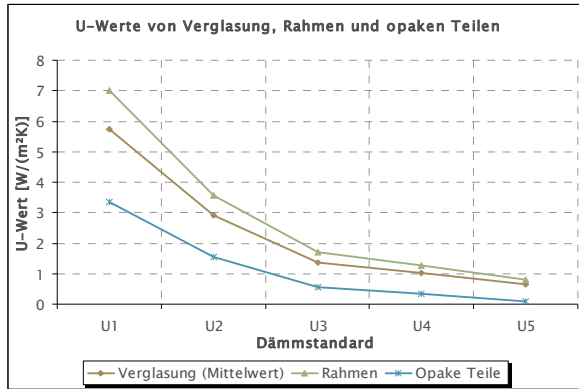


Fig. 150: U-Werte von Verglasung, Rahmen und opaken Teilen abhängig vom Wärmedämmstandard.

In einer Untersuchung wurden „typische Gebäude“ definiert, die in dem jeweiligen Land eines Standortes übliche Fassaden-U-Werte sowie einen Fensterflächenanteil von 65% (mittlerer Wert der Bandbreite) beinhalteten.

Zusätzlich wurde eine Parameterstudie durchgeführt, in welcher der Gesamtprimärenergiebedarf durch Variation von Fensterflächenanteil und Wärmedämmstandard in jeweils fünf Schritten minimiert wurde. Diese Analyse wurde für jeweils einen repräsentativen Standort je Gruppe geographischer Breite wiederholt, wobei auch der Unterschied zwischen Wärme- und Sonnenschutzverglasung untersucht wurde.

Fig. 151 zeigt beispielhaft die Ergebnisse der Parametervariation mit Wärmeschutzverglasung in Praha (50 °N). Der niedrigste Gesamtprimärenergiebedarf wurde bei einem Fensterflächenanteil von 65 % und dem höchsten Wärmedämmstandard festgestellt (roter Kreis).

Der Wärmedämmstandard wurde ebenfalls in fünf Schritten variiert, wobei die obere und untere Grenze der Bandbreite durch technische Grenzen definiert wurde. Fig. 150 zeigt die proportionale Veränderung der U-Werte der Verglasung, der Rahmen sowie der opaken Fassadenelemente in fünf Dämmstandards.

Da der Dämmstandard eines Gebäudes häufig von lokalen Einflüssen wie nationalen Bauvorschriften, Bautraditionen etc. abhängt, wurden zwei verschiedene Untersuchungen durchgeführt.

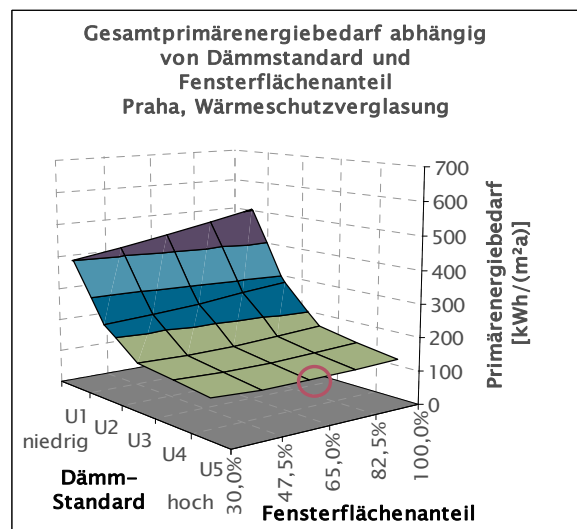


Fig. 151: Gesamtprimärenergiebedarf eines optimierten Gebäudes mit Wärmeschutzverglasung in Praha als Funktion von Wärmedämmstandard und Fensterflächenanteil.

Durch Wiederholung dieser Analyse für jeden der fünf repräsentativen Standorte konnte eine Gruppe von „optimierten Gebäuden“ definiert werden, wobei die Ergebnisse sehr ähnlich waren. Trotz deutlicher, aber teils gegensätzlicher Unterschiede des Primärenergiebedarfes für Heizung, Kühlung und Beleuchtung, wurde in nahezu allen Gruppen geographischer Breite der niedrigste Gesamtprimärenergiebedarf bei höchstem Wärmedämmstandard, einem Fensterflächenanteil von 65 % (Ausnahme:

60 °N mit einem Fensterflächenanteil von 47,5%) und Wärmeschutzverglasung festgestellt. Der höchste Gesamtprimärenergiebedarf trat in allen Fällen bei Ganzglasfassaden ($w_5=100\%$) mit minimalem Dämmstandard auf. Der Unterschied zwischen niedrigstem und höchstem Gesamtprimärenergiebedarf je Standort (also die Bedeutung der Gebäudeoptimierung) nimmt von Süden nach Norden zu, im Wesentlichen aufgrund des zunehmenden Heizwärmebedarfes in kalten Klimaten.

Die Simulation sowohl der typischen als auch der optimierten Gebäude an allen 25 Standorten resultierte in zwei Ergebnisreihen, die mit der geographischen Breite und den Klimabedingungen der Standorte verglichen wurden. Aufgrund der nationalen Unterschiede der Wärmedämmstandards korrelierte der Gesamtprimärenergiebedarf der typischen Gebäude sowohl mit der geographischen Breite als auch mit den klimatischen Bedingungen nur schwach. Die Abweichung des Heizwärmebedarfes war besonders groß und beeinflusste den Gesamtprimärenergiebedarf entsprechend.

Generell wurde mit den optimierten Gebäuden an allen Standorten ein niedrigerer Gesamtprimärenergiebedarf ermittelt, so dass sich ein hoher Wärmedämmstandard mit mäßigen Fensterflächenanteilen an allen Standorten in Europa als optimal erwiesen hat.

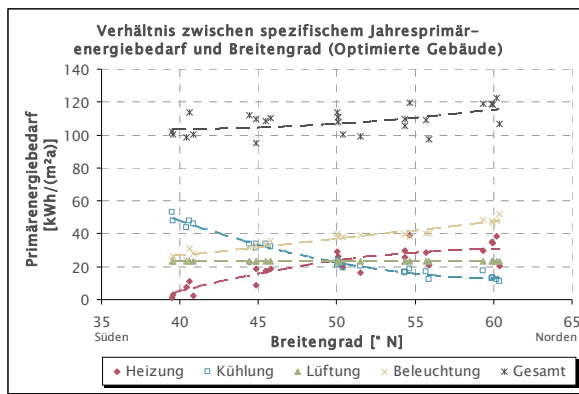


Fig. 152: Jährlicher Primärenergiebedarf von optimierten Gebäuden als Funktion der geographischen Breite.

Fig. 152 zeigt die Ergebnisse der optimierten Gebäude als Funktionen der geographischen Breite. Die Graphen korrelieren überwiegend gut mit dem Breitengrad. Steigender Heiz- und Beleuchtungs- sowie sinkender Kühlenergiebedarf können von Süden nach Norden festgestellt werden, wobei lediglich der Heizwärmebedarf eine bemerkenswerte Streuung der Ergebnisse aufweist. Dies beeinflusst auch die Streuung des Gesamtprimärenergiebedarfes, der nur leicht von Süden nach Norden ansteigt, insgesamt im europäischen Vergleich aber nur um gut 10% schwankt.

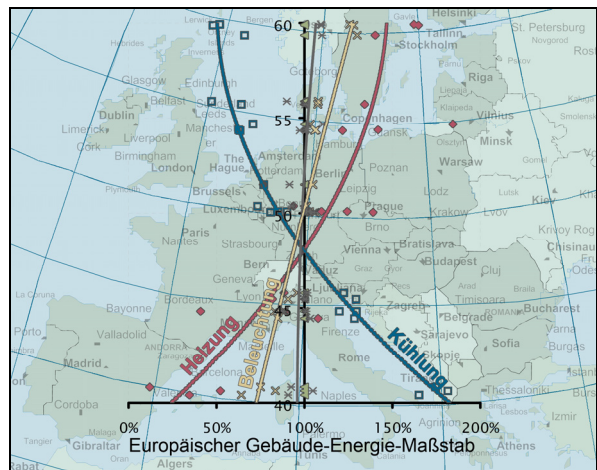


Fig. 153: Europäischer Gebäude-Energie-
 16 - German Summary (Deutsche Zusammenfassung)

Aus diesen Ergebnissen kann eine grobe Abschätzung des klimatischen Einflusses auf den Energiebedarf vom Breitengrad eines Standortes abgeleitet werden. Aufgrund der zahlreichen weiteren Einflüsse auf den absoluten Energiebedarf, wurden die Ergebnisse der optimierten Gebäude auf die Durchschnittswerte ihrer jeweiligen Bandbreiten bezogen. Daraus ergab sich ein grober „Europäischer Gebäude-Energie-Maßstab“ („European Building Energy Benchmark“ – EBEB).

Maßstab (EBEB) für Heizung, Kühlung und Beleuchtung abhängig vom Breitengrad.

Fig. 153 veranschaulicht den Primärenergiebedarf für Heizung, Kühlung und Beleuchtung in optimierten Gebäuden bezogen auf den Europäischen Durchschnitt (100%) und abhängig vom Breitengrad.

Aufgrund der Klimaanalysen wurde eine noch genauere Korrelation der Ergebnisse mit den abgeleiteten Klimagrößen erwartet und konnte nachgewiesen werden. Fig. 154 zeigt den Zusammenhang zwischen Heiz- und Kühlenergiebedarf mit den jeweiligen Gradtagszahlen sowie den Zusammenhang des Beleuchtungsenergiebedarfes mit der jährlichen Gesamtbeleuchtungsstärke auf horizontaler Fläche. Da sowohl Kühl- als auch Beleuchtungsenergiebedarf stark von der Solarstrahlung abhängen, konnte ein Zusammenhang zwischen Beleuchtungsenergiebedarf und Kühlgradtagen nachgewiesen werden.

Die Zusammenhänge in Fig. 154 zeigen den klimatischen Einfluss eines Standortes auf den Energiebedarf eines Gebäudes.

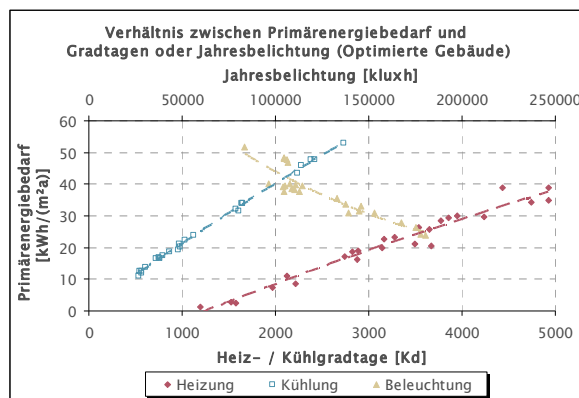


Fig. 154: Primärenergiebedarf optimierter Gebäude als Funktion der Gradtage und der jährlichen Beleuchtungsstärke.

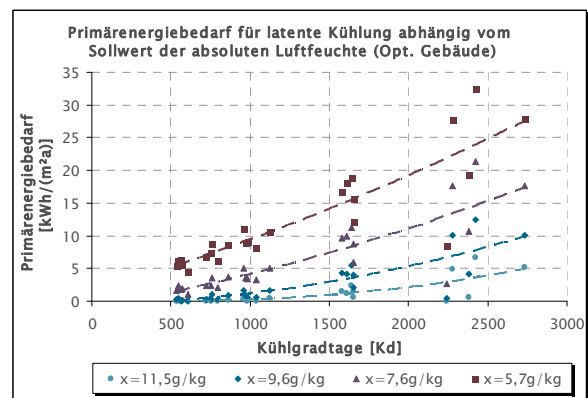


Fig. 155: Einfluss des Sollwertes der Raumluftfeuchte auf den latenten Kühlenergiebedarf als Funktion der Kühlgradtage.

Der Einfluss latenter Kühllasten, resultierend aus der Entfeuchtung der Zuluft, wurde in einer separaten Parameterstudie untersucht, indem der Sollwert variiert wurde, auf den die Zuluft entfeuchtet wird. Fig. 155 zeigt den Primärenergiebedarf für die Kühlung latenter Lasten an den 25 Standorten bei unterschiedlichen Sollwerten (absolute Feuchte) der Zuluft. Ein starker, mit steigenden Kühlgradtagen (d.h. von Norden nach Süden) zunehmender Einfluss des Sollwertes wurde festgestellt.

Dennoch konnte gezeigt werden, dass latente Kühlung auch in Südeuropa eine geringe Bedeutung im Vergleich zum Gesamtprimärenergiebedarf hat (bei $x=5,7\text{g/kg}$ max. 6% in optimierten Gebäuden, 4% bei typischen Gebäuden), solange effiziente Lüftungs- und Kühlsysteme mit niedrigen Luftwechsel- und Entfeuchtungsraten zum

Einsatz kommen. Daher konnte die große Bedeutung der Minimierung sowohl von Luftwechselraten als auch der Luftentfeuchtung für die Minimierung des Energiebedarfes, insbesondere in warmen und feuchten Klimaten, nachgewiesen werden.

Da der tatsächlich Energiebedarf von wesentlich mehr Faktoren als nur dem Klima abhängt, würde die Schätzung absoluter Energiebedarfswerte eine geringe Aussagekraft haben. Daher wurden die Ergebnisse aus der Analyse der 25 optimierten Gebäude innerhalb ihrer eigenen Bandbreite relativiert. Fig. 156 stellt die Zuordnung des resultierenden „Europäischen Gebäudeeffizienz-Klimaindex“ (EBPCI) in sechs Klassen der zugehörigen Klimaklassifikation (EBPCC) dar.

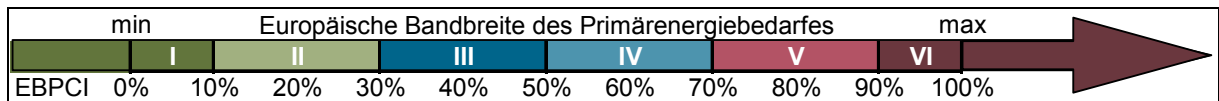


Fig. 156: Definition von Indizes und Klassen des Primärenergiebedarfes innerhalb der Bandbreite der Ergebnisse.

Aufgrund der guten Korrelationen zwischen Heizwärmebedarf und Heizgradtagen einerseits und zwischen Kühl- sowie Beleuchtungsenergiebedarf und den Kühlgradtagen andererseits ermöglicht die EBPC die Abschätzung des klimatischen Einflusses auf den relativen Energiebedarf eines Gebäudes anhand der Heiz- und Kühlgradtage eines Standortklimas.

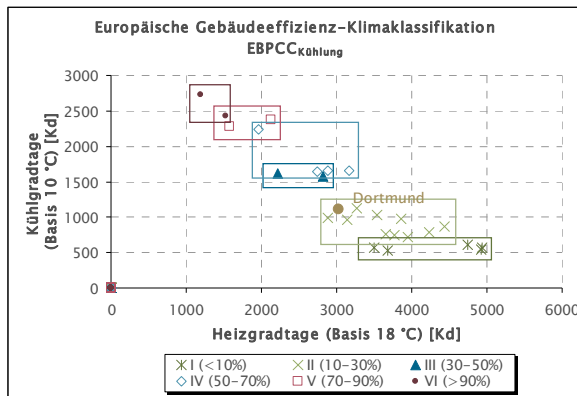


Fig. 157: Felder für die EBPCC_{Kühlung}-Klassen I–VI abhängig von Heiz- und Kühlgradtagen mit beispielhafter Klassifizierung von Dortmund, Deutschland.

im Feld von Klasse II, so dass infolge der klimatischen Bedingungen in Dortmund ein Kühlenergiebedarf zwischen 10% und 30% der europäischen Bandbreite zu erwarten ist. Entsprechende Diagramme wurden ebenfalls für Heiz- und Beleuchtungsenergiebedarf entwickelt

In der Klassifikation müssen Heizung, Kühlung und Beleuchtung separat behandelt werden, da die sehr enge Bandbreite des Gesamtprimärenergiebedarfes optimierter Gebäude in Europa nicht als Bezugswert geeignet ist.

Fig. 157 zeigt beispielhaft die resultierenden Felder für den relativen Kühlenergiebedarf (einschließlich latentem Kühlenergiebedarf), der abhängig von den Heiz- und Kühlgradtagen eines Standortes zu erwarten ist. Als Beispiel wurde Dortmund (Deutschland, HDD₁₈=3021, CDD₁₀=1165) in das Diagramm eingetragen. Der Standort liegt

Die Auswirkungen des Klimawandels auf den Energiebedarf von europäischen Bürogebäuden wurden in einer Nebenanalyse von zwei Standorten im Vereinigten Königreich (UK) untersucht. Dazu wurde ein neuer Wetterdatengenerator verwendet, der Wetterdatensätze für das sich verändernde Klima in UK zur Verwendung in Gebäudesimulationen erzeugt.

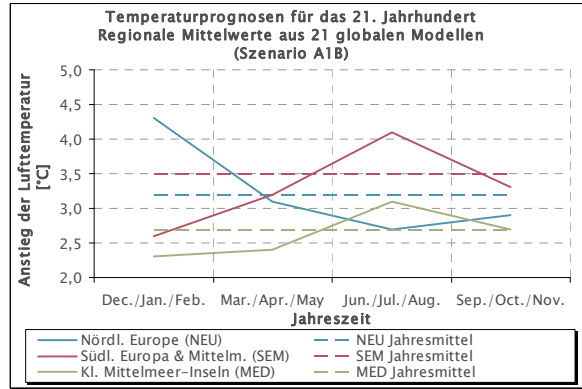


Fig. 158 zeigt die zu erwartenden saisonalen Temperaturänderungen in verschiedenen Teilen Europas gemäß dem vierten IPCC-Bericht. Es ist offensichtlich, dass die Auswirkungen des Klimawandels sich regional und saisonal deutlich unterscheiden werden.

Fig. 158: Saisonale Mittelwerte der Europäischen Temperaturprojektionen im Laufe des 21. Jahrhunderts (basierend auf [IPCC-4 WG I]).

Basierend auf lokalen Vorhersagen wurden die Auswirkungen des Klimawandels auf typische und optimierte Bürogebäude in London und Glasgow unter verschiedenen Szenarien von Treibhausgasemissionen untersucht. Fig. 159 zeigt die Veränderung des Gesamtprimärenergiebedarfes eines optimierten Gebäudes in London während des 21. Jahrhunderts bei verschiedenen Emissionsszenarien. Je nach Szenario ist bis zum Ende des 21. Jahrhunderts ein Anstieg des Gesamtprimärenergiebedarfes bis zu 10% im Vergleich zum Ende des 20. Jahrhunderts zu erwarten.

Die zugehörige Aufteilung des Gesamtprimärenergiebedarfes des Szenarios mit hohen Emissionen ist in Fig. 160 zu sehen. Ein deutlicher Anstieg des Kühlenergiebedarfes und ein Abfallen des Heizwärmebedarfes kann beobachtet werden, was in einem Anstieg des Gesamtprimärenergiebedarfes resultiert.

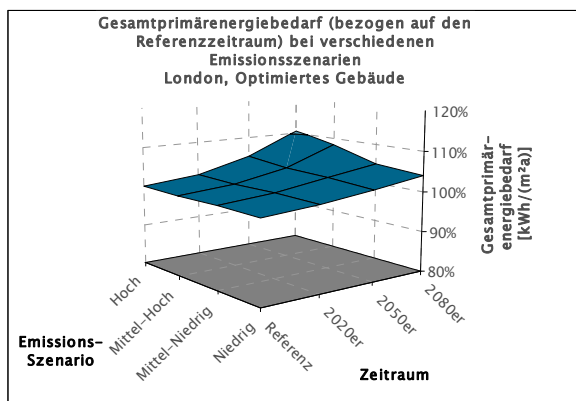


Fig. 159: Veränderung des Primärenergiebedarfes eines optimierten Gebäudes in London während des 21. Jahrhunderts bei verschiedenen Emissionsszenarien und Zeiträumen.

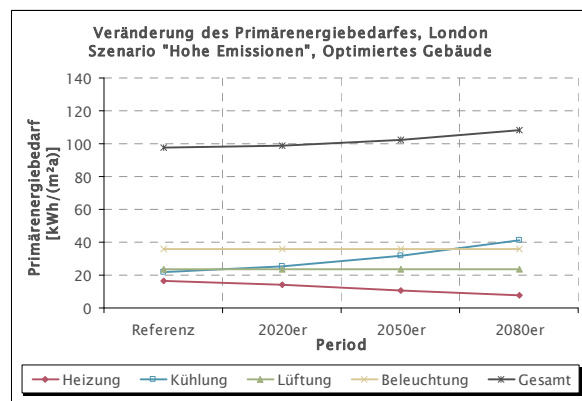


Fig. 160: Veränderung des Primärenergiebedarfes eines optimierten Gebäudes in London während des 21. Jahrhunderts unter dem Szenario hoher Emissionen.

Diese Ergebnisse zeigen, dass die deutlich veränderten Klimabedingungen, denen heutige Gebäude im Laufe ihrer Lebenszeit ausgesetzt sein werden, einen starken Einfluss auf ihren Energiebedarf haben können. Daher sollte die Planung von Ge-

bäuden auf Vorhersagen zukünftiger Klimabedingungen basieren, anstelle von statistischen Wetterdaten aus der Vergangenheit, was immer noch die übliche Vorgehensweise ist. Um zusätzlichen Energiebedarf infolge des Klimawandels zu vermeiden und gleichzeitig die vollen daraus resultierenden Einsparpotentiale zu erschließen, sind dringend angepasste Klimadatensätze erforderlich, welche die Auswirkungen des Klimawandels auf lokale Klimate in Europa und darüber hinaus berücksichtigen.

17. References

- [ASHRAE] Briggs, R.S., Lucas, R.G, Taylor, Z.T.: „ASHRAE 4610/4611 - Climate Classification for Building Energy Codes and Standards”, American Society of Heating, Refrigerating and Air-Conditioning Engineers, 2003.
- [BBR] Gralla, M., Rusch, L.-P., Müller, H.F.O., Schlenger, J. et al.: „Bewertung von Glasfassaden unter Berücksichtigung von Kriterien der Energieeinsparung und Wirtschaftlichkeit“, Schlussbericht BBR-Forschungsprojekt Z6-10.06.03-06.121, 2008. www.bbr.bund.de
- [Butler] Butler, R.: “Cities and urban areas in Europe with population over 100,000 [Source: UN]”, www.mongabay.org
- [Colliver] Colliver, D.G.: “Energy Requirements for Conditioning of Ventilating Air”, Technical Note AIVC 47, Air Infiltration and Ventilation Centre, Coventry, 1995, ISBN 978-0946075867. www.AIVC.org
- [DIN 5034-1] DIN 5034: “Daylight in interiors - Part 1: General requirements”, Beuth, Berlin, 1999-10.
- [DIN 5034-4] DIN 5034: “Daylight in interiors - Part 4: Simplified Determination of Minimum Window Sizes for Dwellings”, Beuth, Berlin, 1994-09.
- [DIN V 4701-10] DIN V 4701: „Energetische Bewertung heiz- und raumluftechnischer Anlagen Teil 10: Heizung, Trinkwassererwärmung, Lüftung“, Beuth, Berlin, 2003-08
„Wiedergegeben mit Erlaubnis des DIN Deutsches Institut für Normung e. V. Maßgebend für das Anwenden der DIN-Norm ist deren Fassung mit dem neuesten Ausgabedatum, die bei der Beuth Verlag GmbH, Burggrafenstraße 6, 10787 Berlin, erhältlich ist.“
- [DIN V 18599-1] DIN V 18599-1: “Energy efficiency of buildings – Calculation of the net, final and primary energy demand for heating, cooling, ventilation, domestic hot water and lighting – Part 1: General balancing procedures, terms and definitions, zoning and evaluation of energy sources”, Beuth, Berlin, 2007-02
- [DIN V 18599-2] DIN V 18599-2: “Energy efficiency of buildings – Calculation of the net, final and primary energy demand for heating, cooling, ventilation, domestic hot water and lighting – Part 2: Net energy demand for heating and cooling of building zones”, Beuth, Berlin, 2007-02
- [DIN V 18599-4] DIN V 18599-4: “Energy efficiency of buildings – Calculation of the net, final and primary energy demand for heating, cooling, ventilation, domestic hot water and lighting – Part 4: Net and final energy demand for lighting”, Beuth, Berlin, 2007-02

- [EN 15251] EN 15251: "Indoor environmental input parameters for design and assessment of energy performance of buildings addressing indoor air quality, thermal environment, lighting and acoustics", Beuth, Berlin, 2007-08
- [EN 15927-1] EN ISO 15927-2: "Hygrothermal performance of buildings – Calculation and presentation of climatic data – Part 2: Hourly data for design cooling load", Beuth, Berlin, 2007-07
- [EN 15927-6] EN ISO 15927-6: "Hygrothermal performance of buildings - Calculation and presentation of climatic data - Part 6: Accumulated temperature differences (degree-days)", Beuth, Berlin 2007-11
- [Energieleitfaden] Müller, H.F.O., Schuster, H., Klein, O.: "Energieleitfaden Bürogebäude", Lehrstuhl Klimagerechte Architektur, Technische Universität Dortmund, 2006.
- [EnPer-TEBuC] Dicke, N., Weber, C. Kjellsson, E., Despretz, H.: "Energy Performance – Towards an European Building Code", Final report of EU-Project DG-TREN 4.1031/C/00-018/2000 ENPER TEBUC, 2003. www.enper.org
- [EnOB-EnBau] Website of the German Research Project „Energieoptimiertes Bauen“, www.enob.info/de/forschungsfelder/enbau/, 2009-01
- [EPBD] DIRECTIVE 2002/91/EC OF THE EUROPEAN PARLIAMENT AND OF THE COUNCIL of 16 December 2002 on the energy performance of buildings, European Commission, Brussels, 2003.
- [EULEB] Müller, H.F.O., Schlenger, J. et al.: "EULEB – EUropean high quality low Energy Buildings", Final report of EU-Project EIE-2003-172 EULEB, 2007. www.EULEB.info
- [Frank] Frank, T.: "Climate change impacts on building heating and cooling energy demand in Switzerland", Energy and Buildings 37, p. 1175–1185, Elsevier, 2005.
- [Ghiaus] Ghiaus, C.: "Equivalence between the load curve and the free-running temperature in energy estimating methods", Energy and Buildings 38, p. 429–435, Elsevier, 2006.
- [IEA] Laustsen, J.: "Energy Efficiency Requirements in Building Codes, Energy Efficiency Policies for New Buildings", International Energy Agency Information Paper in Support of the G8 Plan of Action, OECD/IEA, 2008. www.iea.org
- [IPCC-3 WG I] IPCC, 2001: Climate Change 2001: The Scientific Basis. Contribution of Working Group I to the Third Assessment Report of the Intergovernmental Panel on Climate Change [Houghton, J.T., Y. Ding, D.J. Griggs, M. Noguer, P.J. van der Linden, X. Dai, K. Maskell, and C.A. Johnson (eds.)]. Cambridge University Press, Cambridge, United Kingdom and New York, NY, USA, 881pp. www.IPCC.ch

- [IPCC-4 Syn] IPCC, 2007: Climate Change 2007: Synthesis Report. Contribution of Working Groups I, II and III to the Fourth Assessment Report of the Intergovernmental Panel on Climate Change [Core Writing Team, Pachauri, R.K and Reisinger, A. (eds.)]. IPCC, Geneva, Switzerland, 104 pp. www.IPCC.ch
- [IPCC-4 WG I] IPCC, 2007: Climate Change 2007: The Physical Science Basis. Contribution of Working Group I to the Fourth Assessment Report of the Intergovernmental Panel on Climate Change [Solomon, S., D. Qin, M. Manning, Z. Chen, M. Marquis, K.B. Averyt, M. Tignor and H.L. Miller (eds.)]. Cambridge University Press, Cambridge, United Kingdom and New York, NY, USA, 996 pp. www.IPCC.ch
- [Jacob] Jacob, D., Göttel, H., Kotlarski, S., Lorenz, P., Sieck, K.: "Klimaauswirkungen und Anpassung in Deutschland – Phase 1: Erstellung regionaler Klimaszenarien für Deutschland", Forschungsbericht 204 41 138, UBA-FB 000969, Climate Change - Heft 11/2008, Umweltbundesamt, Dessau, 2008. www.umweltbundesamt.de
- [Jentsch] Jentsch, M.F., Bahaj, A.S., James, P.A.B.: „Climate change future proofing of buildings - Generation and assessment of building simulation weather files“, Energy and Buildings 40, p. 2148–2168, Elsevier, 2008.
- [Keller] Keller, B.: „Klimagerechtes Bauen - Grundlagen, Dimensionierung, Beispiele; mit 18 Tabellen“, Teubner Verlag, Stuttgart, 1997, ISBN 978-3519050803.
- [Kuhn] Kuhn, T.E., Wienold, J.: „Neue Regelstrategien zur simultanen Optimierung von Sonnenschutz, Blendschutz und Tageslichtversorgung“, Konferenzbeitrag, 9. Symposium Innovative Lichttechnik in Gebäuden, OTTI, Staffelstein, 2003.
- [Meteonorm] Remund, J., Kunz, S.: "Meteonorm Handbook, Version 5.0 – Edition 2003", METEOTEST, Fabrikstrasse 14, CH-3012 Bern, Switzerland. www.meteonorm.com
- [Müller] Müller, H.F.O., Emembolu, A., Oetzel, M., Schuster, H., Soylu, I.: Sonnenschutz und Tageslichtbeleuchtung in Büroräumen, in: Bauphysik-Kalender, von Cziesielski, E.; Verlag Ernst & Sohn, Berlin, 2005.
- [Pinpoint] Keller, B., Rutz, S.: „PinPoint Bauphysik: Fakten zu nachhaltigem Bauen“, Vdf Hochschulverlag, Zürich, 2008, ISBN 978-3728131171.
- [Preißler] Preißler, A.: "Einfluss von Fassadenparametern auf den Gesamtprimärenergiebedarf von Gebäuden", Diplomarbeit Lehrstuhl Klimagerechte Architektur, Technische Universität Dortmund, 2008.

- [Spekat] Spekat, A., Enke, W., Kreienkamp, F.: „Neuentwicklung von regional hoch aufgelösten Wetterlagen für Deutschland und Bereitstellung regionaler Klimaszenarios auf der Basis von globalen Klimasimulationen mit dem Regionalisierungsmodell WETTREG auf der Basis von globalen Klimasimulationen mit ECHAM5/MPI-OM T63L31 2010 bis 2100 für die SRES-Szenarios B1, A1B und A2“, Forschungsbericht 204 41 138, Umweltbundesamt, Dessau, 2007. www.umweltbundesamt.de
- [Straesser] Sträßer, M.: „Klimadiagramme zur Köppenschen Klimaklassifikation“, Klett-Perthes, Gotha, 1998, ISBN 978-3623007687.
- [UKCIP] Hacker, JN, Belcher, SE & Connell, RK (2005). Beating the Heat: keeping UK buildings cool in a warming climate. UKCIP Briefing Report. UKCIP, Oxford. Arup and UKCIP, 2005. www.ukcip.org
- [UKCIP02] Hulme, M., Jenkins, G.J., Lu, X., Turnpenny, J.R., Mitchell, T.D., Jones, R.G., Lowe, J., Murphy, J.M., Hassell, D., Boorman, P., McDonald, R. and Hill, S.: “Climate Change Scenarios for the United Kingdom: The UKCIP02 Scientific Report”, 2002, funded by DEFRA, produced by Tyndall and Hadley Centres for UKCIP, Tyndall Centre for Climate Change Research, School of Environmental Sciences, University of East Anglia, Norwich, UK. 120pp. www.ukcip.org
- [WRI] Baumert, K.A., Herzog, T., Pershing, J.: “Navigating the Numbers: Greenhouse Gases And International Climate Change Agreements”, World Resources Institute, 2005, ISBN 978-1569735992.
- [VDI 2071] VDI 2071: “Heat Recovery in heating, ventilation and air conditioning plants”, Beuth, Berlin, 1997-12
- [VDI 3807-2] VDI 3807-2: “Characteristic values of energy and water consumption of buildings – Part 2: Heating and Electricity”, Beuth, Berlin, 1998-06.
- [VDI 3807-4] VDI 3807-4: “Characteristic values of energy and water consumption of buildings – Part 4: Characteristic values for electrical energy”, Beuth, Berlin, 2008-08.
- [Voss] Voss, K., Löhnert, G., Herkel, S., Wagner, A. Wambsganß, M. et al.: “Bürogebäude mit Zukunft - Konzepte, Analysen, Erfahrungen“, Solarpraxis, 2006, ISBN 978-3934595590.
- [Yeang] Yeang, K., Balfour, A., Richards, I.: “Bioclimatic Skyscrapers”, Artemis & Winkler, 1994, ISBN 978-3760884240.

18. List of Diagrams

Fig. 1: Variations of the Earth's Surface Temperature on the Northern Hemisphere for the Past 1000 Years [IPCC-3 WG I].....	1
Fig. 2: Concentration of Carbon Dioxide (CO ₂) in the Atmosphere for the Past 1000 Years [IPCC-3 WG I].....	1
Fig. 3: Share of Buildings in the Global GHG-Emissions [WRI].....	1
Fig. 4: Exemplary Share of Buildings in the GHG-Emissions of the USA [WRI].	1
Fig. 5: Locations and Types of Buildings analysed in [EULEB] (© www.ReginaMueller.de).	3
Fig. 6: Total Primary Energy Demand of EULEB-Buildings, grouped by Building Type and Climatic Zone according to [ASHRAE].	3
Fig. 7: Calculation of Primary Energy Demand [DIN V 4701-10].	4
Fig. 8: Global Distribution of Climatic Zones [Yeang].	6
Fig. 9: Climate Classification of Europe according to KOEPPEN, based on [Straesser], (© www.ReginaMueller.de).	7
Fig. 10: Climate Classification of European Capitals according to ASHRAE 4610/4611.	9
Fig. 11: Example of a Climate Surface (Sum of Heating and Cooling for Zürich, CH) [Keller].	10
Fig. 12: HVAC Operating Zones according to [Ghiaus]: (1) Heating, (2) Ventilation, (3) Free-Cooling, (4) Mechanical Cooling.	11
Fig. 13: Position of the 7.400 Weather Stations in the Software Meteonorm 5.0 [Meteonorm].	12
Fig. 14: Annual Global Irradiation in Europe [Meteonorm].	13
Fig. 15: Map of Europe with Selected Locations.....	14
Fig. 16: Principle of Calculation of Heating Degree Hours (HDH).....	17
Fig. 17: Principle of Calculation of Cooling Degree Hours (CDH).....	18
Fig. 18: Mean, Max. and Min. Air Temperatures as Functions of the Locations' Latitudes.	19
Fig. 19: Heating and Cooling Degree Days as Functions of the Latitude.	20

Fig. 20: Heating and Cooling Degree Days of Selected Locations grouped by Latitude.	20
Fig. 21: Correlation between Heating and Cooling Degree Days.	21
Fig. 22: Ratio between Heating and Cooling Degree Days as Function of Latitude.	21
Fig. 23: Relation between Daylight Hours and Latitude.	21
Fig. 24: Relation between Average Cloudiness and Latitude.	21
Fig. 25: Monthly and Annual Average Illumination in Bergen and Madrid.	22
Fig. 26: Monthly and Annual Average Illumination in Helsinki and Bruxelles.	22
Fig. 27: Global Radiation and Total Illumination on Horizontal Surface as Functions of Latitude.	22
Fig. 28: Total Annual Illumination as Function of Cooling Degree Days.	23
Fig. 29: Correlation between Heating/Cooling Degree Days Ratio and the Annual Illumination.	23
Fig. 30: Relux-Visualisation of Standard Office Room (here: with a Band Façade)..	25
Fig. 31: Principle of Analysing the Combined Influences of Parameters by Deduction of Standardised Gradients in [Preißler].	26
Fig. 32: U-Values of Glazing Types, Frames and Opaque Parts Depending on Insulation Level.	31
Fig. 33: Window U-Values depending on Window Proportion and Insulation Level..	32
Fig. 34: Façade U-Values depending on Window Proportion and Insulation Level. .	32
Fig. 35: Exemplary Distribution of Daylight Factor ($w_3=65\%$, WinID=1031).	33
Fig. 36: Average Daylight Factors depending on Window Proportion and Glazing Type.	33
Fig. 37: Exemplary Visualisation of Daylight Situation inside the Office at Diffuse Sky Conditions.	34
Fig. 38: Typical U-values in European Countries [EnPer-TEBuC].	34
Fig. 39: Number of Climatic Zones in European Countries according to [EnPer-TEBuC].	36
Fig. 40: Selection of Representative Locations per Group of Latitude.	37

Fig. 41: Heating Primary Energy Demand, Praha, Heat Protection Glass.	38
Fig. 42: Cooling Primary Energy Demand, Praha, Heat Protection Glass.	38
Fig. 43: Lighting Primary Energy Demand, Praha, Heat Protection Glass.	39
Fig. 44: Total Primary Energy Demand, Praha, Heat Protection Glass.	39
Fig. 45: Total Primary Energy Demand, Praha, Heat Protection Glass.	40
Fig. 46: Total Primary Energy Demand, Praha, Sun Protection Glass.	40
Fig. 47: Results of Building Optimisation in Representative Location.	42
Fig. 48: Maximum and Minimum Total Primary Energy Demand of Representative Locations.	42
Fig. 49: Monthly Primary Energy Demand of a South-Office in a Typical Building in Praha.	43
Fig. 50: Annual Primary Energy Demand of a Typical Building in Praha.	44
Fig. 51: Total Primary Energy Demand of Typical Buildings in Selected 25 Locations.	44
Fig. 52: Annual Primary Energy Demand for Heating, Cooling, Lighting and Ventilation in Typical Buildings as Function of Latitude.	44
Fig. 53: Total Annual Primary Energy Demand of Typical Buildings as Function of Latitude.	44
Fig. 54: Primary Energy Demand of Typical Buildings as Function of Degree Days and Annual Illumination.	45
Fig. 55: Relative Primary Energy Demand of Typical Buildings as Function of Latitude.	46
Fig. 56: Relative Primary Energy Demand of Typical Buildings as Function of Degree Days and Annual Illumination.	46
Fig. 57: Primary Energy Demand of a Typical Building in Selected Locations relative to European Average (100%).	46
Fig. 58: Monthly Primary Energy Demand of a South-Office in an Optimised Building in Praha.	47
Fig. 59: Annual Primary Energy Demand of an Optimised Building in Praha.	47
Fig. 60: Total Primary Energy Demand of Optimised Buildings in Selected 25 Locations.	48

Fig. 61: Annual Primary Energy Demand for Heating, Cooling, Lighting and Ventilation in Optimised Buildings as Functions of Latitude.	48
Fig. 62: Total Annual Primary Energy Demand of Optimised Buildings as Function of Latitude.	48
Fig. 63: Primary Energy Demand of Optimised Buildings as Function of Degree Days and Annual Illumination.....	49
Fig. 64: Relative Primary Energy Demand of Optimised Buildings as Function of Latitude.	49
Fig. 65: Relative Primary Energy Demand of Optimised Buildings as Functions of Degree Days and Annual Illumination.	49
Fig. 66: Primary Energy Demand of Optimised Buildings in Selected Locations relative to European Average (100%).	50
Fig. 67: European Building Energy Benchmark (EBEB) for Heating, Cooling and Lighting depending on the Latitude.	50
Fig. 68: Comparison of Primary Energy Demand for Heating of Typical and Optimised Buildings per Latitude.	51
Fig. 69: Comparison of Primary Energy Demand for Heating of Typical and Optimised Buildings per Heating Degree Days.	51
Fig. 70: Comparison of Primary Energy Demand for Cooling of Typical and Optimised Buildings per Latitude.....	52
Fig. 71: Comparison of Primary Energy Demand for Cooling of Typical and Optimised Buildings per Cooling Degree Days.	52
Fig. 72: Comparison of Primary Energy Demand for Lighting of Typical and Optimised Buildings per Latitude.	52
Fig. 73: Comparison of Primary Energy Demand for Lighting of Typical and Optimised Buildings per Annual Illumination.	52
Fig. 74: Comparison of Total Primary Energy Demand of Typical and Optimised Buildings per Latitude.....	53
Fig. 75: Exemplary Determination of Mean Values in [VDI 3807-2].....	54
Fig. 76: Exemplary Determination of Guide Values in [VDI 3807-2].	54
Fig. 77: Comparison of Results for Typical and Optimised Buildings in Frankfurt/Main with VDI 3807.....	56

Fig. 78: Latent and Sensible Loads for Cooling of Supply Air in Selected Locations according to [Colliver].....	57
Fig. 79: Latent and Sensible Loads for Cooling of Supply Air in Selected European Locations according to [Colliver].	57
Fig. 80: Annual Primary Energy Demand of 25 Typical Buildings including Latent Cooling (Humidity Ratio Setpoint: 0,0115 kg _{Water} /kg _{Dry Air}) as Function of the Latitude.	58
Fig. 81: Annual Primary Energy Demand of 25 Typical Buildings including Latent Cooling (Humidity Ratio Setpoint: 0,0115 kg _{Water} /kg _{Dry Air}) grouped by Latitude.	58
Fig. 82: Annual Primary Energy Demand of 25 Buildings for Latent Cooling (Humidity Ratio Setpoint: 0,0115 kg _{Water} /kg _{Dry Air}) as Function of the Cooling Degree Days.....	59
Fig. 83: Annual Primary Energy Demand of 25 Optimised Buildings including Latent Cooling (Humidity Ratio Setpoint: 0,0115 kg _{Water} /kg _{Dry Air}) as Function of the Latitude.	59
Fig. 84: Annual Primary Energy Demand of 25 Optimised Buildings including Latent Cooling (Humidity Ratio Setpoint: 0,0115 kg _{Water} /kg _{Dry Air}) grouped by Latitude.	59
Fig. 85: Annual Primary Energy Demand for Latent Cooling with different Humidity Ratio Setpoints as Functions of the Latitude.....	60
Fig. 86: Annual Total Primary Energy Demand including Latent Cooling with different Humidity Ratio Setpoints as Functions of Latitude.....	60
Fig. 87: Influence of the Humidity Ratio Setpoint on the Annual Total Primary Energy Demand as Function of the Cooling Degree Days.	61
Fig. 88: Definition of Indices and Classes of Primary Energy Demand within the Bandwidth of Results.	62
Fig. 89: Arrays for EB _{PCC} _{Heating} -Classes I–VI depending on HDD and CDD with exemplary Classification of Dortmund, Germany.....	63
Fig. 90: Arrays for EB _{PCC} _{Cooling} -Classes I–VI depending on HDD and CDD with exemplary Classification of Dortmund, Germany.....	63
Fig. 91: Arrays for EB _{PCC} _{Ventilation} -Classes I–VI depending on HDD and CDD with exemplary Classification of Dortmund, Germany.....	63
Fig. 92: Arrays for EB _{PCC} _{Lighting} -Classes I–VI depending on HDD and CDD with exemplary Classification of Dortmund, Germany.....	63

Fig. 93: Arrays for EB PCC_{Total} -Classes I–VI depending on HDD and CDD with exemplary Classification of Dortmund, Germany.	64
Fig. 94: Comparison of observed European and Global Changes in Surface Temperature with Results simulated by Climate Models using Natural and Anthropogenic Forcings [IPCC-4 WG I].	66
Fig. 95: Multi-model Averages and Assessed Ranges for Global Emissions of Greenhouse Gases and Global Surface Warming during the 21 st century [IPCC-4 WG I].	67
Fig. 96: Temperature Anomalies in Europe with Respect to 1901 to 1950. Observed (black line) and simulated (red envelope, 1906 to 2005) and Projected (orange envelope, 2001 to 2100, A1B scenario) [IPCC-4 WG I].	68
Fig. 97: Temperature Anomalies in Northern Europe with Respect to 1901 to 1950. Observed (black line) and simulated (red envelope, 1906 to 2005) and Projected (orange envelope, 2001 to 2100, A1B scenario) [IPCC-4 WG I].	68
Fig. 98: Temperature Anomalies in Southern Europe including the Mediterranean Coast with Respect to 1901 to 1950. Observed (black line) and simulated (red envelope, 1906 to 2005) and Projected (orange envelope, 2001 to 2100, A1B scenario) [IPCC-4 WG I].	68
Fig. 99: Temperature Anomalies on Small Islands in the Mediterranean with Respect to 1901 to 1950. Observed (black line) and simulated (red envelope, 1906 to 2005) and Projected (orange envelope, 2001 to 2100, A1B scenario) [IPCC-4 WG I].	68
Fig. 100: Annual Mean, Winter (DJF) and Summer (JJA) Temperature Changes over Europe between 1980 to 1999 and 2080 to 2099, averaged over 21 Models (Scenario A1B) [IPCC-4 WG I].	69
Fig. 101: Seasonal Averages for European Temperature Projections during the 21 st Century (based on [IPCC-4 WG I]).	69
Fig. 102: Increase of Annual Mean Air Temperature (Mean Values of one Decade) in Germany during the 21st Century under the Scenarios A1B, A2 and B1 [Jacob] compared to 1951-1990.	70
Fig. 103: Annual and Seasonal Temperature Changes in Germany by 2071-2100 compared to 1961-1990 under different SRES-Scenarios [Jacob].	70
Fig. 104: Heating Degree Days in Germany during the Reference Period and during 2071-2100 under different SRES-Scenarios [Jacob].	71
Fig. 105: Global Carbon Emissions from all Sources (Energy, Industry and Land-Use Changes) from 1990 to 2100 for the Four Scenarios used in [UKCIP02]. Observed Values to 2000 are grey.	72

Fig. 106: Change in Average Annual Temperature in the UK (with Respect to the Model-Simulated 1961-1990 Climate) for Thirty-Year Periods centred on the 2020s, 2050s and 2080s under different Emission Scenarios [UKCIP02]...	73
Fig. 107: Change in Average Annual and Seasonal Temperature in the UK (with Respect to the Model-Simulated 1961-1990 Climate) for Thirty-Year Periods centred on the 2020s, 2050s and 2080s under the High Emission Scenario [UKCIP02].	73
Fig. 108: Comparison of Predicted Average and Maximum Temperatures in London in the 2080s under the High Emissions Scenario with those in Marseille for 1961-90 [UKCIP].	73
Fig. 109: Trends for mean annual and seasonal air temperature at Zürich–Kloten from 1981 to 2003 [Frank].	74
Fig. 110: Trends for mean annual and seasonal mean solar radiation at Zürich–Kloten from 1981 to 2003 [Frank].	74
Fig. 111: Annual Heating and Cooling Energy Demand of Office Building 1 for Three Levels of Thermal Insulation [Frank].	75
Fig. 112: Annual Heating and Cooling Energy Demand of Office Building 2 for Three Levels of Thermal Insulation [Frank].	75
Fig. 113: Average Discomfort Temperatures, Office Building “as built” [UKCIP].	76
Fig. 114: CO ₂ -emissions, Office Building “as built” [UKCIP].	76
Fig. 115: Average Discomfort Temperatures, Office Building “adapted” [UKCIP].	77
Fig. 116: CO ₂ -emissions, Office Building “adapted” [UKCIP].	77
Fig. 117: Annual Mean Air Temperature in London during the 21 st Century under different Emission Scenarios and Periods.	78
Fig. 118: Annual Mean Air Temperature in Glasgow during the 21 st Century under different Emission Scenarios and Periods.	78
Fig. 119: Annual Solar Radiation in London during the 21 st Century under different Emission Scenarios and Periods.	78
Fig. 120: Annual Solar Radiation in Glasgow during the 21 st Century under different Emission Scenarios and Periods.	78
Fig. 121: Change of Seasonal Mean Air Temperatures during the 21st Century in London under High Emissions Scenario.	79
Fig. 122: Change of Seasonal Mean Air Temperatures during the 21st Century in Glasgow under High Emissions Scenario.	79

Fig. 123: Variation of Primary Energy Demand of an Optimised Building in London during the 21 st Century under High Emissions Scenario.	79
Fig. 124: Variation of Primary Energy Demand of an Optimised Building in Glasgow during the 21 st Century under High Emissions Scenario.	79
Fig. 125: Variation of Primary Energy Demand of an Optimised Building in London during the 21 st Century under different Emissions Scenarios and Periods..	80
Fig. 126: Variation of Primary Energy Demand of an Optimised Building in Glasgow during the 21 st Century under different Emissions Scenarios and Periods..	80
Fig. 127: Variation of Primary Energy Demand of a Typical Building in London during the 21 st Century under High Emissions Scenario.	81
Fig. 128: Variation of Primary Energy Demand of a Typical Building in Glasgow during the 21 st Century under High Emissions Scenario.	81
Fig. 129: Variation of Primary Energy Demand of a Typical Building in London during the 21 st Century under different Emissions Scenarios and Periods.	81
Fig. 130: Variation of Primary Energy Demand of a Typical Building in Glasgow during the 21 st Century under different Emissions Scenarios and Periods..	81
Fig. 131: Share of Buildings in the Global GHG-Emissions [WRI].	84
Fig. 132: Map of Europe with Selected Locations.	84
Fig. 133: Heating and Cooling Degree Days as Functions of the Latitude.	85
Fig. 134: Exemplary Visualisation of five Façades with different Window Proportions and resulting Daylight Situations inside the Office at Diffuse Sky Conditions.	85
Fig. 135: U-values of Glazings, Frames and Opaque Parts Depending on Insulation Level.	86
Fig. 136: Total Primary Energy Demand of an Optimised Building in Praha with Heat Protection Glass as Function of Insulation Level and Window Proportion. .	86
Fig. 137: Annual Primary Energy Demand of Optimised Buildings as Function of Latitude.	87
Fig. 138: European Building Energy Benchmark (EBEB) for Heating, Cooling and Lighting depending on the Latitude.	87
Fig. 139: Primary Energy Demand of Optimised Buildings as Function of Degree Days and Annual Illumination.	88

Fig. 140: Influence of the Humidity Ratio Setpoint on the Latent Cooling Energy Demand as Function of the Cooling Degree Days.	88
Fig. 141: Definition of Indices and Classes of Primary Energy Demand within the Bandwidth of Results.	88
Fig. 142: Arrays for EBPC _{Cooling} -Classes I–VI depending on HDD and CDD with exemplary Classification of Dortmund, Germany.	89
Fig. 143: Seasonal Averages for European Temperature Projections during the 21st Century (based on [IPCC-4 WG I]).	89
Fig. 144: Variation of Primary Energy Demand of an Optimised Building in London during the 21 st Century under different Emissions Scenarios and Periods..	90
Fig. 145: Variation of Primary Energy Demand of an Optimised Building in London during the 21st Century under the High Emissions Scenario.	90
Fig. 146: Anteil von Gebäudeemissionen an den weltweiten Treibhausgasemissionen [WRI].	91
Fig. 147: Landkarte Europas mit ausgewählten Standorten.	91
Fig. 148: Heiz- und Kühlgradtage der ausgewählten Standorte als Funktion der geographischen Breite.	92
Fig. 149: Beispielhafte Visualisierung von fünf Fassaden mit unterschiedlichen Fensterflächenanteilen und resultierender Tageslichtsituation im Büroraum bei bedecktem Himmel.	92
Fig. 150: U-Werte von Verglasung, Rahmen und opaken Teilen abhängig vom Wärmedämmstandard.	93
Fig. 151: Gesamtprimärenergiebedarf eines optimierten Gebäudes mit Wärmeschutzverglasung in Praha als Funktion von Wärmedämmstandard und Fensterflächenanteil.	93
Fig. 152: Jährlicher Primärenergiebedarf von optimierten Gebäuden als Funktion der geographischen Breite.	94
Fig. 153: Europäischer Gebäude-Energie-Maßstab (EBEB) für Heizung, Kühlung und Beleuchtung abhängig vom Breitengrad.	94
Fig. 154: Primärenergiebedarf optimierter Gebäude als Funktion der Gradtage und der jährlichen Beleuchtungsstärke.	95
Fig. 155: Einfluss des Sollwertes der Raumlufffeuchte auf den latenten Kühlenergiebedarf als Funktion der Kühlgradtage.	95

Fig. 156: Definition von Indizes und Klassen des Primärenergiebedarfes innerhalb der Bandbreite der Ergebnisse.	96
Fig. 157: Felder für die $EBPCC_{Kühlung}$ -Klassen I–VI abhängig von Heiz- und Kühlgradtagen mit beispielhafter Klassifizierung von Dortmund, Deutschland.	96
Fig. 158: Saisonale Mittelwerte der Europäischen Temperaturprojektionen im Laufe des 21. Jahrhunderts (basierend auf [IPCC-4 WG I]).....	97
Fig. 159: Veränderung des Primärenergiebedarfes eines optimierten Gebäudes in London während des 21. Jahrhunderts bei verschiedenen Emissionsszenarien und Zeiträumen.	97
Fig. 160: Veränderung des Primärenergiebedarfes eines optimierten Gebäudes in London während des 21. Jahrhunderts unter dem Szenario hoher Emissionen.	97
Fig. 161: Sorted heating and cooling energy demand as Functions of the Outside Air Temperature.	117
Fig. 162: Sunshade Control Strategy resulting from Minimal Primary Energy Demand for Heating and Cooling as Function of the Outside Air Temperature.	117
Fig. 163: Example of Sunshade Control Strategy and resulting Reduction of Solar Transmission.....	118
Fig. 164: Example of Sunshade Control Strategy and resulting Reduction of Light Transmission.....	120
Fig. 165: Local Distribution and Population in Urban Areas of Selected Locations.	125

19. List of Tables

Tab. 1: Visualisations and Dimensions of different Window Proportions.	29
Tab. 2: Characteristics of Selected Glazing Types.	30
Tab. 3: U_f -Values of Frames.	31
Tab. 4: U_{Wall} -Values of Opaque Parts of the Façade.	31
Tab. 5: Window U-Values depending on Window Proportion and Insulation Level. .	32
Tab. 6: Façade U-Values depending on Window Proportion and Insulation Level. .	33
Tab. 7: Assignment of Typical U-Values in EU-Countries to Insulation Levels.	35
Tab. 8: Definition of Window Proportions, Insulation Levels and Glazing Types for Typical Buildings.	36
Tab. 9: Results of Optimisation with lowest Total Primary Energy Demand per Orientation and for Average of Orientations.	41
Tab. 10: Comparison of Results for Typical and Optimised Buildings in Frankfurt/Main with VDI 3807.	55
Tab. 11: Variation of Setpoint Conditions in Terms of Humidity.	60
Tab. 12: SRES-scenarios on Emissions of Greenhouse Gases according to [IPCC-4 WG I].	66
Tab. 13: Building Elements and Materials used in the Dynamic Simulation.	114
Tab. 14: Energy Factors for Heating Energy Demand.	122
Tab. 15: Energy Factors for Cooling Energy Demand.	122
Tab. 16: Energy Factors for Ventilation Energy Demand.	123
Tab. 17: Energy Factors for Lighting Energy Demand.	124
Tab. 18: Characteristics of Selected Locations.	125

20. Appendix

20.1. Boundary Conditions of Building Simulation

20.1.1. Standard Office Room

Room Dimensions:

- Floor / Ceiling area: $2,50 \cdot 4,45 = 11,125 \text{ m}^2$
- Floor-to-floor height: 3,40 m
- Clear height: 3,00 m
- Room volume: $11,125 \cdot 3,00 = 33,375 \text{ m}^3$

Tab. 13: Building Elements and Materials used in the Dynamic Simulation.

Building Element	Height [m]	Width [m]	Area [m ²]	Construction	Thick-ness [m]	U-Value [W/(m ² K)]	Boundary Condition
External Wall (incl. windows)	2,5	3,00	7,50	Depending on Insulation Level	0,40	Depending on Insulation Level	Outside
External Walls (opaque parts)	Depending on Window Proportion			Steel/Insulation /Steel Sand-wich			
External Walls (transparent parts)				Depending on Insulation Level			
Internal Walls	2,50	3,00	7,50	Plasterboard, Insulation	0,10	0,635	Corridor (isotherm)
Internal Walls	4,45		13,35				Office (isotherm)
Ceilings / Floors	2,25	4,45	11,13	Concrete, False Floor, Carpet	0,4	1,412	

20.1.2. Temperature Control

The heating and cooling power has not been limited in the simulations in order to calculate the hourly demand. The temperature limits have been set according to the recommendations for energy calculations using dynamic simulations on an hourly basis in [EN 15251]:

Minimum indoor air temperature: 22 °C

Maximum indoor air temperature: 24,5 °C

20.1.3. Ventilation Control

During the period of use (weekdays, (8h to 18h), a constant air flow rate has been assumed, providing the air change rates recommended in [EN 15251] for new and refurbished buildings with low emissions from materials (category II).

With the assumption of one person per room and the floor area and air volume described in chapter 20.1.1, the required total air current calculates to

$$q_{tot} = 1Person * 7 \frac{l}{(s * Person)} + 11,125m^2 * 0,7 \frac{l}{(s * m^2)} = 14,7875 \frac{l}{s} = 14,7875 \frac{l}{s} * 3,6 \frac{(m^3 * s)}{(h * l)}$$
$$= 53,235 \frac{m^3}{h}$$

The required air change rate calculates to $\frac{53,235 m^3/h}{33,375 m^3} = 1,595 h^{-1}$

Taking into account a permanent leakage rate of $0,2 h^{-1}$, the resulting air change rate is $1,595 - 0,2 = 1,395 h^{-1}$, the resulting air current during the period of use is $1,395 h^{-1} * 33,375 m^3 = 46,56 m^3/h$.

According to [EN 15251], beyond the period of use for non-residential buildings a ventilation rate of $0,1 - 0,2 \frac{l}{(s * m^2)}$ is recommended, i.e. an leakage change rate of $11,125m^2 * 0,16 \frac{l}{(s * m^2)} * 3,6 \frac{(m^3 * s)}{(h * l)} / 33,375m^3 = 0,2 h^{-1}$. Thus the leakage rate provides a sufficient air change beyond the period of use.

A heat recovery system with an average efficiency (recovered heat coefficient) of 50% was assumed. Therefore, depending on the air flow rate, the exhaust and supply (i.e. outdoor) air temperature, a respective reduction of ventilation energy losses (heating and cooling) was taken into account during the period of use according to [VDI 2071].

20.1.4. Dehumidification / Latent Cooling Loads

Only those latent cooling loads were considered, which are required to cool and dehumidify the ventilated air to a certain setpoint. It was further assumed, that the air enters the room at the same setpoint conditions as the indoor air temperature.

It should be recognized that the energy demand resulting from this procedure is for the minimum required enthalpy changes of the air, only. Due to the design and efficiency of the cooling system, the actual latent cooling energy demand may be larger. Effects of indoor sources and sinks of moisture (persons, equipment, moisture storage in materials etc.) were not taken into account.

With these assumptions, the latent cooling load could be calculated from the amount of moisture which must be removed, i.e. from the differences of humidity ratios of outdoor conditions and indoor setpoint conditions. With reference to the air temperature for cooling (see chapter 20.1.2) the setpoint was assumed at

- Air temperature: 24,5 °C
- Relative humidity: 60% (acc. to class II in [EN 15251])

The latent energy calculates to

$$q_{\text{Latent}} = L * (x_{\text{outside}} - x_{\text{setpoint}}) \text{ [kWh/kg]}$$

where

- L: Latent heat of water vaporisation
(0,694805555 kWh / kg_{Water} = 2501,3 kJ / kg_{Water})
- x_{outside} : Humidity ratio of outside air
- x_{setpoint} : Humidity ratio at setpoint (0,0115 kg_{Water} / kg_{Dry Air})

The latent energy removed from a certain air volume flow rate per time step of one hour then calculates to

$$Q_{\text{Latent}} = V * \rho_p * q_{\text{Latent}} \text{ [kWh/h]}$$

where

- V: Volume flow rate [m³/h]
- ρ_p : Density of air (1,2041 kg/m³, assumption: 20°C, sea level)

Latent cooling loads were only taken into account if during occupancy, a sensible cooling load occurred in the room at the same time.

20.1.5. Sunshade Control

20.1.5.1. Control Strategy

The sunshading was controlled automatically depending on the total irradiation on the façade. The level of irradiation required for activation of the sunshading varied depending on the outside air temperature. This control type allows having maximum sunshading in order to prevent high cooling loads and, at the same time, not loose solar gains when desired.

To find the appropriate control function, a sensitivity analysis was performed using an average, South facing façade type (mean window proportion “w3”, mean insulation level “U3” etc.) for a certain constant sunshade control level. The resulting hourly primary energy demands for heating and cooling (mean values) were analysed and arranged in correlation to the outside air temperature during their respective time steps. The example of a sun shade control level of 150 W/m² (see Fig. 161) shows, that the building has no heating and cooling energy demand around 12 °C outside air temperature. Heating and cooling loads occur below and loads above this value.

Repeating this analysis for a set of sunshade control levels between 0 and 450 W/m² brought a set of data with building behaviour under different sun shade control levels (see Fig. 162). The diagram shows that the lowest heating loads at temperatures below 13°C occur at the highest sun shade control level analysed, i.e. 450 W/m². The lowest cooling loads can be achieved at the lowest sunshade control level of 0 W/m², independent from the outside temperature. Between 5 and 15 °C the minimal sum of heating and cooling loads (sum of primary energy demands) shows a transition between the highest and lowest sun shade control levels.

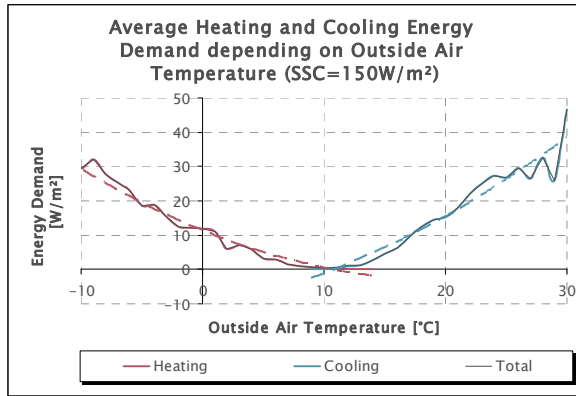


Fig. 161: Sorted heating and cooling energy demand as Functions of the Outside Air Temperature.

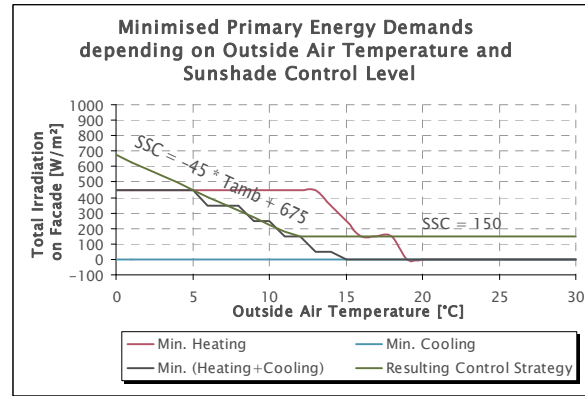


Fig. 162: Sunshade Control Strategy resulting from Minimal Primary Energy Demand for Heating and Cooling as Function of the Outside Air Temperature.

From these results a control strategy could be deduced, activating the sun shading system at a total irradiation on the façade of 150 W/m² when temperatures exceed 11,7 °C. Below this temperature, the sun shade control level increases with decreasing ambient temperature (T_{amb}), in order to take advantage of solar gains as much as possible. The function of this transition was identified as $SSC = -45 * T_{amb} + 675$ [W/m²].

20.1.5.2. Sunshade Systems

The sunshading was realised by external louvers (“venetian blinds”). Depending on different factors such as the colour and the position of the lamellas, these systems reduce the transmission of solar radiation through the window with good efficiency. But as the degree of light transmission is reduced at the same time, the daylight situation in the room and as a result the artificial lighting demand can be affected strongly.

A “cut-off”-strategy has turned out to represent the actual user’s behaviour best: In order to have enough daylight in the room as well as a visual connection to the outside, the lamella will usually be closed by 45° only [Kuhn].

The venetian blinds can usually be used as glare protection at the same time. For the time period where direct (beam) radiation hits the façade and the external shading system is not activated for thermal reasons, a second system for glare protection is needed. This is very often realised by internal textile screens protecting from the glare but still leaving a certain view outside.

[DIN V 18599-2] provides typical values for the resulting solar transmission of different glazing types combined with different shading systems. From these tables an average reduction of solar transmission can be calculated for external louvers in 45° and 10° positions as well as for internal textile screens.

During the period of use, no shading system was activated as long as there was no beam radiation on the façade and the total radiation was lower than the control level for the external shading. As soon as direct radiation occurred on the façade during

the period of use while the total radiation was still low, the internal screen was used to prevent glare effects from the window. The thermal effects of the internal screen were taken into account as an internal shading system. The screen was removed when either the external sun shading system was activated, or when there was no more direct radiation on the façade or beyond the period of use.

Once the total radiation on the façade exceeded the respective control level, the external shading system was activated. If a 10°-position of the louvers resulted in a non-sufficient daylight situation in the room (i.e. less than 500 lux on the desk level), the user brought the lamellas into a 45°-position. If there was no demand for artificial light despite the external shading fully closed, the lamella were left in the 10°-position.

The control strategy and the reduction of transmitted solar radiation resulting from the use of internal screen and external sun shading system has been visualised in Fig. 163 (simplified example for a sunshade control level of 150 W/m² for the whole day).

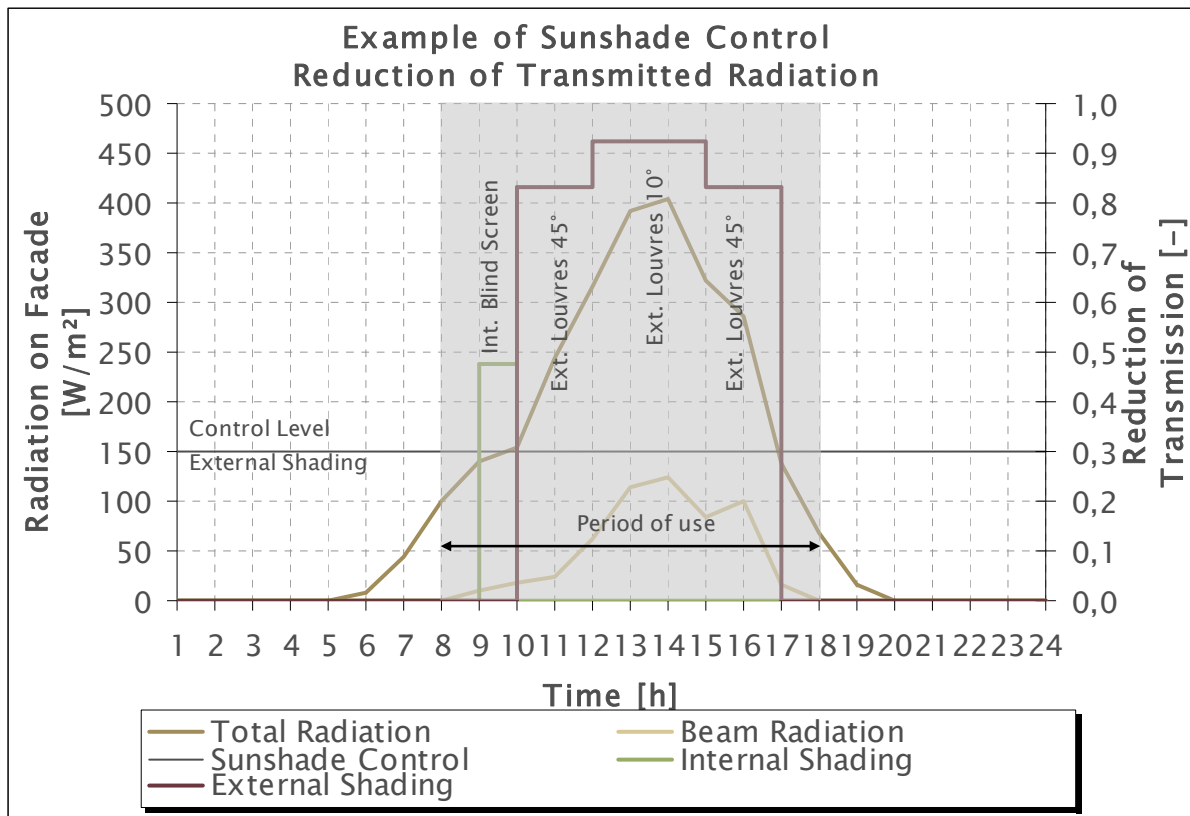


Fig. 163: Example of Sunshade Control Strategy and resulting Reduction of Solar Transmission.

Beyond the period of use, the internal screen was open all the time. The external louvers were then operated depending on the total radiation on the façade and the respective sun shade control level either in open or fully closed (10°) position.

20.1.6. Lighting Energy Demand

20.1.6.1. Daylight factor of the Room

The daylight factor of the room was calculated using the software “Relux Vision”. The reflexion factors of internal surfaces were selected according to the minimum values in [DIN 5034-1]:

- Floor: Reflexion 20%
- Ceiling: Reflexion 70%
- Walls: Reflexion 50%

Depending on the window proportion and the light transmission of the glazing, mean daylight factors were calculated on a height of 85 cm above floor level (according to [DIN 5034-4]) under overcast sky conditions (CIE, acc. to [DIN 5034-1]). Using the daylight factor, the average illumination on the desk level could be calculated.

Based on the assumption of self-dimming lights, during the period of office use the artificial lighting energy demand required to achieve a total of 500 lux on the desk level was calculated. The thermal effects of the partially dimmed artificial lighting were taken into account accordingly.

20.1.6.2. Impacts of the Sun Shading System

As described in chapter 20.1.5.1, due to the combined control of an internal blind screen and an external sun shading system, no relevant amount of direct light could enter the room at any time. Therefore, the daylight factor could be used to calculate the average horizontal illumination on desk level depending on the outside horizontal illumination.

Depending on the activation of the internal blind screen (white) or the external venetian blinds (see chapter 20.1.5.1) the light transmission of the windows had to be reduced. Factors for the respective reduction of light transmission were obtained from [DIN V 18599-4] also taking into account the different lamella positions of the venetian blind. The resulting reduction of daylight transmission depending on the control strategy of the sun shading systems is exemplified in Fig. 164.

A reduction of the transmission of 0,943 means, that for glazing with a given light transmission (τ) of for example 78%, the light transmission including external louvers in 10°-position would be reduced to

$$0,78 * (1 - 0,943) = 0,0445 = 4,45\%.$$

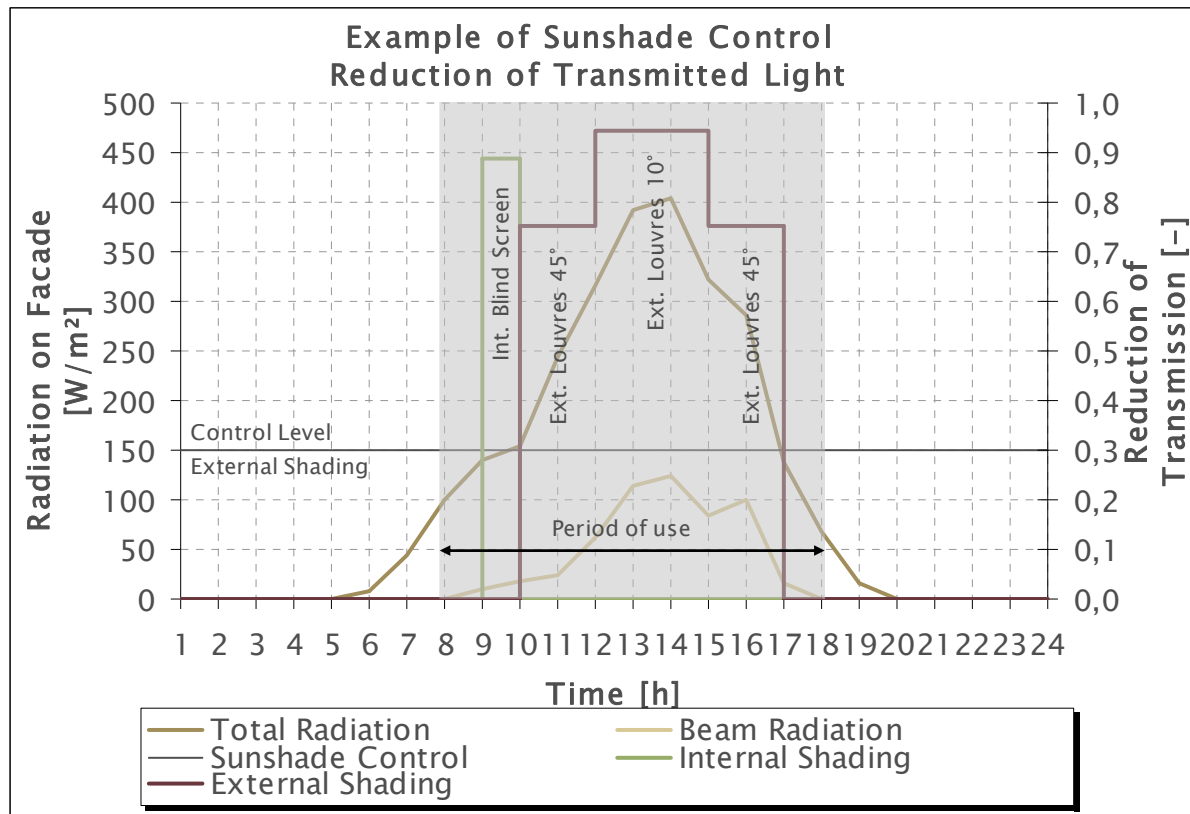


Fig. 164: Example of Sunshade Control Strategy and resulting Reduction of Light Transmission.

Depending on the sunshade control strategy, these factors were multiplied with the daylight factor of the room. With this procedure, the average indoor illumination on desk level could be calculated for each time step depending on the outside illumination on a horizontal surface, the window proportion and glazing type, the corresponding daylight factor of the room and the control strategy of the internal blind screen and the external venetian blinds.

Again, depending on the illumination on the desk level, the lighting energy demand required to achieve 500 lux on the desk was calculated. The thermal effects of the partially dimmed artificial lighting were taken into account accordingly.

20.1.7. Energy Factors

20.1.7.1. General

The energy demand was evaluated on a level of primary energy. Since the outcomes of the building simulation usually are use energy, i.e. the energy demand of the room itself, assumptions had to be made for the efficiency of technical systems and for the energy resources used. The assumptions of efficiencies were made based on typical values for standard systems.

Since primary energy factors do not exist for all parts of Europe, German values taken from [DIN V 18599-1] have been used uniformly for all locations. For gas and oil the primary energy factors can be assumed to be more or less the same all over Europe. Depending on the mix of power generation types (especially in terms of the

share of renewable and nuclear energies), the actual primary energy factors for electricity may vary from country to country. Since there is an active trade of electricity within the European countries, it was considered acceptable to use the German Factors as average values for Europe.

The calculation from one energy level to the next is done by multiplication of the lower level with the respective energy factor for the next level:

$$\text{End Energy} = \text{Use Energy} * \text{EndEnergyFactor}$$

$$\text{Primary Energy} = \text{End Energy} * \text{PrimaryEnergyFactor}$$

The total energy factors indicated in the following tables Tab. 14 to Tab. 17 describe the ratio between use and primary energy:

$$\text{Primary Energy} = \text{Use Energy} * \text{TotalEnergyFactor}$$

where

$$\text{TotalEnergyFactor} = \text{EndEnergyFactor} * \text{PrimaryEnergyFactor}$$

20.1.7.2. Heating

The use energy for heating was a direct outcome of the dynamic building simulation. The energy factors assumed in this work for the calculation of further energy levels can be found in Tab. 14.

Tab. 14: Energy Factors for Heating Energy Demand.

Heating Energy	Factor	Unit	Comment
EndEnergyFactor	1,15	kWh _{End} /kWh _{Use}	Typical Heating System [Energieleitfaden]
PrimaryEnergyFactor	1,1	kWh _{Prim} /kWh _{End}	Oil or Gas (non-renewable part) [DIN V 18599-1]
TotalEnergyFactor	1,265	kWh _{Prim} /kWh _{Use}	-

20.1.7.3. Cooling

The use energy for cooling was a direct outcome of the dynamic building simulation. The energy factors assumed in this work for the calculation of further energy levels can be found in Tab. 15.

Tab. 15: Energy Factors for Cooling Energy Demand.

Cooling Energy	Cooling	Unit	Comment
EndEnergyFactor	0,33	kWh _{End} /kWh _{Use}	Typical Compression Chiller System [Energieleitfaden]
PrimaryEnergyFactor	2,7	kWh _{Prim} /kWh _{End}	Electricity Mix (non-renewable part) [DIN V 18599-1]
TotalEnergyFactor	0,891	kWh _{Prim} /kWh _{Use}	-

20.1.7.4. Ventilation

The energy demand for ventilation is highly influenced by the ventilation concept (natural or mechanical ventilation) of a building and the technical systems (centralised or decentralised ventilation etc.) in case of mechanical ventilation. Thus it was decided to assume a standard ventilation energy demand for all calculations, representing a typical centralised mechanical ventilation system.

Since the ventilation system was not simulated in detail, the energy demand for ventilation was calculated from standard consumptions and the operating hours, i.e. the period of office use.

With the required air current (see chapter 20.1.3) and an average specific ventilation energy demand [Energieleitfaden] the electrical use energy for ventilation was calculated per hour:

$$46,56 \text{ m}^3/\text{h} * 0,56 \text{ W}_{\text{Use,el}}/(\text{m}^3/\text{h}) = 26,07 \text{ Wh}_{\text{Use,el}}/\text{h}$$

The annual use energy was calculated by multiplication of the hourly energy demand with the number of hours with mechanical ventilation (see 20.1.3). The energy factors assumed in this work for the calculation of further energy levels can be found in Tab. 16.

Tab. 16: Energy Factors for Ventilation Energy Demand.

Ventilation Energy	Factor	Unit	Comment
EndEnergyFactor	1,43	kWh _{End} /kWh _{Use}	Typical Centralised Mechanical Ventilation System (pressure losses etc.) [Energieleitfaden]
PrimaryEnergyFactor	2,7	kWh _{Prim} /kWh _{End}	Electricity Mix (non-renewable part) [DIN V 18599-1]
TotalEnergyFactor	3,861	kWh _{Prim} /kWh _{Use}	-

20.1.7.5. Lighting

As described in chapter 20.1.6, an artificial lighting self-dimming depending on the amount of daylight in the room was assumed. Thus, for each time step the fraction of the maximum installed lighting energy demand was calculated. With the installed specific lighting capacity and the floor area, the use energy demand for 100% lighting (maximum light use) in one time step calculates to:

$$13 \text{ W/m}^2 * 11,125 \text{ m}^2 = 144,625 \text{ Wh}_{\text{Use,el}}$$

The energy factors assumed in this work for the calculation of further energy levels can be found in Tab. 17.

Tab. 17: Energy Factors for Lighting Energy Demand.

Lighting Energy	Factor	Unit	Comment
EndEnergyFactor	1,05	kWh _{End} /kWh _{Use}	Typical Efficiency of Lighting Systems (control losses etc.) [Energieleitfaden]
PrimaryEnergyFactor	2,7	kWh _{Prim} /kWh _{End}	Electricity Mix (non-renewable part) [DIN V 18599-1]
TotalEnergyFactor	2,835	kWh _{Prim} /kWh _{Use}	-

20.2. Characteristics of Selected Locations

Tab. 18: Characteristics of Selected Locations.

Latitude Group	Location number	Location name	Country	Latitude	Longitude	Height above sea level	Number of inhabitants
				[°N]	[°E]	[m]	[-]
60°N	01	Bergen	Norway	60,38	5,33	0	200.600
	02	Oslo	Norway	59,93	10,75	154	787.400
	03	Uppsala	Sweden	59,88	17,7	29	126.400
	04	Stockholm	Sweden	59,35	18,08	15	1.621.700
	05	Helsinki	Finland	60,22	25	12	1.147.000
55°N	06	Glasgow	United Kingdom	55,88	-4,25	56	1.086.200
	07	Kiel	Germany	54,33	10,13	22	231.700
	08	Kobenhavn	Germany	55,72	12,57	19	1.096.100
	09	Gdansk	Poland	54,37	18,68	0	866.800
	10	Vilnius	Lithuania	54,67	25,32	121	555.500
50°N	11	London	United Kingdom	51,5	-0,17	36	11.230.500
	12	Brussels	Belgium	50,38	4,35	100	1.740.300
	13	Frankfurt/Main	Germany	50,1	8,68	125	2.717.800
	14	Praha	Czech Republic	50,1	14,43	256	1.379.200
	15	Krakow	Poland	50,05	19,92	216	783.100
45°N	16	Bordeaux	France	44,83	-0,57	11	935.100
	17	Milano	Italy	45,47	9,2	98	4.051.500
	18	Zagreb	Croatia	45,8	15,97	146	890.900
	19	Beograd	Serbia	44,83	20,5	200	1.695.300
	20	Bucuresti	Romania	44,45	26,17	79	2.249.400
40°N	21	Madrid	Spain	40,41	-3,71	608	5.078.100
	22	Valencia	Spain	39,48	-0,4	47	1.406.600
	23	Palma de Mallorca	Spain	39,58	2,65	1	350.700
	24	Napoli	Italy	40,83	14,25	0	3.620.300
	25	Salonika	Greece	40,63	22,93	149	798.100

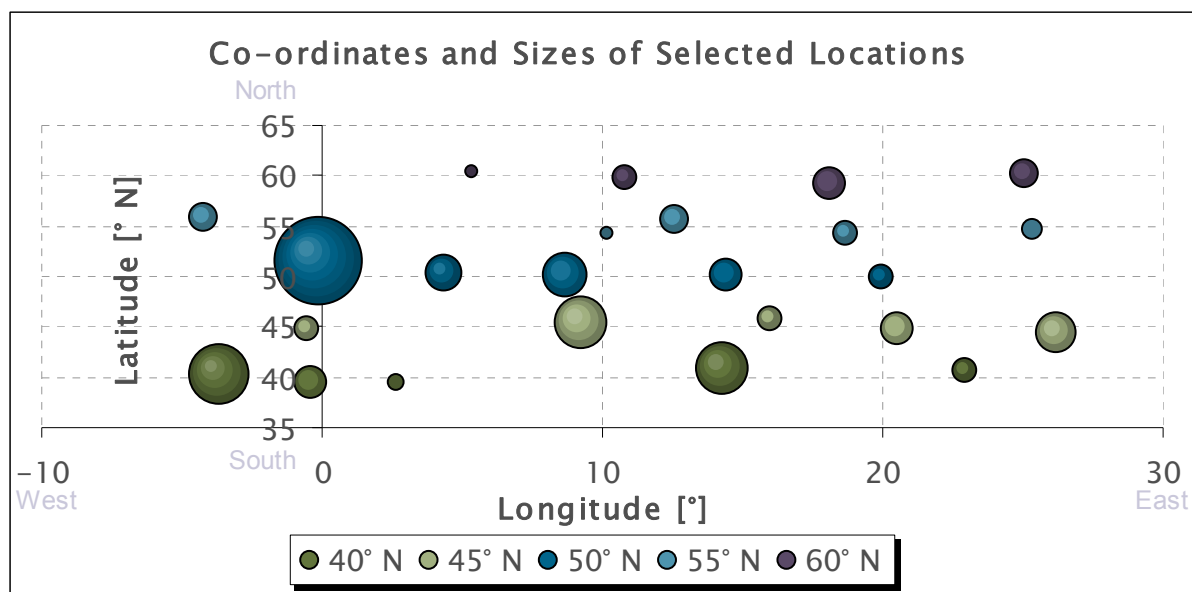


Fig. 165: Local Distribution and Population in Urban Areas of Selected Locations.

20.3. Climatic Data and Results of Selected Locations

20.3.1. Location 01 - Bergen

Location	Location name	Bergen (N)	
	Latitude (North positive)	[°]	50,1
	Longitude (East positive)	[°]	8,68
	Height above sealevel	[m]	125

Assumed Period of Office Use	Begin (local time)	[h]	8
	End (local time)	[h]	18
	Office use per day	[h]	10
	Office use per year	[h]	2607,14

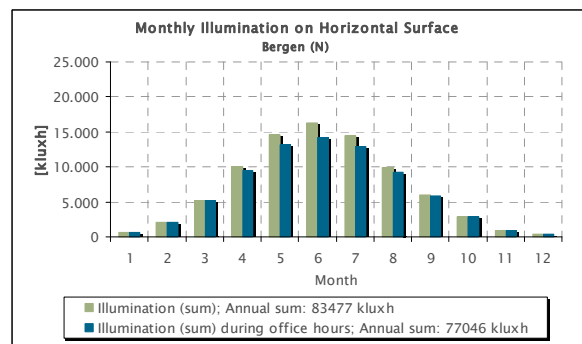
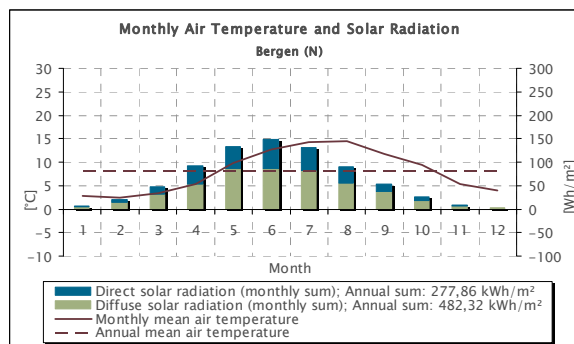
Temperature	Max. daily mean air temperature	[°C]	20,60
	Min. daily mean air temperature	[°C]	-5,28
	Max. monthly mean air temperature	[°C]	14,39
	Min. monthly mean air temperature	[°C]	2,34
	Annual mean air temperature	[°C]	8,00
	Standard deviation of daily mean from annual mean air temperature	[°C]	5,3

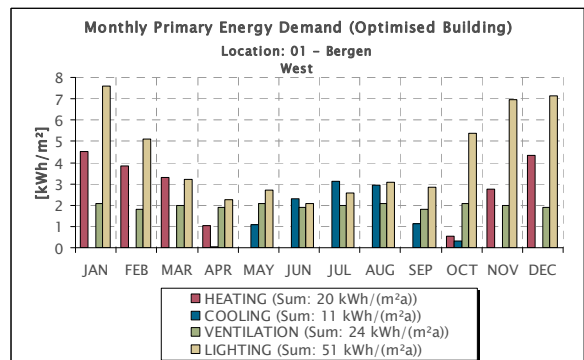
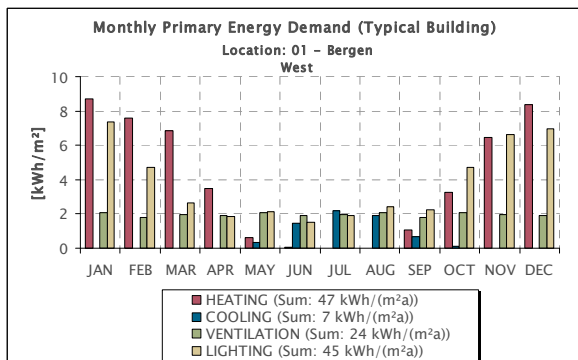
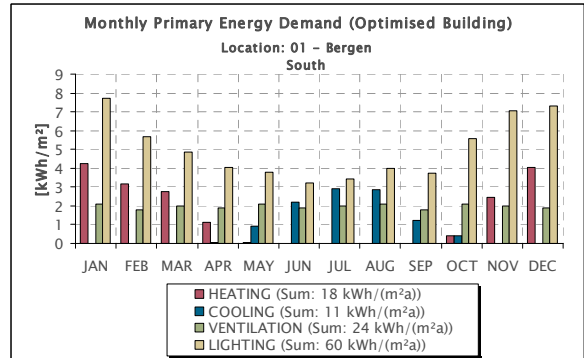
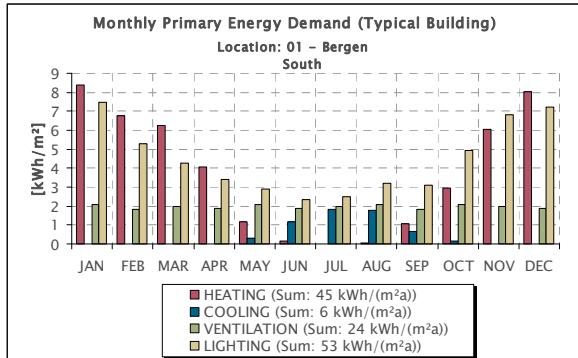
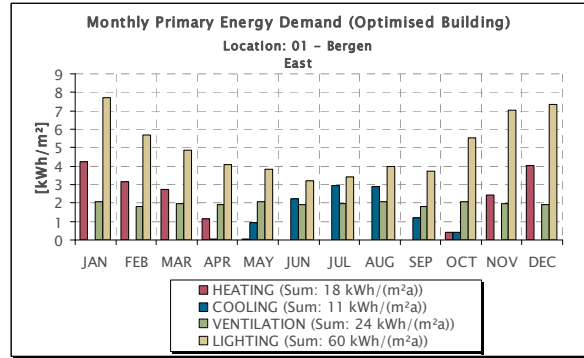
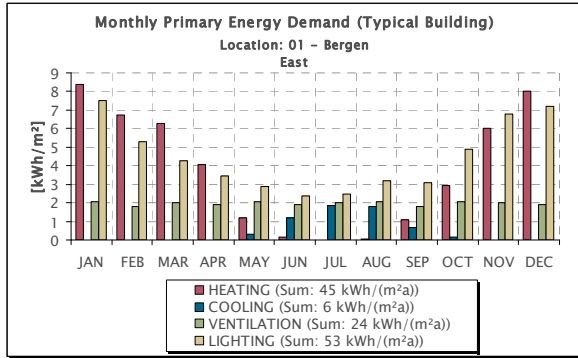
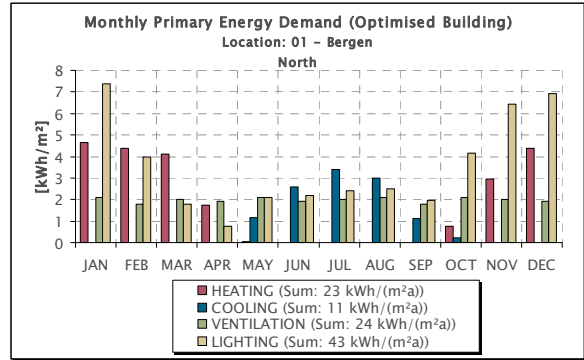
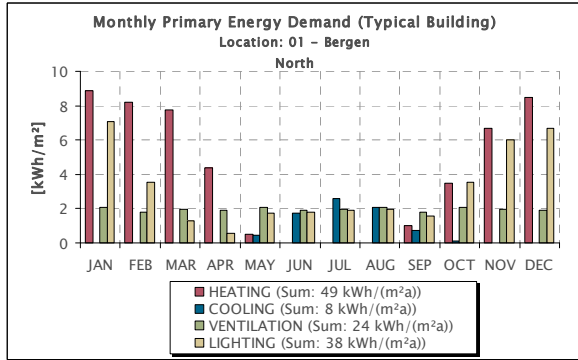
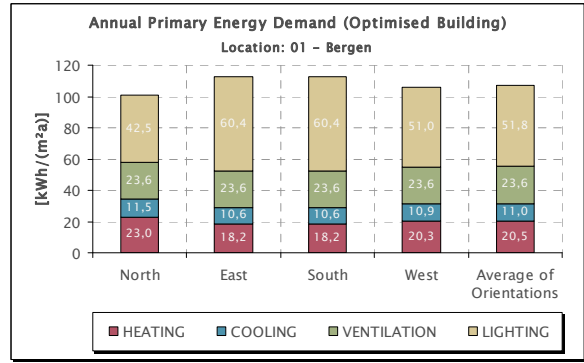
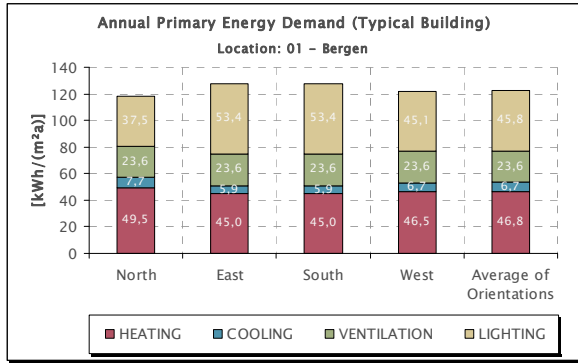
Heat. / Cool. Degree Days	Heating Degree Days (Base 18°C)	[Kd]	3674,00
	Cooling Degree Days (Base 10°C)	[Kd]	534,08

Solar Radiation	Annual total diffuse rad. on horiz. surf.	[kWh/m ²]	482,32
	Annual total direct rad. on horiz. surf.	[kWh/m ²]	277,86
	Annual total global rad. on horiz. surf.	[kWh/m ²]	760,18

Daylight	Annual total illumination on horiz. surf.	[kluxh]	83.477
	Annual total daylight hours	[h]	4.285
	Average illuminance on horiz. surf.	[lux]	19.481
	Annual total illumination on horiz. surf. during office use	[kluxh]	77.046
	Annual total daylight hours during office use	[h]	3.431
	Average illuminance on horiz. surf. during office use	[lux]	22.456

Air Humidity	Mean relative humidity	[-]	0,75
--------------	------------------------	-----	------





20.3.2. Location 02 – Oslo

Location	Location name	Oslo (N)	
	Latitude (North positive)	[°]	50,1
	Longitude (East positive)	[°]	8,68
	Height above sealevel	[m]	125

Assumed Period of Office Use	Begin (local time)	[h]	8
	End (local time)	[h]	18
	Office use per day	[h]	10
	Office use per year	[h]	2607,14

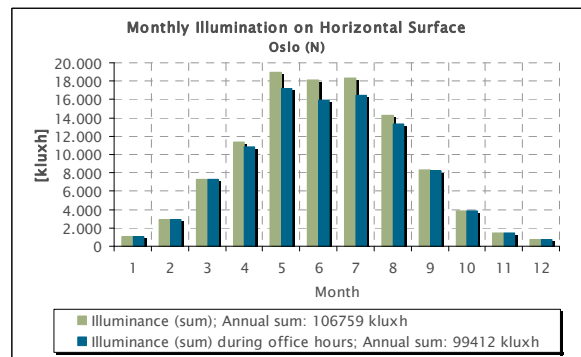
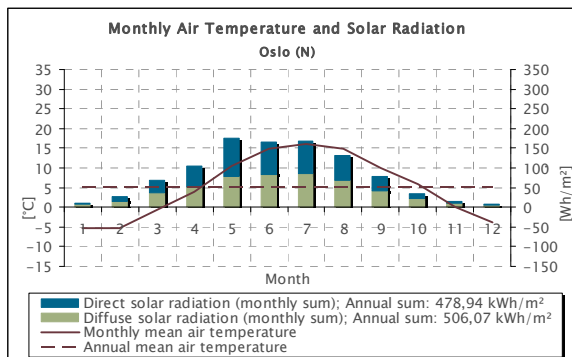
Temperature	Max. daily mean air temperature	[°C]	20,64
	Min. daily mean air temperature	[°C]	-16,36
	Max. monthly mean air temperature	[°C]	16,11
	Min. monthly mean air temperature	[°C]	-5,29
	Annual mean air temperature	[°C]	5,14
	Standard deviation of daily mean from annual mean air temperature	[°C]	8,4

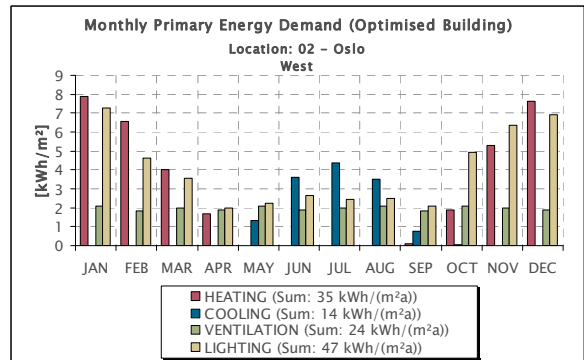
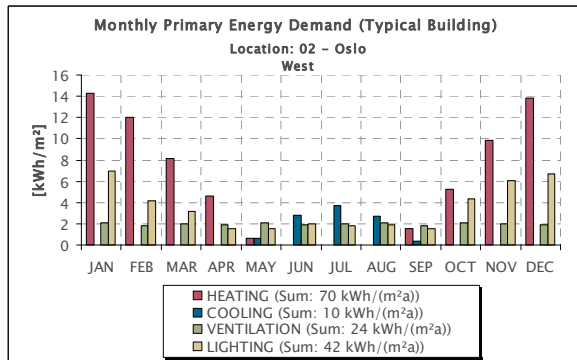
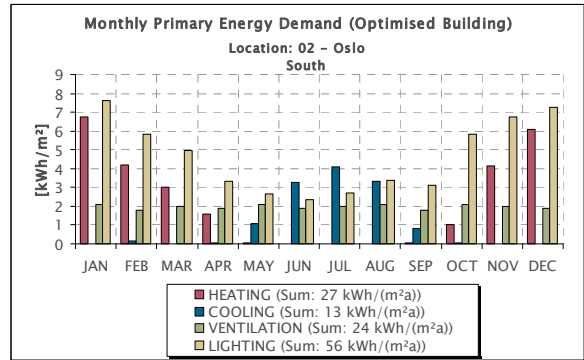
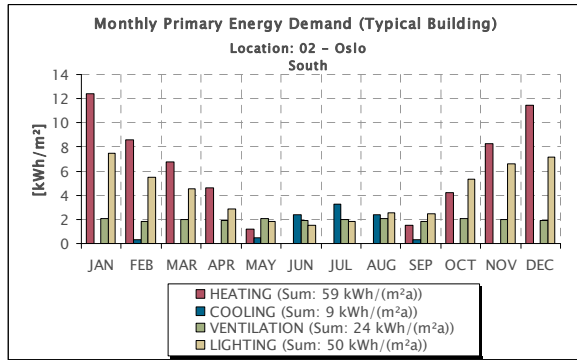
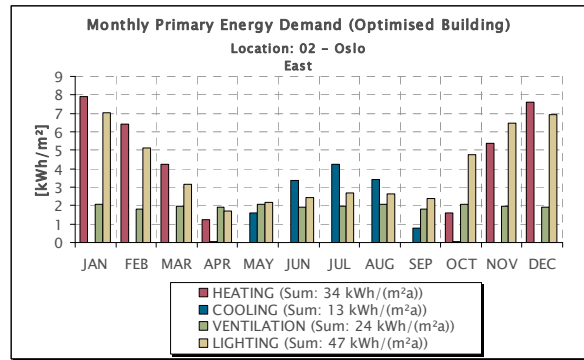
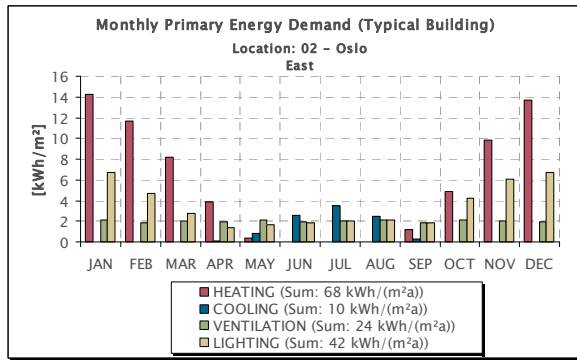
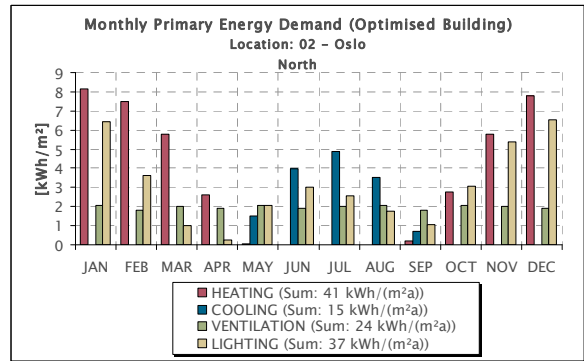
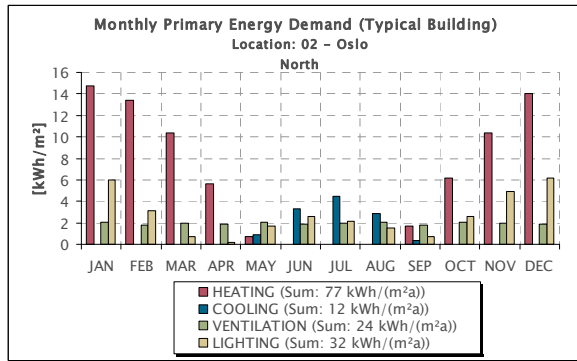
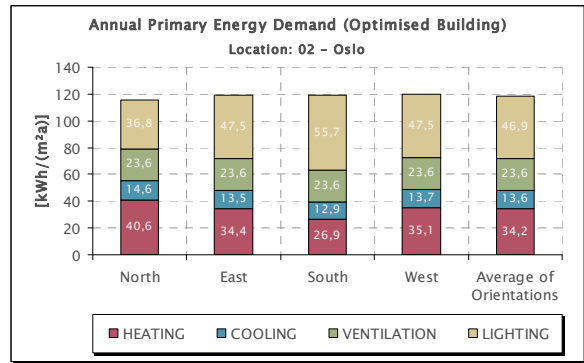
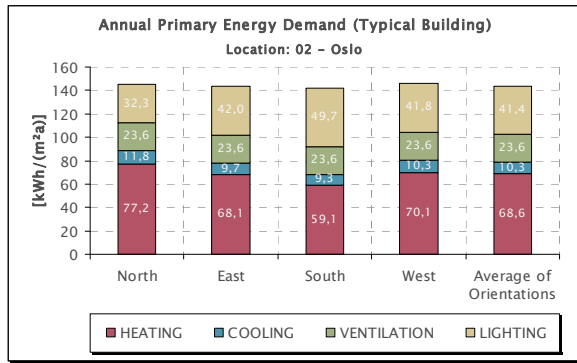
Heat. / Cool. Degree Days	Heating Degree Days (Base 18°C)	[Kd]	4744,26
	Cooling Degree Days (Base 10°C)	[Kd]	607,50

Solar Radiation	Annual total diffuse rad. on horiz. surf.	[kWh/m ²]	506,07
	Annual total direct rad. on horiz. surf.	[kWh/m ²]	478,94
	Annual total global rad. on horiz. surf.	[kWh/m ²]	985,01

Daylight	Annual total illumination on horiz. surf.	[kluxh]	106.759
	Annual total daylight hours	[h]	4.291
	Average illuminance on horiz. surf.	[lux]	24.880
	Annual total illumination on horiz. surf. during office use	[kluxh]	99.412
	Annual total daylight hours during office use	[h]	3.446
	Average illuminance on horiz. surf. during office use	[lux]	28.848

Air Humidity	Mean relative humidity	[-]	0,72
--------------	------------------------	-----	------





20.3.3. Location 03 – Uppsala

Location	Location name	Uppsala (S)	
	Latitude (North positive)	[°]	50,1
	Longitude (East positive)	[°]	8,68
	Height above sealevel	[m]	125

Assumed Period of Office Use	Begin (local time)	[h]	8
	End (local time)	[h]	18
	Office use per day	[h]	10
	Office use per year	[h]	2607,14

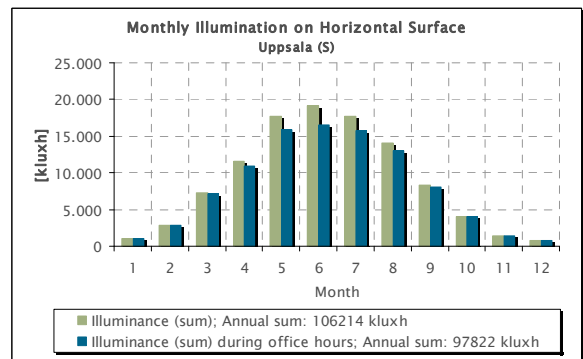
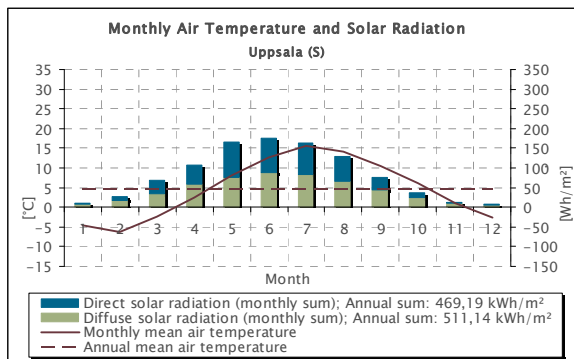
Temperature	Max. daily mean air temperature	[°C]	22,46
	Min. daily mean air temperature	[°C]	-18,41
	Max. monthly mean air temperature	[°C]	15,59
	Min. monthly mean air temperature	[°C]	-6,29
	Annual mean air temperature	[°C]	4,63
	Standard deviation of daily mean from annual mean air temperature	[°C]	8,28

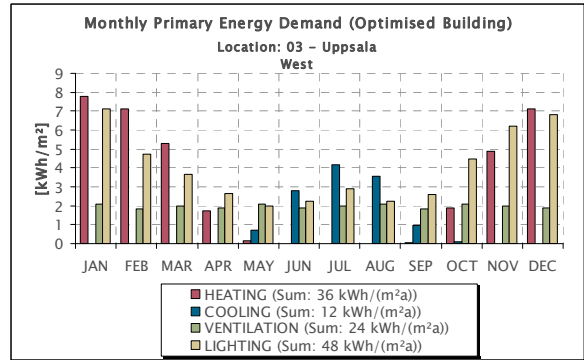
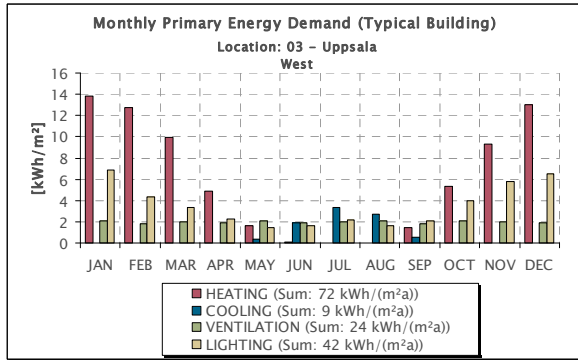
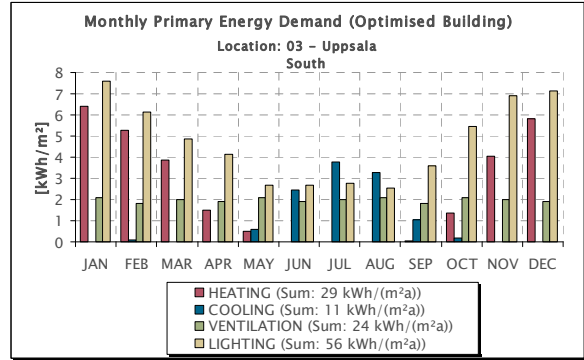
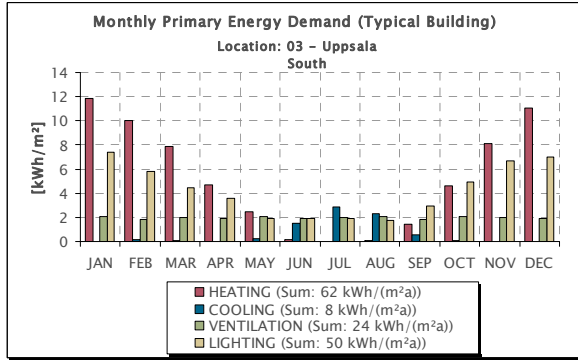
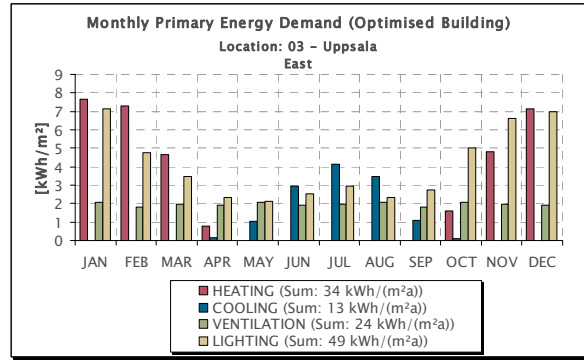
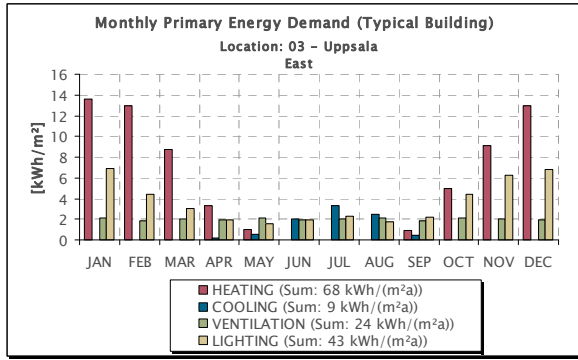
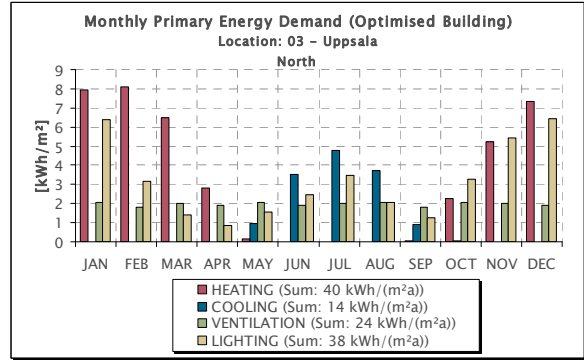
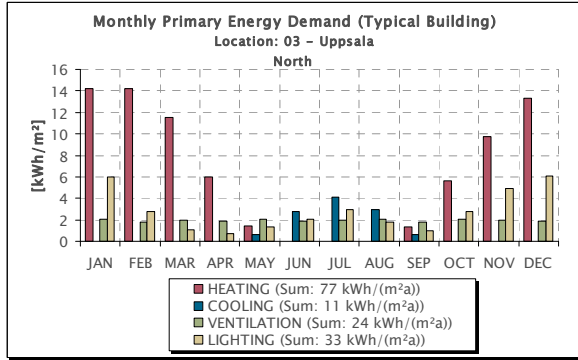
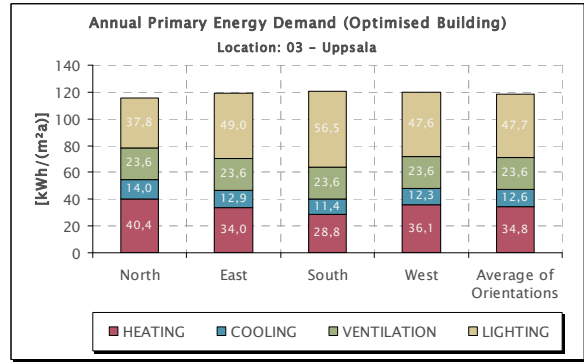
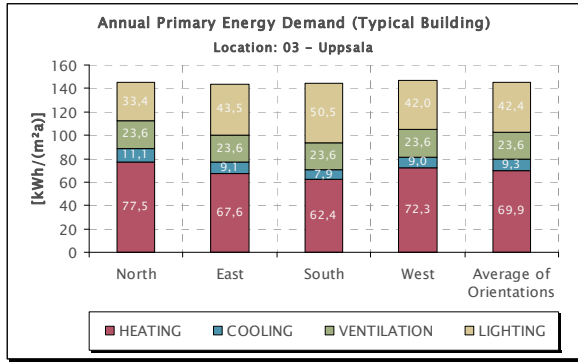
Heat. / Cool. Degree Days	Heating Degree Days (Base 18°C)	[Kd]	4928,78
	Cooling Degree Days (Base 10°C)	[Kd]	543,60

Solar Radiation	Annual total diffuse rad. on horiz. surf.	[kWh/m²]	511,14
	Annual total direct rad. on horiz. surf.	[kWh/m²]	469,19
	Annual total global rad. on horiz. surf.	[kWh/m²]	980,33

Daylight	Annual total illumination on horiz. surf.	[kluxh]	106.214
	Annual total daylight hours	[h]	4.302
	Average illuminance on horiz. surf.	[lux]	24.689
	Annual total illumination on horiz. surf. during office use	[kluxh]	97.822
	Annual total daylight hours during office use	[h]	3.432
	Average illuminance on horiz. surf. during office use	[lux]	28.503

Air Humidity	Mean relative humidity	[-]	0,79
--------------	------------------------	-----	------





20.3.4. Location 04 – Stockholm

Location	Location name	Stockholm (S)	
	Latitude (North positive)	[°]	50,1
	Longitude (East positive)	[°]	8,68
	Height above sealevel	[m]	125

Assumed Period of Office Use	Begin (local time)	[h]	8
	End (local time)	[h]	18
	Office use per day	[h]	10
	Office use per year	[h]	2607,14

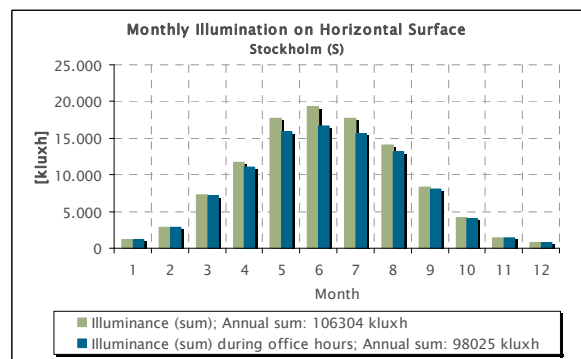
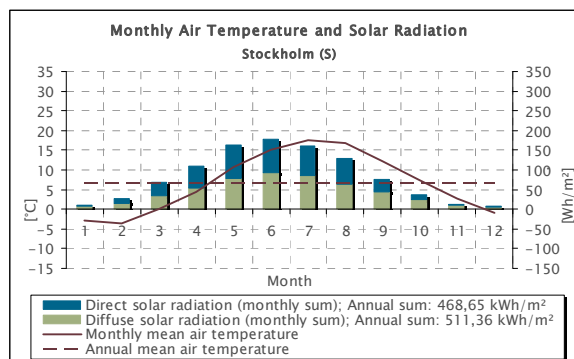
Temperature	Max. daily mean air temperature	[°C]	24,41
	Min. daily mean air temperature	[°C]	-15,08
	Max. monthly mean air temperature	[°C]	17,44
	Min. monthly mean air temperature	[°C]	-3,49
	Annual mean air temperature	[°C]	6,69
	Standard deviation of daily mean from annual mean air temperature	[°C]	8,2

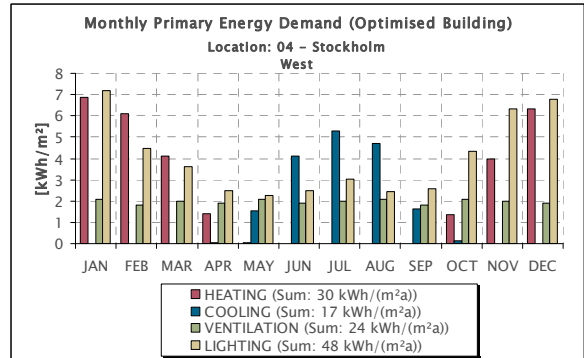
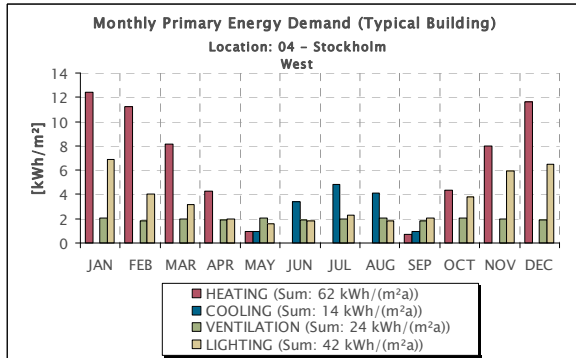
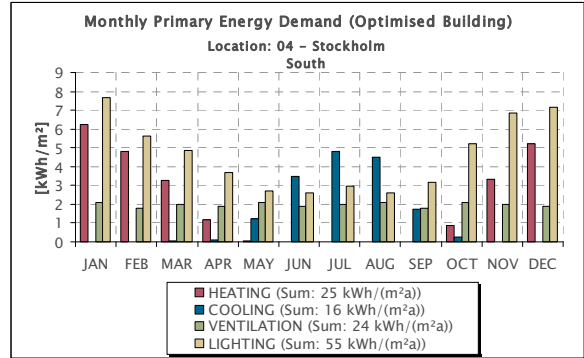
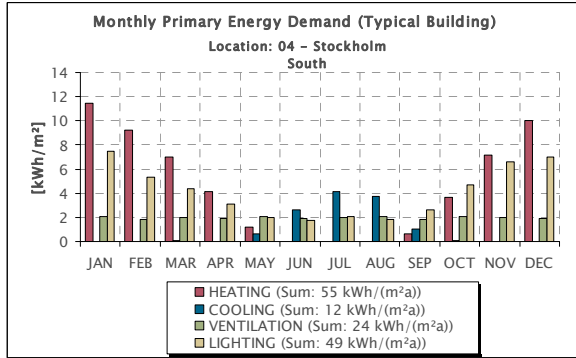
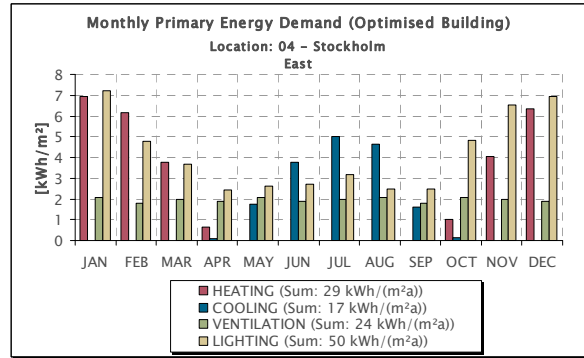
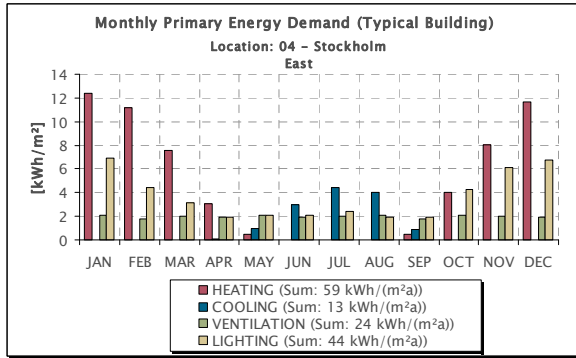
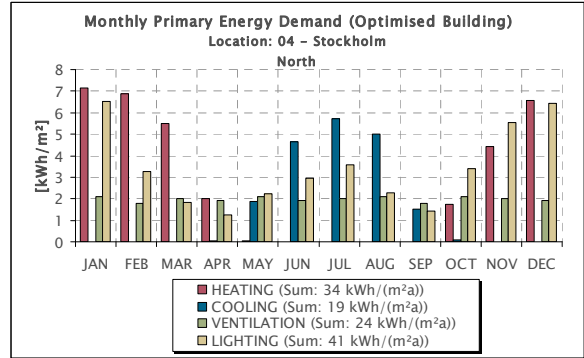
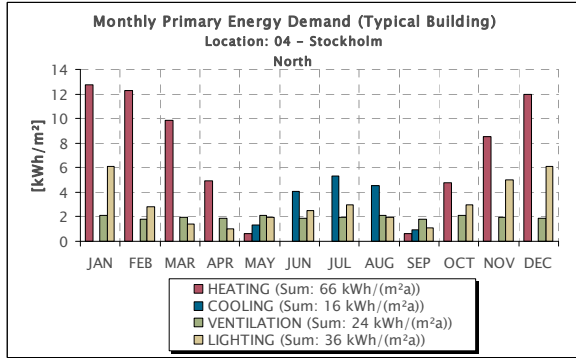
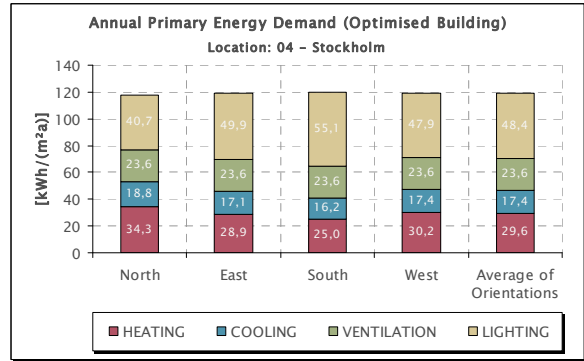
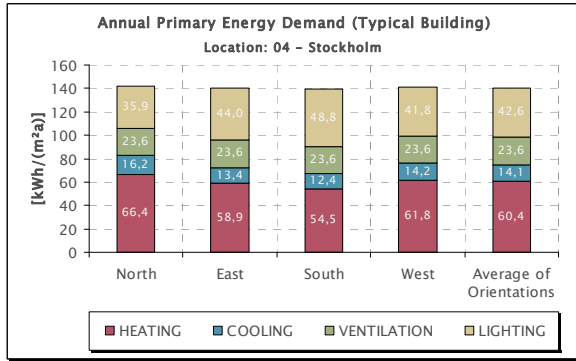
Heat. / Cool. Degree Days	Heating Degree Days (Base 18°C)	[Kd]	4235,33
	Cooling Degree Days (Base 10°C)	[Kd]	792,62

Solar Radiation	Annual total diffuse rad. on horiz. surf.	[kWh/m ²]	511,36
	Annual total direct rad. on horiz. surf.	[kWh/m ²]	468,65
	Annual total global rad. on horiz. surf.	[kWh/m ²]	980,01

Daylight	Annual total illumination on horiz. surf.	[kluxh]	106.304
	Annual total daylight hours	[h]	4.308
	Average illuminance on horiz. surf.	[lux]	24.676
	Annual total illumination on horiz. surf. during office use	[kluxh]	98.025
	Annual total daylight hours during office use	[h]	3.448
	Average illuminance on horiz. surf. during office use	[lux]	28.429

Air Humidity	Mean relative humidity	[-]	0,72
--------------	------------------------	-----	------





20.3.5. Location 05 – Helsinki

Location	Location name	Helsinki (FIN)	
	Latitude (North positive)	[°]	50,1
	Longitude (East positive)	[°]	8,68
	Height above sealevel	[m]	125

Assumed Period of Office Use	Begin (local time)	[h]	8
	End (local time)	[h]	18
	Office use per day	[h]	10
	Office use per year	[h]	2607,14

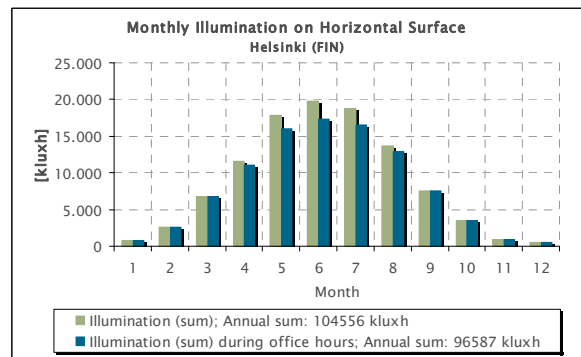
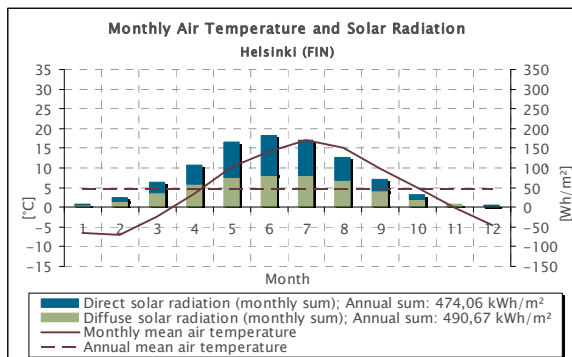
Temperature	Max. daily mean air temperature	[°C]	22,18
	Min. daily mean air temperature	[°C]	-18,54
	Max. monthly mean air temperature	[°C]	16,94
	Min. monthly mean air temperature	[°C]	-6,95
	Annual mean air temperature	[°C]	4,59
	Standard deviation of daily mean from annual mean air temperature	[°C]	8,9

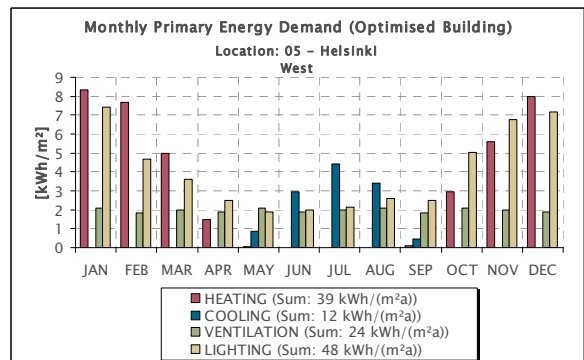
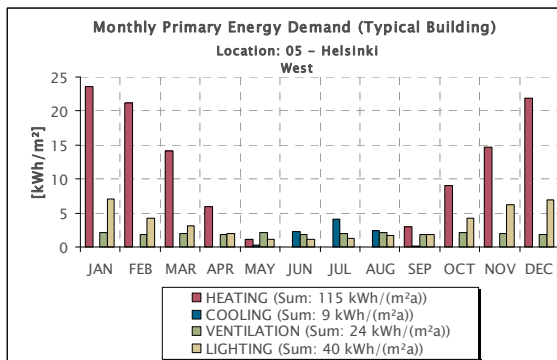
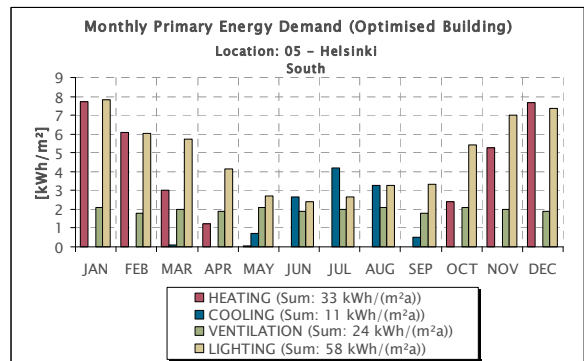
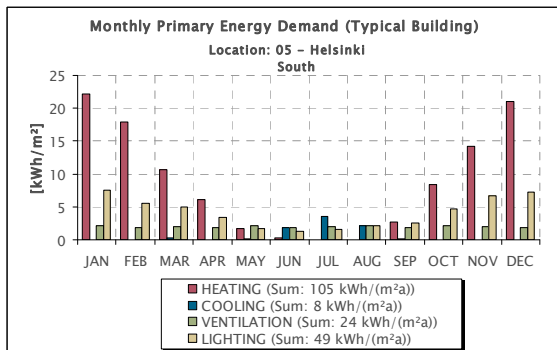
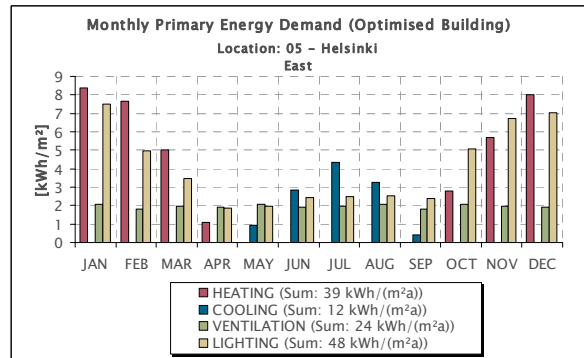
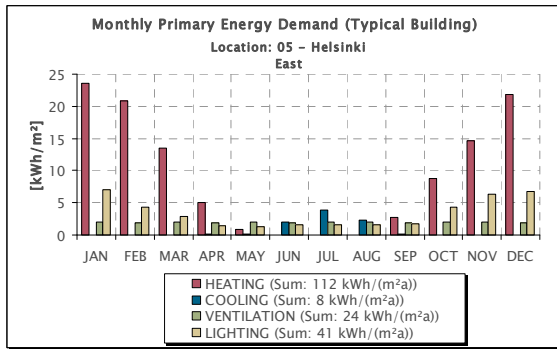
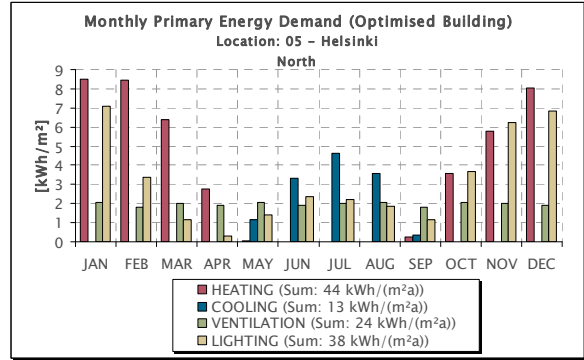
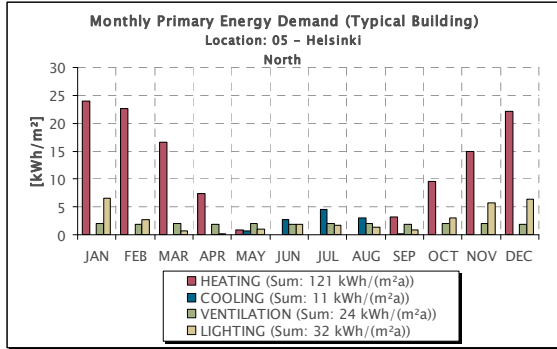
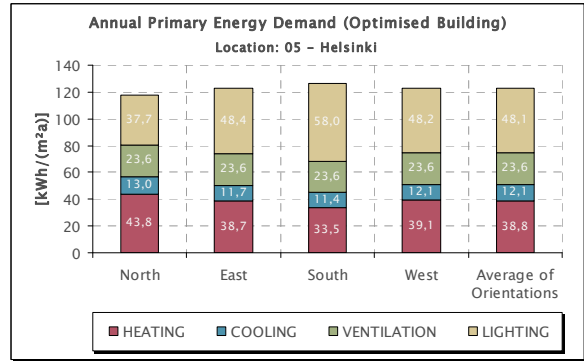
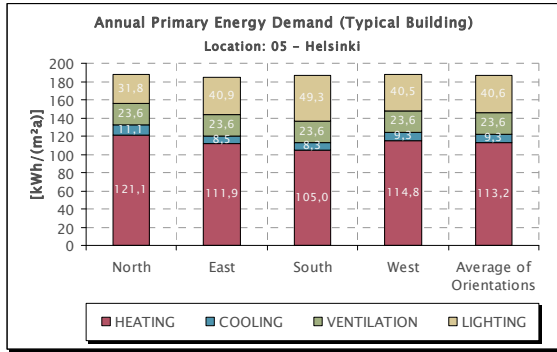
Heat. / Cool. Degree Days	Heating Degree Days (Base 18°C)	[Kd]	4930,85
	Cooling Degree Days (Base 10°C)	[Kd]	570,89

Solar Radiation	Annual total diffuse rad. on horiz. surf.	[kWh/m ²]	490,67
	Annual total direct rad. on horiz. surf.	[kWh/m ²]	474,06
	Annual total global rad. on horiz. surf.	[kWh/m ²]	964,73

Daylight	Annual total illumination on horiz. surf.	[kluxh]	104.556
	Annual total daylight hours	[h]	4.287
	Average illuminance on horiz. surf.	[lux]	24.389
	Annual total illumination on horiz. surf. during office use	[kluxh]	96.587
	Annual total daylight hours during office use	[h]	3.438
	Average illuminance on horiz. surf. during office use	[lux]	28.094

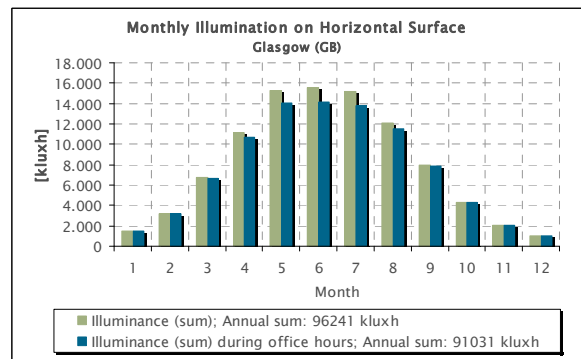
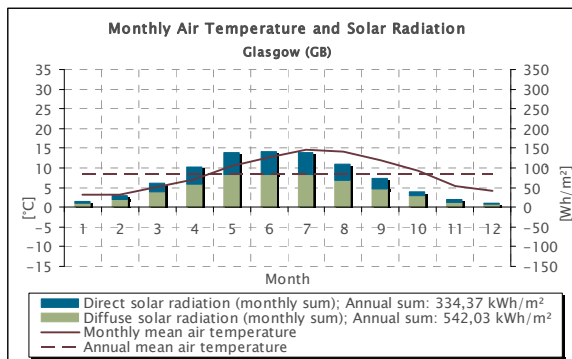
Air Humidity	Mean relative humidity	[-]	0,77
--------------	------------------------	-----	------

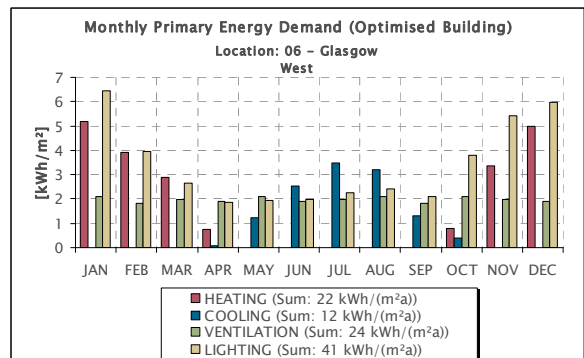
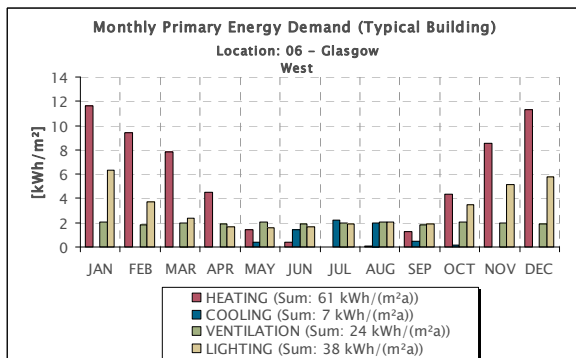
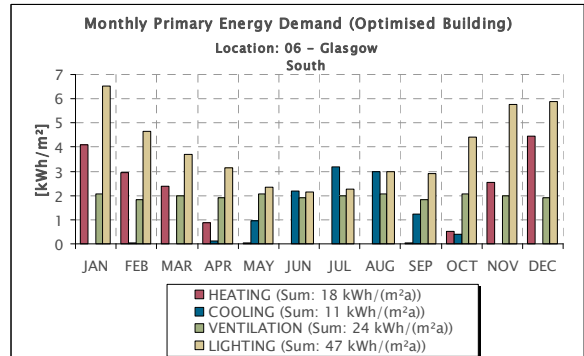
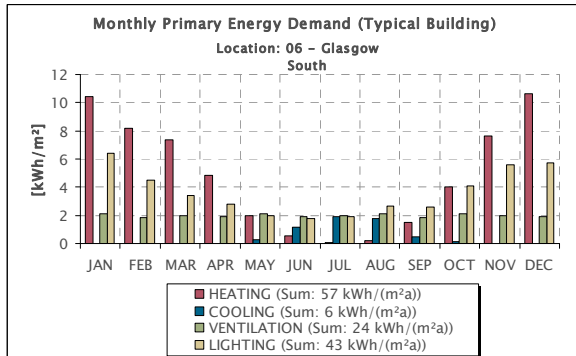
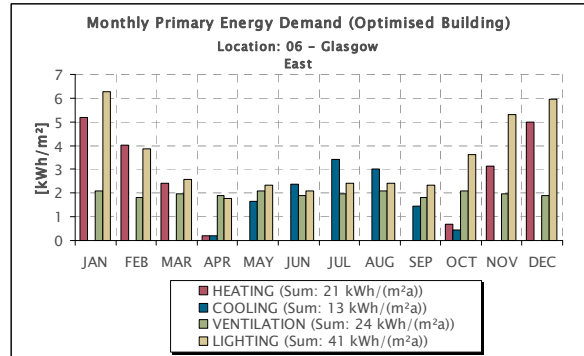
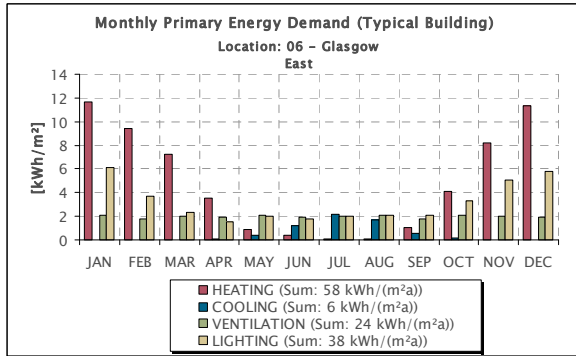
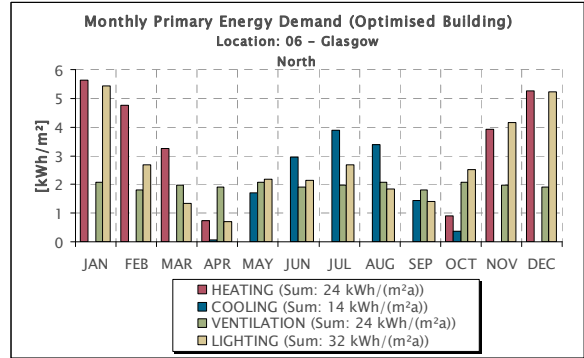
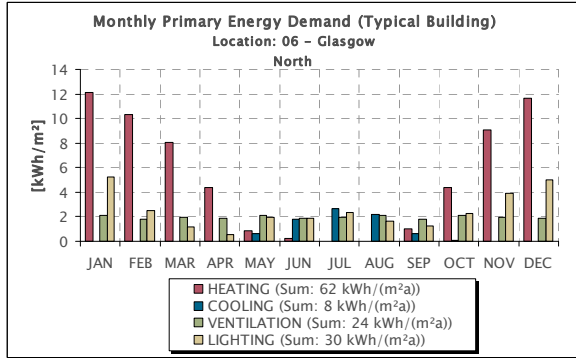
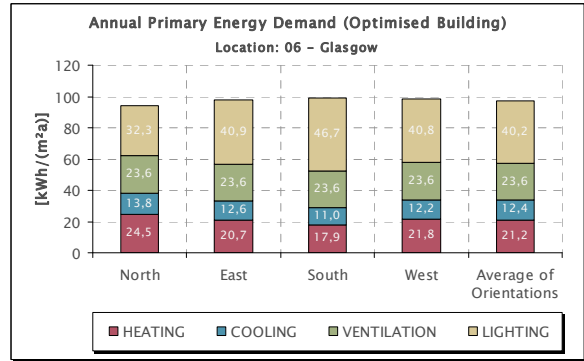
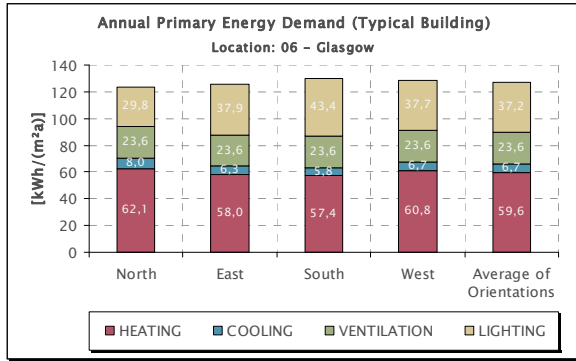




20.3.6. Location 06 – Glasgow

Location	Location name	Glasgow (GB)	
	Latitude (North positive)	[°]	50,1
	Longitude (East positive)	[°]	8,68
	Height above sealevel	[m]	125
Assumed Period of Office Use	Begin (local time)	[h]	8
	End (local time)	[h]	18
	Office use per day	[h]	10
	Office use per year	[h]	2607,14
Temperature	Max. daily mean air temperature	[°C]	19,06
	Min. daily mean air temperature	[°C]	-5,88
	Max. monthly mean air temperature	[°C]	14,51
	Min. monthly mean air temperature	[°C]	3,16
	Annual mean air temperature	[°C]	8,48
	Standard deviation of daily mean from annual mean air temperature	[°C]	4,9
Heat. / Cool. Degree Days	Heating Degree Days (Base 18°C)	[Kd]	3496,30
	Cooling Degree Days (Base 10°C)	[Kd]	567,40
Solar Radiation	Annual total diffuse rad. on horiz. surf.	[kWh/m ²]	542,03
	Annual total direct rad. on horiz. surf.	[kWh/m ²]	334,37
	Annual total global rad. on horiz. surf.	[kWh/m ²]	876,40
Daylight	Annual total illumination on horiz. surf.	[kluxh]	96.241
	Annual total daylight hours	[h]	4.313
	Average illuminance on horiz. surf.	[lux]	22.314
	Annual total illumination on horiz. surf. during office use	[kluxh]	91.031
	Annual total daylight hours during office use	[h]	3.568
	Average illuminance on horiz. surf. during office use	[lux]	25.513
Air Humidity	Mean relative humidity	[-]	0,80





20.3.7. Location 07 – Kiel

Location	Location name	Kiel (D)	
	Latitude (North positive)	[°]	50,1
	Longitude (East positive)	[°]	8,68
	Height above sealevel	[m]	125

Assumed Period of Office Use	Begin (local time)	[h]	8
	End (local time)	[h]	18
	Office use per day	[h]	10
	Office use per year	[h]	2607,14

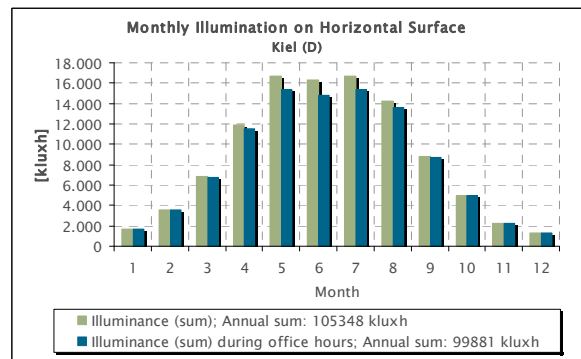
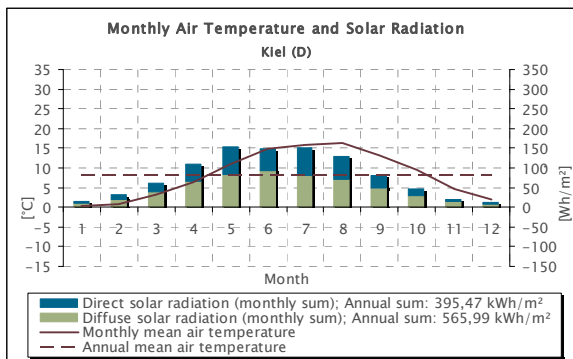
Temperature	Max. daily mean air temperature	[°C]	23,40
	Min. daily mean air temperature	[°C]	-8,76
	Max. monthly mean air temperature	[°C]	16,26
	Min. monthly mean air temperature	[°C]	0,35
	Annual mean air temperature	[°C]	8,21
	Standard deviation of daily mean from annual mean air temperature	[°C]	6,6

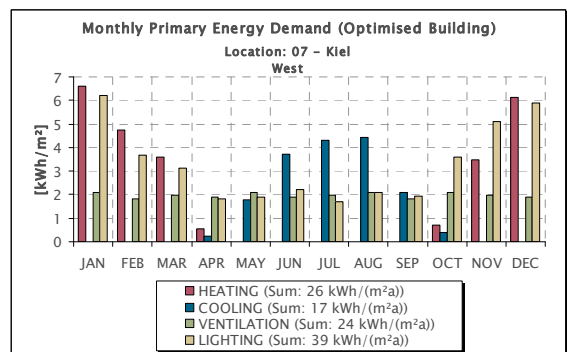
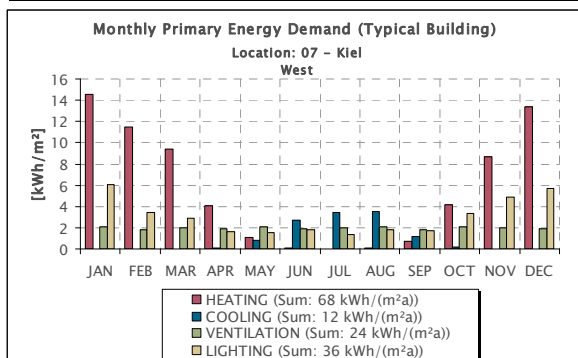
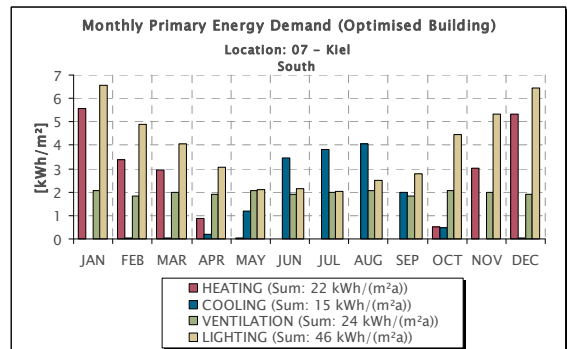
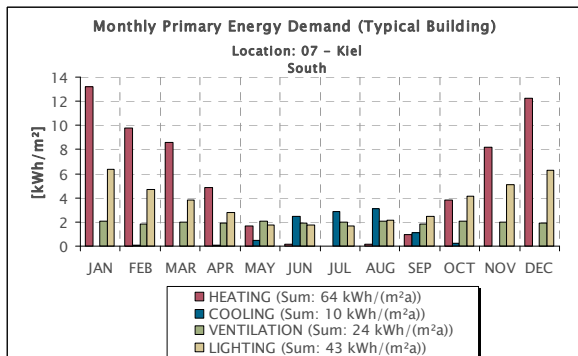
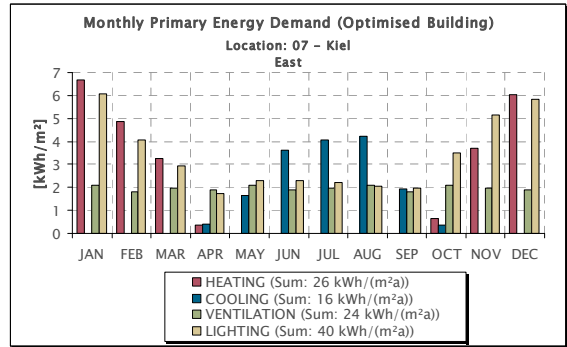
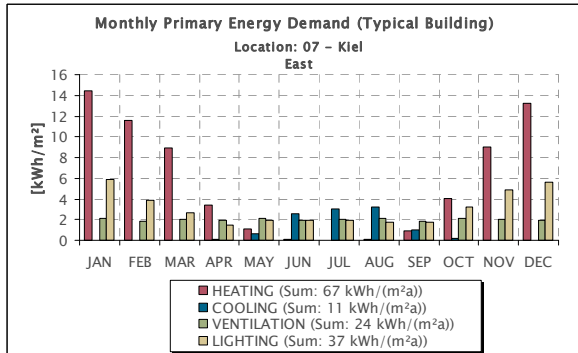
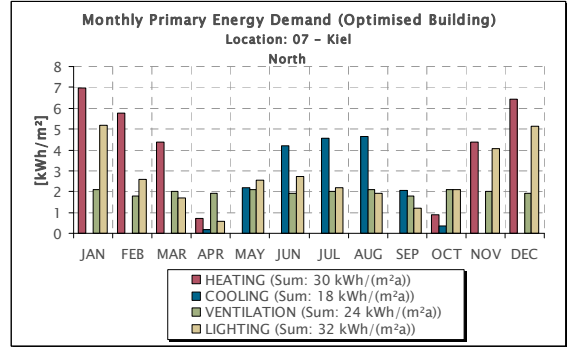
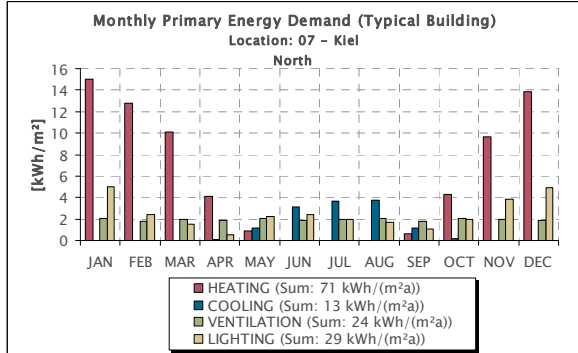
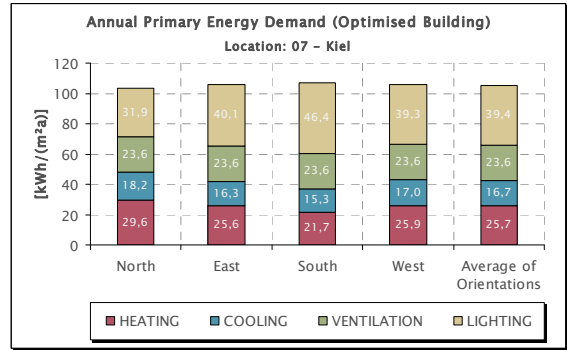
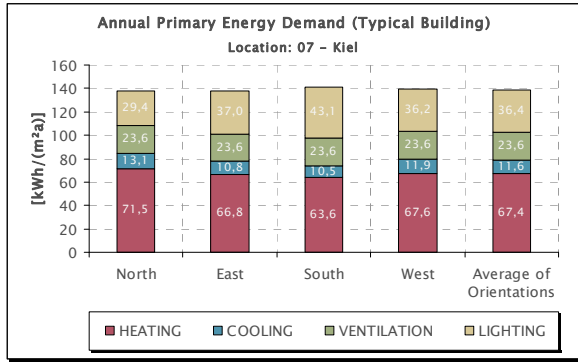
Heat. / Cool. Degree Days	Heating Degree Days (Base 18°C)	[Kd]	3650,12
	Cooling Degree Days (Base 10°C)	[Kd]	758,58

Solar Radiation	Annual total diffuse rad. on horiz. surf.	[kWh/m²]	565,99
	Annual total direct rad. on horiz. surf.	[kWh/m²]	395,47
	Annual total global rad. on horiz. surf.	[kWh/m²]	961,46

Daylight	Annual total illumination on horiz. surf.	[kluxh]	105.348
	Annual total daylight hours	[h]	4.331
	Average illuminance on horiz. surf.	[lux]	24.324
	Annual total illumination on horiz. surf. during office use	[kluxh]	99.881
	Annual total daylight hours during office use	[h]	3.614
	Average illuminance on horiz. surf. during office use	[lux]	27.637

Air Humidity	Mean relative humidity	[-]	0,80
--------------	------------------------	-----	------





20.3.8. Location 08 – Kobenhavn

Location	Location name	Kobenhavn (DK)	
	Latitude (North positive)	[°]	50,1
	Longitude (East positive)	[°]	8,68
	Height above sealevel	[m]	125

Assumed Period of Office Use	Begin (local time)	[h]	8
	End (local time)	[h]	18
	Office use per day	[h]	10
	Office use per year	[h]	2607,14

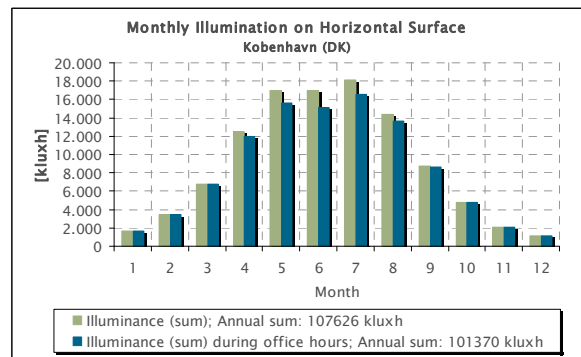
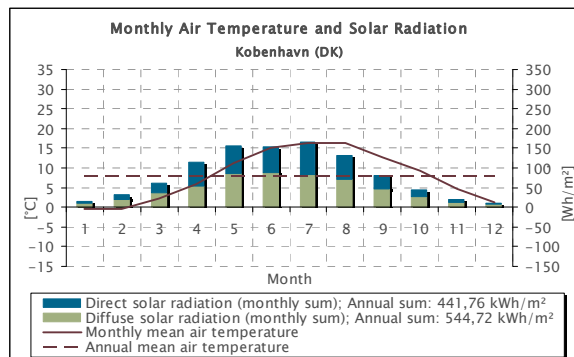
Temperature	Max. daily mean air temperature	[°C]	22,39
	Min. daily mean air temperature	[°C]	-8,08
	Max. monthly mean air temperature	[°C]	16,39
	Min. monthly mean air temperature	[°C]	-0,43
	Annual mean air temperature	[°C]	7,87
	Standard deviation of daily mean from annual mean air temperature	[°C]	6,8

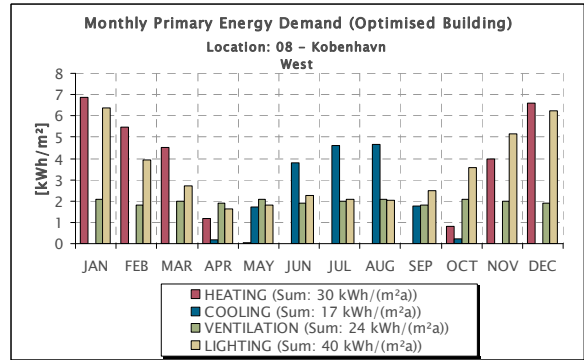
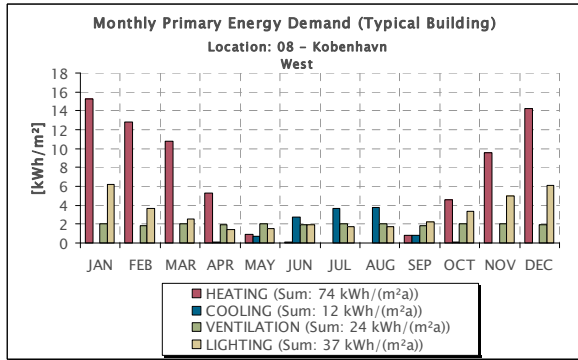
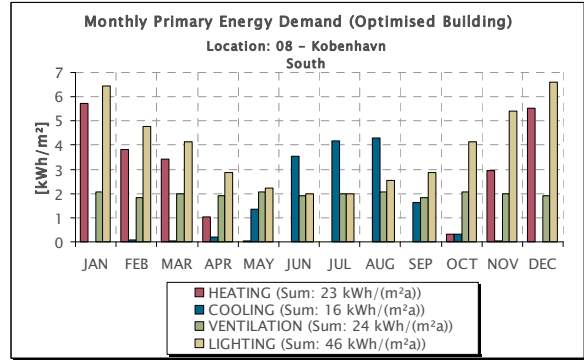
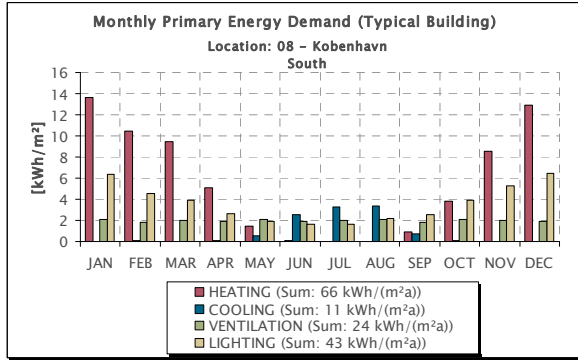
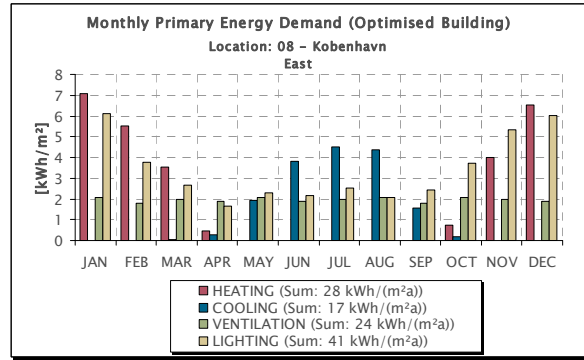
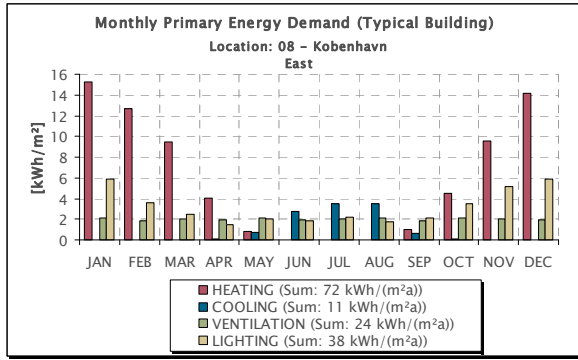
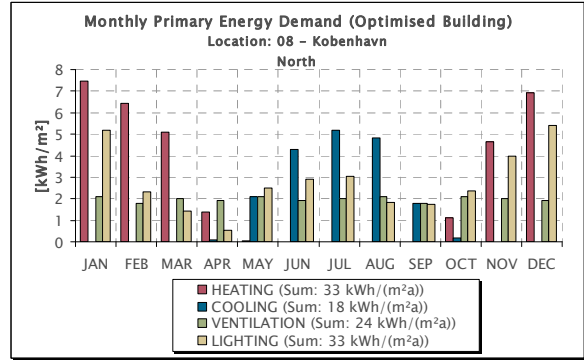
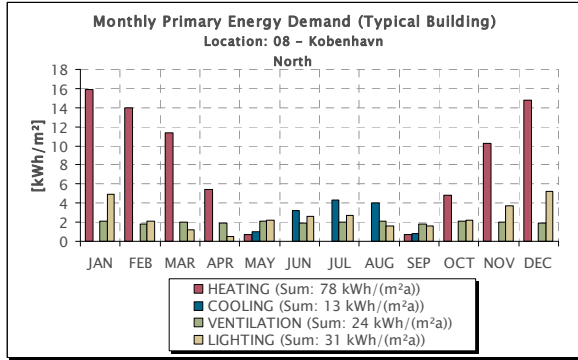
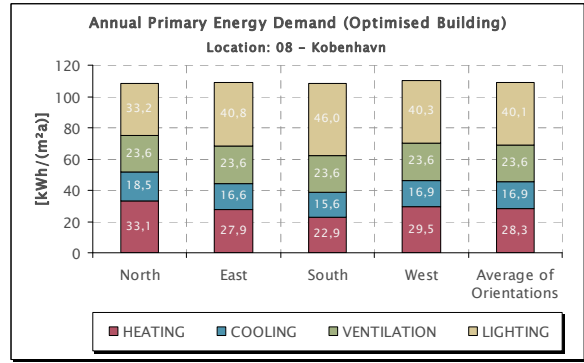
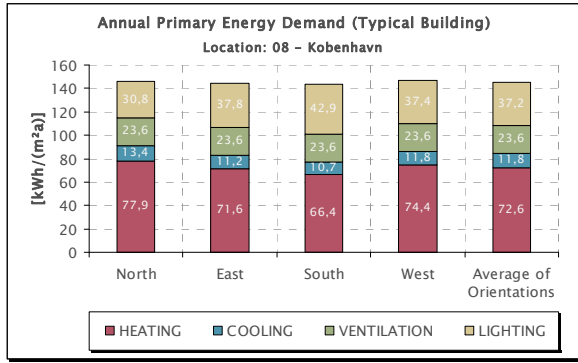
Heat. / Cool. Degree Days	Heating Degree Days (Base 18°C)	[Kd]	3770,15
	Cooling Degree Days (Base 10°C)	[Kd]	750,63

Solar Radiation	Annual total diffuse rad. on horiz. surf.	[kWh/m ²]	544,72
	Annual total direct rad. on horiz. surf.	[kWh/m ²]	441,76
	Annual total global rad. on horiz. surf.	[kWh/m ²]	986,47

Daylight	Annual total illumination on horiz. surf.	[kluxh]	107.626
	Annual total daylight hours	[h]	4.300
	Average illuminance on horiz. surf.	[lux]	25.029
	Annual total illumination on horiz. surf. during office use	[kluxh]	101.370
	Annual total daylight hours during office use	[h]	3.560
	Average illuminance on horiz. surf. during office use	[lux]	28.475

Air Humidity	Mean relative humidity	[-]	0,76
--------------	------------------------	-----	------





20.3.9. Location 09 – Gdansk

Location	Location name	Gdansk (PL)	
	Latitude (North positive)	[°]	50,1
	Longitude (East positive)	[°]	8,68
	Height above sealevel	[m]	125

Assumed Period of Office Use	Begin (local time)	[h]	8
	End (local time)	[h]	18
	Office use per day	[h]	10
	Office use per year	[h]	2607,14

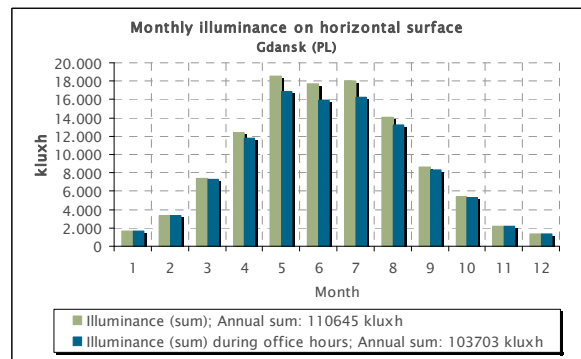
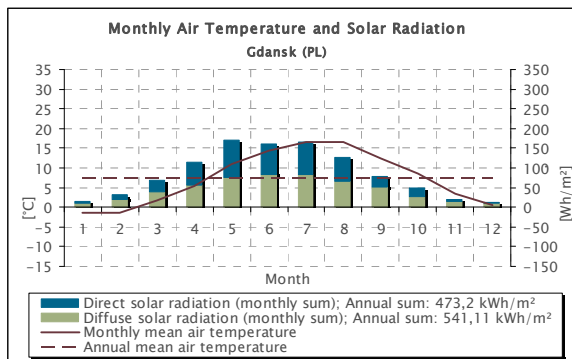
Temperature	Max. daily mean air temperature	[°C]	21,66
	Min. daily mean air temperature	[°C]	-9,91
	Max. monthly mean air temperature	[°C]	16,47
	Min. monthly mean air temperature	[°C]	-1,48
	Annual mean air temperature	[°C]	7,36
	Standard deviation of daily mean from annual mean air temperature	[°C]	7,1

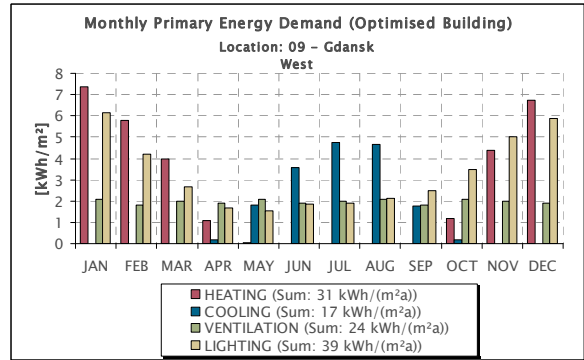
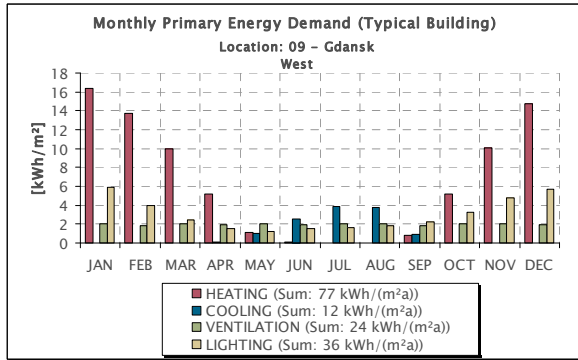
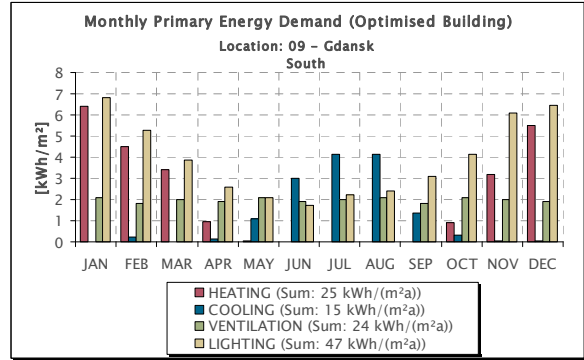
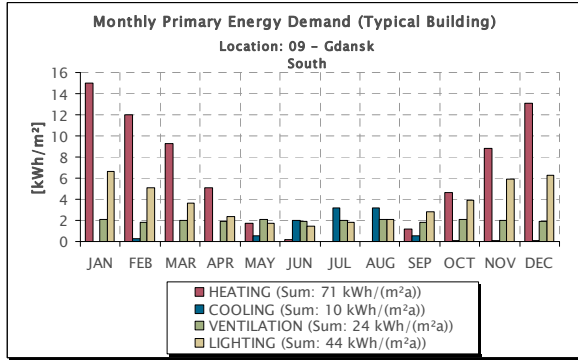
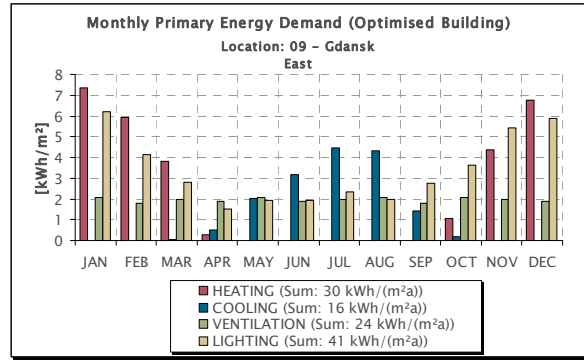
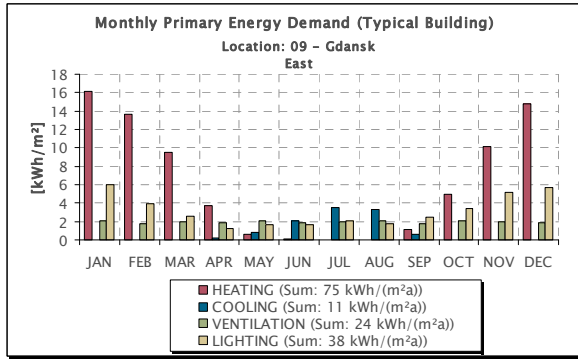
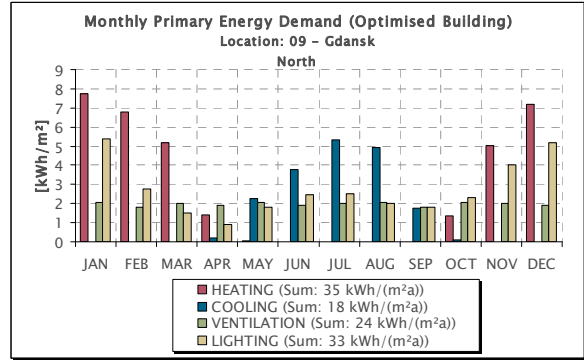
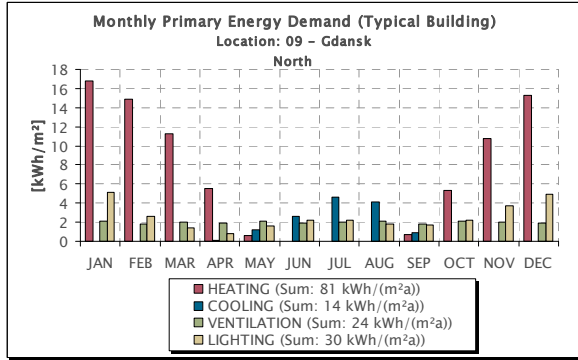
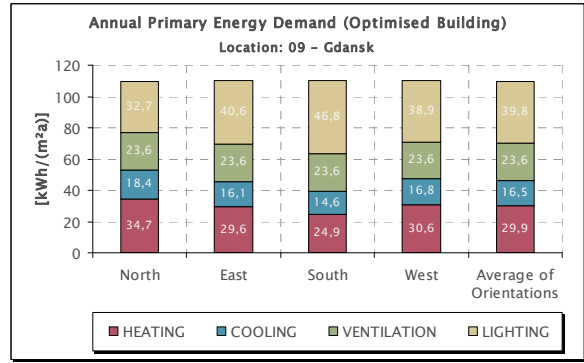
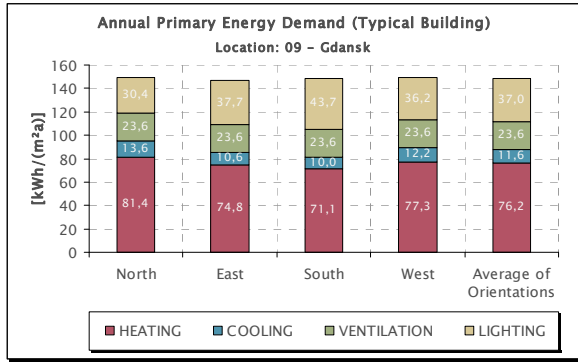
Heat. / Cool. Degree Days	Heating Degree Days (Base 18°C)	[Kd]	3946,95
	Cooling Degree Days (Base 10°C)	[Kd]	720,31

Solar Radiation	Annual total diffuse rad. on horiz. surf.	[kWh/m²]	541,11
	Annual total direct rad. on horiz. surf.	[kWh/m²]	473,20
	Annual total global rad. on horiz. surf.	[kWh/m²]	1.014,31

Daylight	Annual total illumination on horiz. surf.	[kluxh]	110.645
	Annual total daylight hours	[h]	4.322
	Average illuminance on horiz. surf.	[lux]	25.601
	Annual total illumination on horiz. surf. during office use	[kluxh]	103.703
	Annual total daylight hours during office use	[h]	3.585
	Average illuminance on horiz. surf. during office use	[lux]	28.927

Air Humidity	Mean relative humidity	[-]	0,76
--------------	------------------------	-----	------





20.3.10. Location 10 – Vilnius

Location	Location name	Vilnius (LT)	
	Latitude (North positive)	[°]	50,1
	Longitude (East positive)	[°]	8,68
	Height above sealevel	[m]	125

Assumed Period of Office Use	Begin (local time)	[h]	8
	End (local time)	[h]	18
	Office use per day	[h]	10
	Office use per year	[h]	2607,14

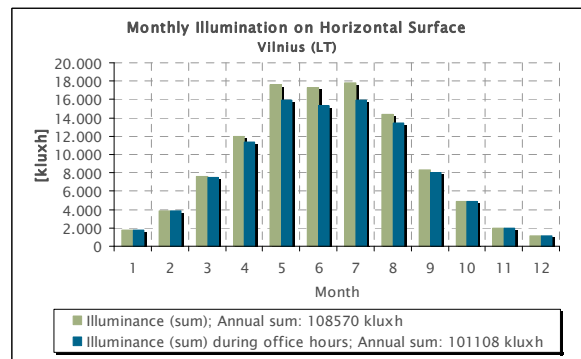
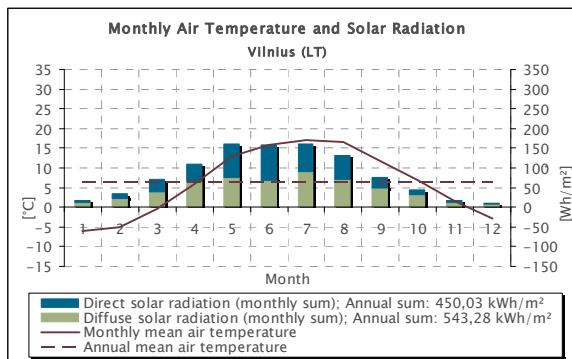
Temperature	Max. daily mean air temperature	[°C]	24,36
	Min. daily mean air temperature	[°C]	-19,61
	Max. monthly mean air temperature	[°C]	17,14
	Min. monthly mean air temperature	[°C]	-5,92
	Annual mean air temperature	[°C]	6,24
	Standard deviation of daily mean from annual mean air temperature	[°C]	9,3

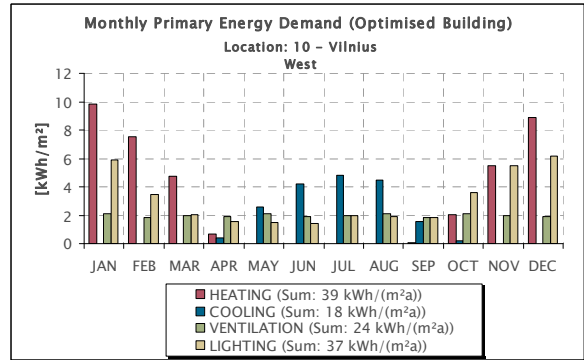
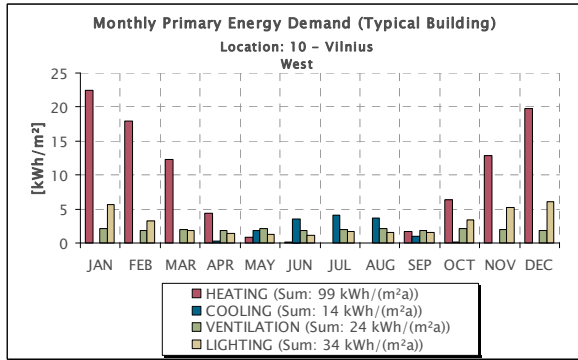
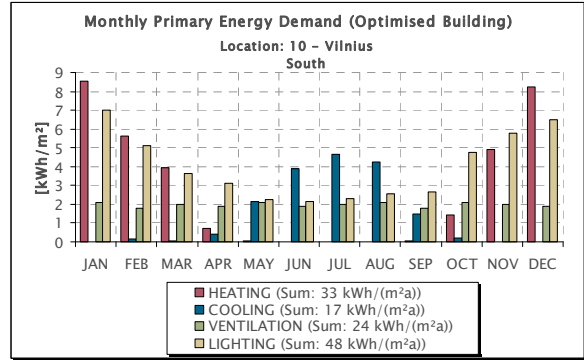
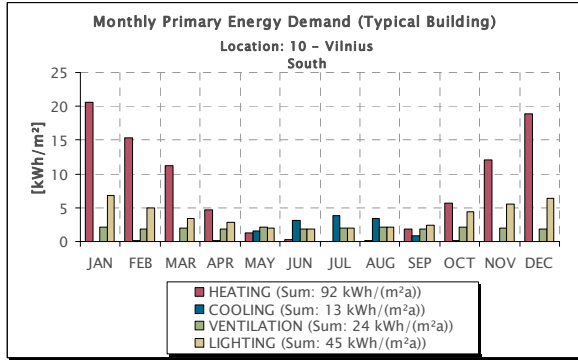
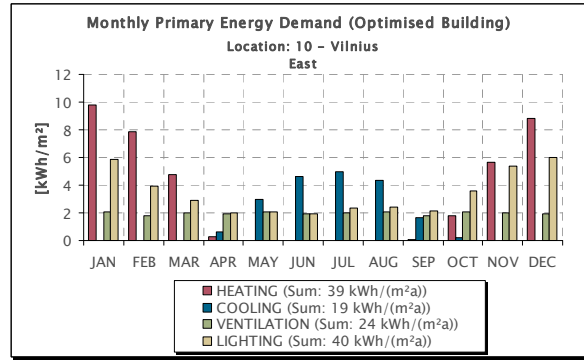
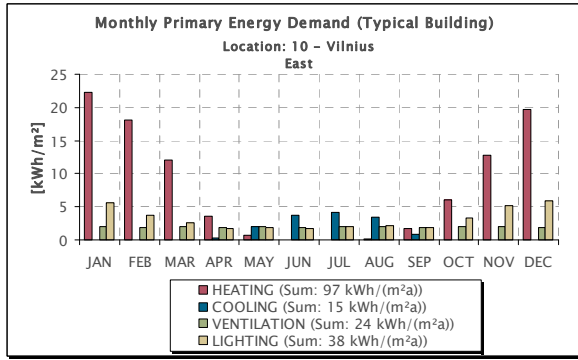
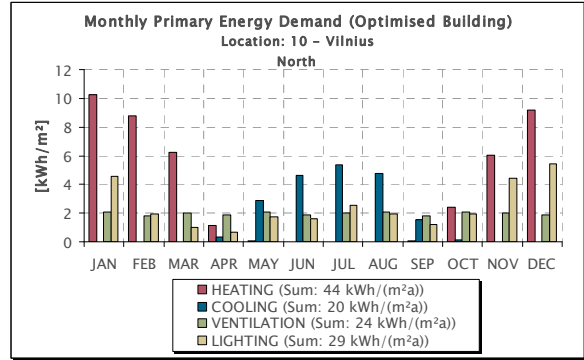
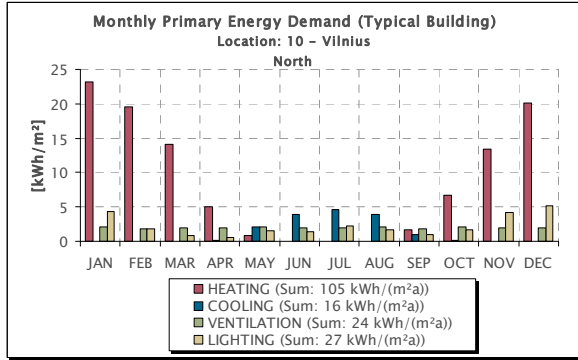
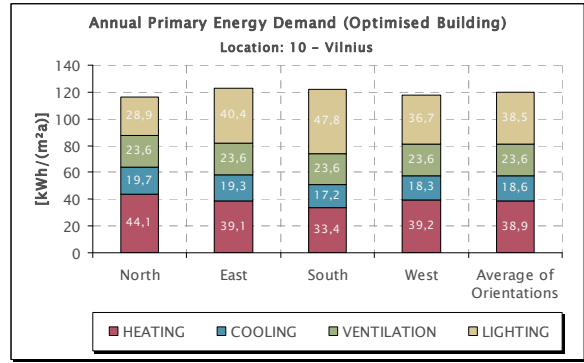
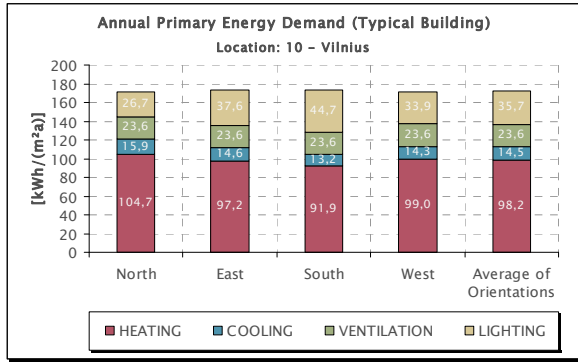
Heat. / Cool. Degree Days	Heating Degree Days (Base 18°C)	[Kd]	4434,09
	Cooling Degree Days (Base 10°C)	[Kd]	864,36

Solar Radiation	Annual total diffuse rad. on horiz. surf.	[kWh/m²]	543,28
	Annual total direct rad. on horiz. surf.	[kWh/m²]	450,03
	Annual total global rad. on horiz. surf.	[kWh/m²]	993,31

Daylight	Annual total illumination on horiz. surf.	[kluxh]	108.570
	Annual total daylight hours	[h]	4.333
	Average illuminance on horiz. surf.	[lux]	25.057
	Annual total illumination on horiz. surf. during office use	[kluxh]	101.108
	Annual total daylight hours during office use	[h]	3.575
	Average illuminance on horiz. surf. during office use	[lux]	28.282

Air Humidity	Mean relative humidity	[-]	0,75
--------------	------------------------	-----	------





20.3.11. Location 11 – London

Location	Location name	London (GB)	
	Latitude (North positive)	[°]	50,1
	Longitude (East positive)	[°]	8,68
	Height above sealevel	[m]	125

Assumed Period of Office Use	Begin (local time)	[h]	8
	End (local time)	[h]	18
	Office use per day	[h]	10
	Office use per year	[h]	2607,14

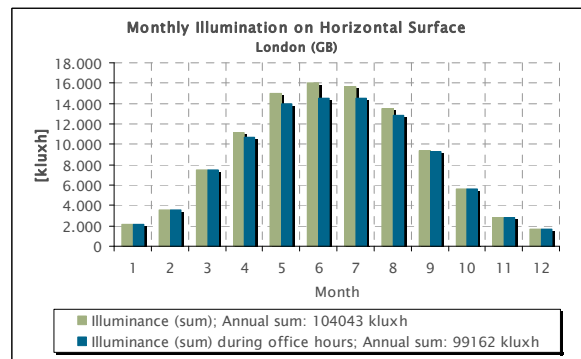
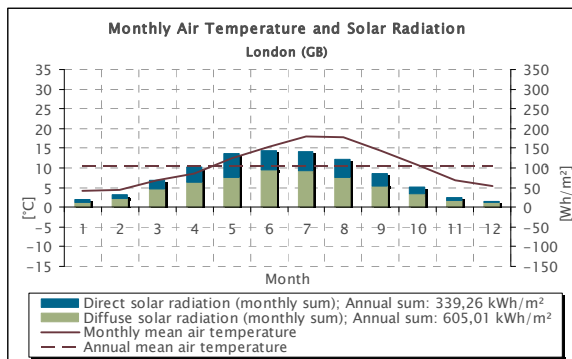
Temperature	Max. daily mean air temperature	[°C]	24,89
	Min. daily mean air temperature	[°C]	-2,35
	Max. monthly mean air temperature	[°C]	17,93
	Min. monthly mean air temperature	[°C]	4,22
	Annual mean air temperature	[°C]	10,43
	Standard deviation of daily mean from annual mean air temperature	[°C]	5,6

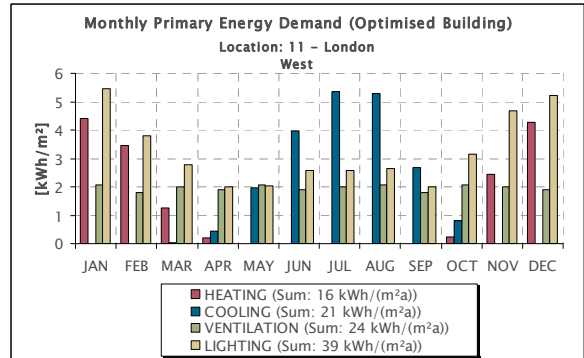
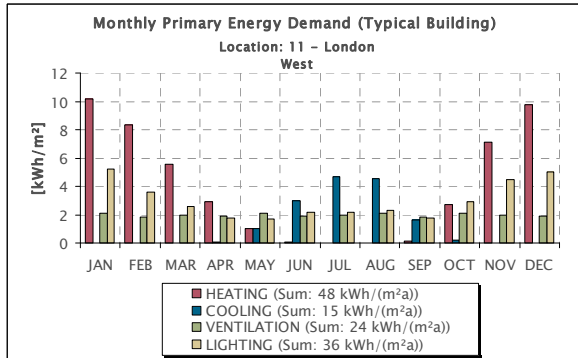
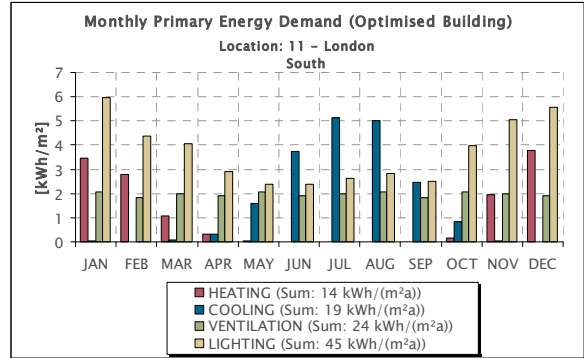
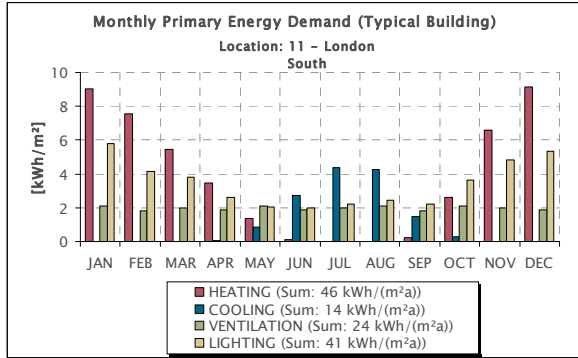
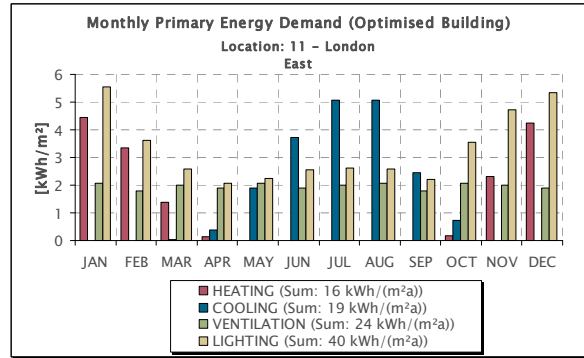
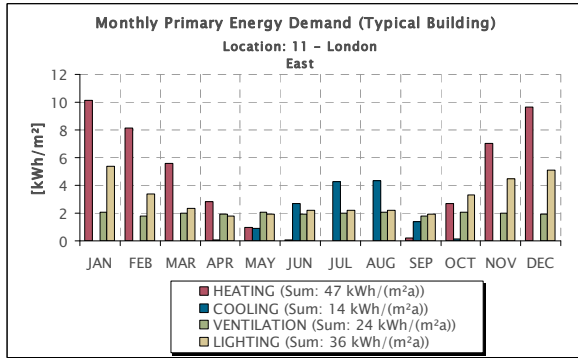
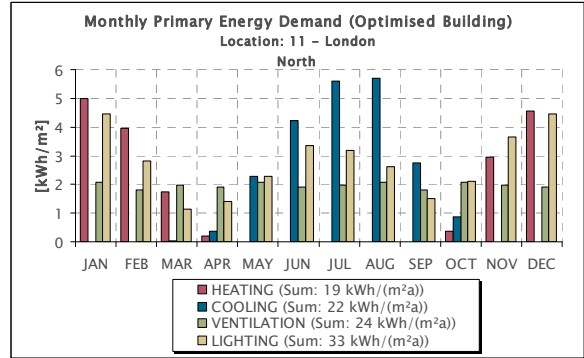
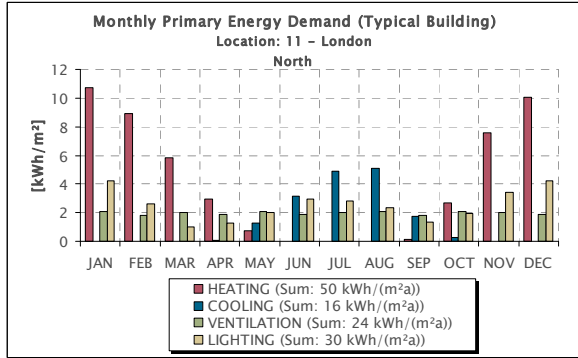
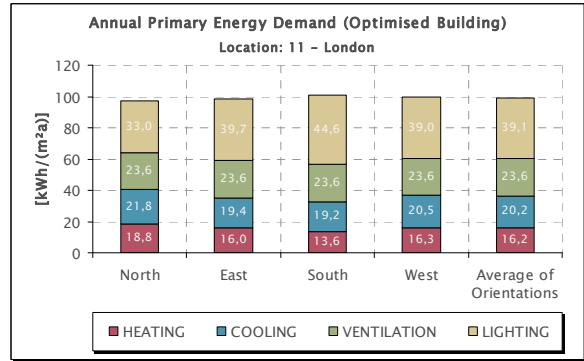
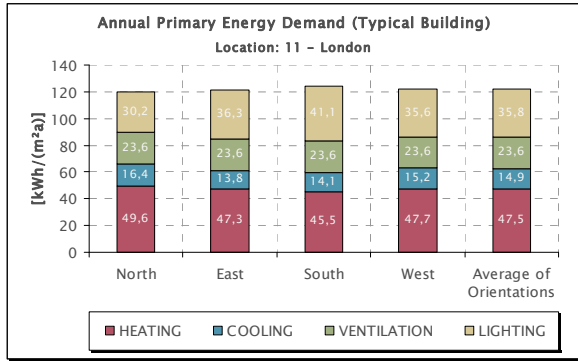
Heat. / Cool. Degree Days	Heating Degree Days (Base 18°C)	[Kd]	2880,01
	Cooling Degree Days (Base 10°C)	[Kd]	984,21

Solar Radiation	Annual total diffuse rad. on horiz. surf.	[kWh/m ²]	605,01
	Annual total direct rad. on horiz. surf.	[kWh/m ²]	339,26
	Annual total global rad. on horiz. surf.	[kWh/m ²]	944,27

Daylight	Annual total illumination on horiz. surf.	[kluxh]	104.043
	Annual total daylight hours	[h]	4.346
	Average illuminance on horiz. surf.	[lux]	23.940
	Annual total illumination on horiz. surf. during office use	[kluxh]	99.162
	Annual total daylight hours during office use	[h]	3.677
	Average illuminance on horiz. surf. during office use	[lux]	26.968

Air Humidity	Mean relative humidity	[-]	0,76
--------------	------------------------	-----	------





20.3.12. Location 12 – Bruxelles

Location	Location name	Bruxelles (B)	
	Latitude (North positive)	[°]	50,1
	Longitude (East positive)	[°]	8,68
	Height above sealevel	[m]	125

Assumed Period of Office Use	Begin (local time)	[h]	8
	End (local time)	[h]	18
	Office use per day	[h]	10
	Office use per year	[h]	2607,14

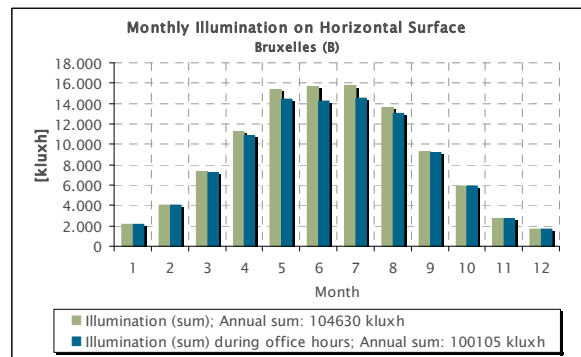
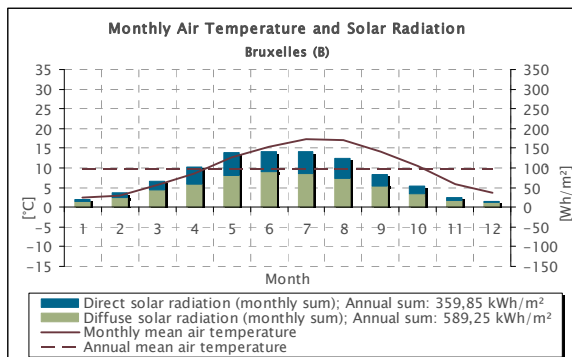
Temperature	Max. daily mean air temperature	[°C]	24,86
	Min. daily mean air temperature	[°C]	-6,00
	Max. monthly mean air temperature	[°C]	17,37
	Min. monthly mean air temperature	[°C]	2,52
	Annual mean air temperature	[°C]	9,75
	Standard deviation of daily mean from annual mean air temperature	[°C]	6,3

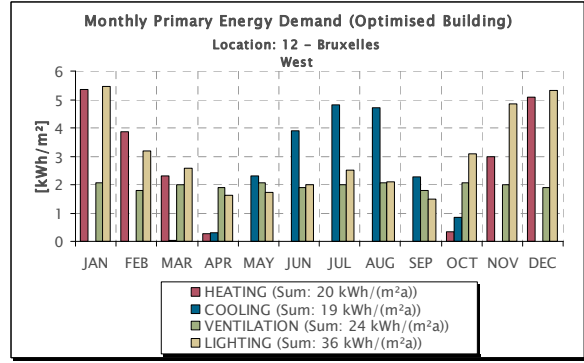
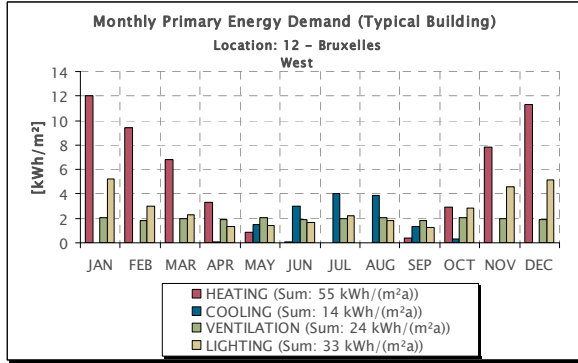
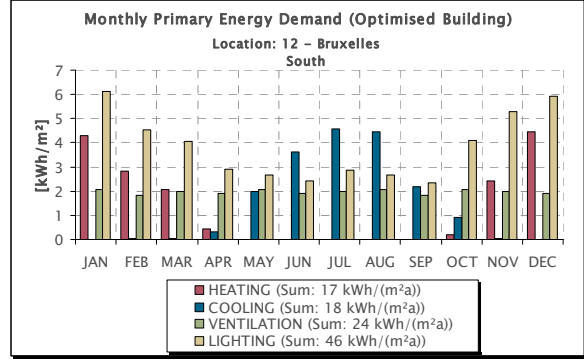
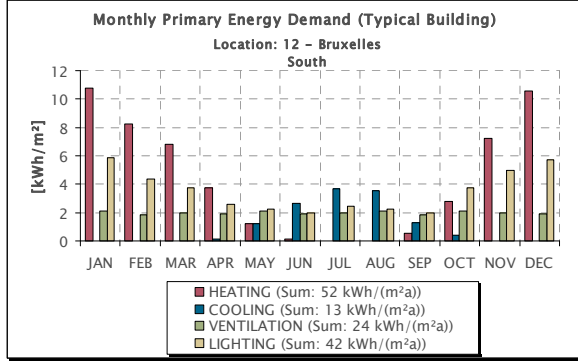
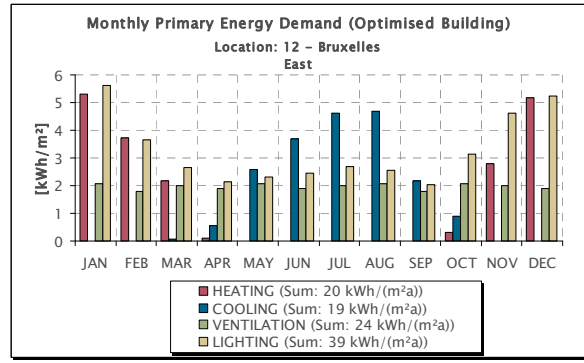
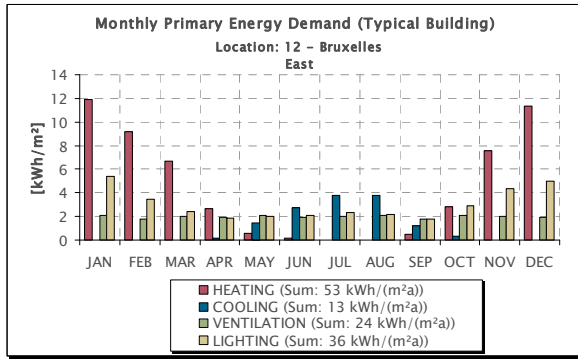
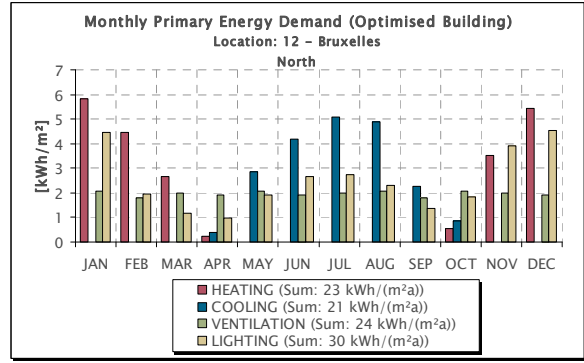
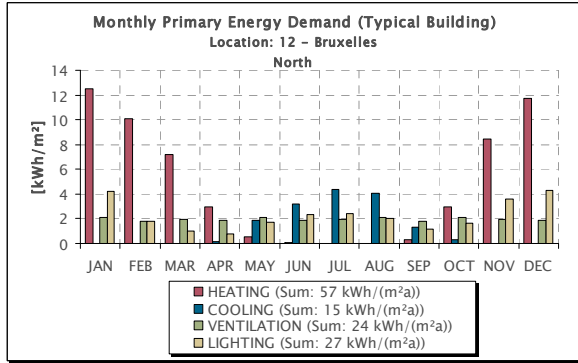
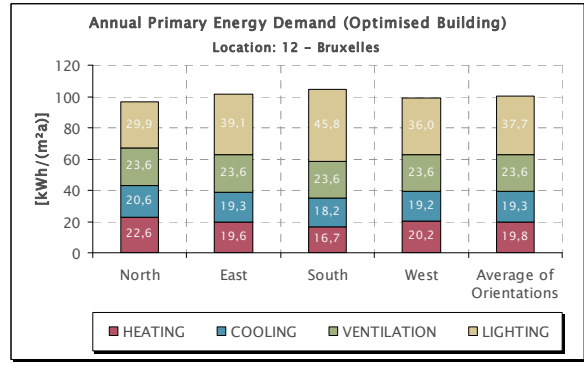
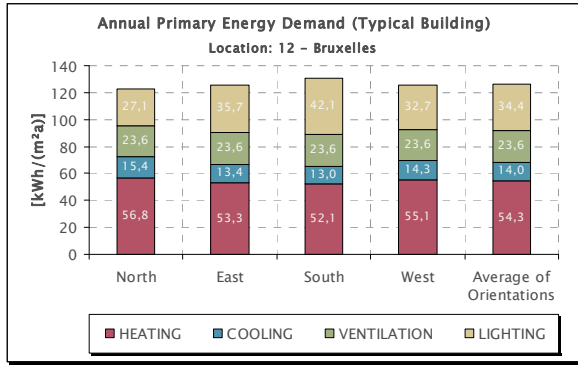
Heat. / Cool. Degree Days	Heating Degree Days (Base 18°C)	[Kd]	3141,65
	Cooling Degree Days (Base 10°C)	[Kd]	961,47

Solar Radiation	Annual total diffuse rad. on horiz. surf.	[kWh/m ²]	589,25
	Annual total direct rad. on horiz. surf.	[kWh/m ²]	359,85
	Annual total global rad. on horiz. surf.	[kWh/m ²]	949,10

Daylight	Annual total illumination on horiz. surf.	[kluxh]	104.630
	Annual total daylight hours	[h]	4.313
	Average illuminance on horiz. surf.	[lux]	24.259
	Annual total illumination on horiz. surf. during office use	[kluxh]	100.105
	Annual total daylight hours during office use	[h]	3.670
	Average illuminance on horiz. surf. during office use	[lux]	27.276

Air Humidity	Mean relative humidity	[-]	0,78
--------------	------------------------	-----	------





20.3.13. Location 13 – Frankfurt/Main

Location	Location name	Frankfurt/Main (D)	
	Latitude (North positive)	[°]	50,1
	Longitude (East positive)	[°]	8,68
	Height above sealevel	[m]	125

Assumed Period of Office Use	Begin (local time)	[h]	8
	End (local time)	[h]	18
	Office use per day	[h]	10
	Office use per year	[h]	2607,14

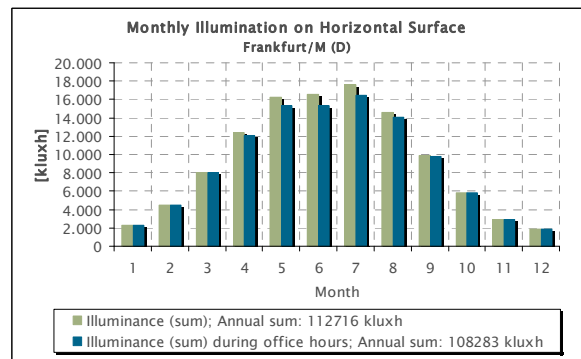
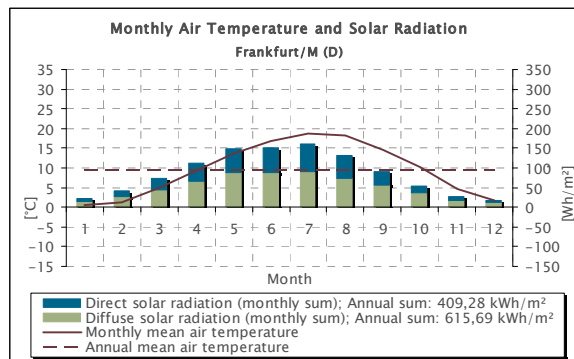
Temperature	Max. daily mean air temperature	[°C]	26,61
	Min. daily mean air temperature	[°C]	-9,28
	Max. monthly mean air temperature	[°C]	18,78
	Min. monthly mean air temperature	[°C]	0,60
	Annual mean air temperature	[°C]	9,62
	Standard deviation of daily mean from annual mean air temperature	[°C]	7,4

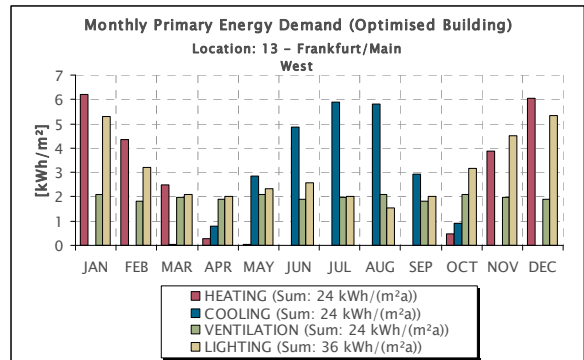
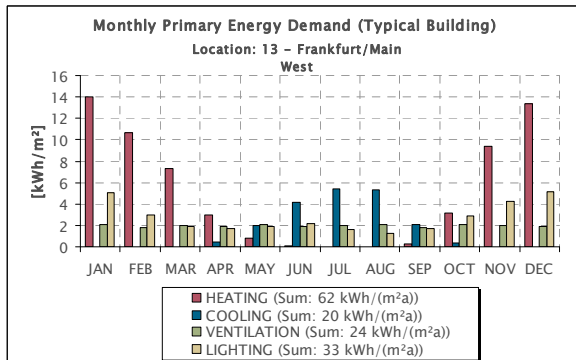
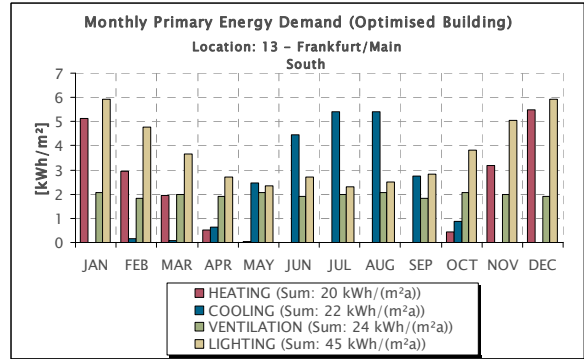
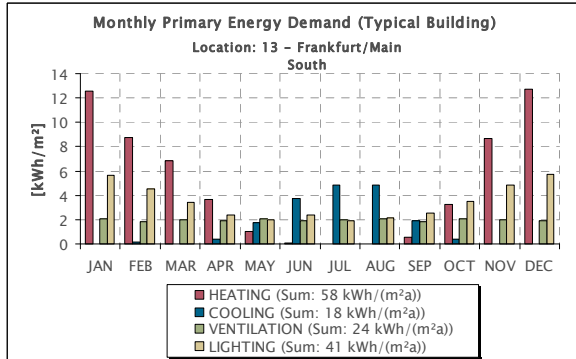
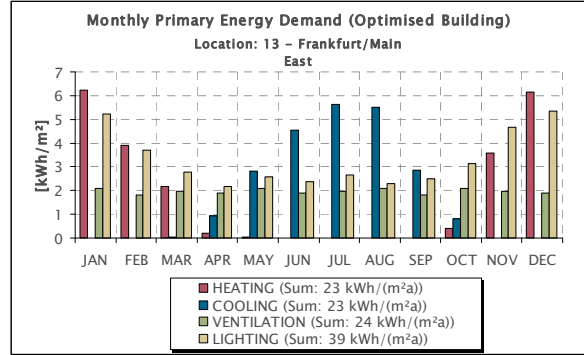
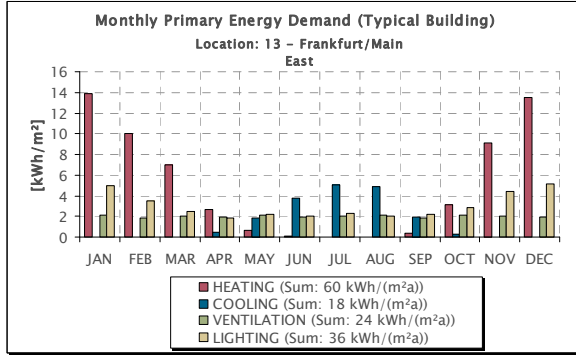
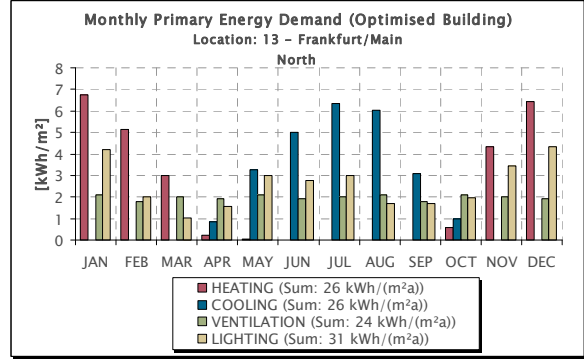
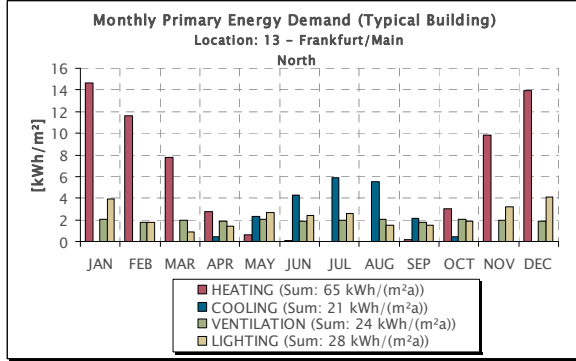
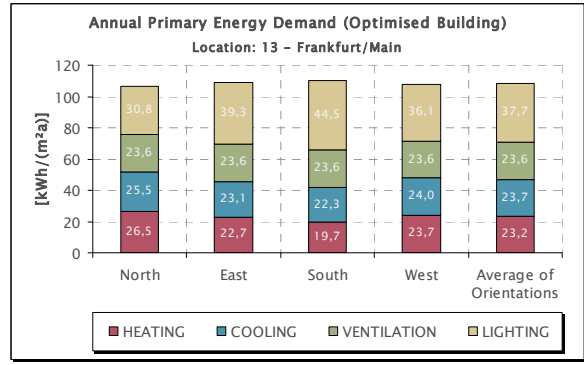
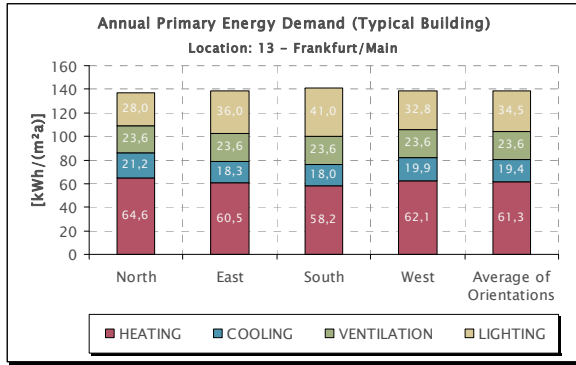
Heat. / Cool. Degree Days	Heating Degree Days (Base 18°C)	[Kd]	3273,60
	Cooling Degree Days (Base 10°C)	[Kd]	1124,49

Solar Radiation	Annual total diffuse rad. on horiz. surf.	[kWh/m ²]	615,69
	Annual total direct rad. on horiz. surf.	[kWh/m ²]	409,28
	Annual total global rad. on horiz. surf.	[kWh/m ²]	1.024,98

Daylight	Annual total illumination on horiz. surf.	[kluxh]	112.716
	Annual total daylight hours	[h]	4.282
	Average illuminance on horiz. surf.	[lux]	26.323
	Annual total illumination on horiz. surf. during office use	[kluxh]	108.283
	Annual total daylight hours during office use	[h]	3.682
	Average illuminance on horiz. surf. during office use	[lux]	29.409

Air Humidity	Mean relative humidity	[-]	0,73
--------------	------------------------	-----	------





20.3.14. Location 14 – Praha

Location	Location name	Praha (CZ)	
	Latitude (North positive)	[°]	50,1
	Longitude (East positive)	[°]	8,68
	Height above sealevel	[m]	125

Assumed Period of Office Use	Begin (local time)	[h]	8
	End (local time)	[h]	18
	Office use per day	[h]	10
	Office use per year	[h]	2607,14

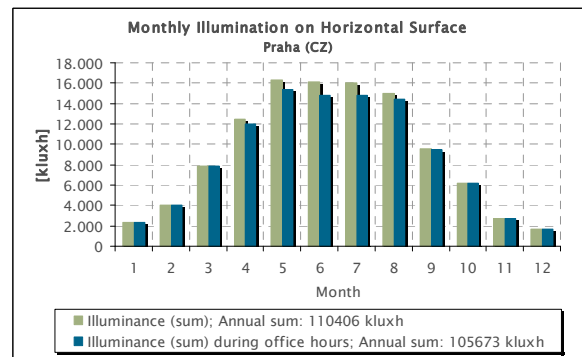
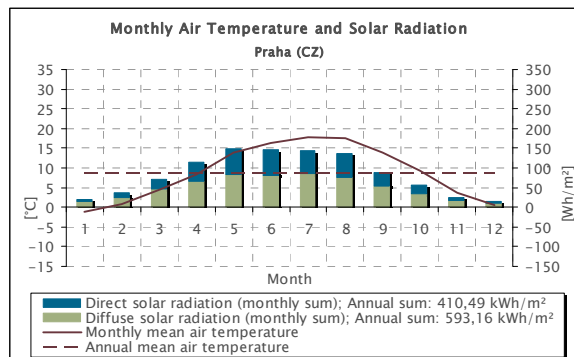
Temperature	Max. daily mean air temperature	[°C]	24,99
	Min. daily mean air temperature	[°C]	-12,50
	Max. monthly mean air temperature	[°C]	17,73
	Min. monthly mean air temperature	[°C]	-1,19
	Annual mean air temperature	[°C]	8,80
	Standard deviation of daily mean from annual mean air temperature	[°C]	7,7

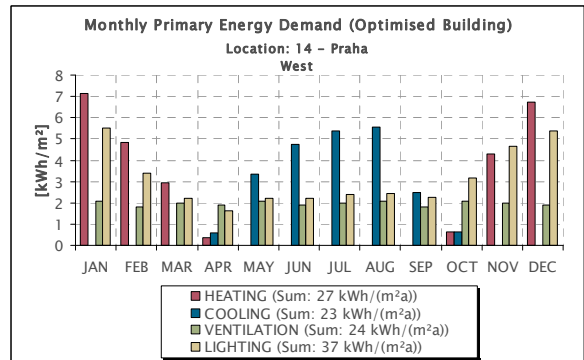
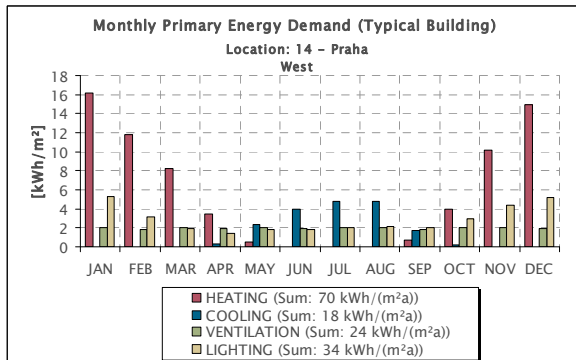
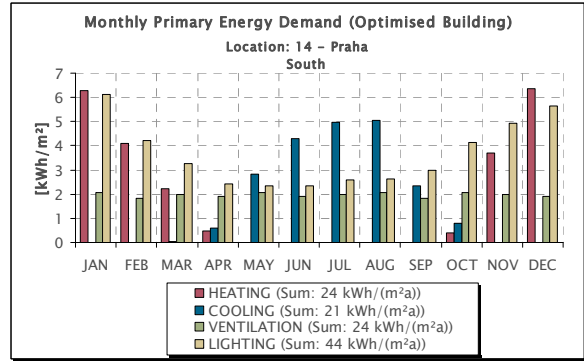
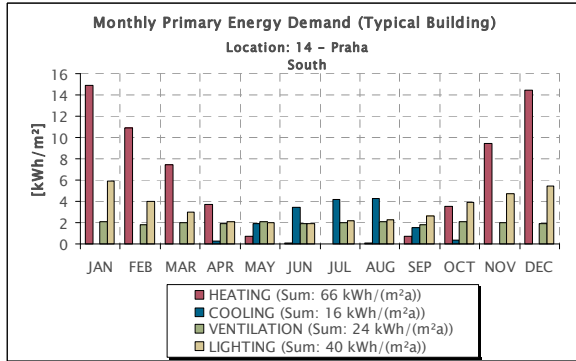
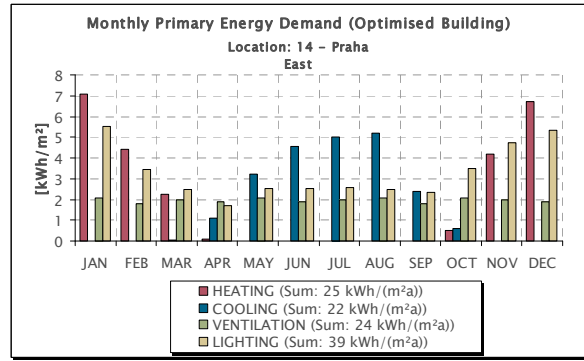
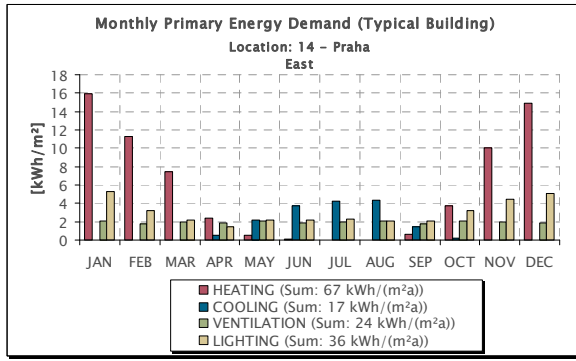
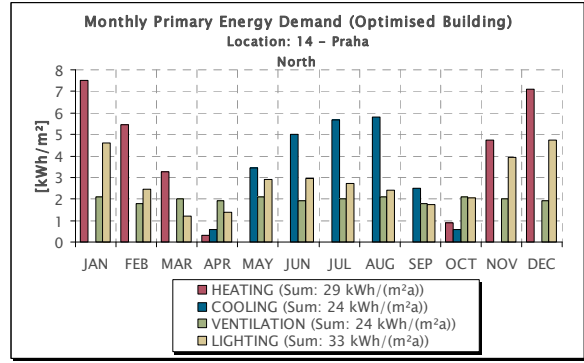
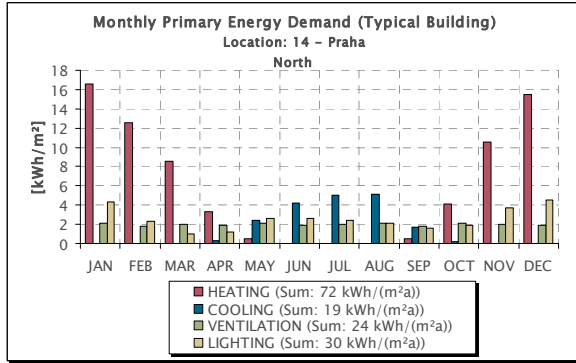
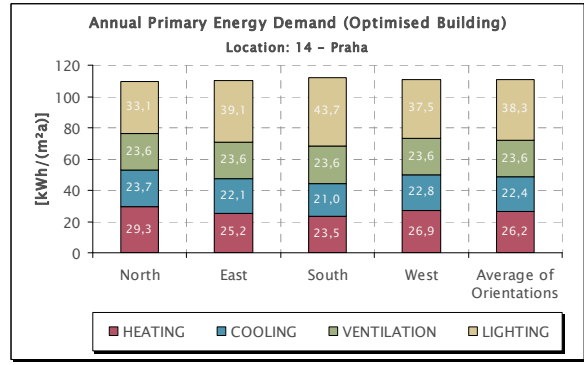
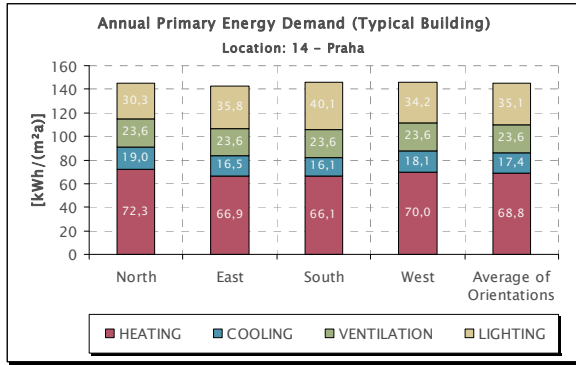
Heat. / Cool. Degree Days	Heating Degree Days (Base 18°C)	[Kd]	3536,53
	Cooling Degree Days (Base 10°C)	[Kd]	1036,04

Solar Radiation	Annual total diffuse rad. on horiz. surf.	[kWh/m ²]	593,16
	Annual total direct rad. on horiz. surf.	[kWh/m ²]	410,49
	Annual total global rad. on horiz. surf.	[kWh/m ²]	1.003,65

Daylight	Annual total illumination on horiz. surf.	[kluxh]	110.406
	Annual total daylight hours	[h]	4.344
	Average illuminance on horiz. surf.	[lux]	25.416
	Annual total illumination on horiz. surf. during office use	[kluxh]	105.673
	Annual total daylight hours during office use	[h]	3.690
	Average illuminance on horiz. surf. during office use	[lux]	28.638

Air Humidity	Mean relative humidity	[-]	0,68
--------------	------------------------	-----	------





20.3.15. Location 15 – Krakow

Location	Location name	Krakow (PL)	
	Latitude (North positive)	[°]	50,1
	Longitude (East positive)	[°]	8,68
	Height above sealevel	[m]	125

Assumed Period of Office Use	Begin (local time)	[h]	8
	End (local time)	[h]	18
	Office use per day	[h]	10
	Office use per year	[h]	2607,14

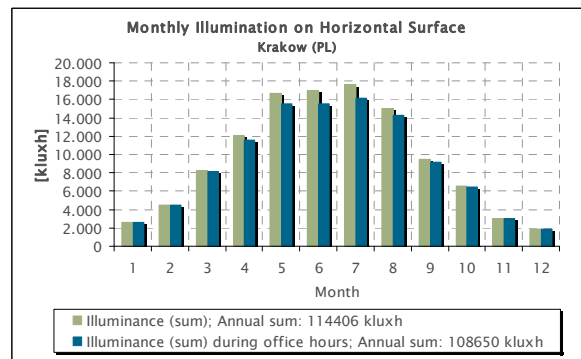
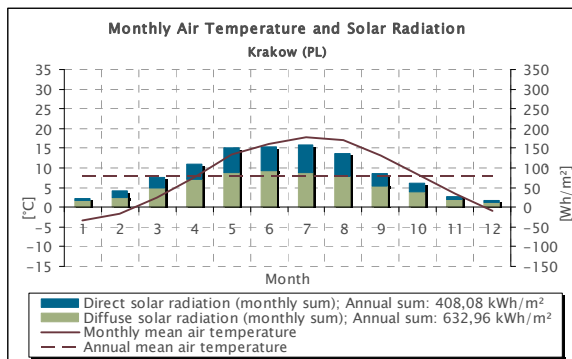
Temperature	Max. daily mean air temperature	[°C]	24,55
	Min. daily mean air temperature	[°C]	-14,58
	Max. monthly mean air temperature	[°C]	17,72
	Min. monthly mean air temperature	[°C]	-3,29
	Annual mean air temperature	[°C]	7,86
	Standard deviation of daily mean from annual mean air temperature	[°C]	8,3

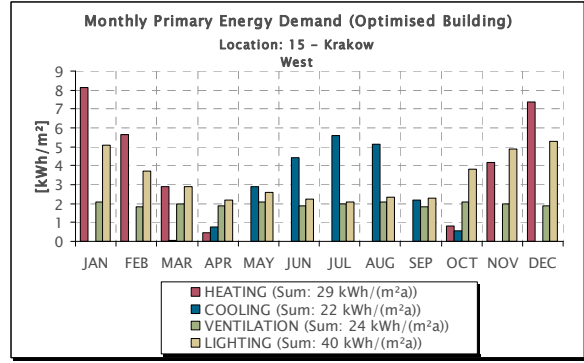
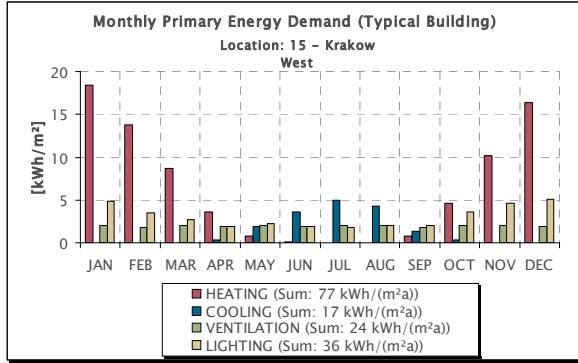
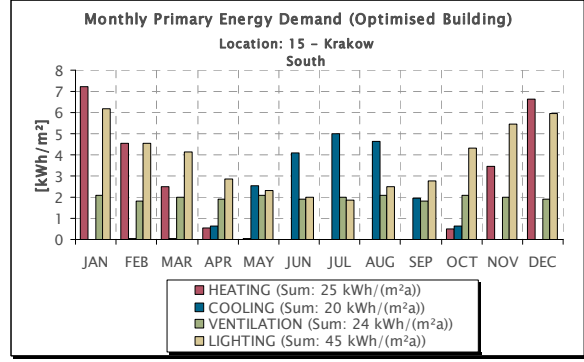
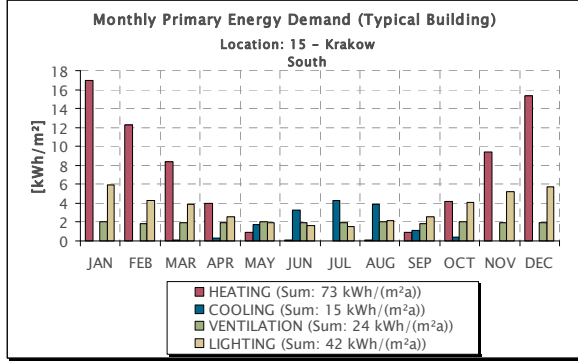
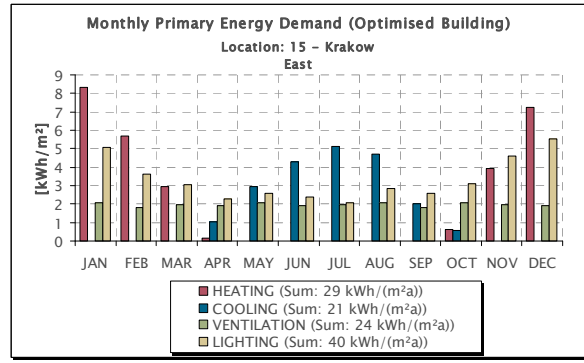
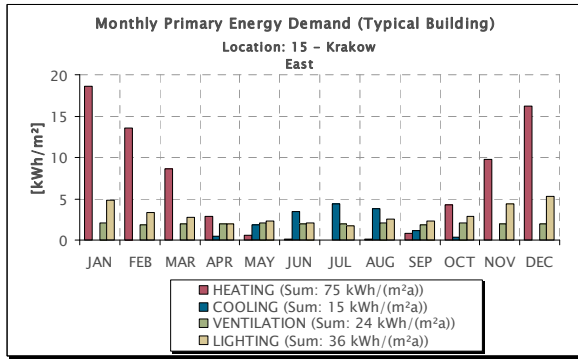
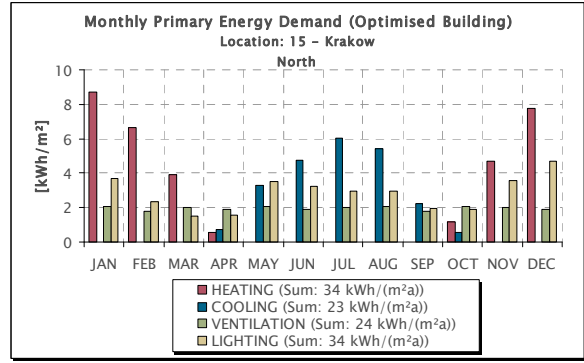
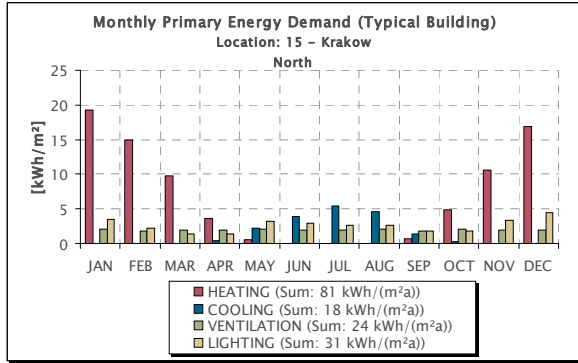
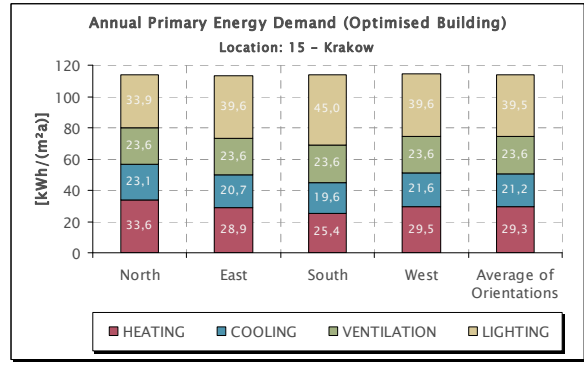
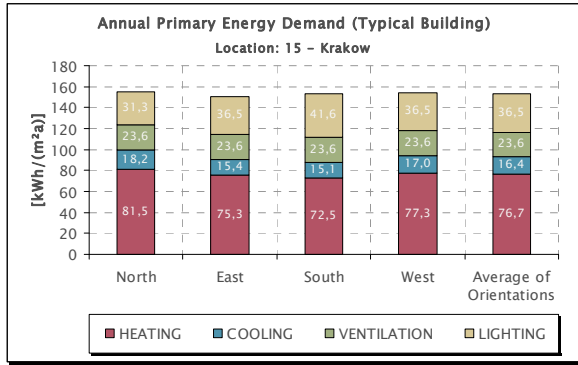
Heat. / Cool. Degree Days	Heating Degree Days (Base 18°C)	[Kd]	3859,89
	Cooling Degree Days (Base 10°C)	[Kd]	973,25

Solar Radiation	Annual total diffuse rad. on horiz. surf.	[kWh/m²]	632,96
	Annual total direct rad. on horiz. surf.	[kWh/m²]	408,08
	Annual total global rad. on horiz. surf.	[kWh/m²]	1.041,03

Daylight	Annual total illumination on horiz. surf.	[kluxh]	114.406
	Annual total daylight hours	[h]	4.313
	Average illuminance on horiz. surf.	[lux]	26.526
	Annual total illumination on horiz. surf. during office use	[kluxh]	108.650
	Annual total daylight hours during office use	[h]	3.643
	Average illuminance on horiz. surf. during office use	[lux]	29.824

Air Humidity	Mean relative humidity	[-]	0,72
--------------	------------------------	-----	------





20.3.16. Location 16 – Bordeaux

Location	Location name	Bordeaux (F)	
	Latitude (North positive)	[°]	50,1
	Longitude (East positive)	[°]	8,68
	Height above sealevel	[m]	125

Assumed Period of Office Use	Begin (local time)	[h]	8
	End (local time)	[h]	18
	Office use per day	[h]	10
	Office use per year	[h]	2607,14

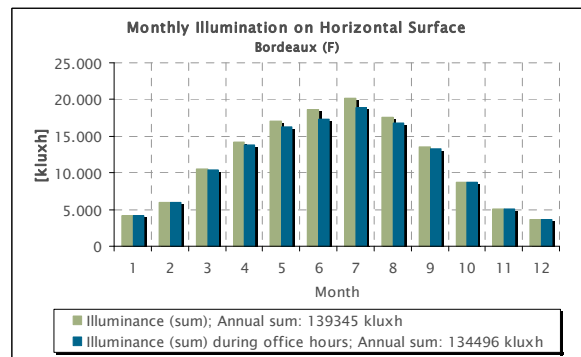
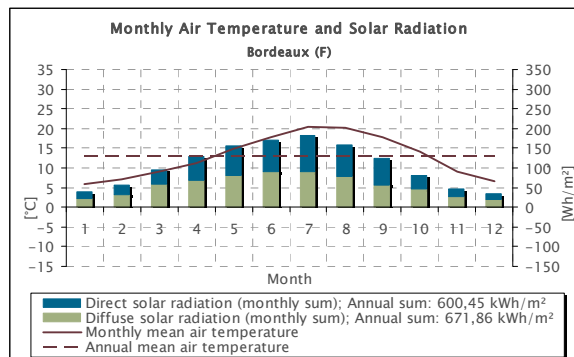
Temperature	Max. daily mean air temperature	[°C]	26,81
	Min. daily mean air temperature	[°C]	-3,21
	Max. monthly mean air temperature	[°C]	20,50
	Min. monthly mean air temperature	[°C]	5,98
	Annual mean air temperature	[°C]	12,88
	Standard deviation of daily mean from annual mean air temperature	[°C]	6,0

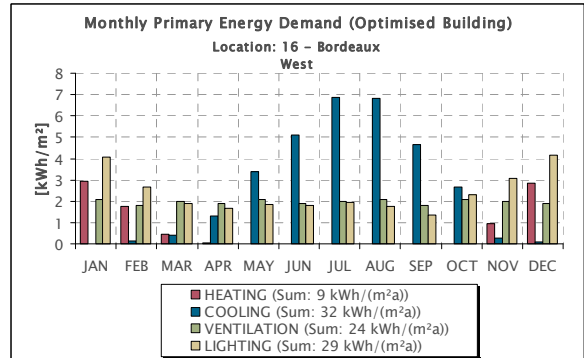
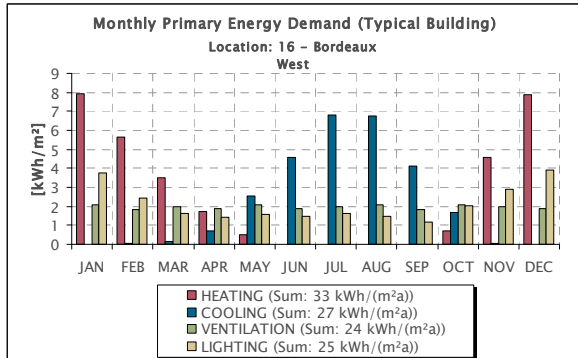
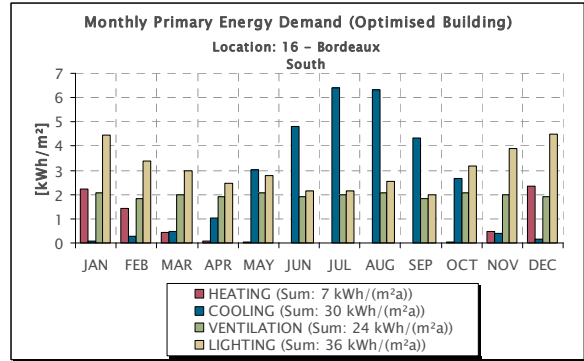
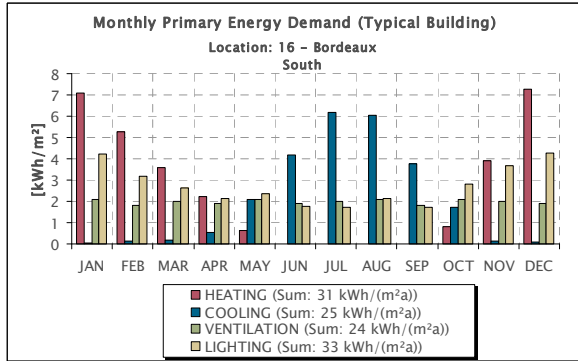
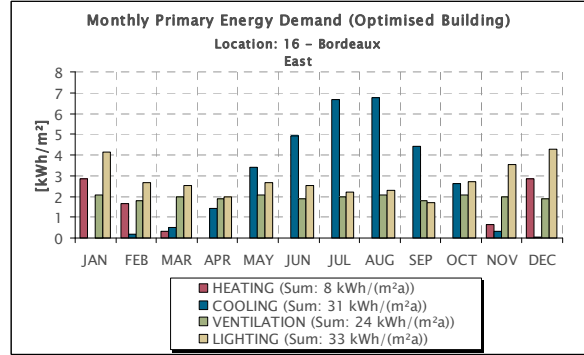
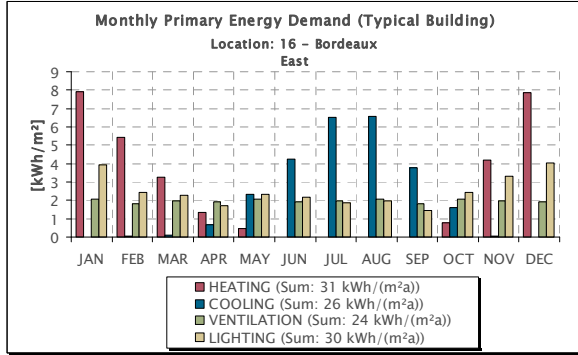
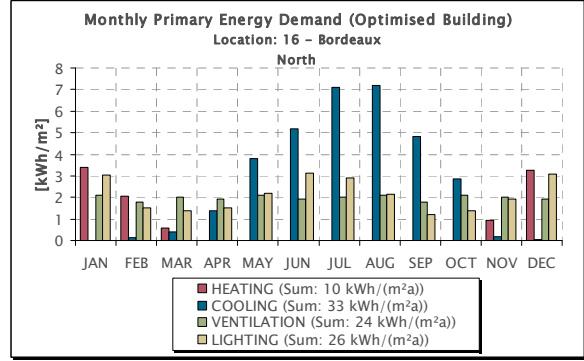
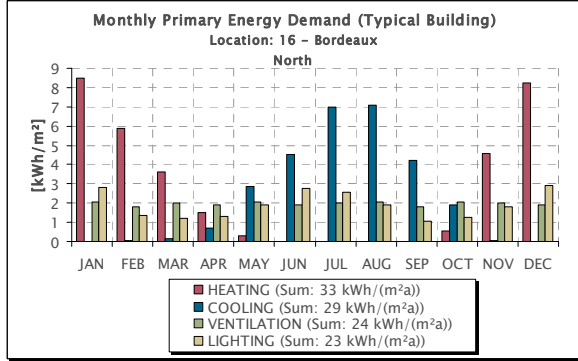
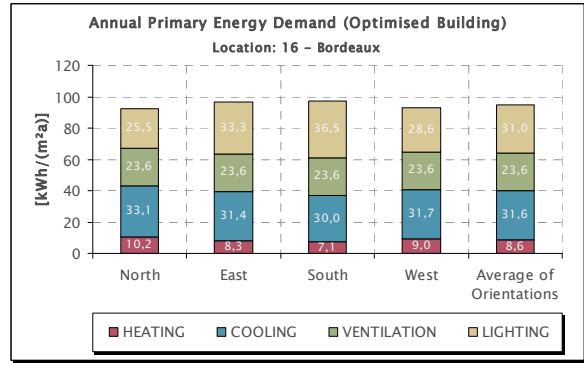
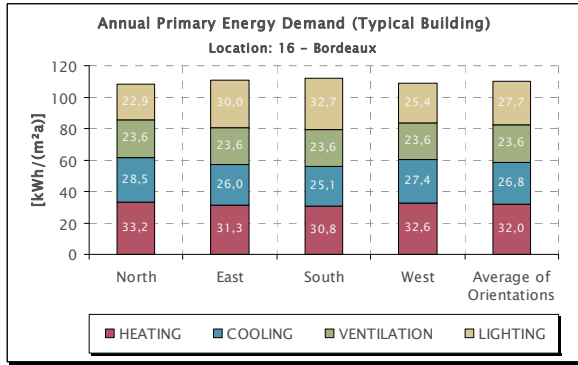
Heat. / Cool. Degree Days	Heating Degree Days (Base 18°C)	[Kd]	2218,08
	Cooling Degree Days (Base 10°C)	[Kd]	1611,89

Solar Radiation	Annual total diffuse rad. on horiz. surf.	[kWh/m ²]	671,86
	Annual total direct rad. on horiz. surf.	[kWh/m ²]	600,45
	Annual total global rad. on horiz. surf.	[kWh/m ²]	1.272,31

Daylight	Annual total illumination on horiz. surf.	[kluxh]	139.345
	Annual total daylight hours	[h]	4.310
	Average illuminance on horiz. surf.	[lux]	32.331
	Annual total illumination on horiz. surf. during office use	[kluxh]	134.496
	Annual total daylight hours during office use	[h]	3.739
	Average illuminance on horiz. surf. during office use	[lux]	35.971

Air Humidity	Mean relative humidity	[-]	0,74
--------------	------------------------	-----	------





20.3.17. Location 17 – Milano

Location	Location name	Milano (I)	
	Latitude (North positive)	[°]	50,1
	Longitude (East positive)	[°]	8,68
	Height above sealevel	[m]	125

Assumed Period of Office Use	Begin (local time)	[h]	8
	End (local time)	[h]	18
	Office use per day	[h]	10
	Office use per year	[h]	2607,14

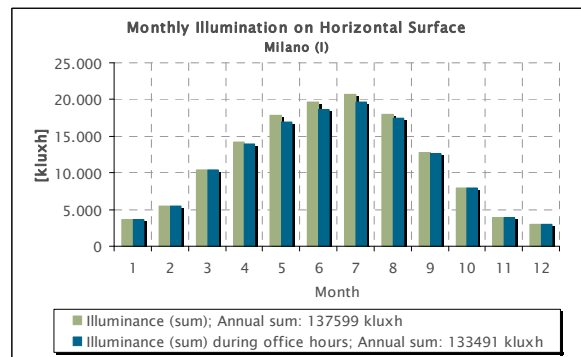
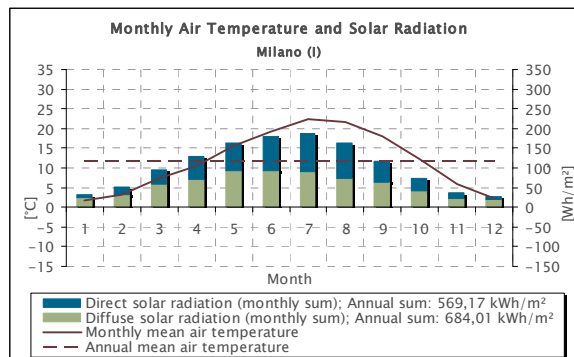
Temperature	Max. daily mean air temperature	[°C]	26,50
	Min. daily mean air temperature	[°C]	-3,70
	Max. monthly mean air temperature	[°C]	22,34
	Min. monthly mean air temperature	[°C]	1,64
	Annual mean air temperature	[°C]	11,72
	Standard deviation of daily mean from annual mean air temperature	[°C]	7,8

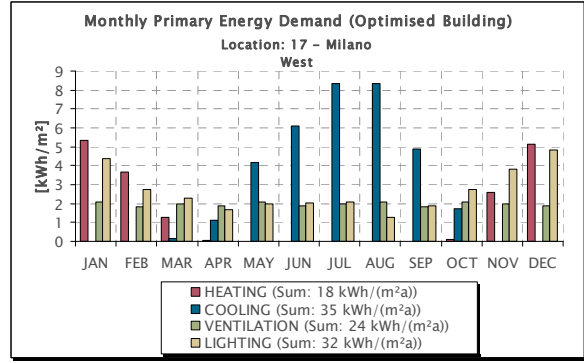
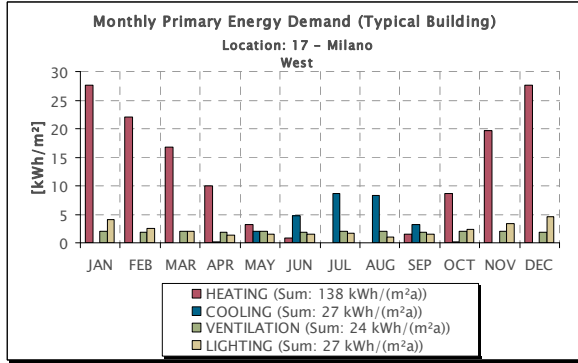
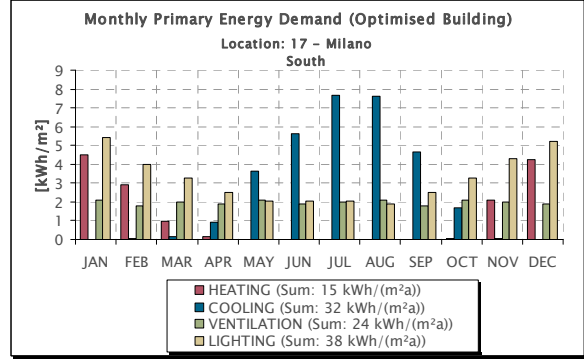
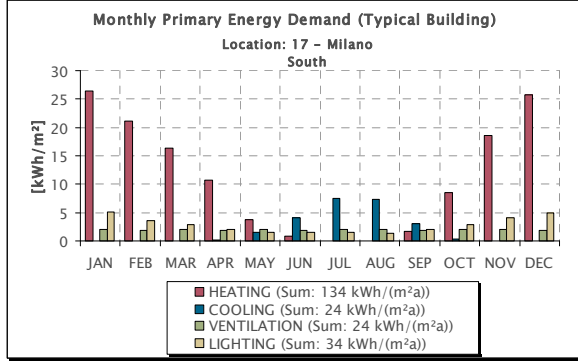
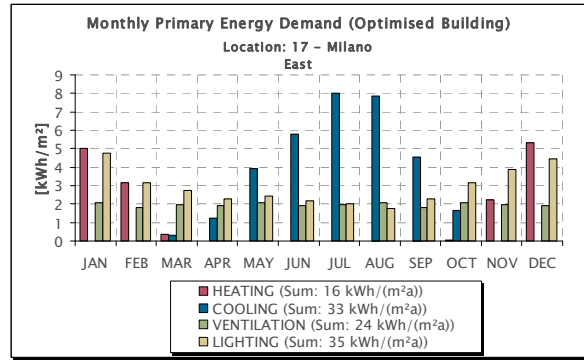
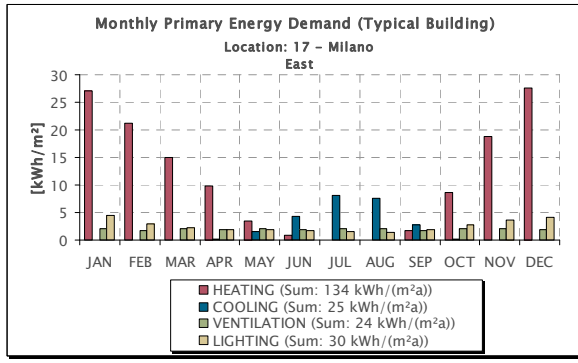
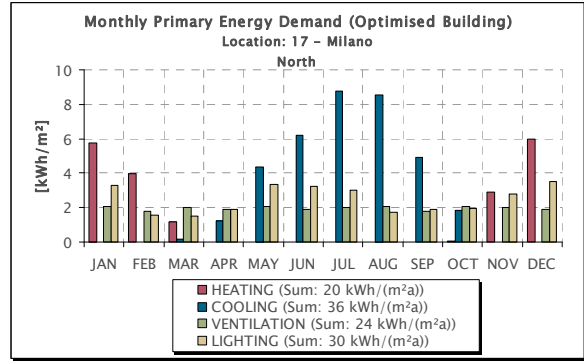
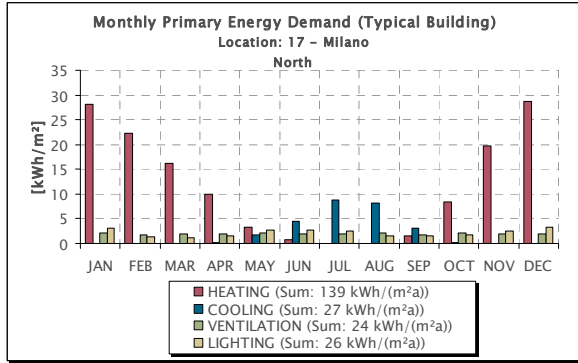
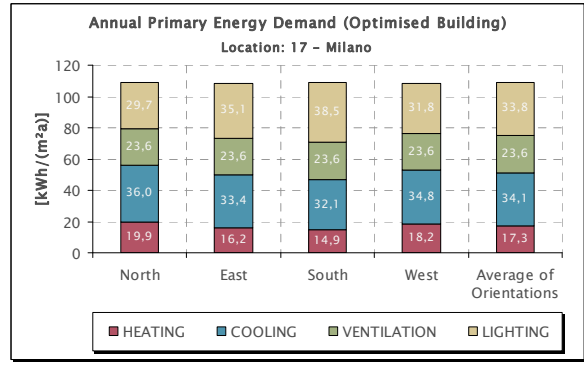
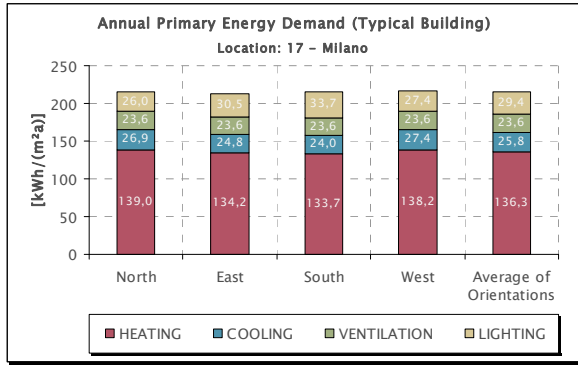
Heat. / Cool. Degree Days	Heating Degree Days (Base 18°C)	[Kd]	2738,24
	Cooling Degree Days (Base 10°C)	[Kd]	1642,62

Solar Radiation	Annual total diffuse rad. on horiz. surf.	[kWh/m ²]	684,01
	Annual total direct rad. on horiz. surf.	[kWh/m ²]	569,17
	Annual total global rad. on horiz. surf.	[kWh/m ²]	1.253,19

Daylight	Annual total illumination on horiz. surf.	[kluxh]	137.599
	Annual total daylight hours	[h]	4.337
	Average illuminance on horiz. surf.	[lux]	31.727
	Annual total illumination on horiz. surf. during office use	[kluxh]	133.491
	Annual total daylight hours during office use	[h]	3.778
	Average illuminance on horiz. surf. during office use	[lux]	35.334

Air Humidity	Mean relative humidity	[-]	0,73
--------------	------------------------	-----	------





20.3.18. Location 18 – Zagreb

Location	Location name	Zagreb (HR)	
	Latitude (North positive)	[°]	50,1
	Longitude (East positive)	[°]	8,68
	Height above sealevel	[m]	125

Assumed Period of Office Use	Begin (local time)	[h]	8
	End (local time)	[h]	18
	Office use per day	[h]	10
	Office use per year	[h]	2607,14

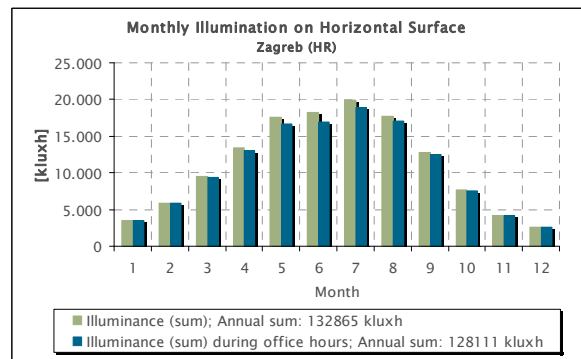
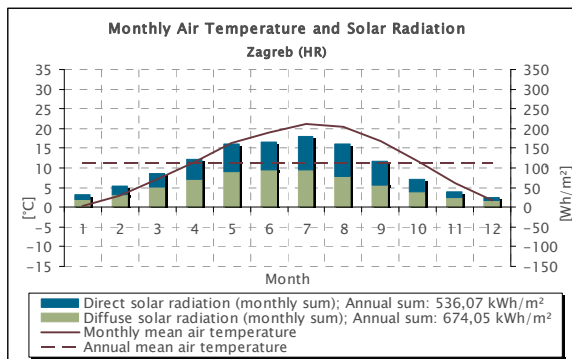
Temperature	Max. daily mean air temperature	[°C]	27,77
	Min. daily mean air temperature	[°C]	-8,83
	Max. monthly mean air temperature	[°C]	21,26
	Min. monthly mean air temperature	[°C]	0,22
	Annual mean air temperature	[°C]	11,28
	Standard deviation of daily mean from annual mean air temperature	[°C]	8,3

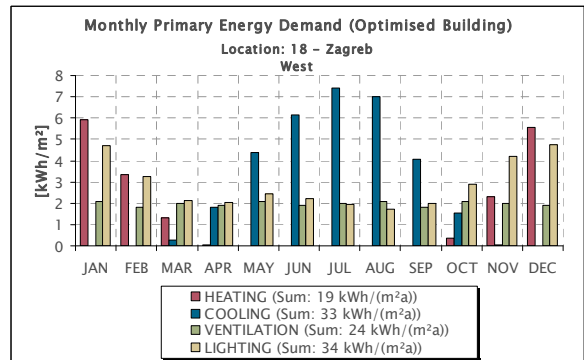
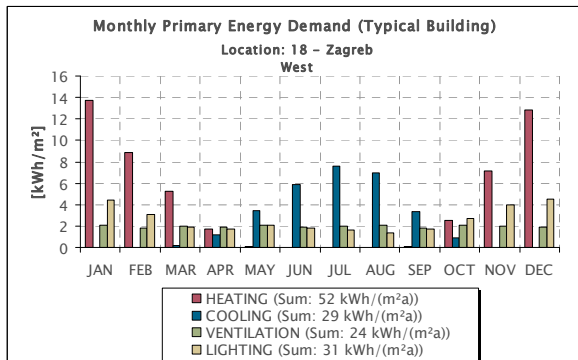
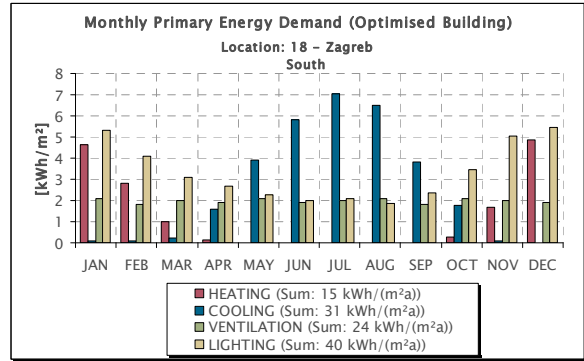
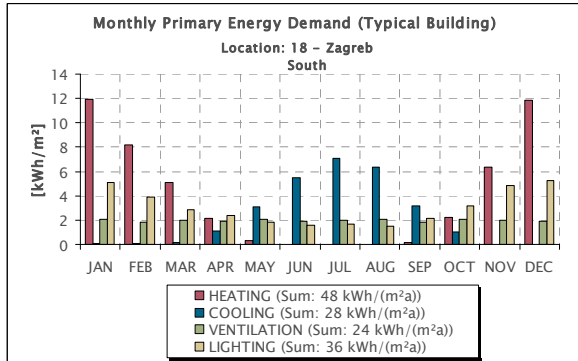
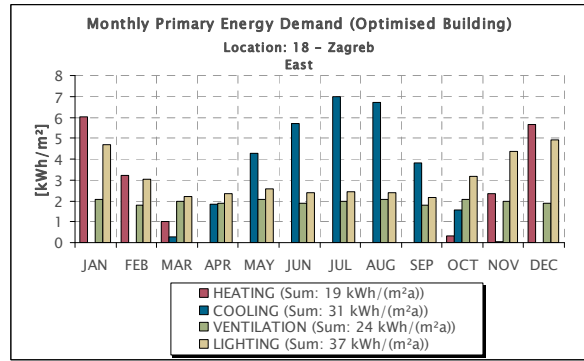
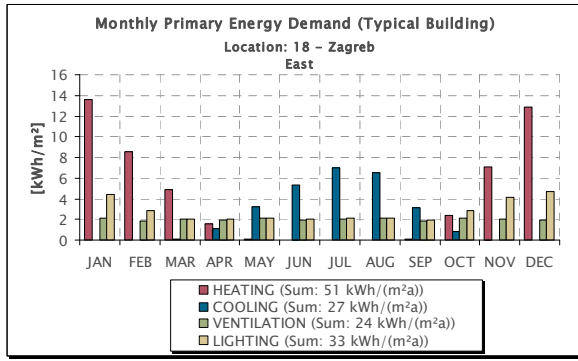
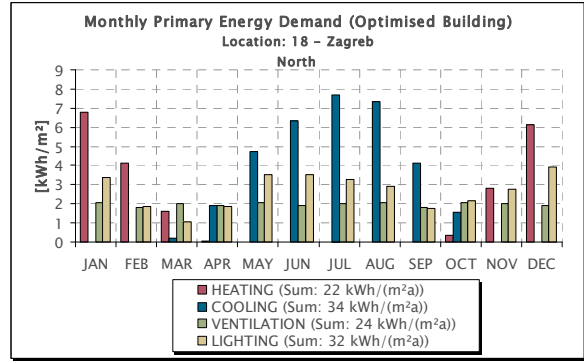
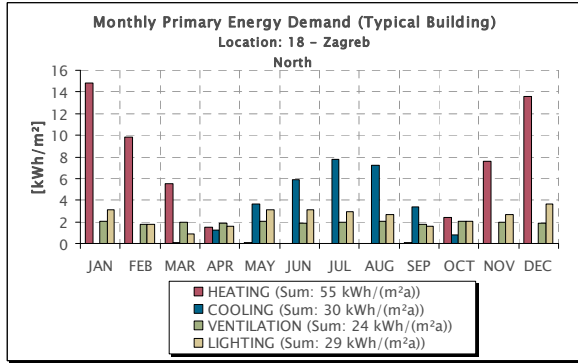
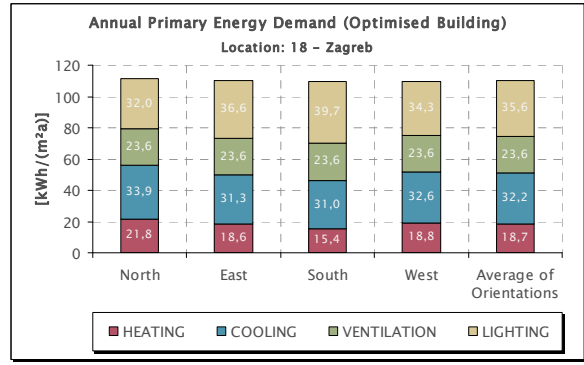
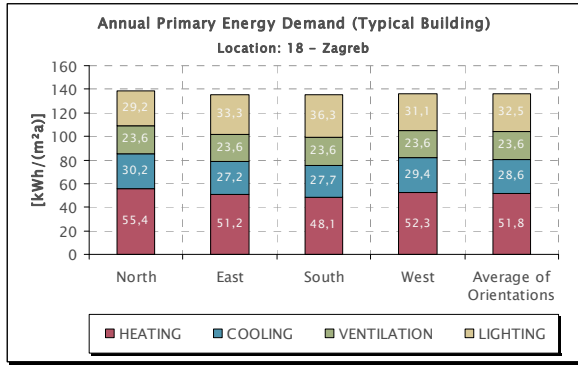
Heat. / Cool. Degree Days	Heating Degree Days (Base 18°C)	[Kd]	2822,15
	Cooling Degree Days (Base 10°C)	[Kd]	1578,89

Solar Radiation	Annual total diffuse rad. on horiz. surf.	[kWh/m²]	674,05
	Annual total direct rad. on horiz. surf.	[kWh/m²]	536,07
	Annual total global rad. on horiz. surf.	[kWh/m²]	1.210,12

Daylight	Annual total illumination on horiz. surf.	[kluxh]	132.865
	Annual total daylight hours	[h]	4.326
	Average illuminance on horiz. surf.	[lux]	30.713
	Annual total illumination on horiz. surf. during office use	[kluxh]	128.111
	Annual total daylight hours during office use	[h]	3.726
	Average illuminance on horiz. surf. during office use	[lux]	34.383

Air Humidity	Mean relative humidity	[-]	0,73
--------------	------------------------	-----	------





20.3.19. Location 19 – Beograd

Location	Location name	Beograd (SRB)	
	Latitude (North positive)	[°]	50,1
	Longitude (East positive)	[°]	8,68
	Height above sealevel	[m]	125

Assumed Period of Office Use	Begin (local time)	[h]	8
	End (local time)	[h]	18
	Office use per day	[h]	10
	Office use per year	[h]	2607,14

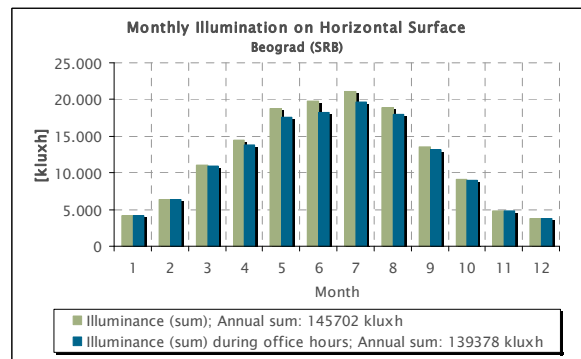
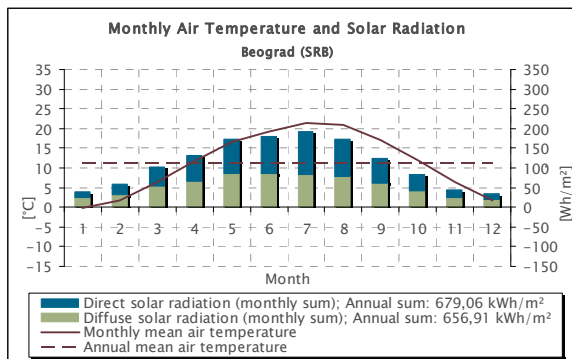
Temperature	Max. daily mean air temperature	[°C]	28,60
	Min. daily mean air temperature	[°C]	-9,05
	Max. monthly mean air temperature	[°C]	21,34
	Min. monthly mean air temperature	[°C]	-0,15
	Annual mean air temperature	[°C]	11,28
	Standard deviation of daily mean from annual mean air temperature	[°C]	8,6

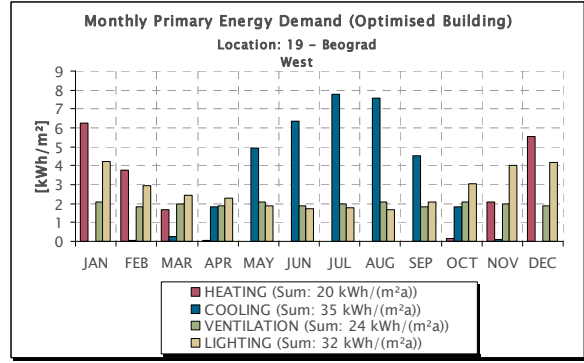
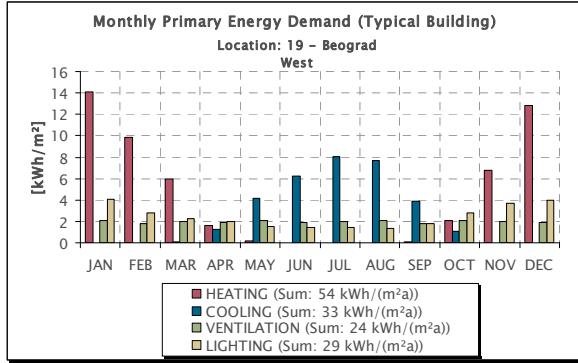
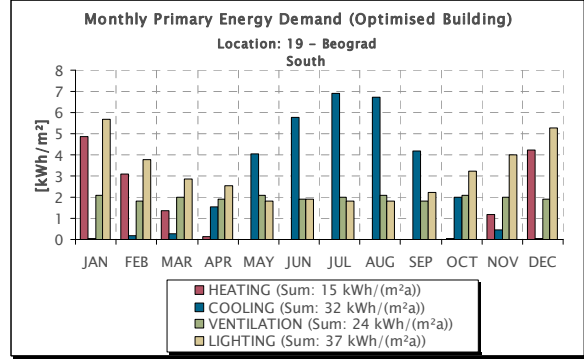
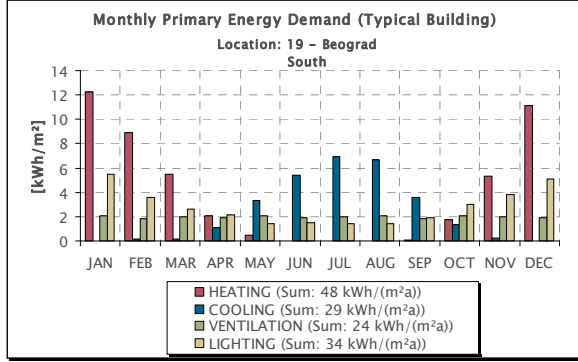
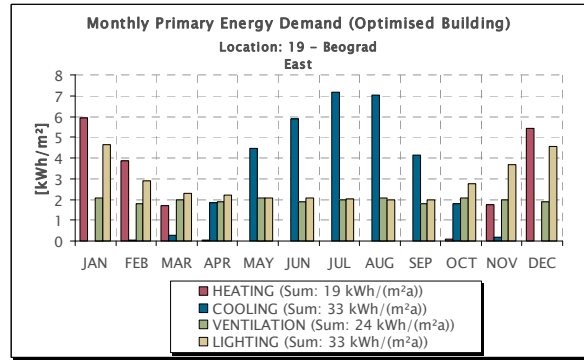
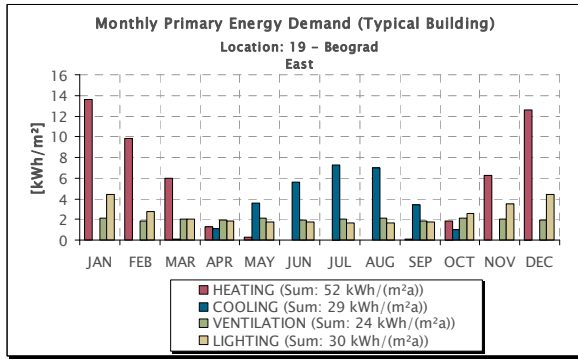
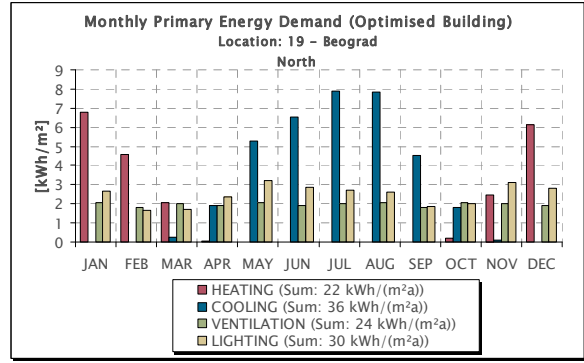
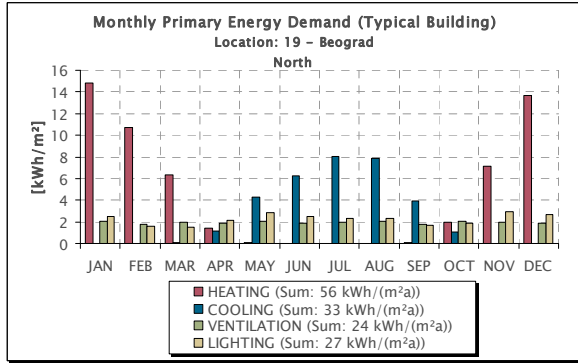
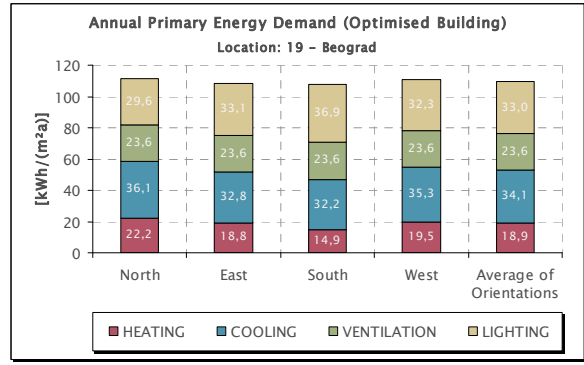
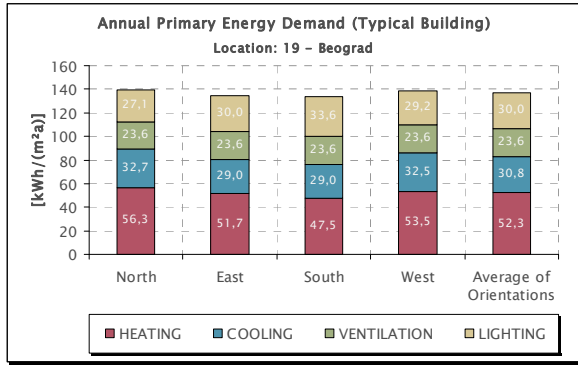
Heat. / Cool. Degree Days	Heating Degree Days (Base 18°C)	[Kd]	2881,83
	Cooling Degree Days (Base 10°C)	[Kd]	1654,09

Solar Radiation	Annual total diffuse rad. on horiz. surf.	[kWh/m ²]	656,91
	Annual total direct rad. on horiz. surf.	[kWh/m ²]	679,06
	Annual total global rad. on horiz. surf.	[kWh/m ²]	1.335,97

Daylight	Annual total illumination on horiz. surf.	[kluxh]	145.702
	Annual total daylight hours	[h]	4.353
	Average illuminance on horiz. surf.	[lux]	33.472
	Annual total illumination on horiz. surf. during office use	[kluxh]	139.378
	Annual total daylight hours during office use	[h]	3.743
	Average illuminance on horiz. surf. during office use	[lux]	37.237

Air Humidity	Mean relative humidity	[-]	0,65
--------------	------------------------	-----	------





20.3.20. Location 20 – Bucuresti

Location	Location name	Bucuresti (RO)	
	Latitude (North positive)	[°]	50,1
	Longitude (East positive)	[°]	8,68
	Height above sealevel	[m]	125

Assumed Period of Office Use	Begin (local time)	[h]	8
	End (local time)	[h]	18
	Office use per day	[h]	10
	Office use per year	[h]	2607,14

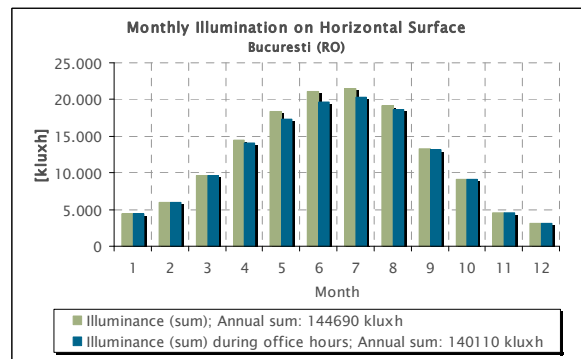
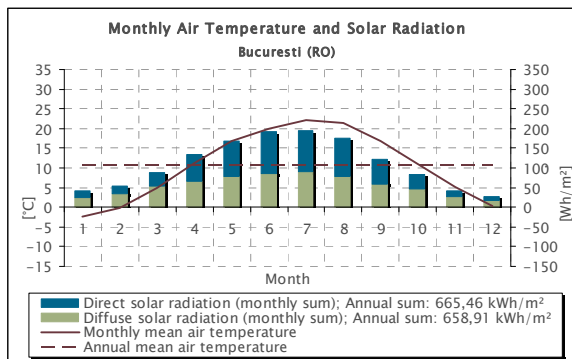
Temperature	Max. daily mean air temperature	[°C]	29,83
	Min. daily mean air temperature	[°C]	-11,63
	Max. monthly mean air temperature	[°C]	22,15
	Min. monthly mean air temperature	[°C]	-2,41
	Annual mean air temperature	[°C]	10,63
	Standard deviation of daily mean from annual mean air temperature	[°C]	9,4

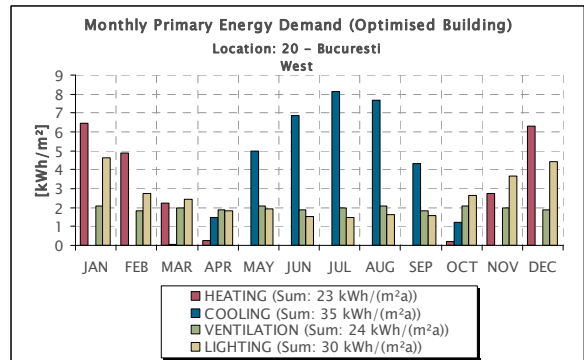
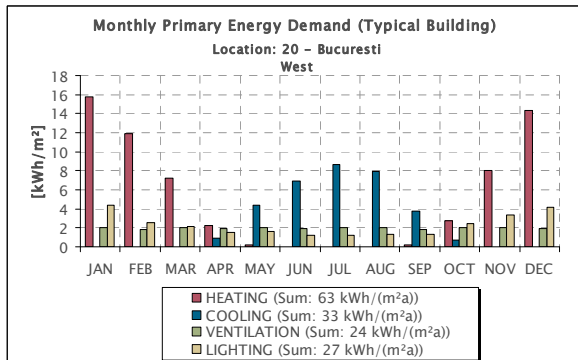
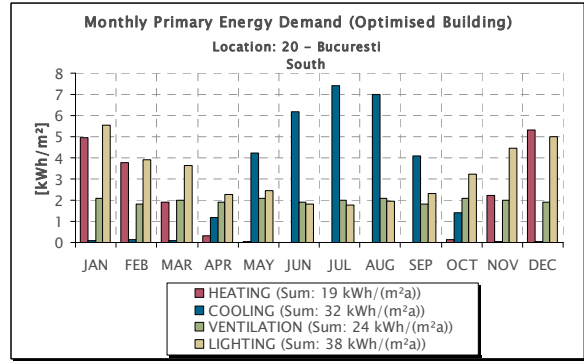
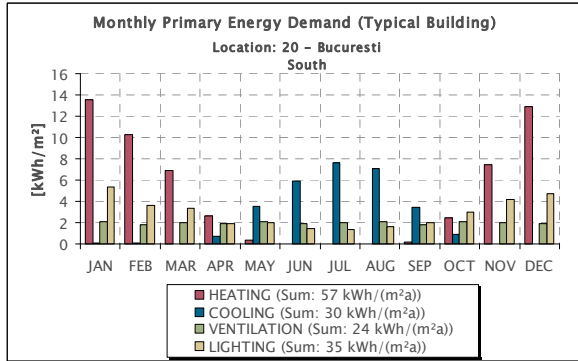
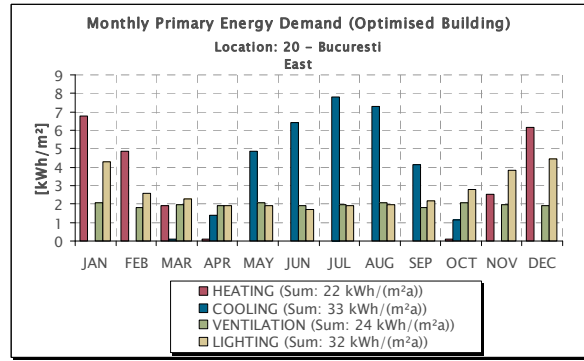
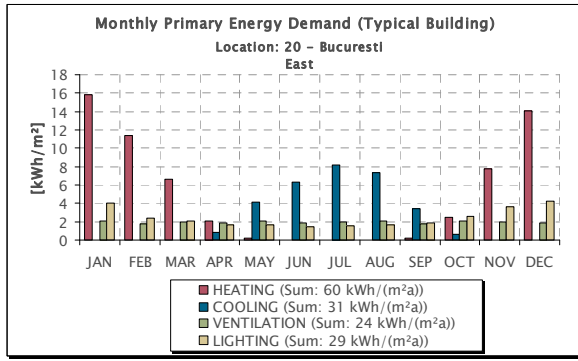
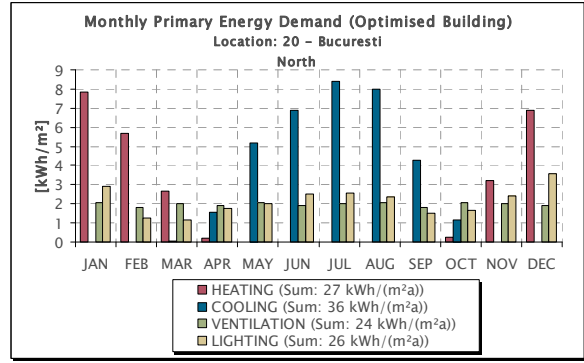
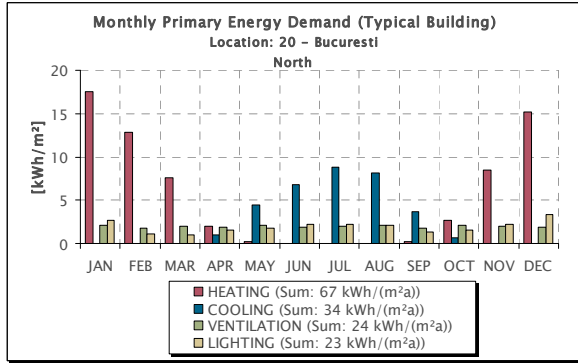
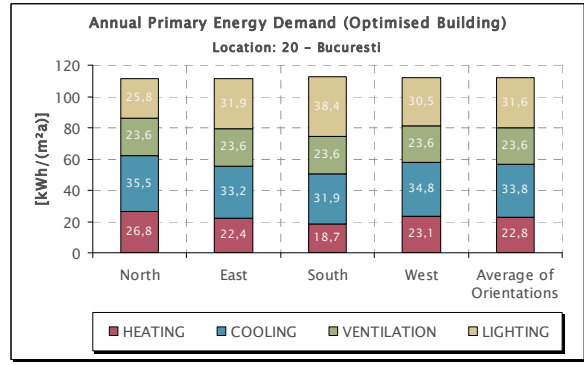
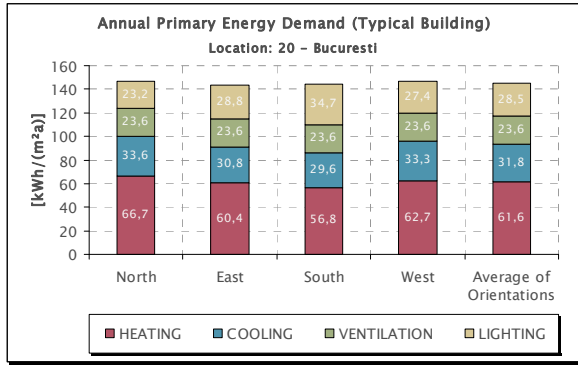
Heat. / Cool. Degree Days	Heating Degree Days (Base 18°C)	[Kd]	3167,02
	Cooling Degree Days (Base 10°C)	[Kd]	1651,04

Solar Radiation	Annual total diffuse rad. on horiz. surf.	[kWh/m ²]	658,91
	Annual total direct rad. on horiz. surf.	[kWh/m ²]	665,46
	Annual total global rad. on horiz. surf.	[kWh/m ²]	1.324,37

Daylight	Annual total illumination on horiz. surf.	[kluxh]	144.690
	Annual total daylight hours	[h]	4.323
	Average illuminance on horiz. surf.	[lux]	33.470
	Annual total illumination on horiz. surf. during office use	[kluxh]	140.110
	Annual total daylight hours during office use	[h]	3.771
	Average illuminance on horiz. surf. during office use	[lux]	37.155

Air Humidity	Mean relative humidity	[-]	0,69
--------------	------------------------	-----	------





20.3.21. Location 21 – Madrid

Location	Location name	Madrid (E)	
	Latitude (North positive)	[°]	50,1
	Longitude (East positive)	[°]	8,68
	Height above sealevel	[m]	125

Assumed Period of Office Use	Begin (local time)	[h]	8
	End (local time)	[h]	18
	Office use per day	[h]	10
	Office use per year	[h]	2607,14

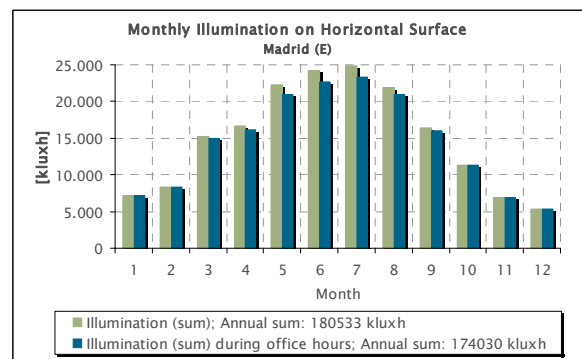
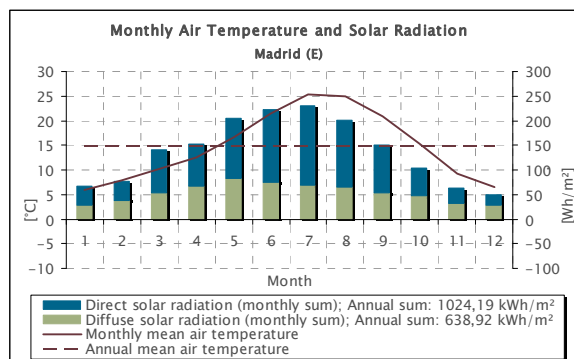
Temperature	Max. daily mean air temperature	[°C]	30,63
	Min. daily mean air temperature	[°C]	-0,66
	Max. monthly mean air temperature	[°C]	25,37
	Min. monthly mean air temperature	[°C]	5,98
	Annual mean air temperature	[°C]	14,78
	Standard deviation of daily mean from annual mean air temperature	[°C]	7,4

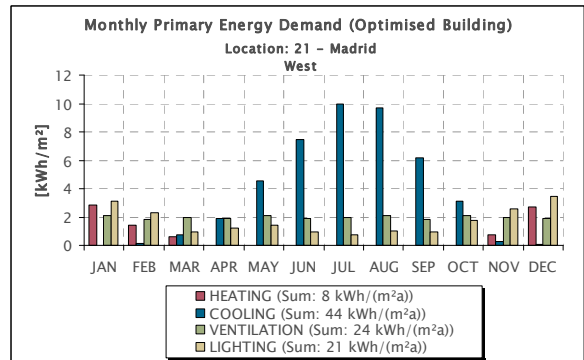
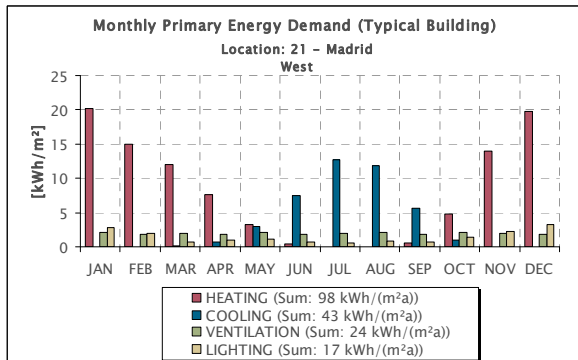
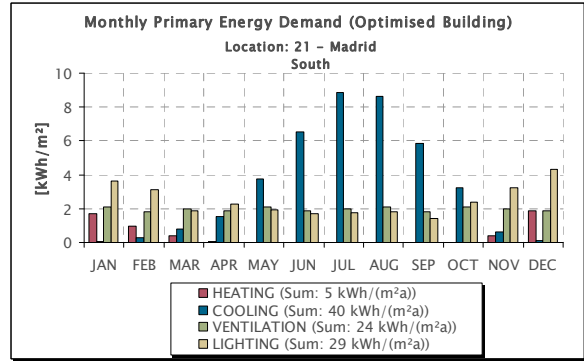
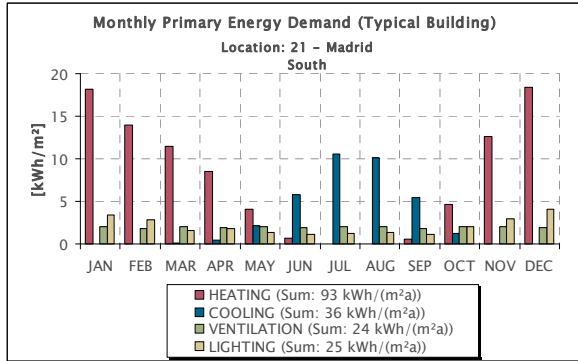
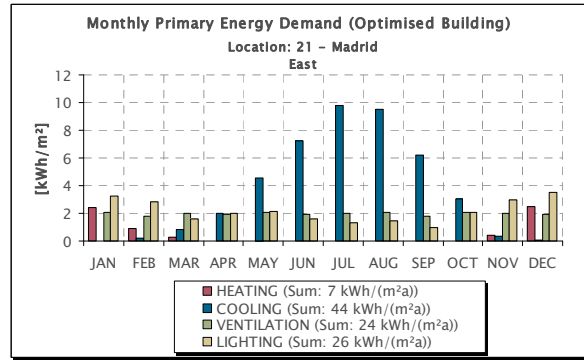
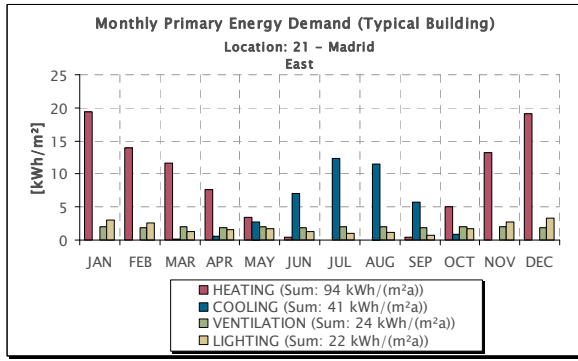
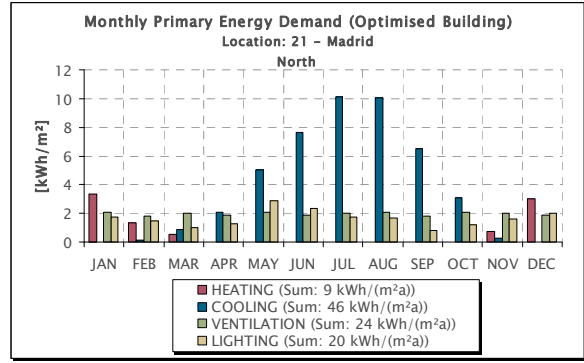
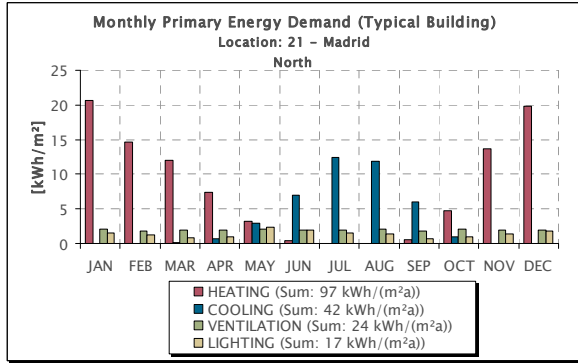
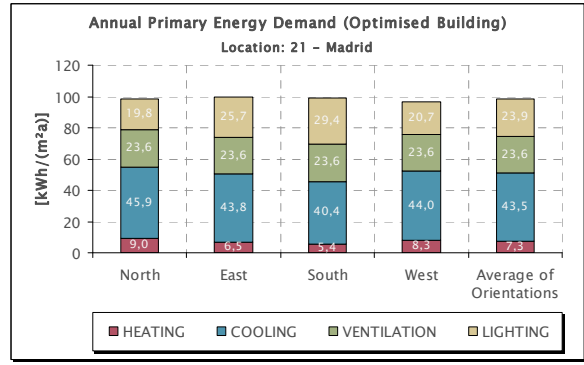
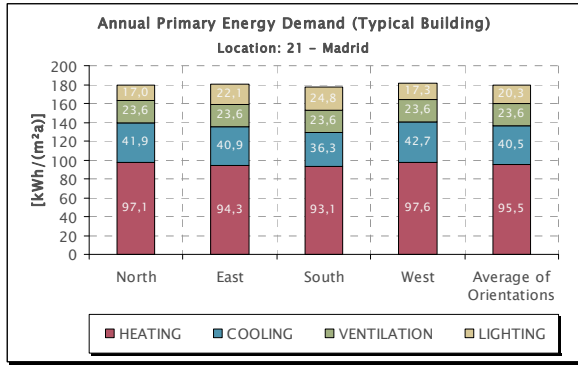
Heat. / Cool. Degree Days	Heating Degree Days (Base 18°C)	[Kd]	1965,35
	Cooling Degree Days (Base 10°C)	[Kd]	2241,20

Solar Radiation	Annual total diffuse rad. on horiz. surf.	[kWh/m ²]	638,92
	Annual total direct rad. on horiz. surf.	[kWh/m ²]	1.024,19
	Annual total global rad. on horiz. surf.	[kWh/m ²]	1.663,11

Daylight	Annual total illumination on horiz. surf.	[kluxh]	180.533
	Annual total daylight hours	[h]	4.346
	Average illuminance on horiz. surf.	[lux]	41.540
	Annual total illumination on horiz. surf. during office use	[kluxh]	174.030
	Annual total daylight hours during office use	[h]	3.790
	Average illuminance on horiz. surf. during office use	[lux]	45.918

Air Humidity	Mean relative humidity	[-]	0,52
--------------	------------------------	-----	------





20.3.22. Location 22 – Valencia

Location	Location name	Valencia (E)	
	Latitude (North positive)	[°]	50,1
	Longitude (East positive)	[°]	8,68
	Height above sealevel	[m]	125

Assumed Period of Office Use	Begin (local time)	[h]	8
	End (local time)	[h]	18
	Office use per day	[h]	10
	Office use per year	[h]	2607,14

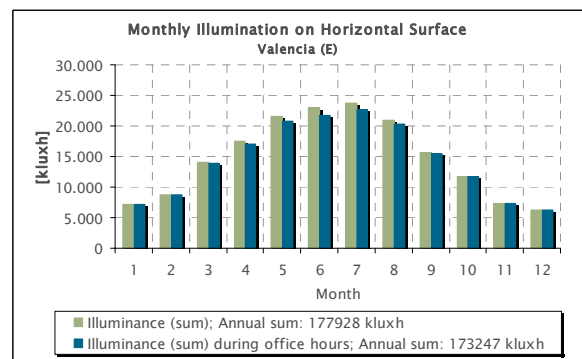
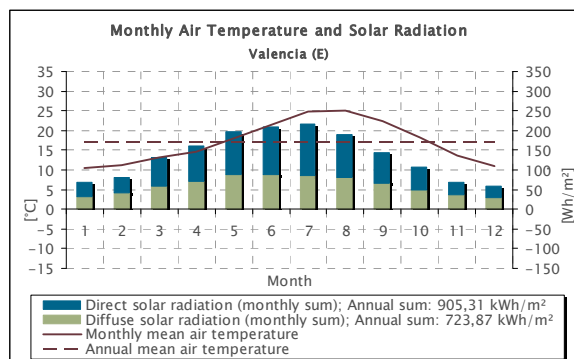
Temperature	Max. daily mean air temperature	[°C]	28,63
	Min. daily mean air temperature	[°C]	4,21
	Max. monthly mean air temperature	[°C]	24,96
	Min. monthly mean air temperature	[°C]	10,39
	Annual mean air temperature	[°C]	17,01
	Standard deviation of daily mean from annual mean air temperature	[°C]	5,7

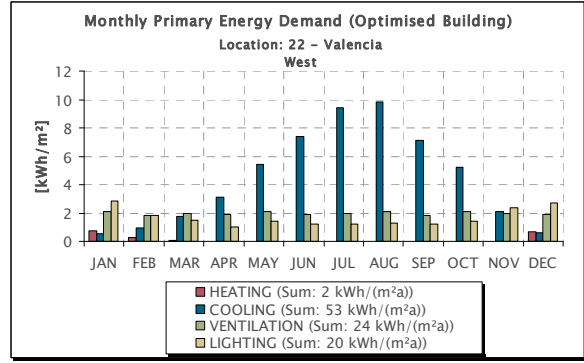
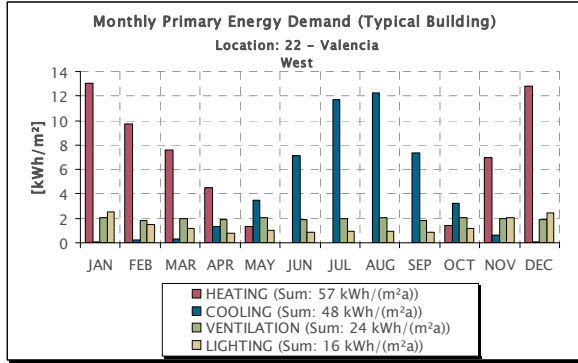
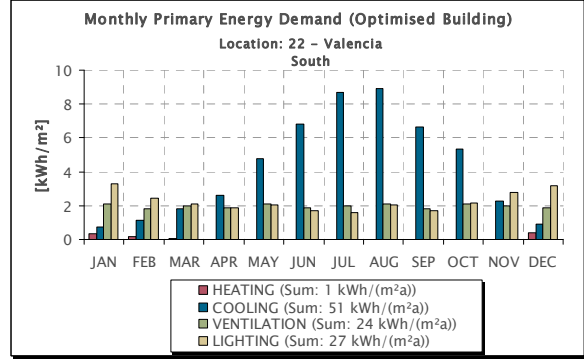
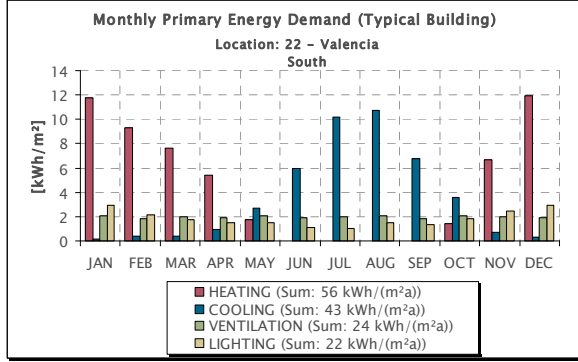
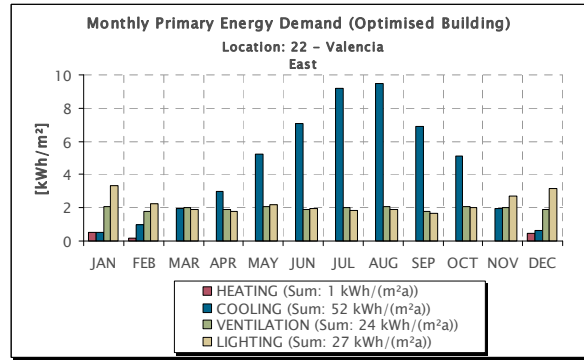
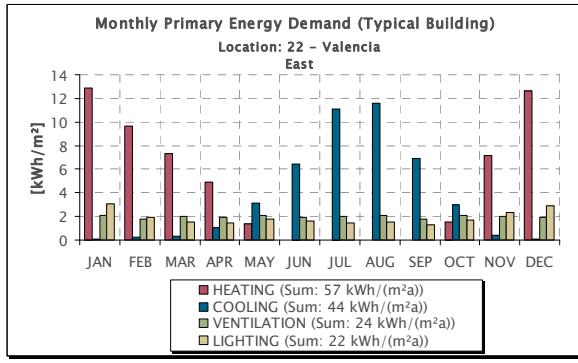
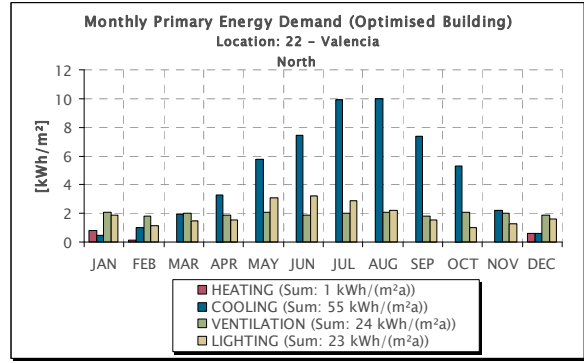
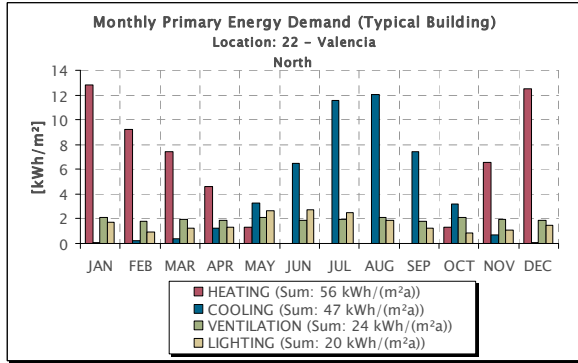
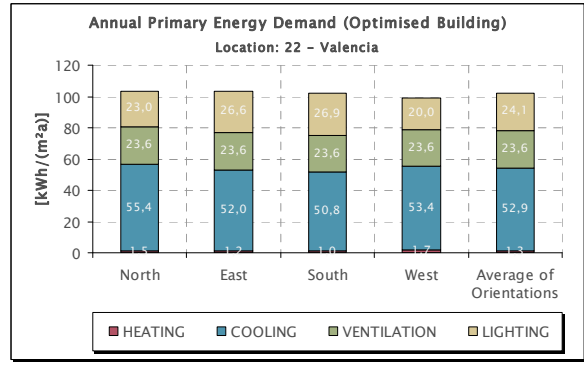
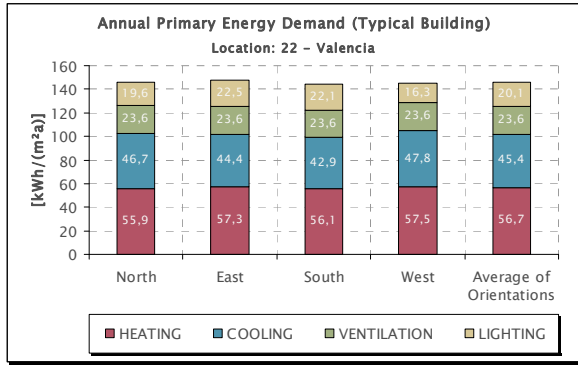
Heat. / Cool. Degree Days	Heating Degree Days (Base 18°C)	[Kd]	1194,34
	Cooling Degree Days (Base 10°C)	[Kd]	2731,93

Solar Radiation	Annual total diffuse rad. on horiz. surf.	[kWh/m ²]	723,87
	Annual total direct rad. on horiz. surf.	[kWh/m ²]	905,31
	Annual total global rad. on horiz. surf.	[kWh/m ²]	1.629,18

Daylight	Annual total illumination on horiz. surf.	[kluxh]	177.928
	Annual total daylight hours	[h]	4.319
	Average illuminance on horiz. surf.	[lux]	41.197
	Annual total illumination on horiz. surf. during office use	[kluxh]	173.247
	Annual total daylight hours during office use	[h]	3.828
	Average illuminance on horiz. surf. during office use	[lux]	45.258

Air Humidity	Mean relative humidity	[-]	0,67
--------------	------------------------	-----	------





20.3.23. Location 23 – Palma de Mallorca

Location	Location name	Palma de Mallorca (E)	
	Latitude (North positive)	[°]	50,1
	Longitude (East positive)	[°]	8,68
	Height above sealevel	[m]	125

Assumed Period of Office Use	Begin (local time)	[h]	8
	End (local time)	[h]	18
	Office use per day	[h]	10
	Office use per year	[h]	2607,14

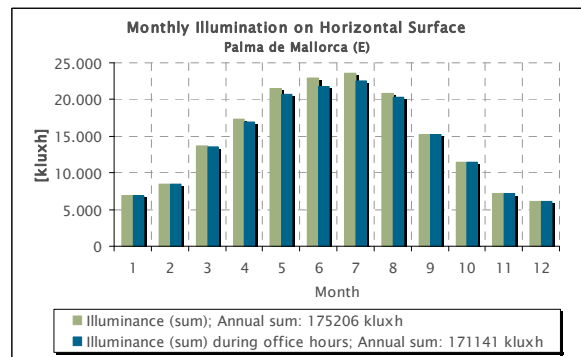
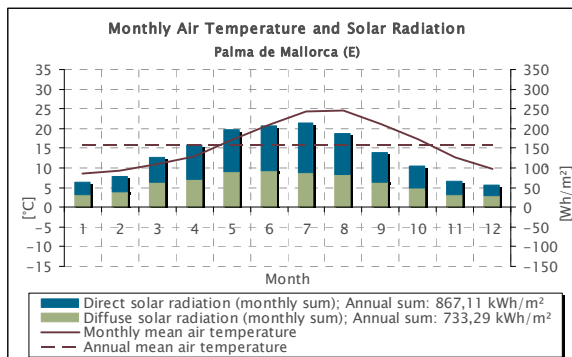
Temperature	Max. daily mean air temperature	[°C]	28,57
	Min. daily mean air temperature	[°C]	3,25
	Max. monthly mean air temperature	[°C]	24,48
	Min. monthly mean air temperature	[°C]	8,56
	Annual mean air temperature	[°C]	15,84
	Standard deviation of daily mean from annual mean air temperature	[°C]	6,0

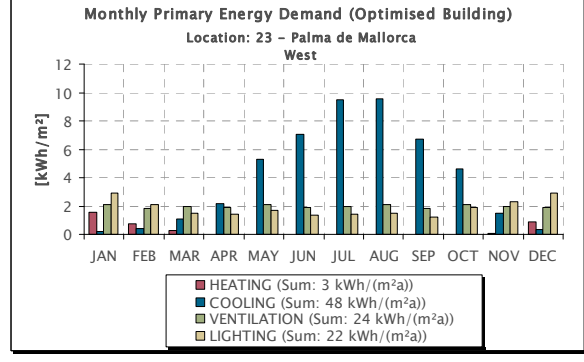
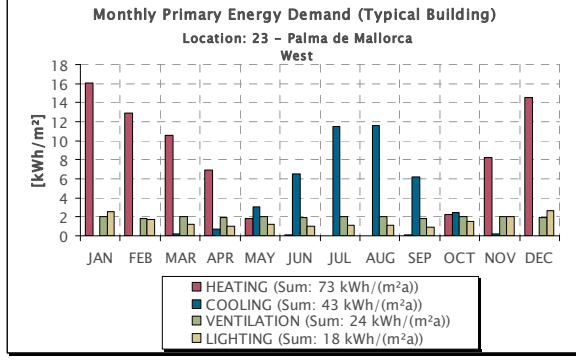
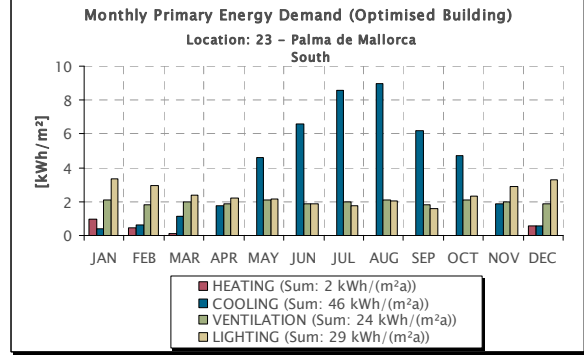
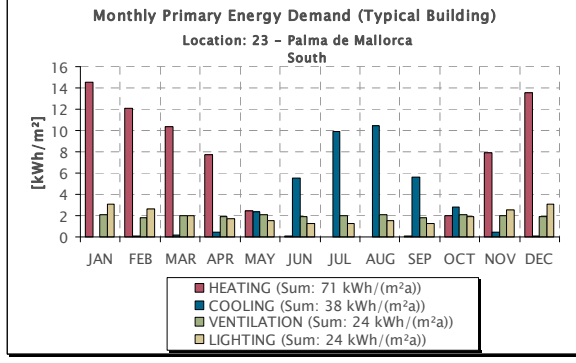
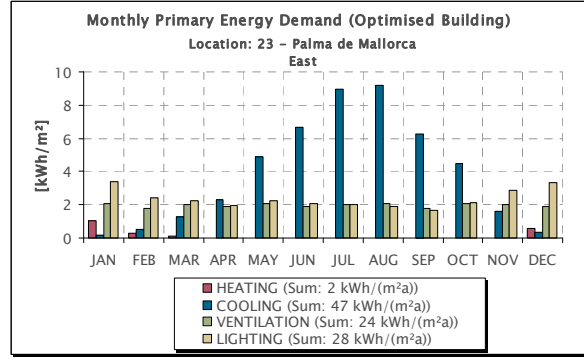
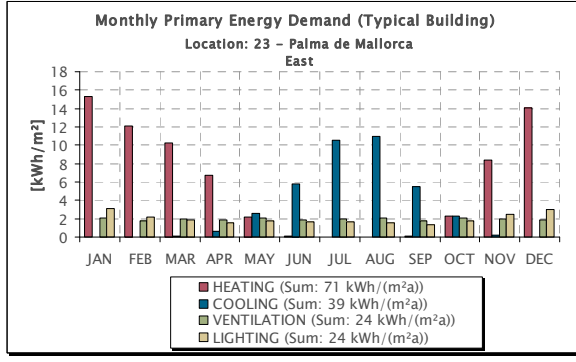
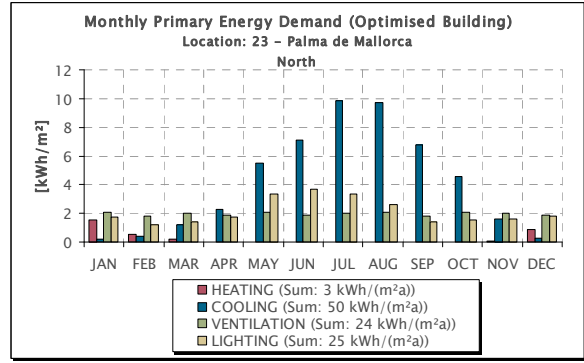
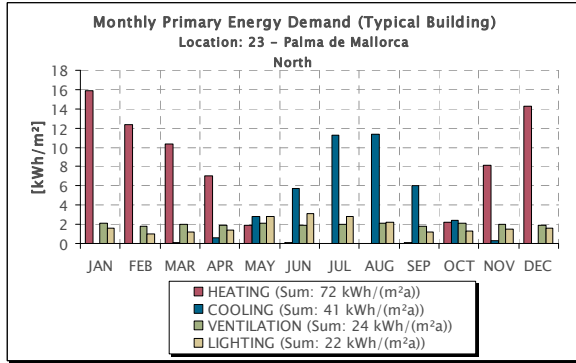
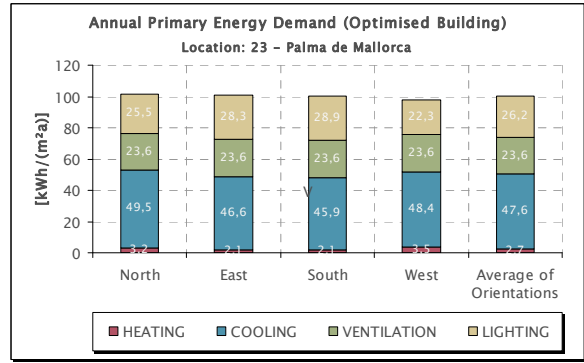
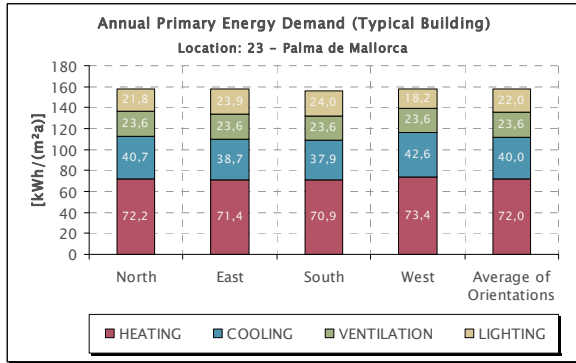
Heat. / Cool. Degree Days	Heating Degree Days (Base 18°C)	[Kd]	1523,56
	Cooling Degree Days (Base 10°C)	[Kd]	2424,14

Solar Radiation	Annual total diffuse rad. on horiz. surf.	[kWh/m ²]	733,29
	Annual total direct rad. on horiz. surf.	[kWh/m ²]	867,11
	Annual total global rad. on horiz. surf.	[kWh/m ²]	1.600,40

Daylight	Annual total illumination on horiz. surf.	[kluxh]	175.206
	Annual total daylight hours	[h]	4.307
	Average illuminance on horiz. surf.	[lux]	40.679
	Annual total illumination on horiz. surf. during office use	[kluxh]	171.141
	Annual total daylight hours during office use	[h]	3.835
	Average illuminance on horiz. surf. during office use	[lux]	44.626

Air Humidity	Mean relative humidity	[-]	0,75
--------------	------------------------	-----	------





20.3.24. Location 24 – Napoli

Location	Location name	Napoli (I)	
	Latitude (North positive)	[°]	50,1
	Longitude (East positive)	[°]	8,68
	Height above sealevel	[m]	125

Assumed Period of Office Use	Begin (local time)	[h]	8
	End (local time)	[h]	18
	Office use per day	[h]	10
	Office use per year	[h]	2607,14

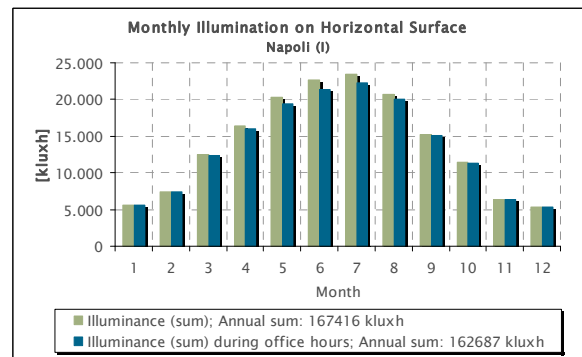
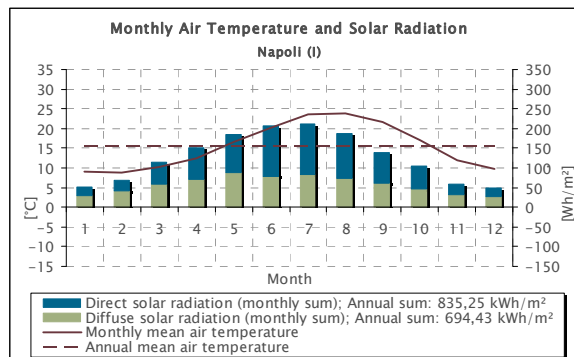
Temperature	Max. daily mean air temperature	[°C]	27,11
	Min. daily mean air temperature	[°C]	2,90
	Max. monthly mean air temperature	[°C]	23,94
	Min. monthly mean air temperature	[°C]	8,70
	Annual mean air temperature	[°C]	15,47
	Standard deviation of daily mean from annual mean air temperature	[°C]	6,0

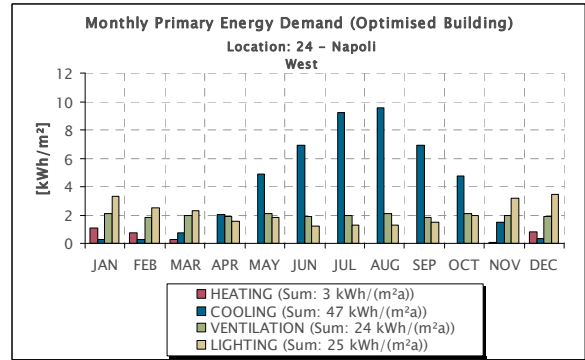
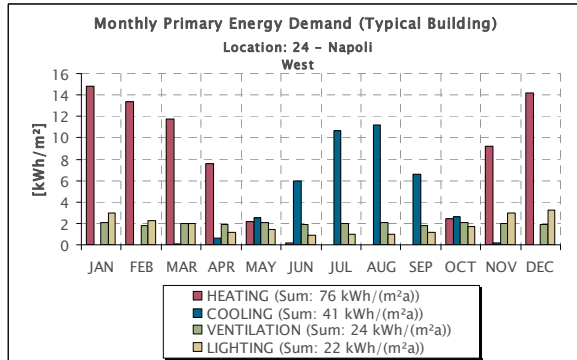
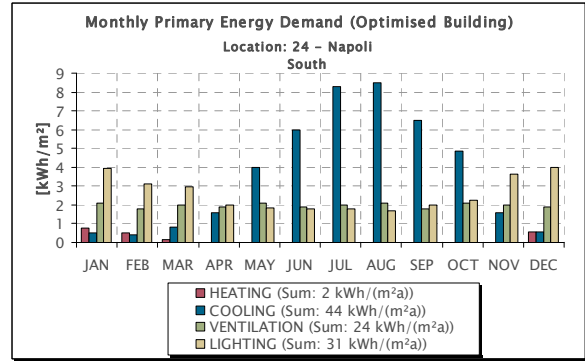
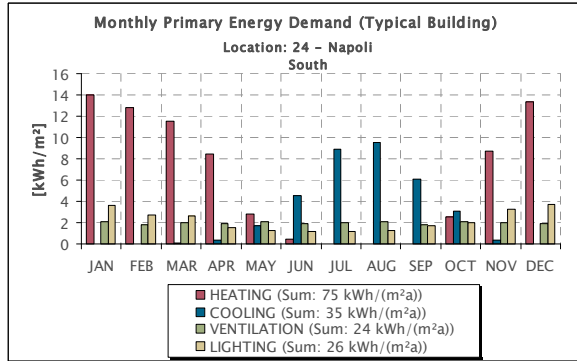
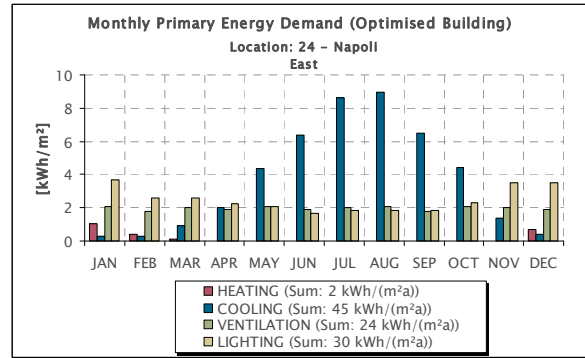
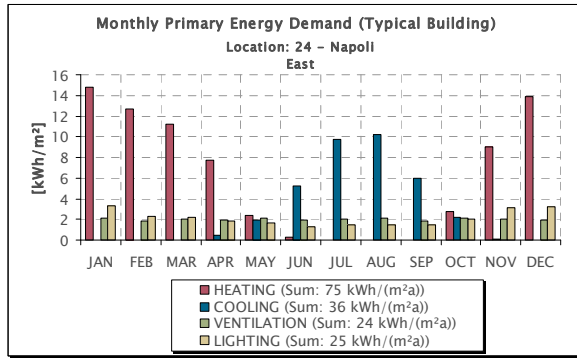
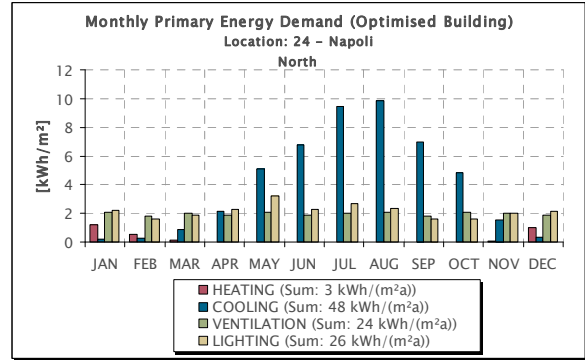
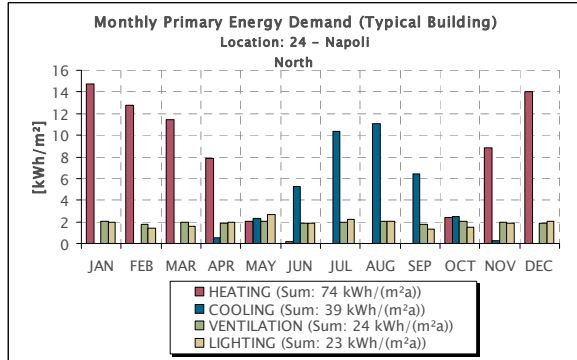
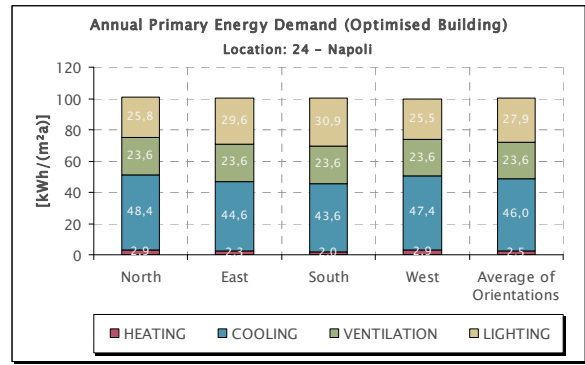
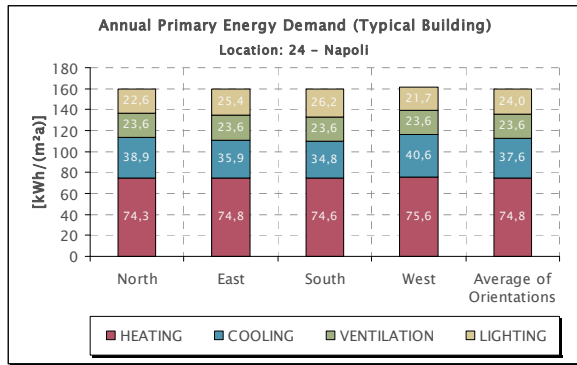
Heat. / Cool. Degree Days	Heating Degree Days (Base 18°C)	[Kd]	1578,93
	Cooling Degree Days (Base 10°C)	[Kd]	2278,90

Solar Radiation	Annual total diffuse rad. on horiz. surf.	[kWh/m²]	694,43
	Annual total direct rad. on horiz. surf.	[kWh/m²]	835,25
	Annual total global rad. on horiz. surf.	[kWh/m²]	1.529,68

Daylight	Annual total illumination on horiz. surf.	[kluxh]	167.416
	Annual total daylight hours	[h]	4.288
	Average illuminance on horiz. surf.	[lux]	39.043
	Annual total illumination on horiz. surf. during office use	[kluxh]	162.687
	Annual total daylight hours during office use	[h]	3.800
	Average illuminance on horiz. surf. during office use	[lux]	42.812

Air Humidity	Mean relative humidity	[-]	0,73
--------------	------------------------	-----	------





20.3.25. Location 25 – Salonika

Location	Location name	Salonika (GR)	
	Latitude (North positive)	[°]	40,63
	Longitude (East positive)	[°]	22,93
	Height above sealevel	[m]	149

Assumed Period of Office Use	Begin (local time)	[h]	8
	End (local time)	[h]	18
	Office use per day	[h]	10
	Office use per year	[h]	2607,14

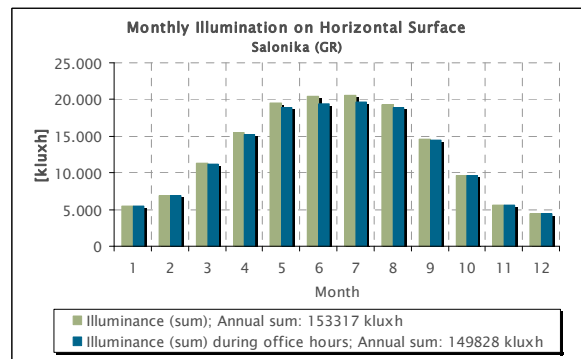
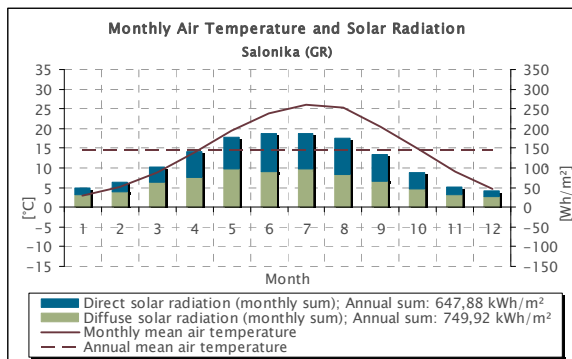
Temperature	Max. daily mean air temperature	[°C]	29,93
	Min. daily mean air temperature	[°C]	-4,08
	Max. monthly mean air temperature	[°C]	26,07
	Min. monthly mean air temperature	[°C]	2,92
	Annual mean air temperature	[°C]	14,59
	Standard deviation of daily mean from annual mean air temperature	[°C]	8,5

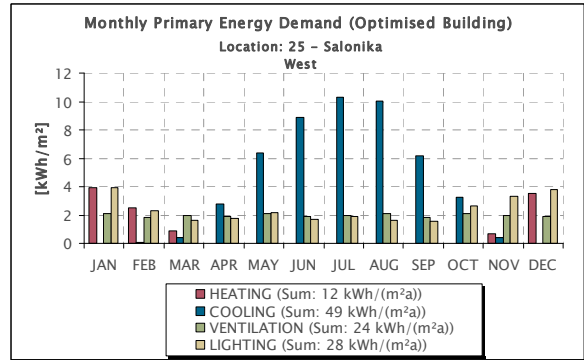
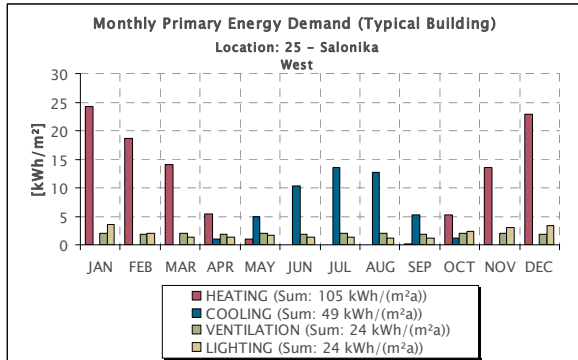
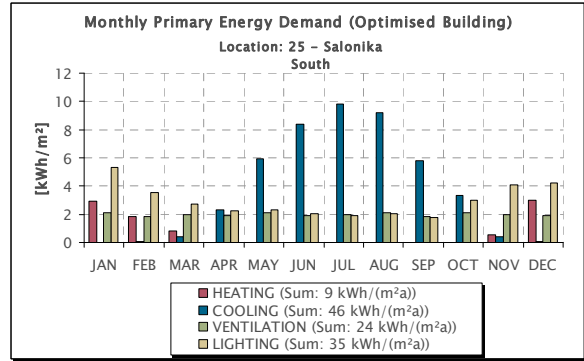
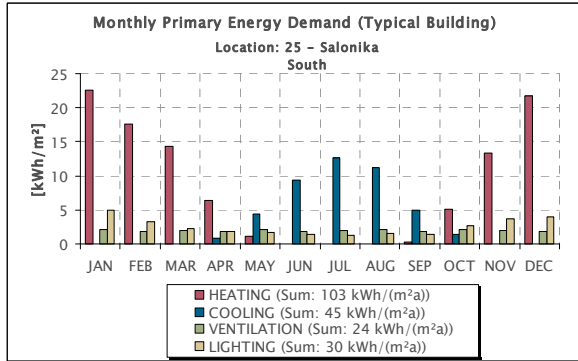
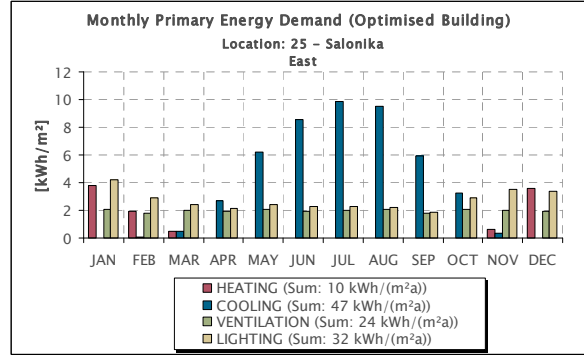
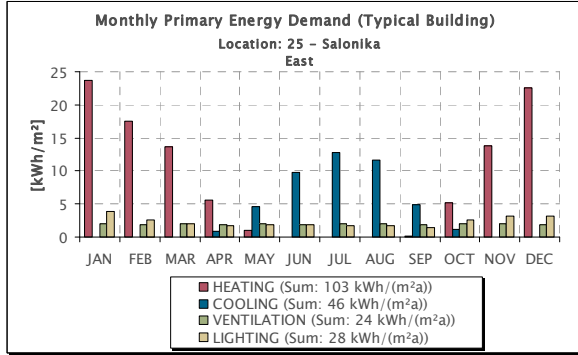
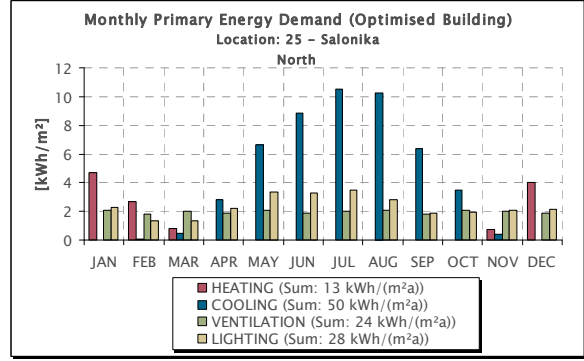
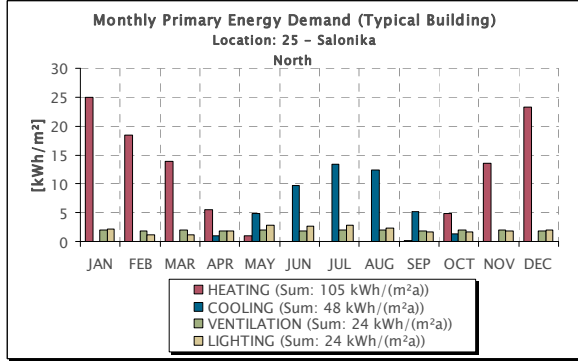
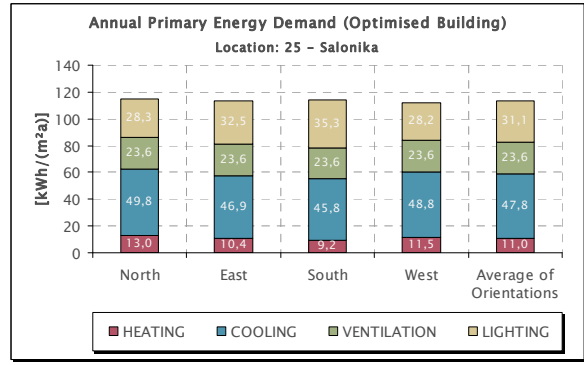
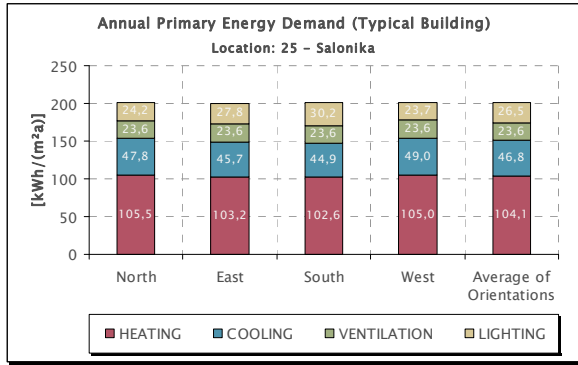
Heat. / Cool. Degree Days	Heating Degree Days (Base 18°C)	[Kd]	2123,26
	Cooling Degree Days (Base 10°C)	[Kd]	2381,95

Solar Radiation	Annual total diffuse rad. on horiz. surf.	[kWh/m²]	749,92
	Annual total direct rad. on horiz. surf.	[kWh/m²]	647,88
	Annual total global rad. on horiz. surf.	[kWh/m²]	1.397,80

Daylight	Annual total illumination on horiz. surf.	[kluxh]	153.317
	Annual total daylight hours	[h]	4.345
	Average illuminance on horiz. surf.	[lux]	35.286
	Annual total illumination on horiz. surf. during office use	[kluxh]	149.828
	Annual total daylight hours during office use	[h]	3.824
	Average illuminance on horiz. surf. during office use	[lux]	39.181

Air Humidity	Mean relative humidity	[-]	0,62
--------------	------------------------	-----	------





Curriculum vitae

Name Jörg Schlenger

Date of Birth 5. June 1973

Place of Birth Essen, Germany

Education

- 1997-2001 Dipl.-Ing. (Civil Engineering) at Darmstadt University of Technology, Darmstadt, Germany
- 1993-1997 cand.-Ing. (Civil Engineering) at University of Essen, Essen, Germany
- 1992-1993 Civilian Service at German Red Cross, Essen, Germany
- 1983-1992 Abitur at Helmholtz-Gymnasium, Essen, Germany

Work Experience

- Since 2009 Project Manager at Drees&Sommer Advanced Building Technologies GmbH, Frankfurt/Main, Germany
- 2004-2009 Assistant Researcher and Lecturer at Chair of Environmental Architecture, Faculty of Building, Dortmund University of Technology, Dortmund, Germany
- 2002-2004 Project Engineer at Institute for applied Energysimulations (ifes) GmbH, Frechen (near Cologne), Germany